NCHRP

REPORT 611

NATIONAL COOPERATIVE HIGHWAY RESEARCH PROGRAM

Seismic Analysis and Design of Retaining Walls, Buried Structures, Slopes, and Embankments

TRANSPORTATION RESEARCH BOARD
OF THE NATIONAL ACADEMIES

TRANSPORTATION RESEARCH BOARD 2008 EXECUTIVE COMMITTEE*

OFFICERS

CHAIR: **Debra L. Miller,** *Secretary, Kansas DOT, Topeka*
VICE CHAIR: **Adib K. Kanafani,** *Cahill Professor of Civil Engineering, University of California, Berkeley*
EXECUTIVE DIRECTOR: **Robert E. Skinner, Jr.,** *Transportation Research Board*

MEMBERS

J. Barry Barker, *Executive Director, Transit Authority of River City, Louisville, KY*
Allen D. Biehler, *Secretary, Pennsylvania DOT, Harrisburg*
John D. Bowe, *President, Americas Region, APL Limited, Oakland, CA*
Larry L. Brown, Sr., *Executive Director, Mississippi DOT, Jackson*
Deborah H. Butler, *Executive Vice President, Planning, and CIO, Norfolk Southern Corporation, Norfolk, VA*
William A.V. Clark, *Professor, Department of Geography, University of California, Los Angeles*
David S. Ekern, *Commissioner, Virginia DOT, Richmond*
Nicholas J. Garber, *Henry L. Kinnier Professor, Department of Civil Engineering, University of Virginia, Charlottesville*
Jeffrey W. Hamiel, *Executive Director, Metropolitan Airports Commission, Minneapolis, MN*
Edward A. (Ned) Helme, *President, Center for Clean Air Policy, Washington, DC*
Will Kempton, *Director, California DOT, Sacramento*
Susan Martinovich, *Director, Nevada DOT, Carson City*
Michael D. Meyer, *Professor, School of Civil and Environmental Engineering, Georgia Institute of Technology, Atlanta*
Michael R. Morris, *Director of Transportation, North Central Texas Council of Governments, Arlington*
Neil J. Pedersen, *Administrator, Maryland State Highway Administration, Baltimore*
Pete K. Rahn, *Director, Missouri DOT, Jefferson City*
Sandra Rosenbloom, *Professor of Planning, University of Arizona, Tucson*
Tracy L. Rosser, *Vice President, Corporate Traffic, Wal-Mart Stores, Inc., Bentonville, AR*
Rosa Clausell Rountree, *Executive Director, Georgia State Road and Tollway Authority, Atlanta*
Henry G. (Gerry) Schwartz, Jr., *Chairman (retired), Jacobs/Sverdrup Civil, Inc., St. Louis, MO*
C. Michael Walton, *Ernest H. Cockrell Centennial Chair in Engineering, University of Texas, Austin*
Linda S. Watson, *CEO, LYNX–Central Florida Regional Transportation Authority, Orlando*
Steve Williams, *Chairman and CEO, Maverick Transportation, Inc., Little Rock, AR*

EX OFFICIO MEMBERS

Thad Allen (Adm., U.S. Coast Guard), *Commandant, U.S. Coast Guard, Washington, DC*
Joseph H. Boardman, *Federal Railroad Administrator, U.S.DOT*
Rebecca M. Brewster, *President and COO, American Transportation Research Institute, Smyrna, GA*
Paul R. Brubaker, *Research and Innovative Technology Administrator, U.S.DOT*
George Bugliarello, *President Emeritus and University Professor, Polytechnic Institute of New York University, Brooklyn; Foreign Secretary, National Academy of Engineering, Washington, DC*
Sean T. Connaughton, *Maritime Administrator, U.S.DOT*
LeRoy Gishi, *Chief, Division of Transportation, Bureau of Indian Affairs, U.S. Department of the Interior, Washington, DC*
Edward R. Hamberger, *President and CEO, Association of American Railroads, Washington, DC*
John H. Hill, *Federal Motor Carrier Safety Administrator, U.S.DOT*
John C. Horsley, *Executive Director, American Association of State Highway and Transportation Officials, Washington, DC*
Carl T. Johnson, *Pipeline and Hazardous Materials Safety Administrator, U.S.DOT*
J. Edward Johnson, *Director, Applied Science Directorate, National Aeronautics and Space Administration, John C. Stennis Space Center, MS*
David Kelly, *Acting Administrator, National Highway Traffic Safety Administration, U.S.DOT*
Thomas J. Madison, Jr., *Administrator, Federal Highway Administration, U.S.DOT*
William W. Millar, *President, American Public Transportation Association, Washington, DC*
James S. Simpson, *Federal Transit Administrator, U.S.DOT*
Robert A. Sturgell, *Acting Administrator, Federal Aviation Administration, U.S.DOT*
Robert L. Van Antwerp (Lt. Gen., U.S. Army), *Chief of Engineers and Commanding General, U.S. Army Corps of Engineers, Washington, DC*

*Membership as of November 2008.

NATIONAL COOPERATIVE HIGHWAY RESEARCH PROGRAM

NCHRP REPORT 611

Seismic Analysis and Design of Retaining Walls, Buried Structures, Slopes, and Embankments

Donald G. Anderson
CH2M HILL
Bellevue, WA

Geoffrey R. Martin
University of Southern California
Los Angeles, CA

Ignatius (Po) Lam
Earth Mechanics, Inc.
Fountain Valley, CA

J. N. (Joe) Wang
Parsons Brinckerhoff Inc.
New York, NY

Subject Areas
Bridges, Other Structures, and Hydraulics and Hydrology

Research sponsored by the American Association of State Highway and Transportation Officials
in cooperation with the Federal Highway Administration

TRANSPORTATION RESEARCH BOARD

WASHINGTON, D.C.
2008
www.TRB.org

NATIONAL COOPERATIVE HIGHWAY RESEARCH PROGRAM

Systematic, well-designed research provides the most effective approach to the solution of many problems facing highway administrators and engineers. Often, highway problems are of local interest and can best be studied by highway departments individually or in cooperation with their state universities and others. However, the accelerating growth of highway transportation develops increasingly complex problems of wide interest to highway authorities. These problems are best studied through a coordinated program of cooperative research.

In recognition of these needs, the highway administrators of the American Association of State Highway and Transportation Officials initiated in 1962 an objective national highway research program employing modern scientific techniques. This program is supported on a continuing basis by funds from participating member states of the Association and it receives the full cooperation and support of the Federal Highway Administration, United States Department of Transportation.

The Transportation Research Board of the National Academies was requested by the Association to administer the research program because of the Board's recognized objectivity and understanding of modern research practices. The Board is uniquely suited for this purpose as it maintains an extensive committee structure from which authorities on any highway transportation subject may be drawn; it possesses avenues of communications and cooperation with federal, state and local governmental agencies, universities, and industry; its relationship to the National Research Council is an insurance of objectivity; it maintains a full-time research correlation staff of specialists in highway transportation matters to bring the findings of research directly to those who are in a position to use them.

The program is developed on the basis of research needs identified by chief administrators of the highway and transportation departments and by committees of AASHTO. Each year, specific areas of research needs to be included in the program are proposed to the National Research Council and the Board by the American Association of State Highway and Transportation Officials. Research projects to fulfill these needs are defined by the Board, and qualified research agencies are selected from those that have submitted proposals. Administration and surveillance of research contracts are the responsibilities of the National Research Council and the Transportation Research Board.

The needs for highway research are many, and the National Cooperative Highway Research Program can make significant contributions to the solution of highway transportation problems of mutual concern to many responsible groups. The program, however, is intended to complement rather than to substitute for or duplicate other highway research programs.

NCHRP REPORT 611

Project 12-70
ISSN 0077-5614
ISBN: 978-0-309-11765-4
Library of Congress Control Number 2008911003

COPYRIGHT PERMISSION

NOTICE

The project that is the subject of this report was a part of the National Cooperative Highway Research Program conducted by the Transportation Research Board with the approval of the Governing Board of the National Research Council. Such approval reflects the Governing Board's judgment that the program concerned is of national importance and appropriate with respect to both the purposes and resources of the National Research Council.

The members of the technical committee selected to monitor this project and to review this report were chosen for recognized scholarly competence and with due consideration for the balance of disciplines appropriate to the project. The opinions and conclusions expressed or implied are those of the research agency that performed the research, and, while they have been accepted as appropriate by the technical committee, they are not necessarily those of the Transportation Research Board, the National Research Council, the American Association of State Highway and Transportation Officials, or the Federal Highway Administration, U.S. Department of Transportation.

Each report is reviewed and accepted for publication by the technical committee according to procedures established and monitored by the Transportation Research Board Executive Committee and the Governing Board of the National Research Council.

The Transportation Research Board of the National Academies, the National Research Council, the Federal Highway Administration, the American Association of State Highway and Transportation Officials, and the individual states participating in the National Cooperative Highway Research Program do not endorse products or manufacturers. Trade or manufacturers' names appear herein solely because they are considered essential to the object of this report.

Published reports of the

NATIONAL COOPERATIVE HIGHWAY RESEARCH PROGRAM

are available from:

Transportation Research Board
Business Office
500 Fifth Street, NW
Washington, DC 20001

and can be ordered through the Internet at:

http://www.national-academies.org/trb/bookstore

Printed in the United States of America

THE NATIONAL ACADEMIES

Advisers to the Nation on Science, Engineering, and Medicine

The **National Academy of Sciences** is a private, nonprofit, self-perpetuating society of distinguished scholars engaged in scientific and engineering research, dedicated to the furtherance of science and technology and to their use for the general welfare. On the authority of the charter granted to it by the Congress in 1863, the Academy has a mandate that requires it to advise the federal government on scientific and technical matters. Dr. Ralph J. Cicerone is president of the National Academy of Sciences.

The **National Academy of Engineering** was established in 1964, under the charter of the National Academy of Sciences, as a parallel organization of outstanding engineers. It is autonomous in its administration and in the selection of its members, sharing with the National Academy of Sciences the responsibility for advising the federal government. The National Academy of Engineering also sponsors engineering programs aimed at meeting national needs, encourages education and research, and recognizes the superior achievements of engineers. Dr. Charles M. Vest is president of the National Academy of Engineering.

The **Institute of Medicine** was established in 1970 by the National Academy of Sciences to secure the services of eminent members of appropriate professions in the examination of policy matters pertaining to the health of the public. The Institute acts under the responsibility given to the National Academy of Sciences by its congressional charter to be an adviser to the federal government and, on its own initiative, to identify issues of medical care, research, and education. Dr. Harvey V. Fineberg is president of the Institute of Medicine.

The **National Research Council** was organized by the National Academy of Sciences in 1916 to associate the broad community of science and technology with the Academy's purposes of furthering knowledge and advising the federal government. Functioning in accordance with general policies determined by the Academy, the Council has become the principal operating agency of both the National Academy of Sciences and the National Academy of Engineering in providing services to the government, the public, and the scientific and engineering communities. The Council is administered jointly by both the Academies and the Institute of Medicine. Dr. Ralph J. Cicerone and Dr. Charles M. Vest are chair and vice chair, respectively, of the National Research Council.

The **Transportation Research Board** is one of six major divisions of the National Research Council. The mission of the Transportation Research Board is to provide leadership in transportation innovation and progress through research and information exchange, conducted within a setting that is objective, interdisciplinary, and multimodal. The Board's varied activities annually engage about 7,000 engineers, scientists, and other transportation researchers and practitioners from the public and private sectors and academia, all of whom contribute their expertise in the public interest. The program is supported by state transportation departments, federal agencies including the component administrations of the U.S. Department of Transportation, and other organizations and individuals interested in the development of transportation. **www.TRB.org**

www.national-academies.org

CRP STAFF FOR NCHRP REPORT 611

Christopher W. Jenks, *Director, Cooperative Research Programs*
Crawford F. Jencks, *Deputy Director, Cooperative Research Programs*
David B. Beal, *Senior Program Officer*
Eileen P. Delaney, *Director of Publications*
Margaret B. Hagood, *Editor*

NCHRP PROJECT 12-70 PANEL
Field of Design—Area of Bridges

Harry A. Capers, Jr., *Arora and Associates, P.C., Lawrenceville, NJ* (Chair)
Darrin Beckett, *Kentucky Transportation Cabinet, Frankfort, KY*
Donald Dwyer, *New York State DOT, Albany, NY*
Ian M. Friedland, *Federal Highway Administration, McLean, VA*
Michael G. Katona, *Gig Harbor, WA*
Scott M. Olson, *University of Illinois–Urbana-Champaign, Urbana, IL*
M. "Saiid" Saiidi, *University of Nevada–Reno, Reno, NV*
Anoosh Shamsabadi, *California DOT, Irvine, CA*
Munindra Talukdar, *Washington State DOT, Tumwater, WA*
Jerry A. DiMaggio, *FHWA Liaison*
G. P. Jayaprakash, *TRB Liaison*

AUTHOR ACKNOWLEDGMENTS

Work for the NCHRP 12-70 Project was carried out by a Project Team led by CH2M HILL of Bellevue, Washington, with major support from Earth Mechanics, Inc. of Fountain Valley, California and Parsons Brinckerhoff Inc. of New York City, New York. Leadership for the Project Team was provided by the following individuals: Dr. Donald Anderson, P.E. from CH2M HILL in Bellevue, Washington, who was the project manager for the work; Professor Geoffrey R. Martin, P.E. from the University of Southern California, who served as a Principal Investigator; Mr. Ignatius (Po) Lam, P.E. from Earth Mechanics, who served as another Principal Investigator; and Dr. J.N. (Joe) Wang, P.E. from Parsons Brinckerhoff, who also served as a principal investigator.

The Project included a Technical Advisory Panel that provided technical input to the Project at various points during the project duration. The panel members included: Professor Robert Holtz, P.E. from the University of Washington; Dr. Lee Marsh, P.E. from Berger ABAM in Federal Way, Washington; Professor Edward Kavazanjian, P.E. from Arizona State University; and Professor Tom O'Rourke, P.E. from Cornell University

A number of other individuals provided important input to the project, including Mr. Tony Allen, P.E., Chief Geotechnical Engineer with the Washington State Department of Transportation, and Dr. Anoosh Shamsabadi, P.E, structural research engineer with the California Department of Transportation (Caltrans). The practical feedback from both individuals was particularly helpful. Mr. Amir Zand and Dr. Hubert Law from Earth Mechanics also provided major support by conducting analyses and assisting with the development of example problems.

FOREWORD

By David B. Beal
Staff Officer
Transportation Research Board

This report provides analytical and design methods for the seismic design of retaining walls, buried structures, slopes, and embankments. The report details the development of the design procedures. Recommended LRFD specifications and design examples illustrating the application of the design methods and specifications are included in an Appendix. The material in this report will be of immediate interest to roadway and bridge designers.

A comprehensive load and resistance factor design (LRFD) specification for the seismic design of highway bridges has been developed by AASHTO. Those specifications reflect the latest bridge design philosophies for achieving high levels of seismic performance. Because these specifications are limited to highway bridges and components that are directly attached to them, such as abutments and wing walls, they do not address new or improved analytical methods or seismic design provisions for retaining walls, buried structures, slopes, or embankments.

The objective of NCHRP Project 12-70 was to remove the limitations of the current specifications through the development of analytical and design methods for the seismic design of retaining walls, buried structures, slopes, and embankments. This research was managed by Donald Anderson, CH2M HILL, Bellevue, Washington, with the assistance of Geoffrey Martin, University of Southern California; Po Lam, Earth Mechanics; and Joe Wang, Parson Brinckerhoff, New York. The report fully documents the program used to develop the design procedures.

The Final Report is organized into two volumes. Volume 1 is published here as NCHRP Report 611. Volume 2 is available at the TRB website at http://trb.org/news/blurb_detail.asp?id=9631.

CONTENTS

VOLUME 1 Final Report

CHAPTER 1

Introduction

This Final Report summarizes work that was carried out on National Cooperative Highway Research Program (NCHRP) Project 12-70 *Seismic Analysis and Design of Retaining Walls, Buried Structures, Slopes, and Embankments.* This project involved an effort to develop analysis and design methods and recommended load and resistance factor design (LRFD) specifications for the seismic design of retaining walls, slopes and embankments, and buried structures.

1.1 Overall Project Objectives, Approach, and Schedule

The overall objectives of the Project were to develop analysis and design methods and to prepare LRFD specifications and example problems for the design of retaining walls, slopes and embankments, and buried structures. These overall objectives were intended to address short-comings in AASHTO *LRFD Bridge Design Specifications* or in some cases the absence of a recommended design methodology in the LRFD Specifications.

The approach used to address these two objectives was outlined in a Working Plan submitted by the Project Team to NCHRP in May of 2004. The Working Plan is based on CH2M HILL's proposal to NCHRP in November of 2003, with modifications summarized in Attachment 2 of CH2M HILL's letter dated January 13, 2004, to Dr. Robert Reilly of the Transportation Research Board. Also included in this Working Plan was a Progress Schedule tied to the Project start date of March 29, 2004, and a Table of Deliverables for this Project. A copy of the Working Plan for the Project is included in Appendix A to Volume 1 of this Final Report.

Five fundamental goals were identified during the planning of the Project in 2004. These goals formed the basis for the work that was to be done during each Project activity. The five goals involved

- Improving existing or developing new analytical methods to overcome the shortcomings of existing technology, based on sound soil-structure interaction principles;
- Optimizing design approaches for both routine design and special design cases using more comprehensive methods;
- Avoiding hidden conservatism in design approaches;
- Ensuring applicability of specifications to seismic zones nationwide, including provisions for "no seismic design" in low seismicity regions; and
- Satisfying LRFD philosophy and providing flexibility in establishing serviceability criteria.

The approach for the Project initially focused on data collection and review during Task 1, leading to the documentation of problems and knowledge gaps in Task 2. The problems and knowledge gaps identified in Task 2 were used to recommend analytical methodology developments in Task 3, and a detailed work plan in Task 4. The results of these four tasks were summarized in Task 5, the first Interim Report. This phase of the work occurred within the first 9 months of the planned 39-month project duration.

Following submittal of the first Interim Report and the NCHRP Oversight Panel's review and approval of the work plan described in the first Interim Report, the approved work plan was implemented in Task 6. An outline of the LRFD specifications was prepared in Task 7, and the results of the analytical developments and LRFD specification outline were summarized in Task 8, which was identified as the second Interim Report. The submittal of the second Interim Report concluded Phase 1 of the Project. The schedule for completing the second Interim Report was originally planned to be approximately 22 months after the initiation of the Project; however, actual work took approximately 24 months.

Phase 2 was initiated upon completion of Task 8. This phase involved Task Orders 9-12, where specifications, commentaries, and example problems were prepared and submitted to the NCHRP Oversight Panel for review. The third Interim Report provided the first draft of the specifications, commentaries, and example problems, in accordance with the requirements of Task 10. Following receipt of comments

from the NCHRP Oversight Panel, Task 11 was implemented. This task involved (1) making further modifications to the specifications, commentaries, and example problems; (2) addressing the Oversight Panel's comments on the third Interim Report, and (3) and preparing a Final Report. This work was scheduled to be completed after 35 months but took approximately 39 months.

The final work activity in Phase 2 on the Project, Task 12, involved preparation of this Final Report and the revised specifications, commentaries, and example problems. This task was finalized in November of 2007, approximately 44 months following initiation of the Working Plan in April of 2004. Following this submittal, an additional example problem was completed, specifications and commentaries were revised, and the Final Report finalized in June 2008.

Throughout work on each task within the Project there was a continuing effort to focus on the final product of the Project. This product involved a methodology that could be used in areas that are both highly seismic and relatively aseismic; that could be implemented by staff from DOTs, vendors, and consulting firms using existing software without the need for extensive training; and that "made sense" relative to observed performance during past earthquakes. This theme was implemented throughout the Project, from start to finish. To the extent practical, this theme is followed in the presentation of each chapter of this Draft Final Report.

1.2 Project Background

Work on the NCHRP 12-70 Project was initiated in April of 2004. The following three subsections provide background information for the work that has been accomplished. This background information includes a summary of plans for implementing the overall LRFD design methodology and overviews of interim conclusions from the work performed on the Project. The overview of conclusions helps provide a perspective for the development work that is being summarized in subsequent chapters.

1.2.1 Plans for Implementing the LRFD Design Methodology

The work carried out for the NCHRP 12-70 Project must be consistent with the philosophy and format of the AASHTO *LRFD Bridge Design Specifications* and the seismic provisions for highway bridges. In this philosophy, "Bridges shall be designed for specified limit states to achieve the objectives of constructibility, safety, and serviceability, with due regard to issues of inspectibility, economy, and aesthetics. . . ." In the LRFD procedure, margins of safety are incorporated through load (γ_p) factors and performance (or resistance, ϕ_r) factors.

1.2.1.1 Factors to Consider

The basic requirement for this Project is to ensure that factored capacity exceeds factored load as defined by the following equation for various limit states (or acceptable performance):

$$\phi_r R_n \geq \Sigma \gamma_{pi} Q_i \tag{1-1}$$

where

ϕ_r = performance factor;
R_n = nominal resistance;
γ_{pi} = load factor for load component *I;* and
Q_i = load effect due to load component *i.*

During the initial phase of work for this Project, the LRFD methodology was not formerly introduced. Rather, the focus of the work was on the identification and evaluation of a design methodology without load or resistance factors. Once the methodologies were developed and approved, then an approach for incorporating load and resistance factors was established relative to the recommended methodologies.

Although work on the initial phase of work did not present recommendations on load and resistance factors to use with the proposed methodologies, consideration was given by the Project Team to how load and resistance factors might eventually be used during seismic design. Ideally this approach would build on the load and resistance factors used in the conventional static load case presented in the current version of the AASHTO *LRFD Bridge Design Specifications.*

For the static design case the appropriate load and resistance factors have been developed to yield a consistent margin of safety in the designed structure. This same logic needs to be followed for seismic loading to retaining walls, slopes and embankments, and buried structures. However, the approach for defining a consistent margin of safety is more difficult to define for the following reasons:

- The load factors and load cases (that is, on the right-hand-side of the above equation) had to be consistent with those recommended by the NCHRP Project 20-07 *Recommended LRFD Guidelines for the Seismic Design of Highway Bridges* (Imbsen, 2006). At the time the NCHRP 12-70 Project was initiated, the NCHRP 20-07 Project was establishing the appropriate earthquake loading return period—subject to the approval of the AASHTO Highway Subcommittee on Bridges and Structures (HSCOBS T-3) and eventually the AASHTO voting members. These recommendations would result in larger loads associated with a seismic event at a specific site relative to the then current AASHTO requirements, but the likelihood of the load occurring decreased and would be relatively infrequent. Under this situation use of a load factor on the seismic load was believed to be overly conservative. (The NCHRP 20-07 Project was originally referred to as the NCHRP 12-49 Update Project.

The intent of the NCHRP 12-07 Project was to revise recommendations given in the NCHRP 12-49 Project (NCHRP Report 472, 2003) for use in updating seismic provisions in the AASHTO *LRFD Bridge Design Specifications.* One of the key recommendations initially made by the NCHRP 20-07 Project was to increase the return period for seismic design from the 500-year level in the then current (2006) LRFD specifications to a 1,000-year return period. The probability of occurrence for the 1,000-year event is approximately 7 percent in 75 years. This recommendation was approved by AASHTO in July of 2007, at the time that the NCHRP 12-70 Project report was being finalized.)

- From a resistance factor standpoint, design could be performed using either a limit equilibrium or displacement-based approach. The selection of resistance factors for these two cases will differ. For example, use of a resistance factor less than 1.0 often will result in a conservative design using limit equilibrium methods, but could lead to an unconservative design for a displacement-based approach.

While the starting point involved use of load and resistance factors equal to 1.0, in certain geographic areas and for certain categories of design, use of a resistance factor less than 1.0 (that is, $\phi < 1.0$) was considered for simplifying the design process. An example of this was for the evaluation of seismic stability of slopes. If a deformational approach is not taken and the owner wants to base the evaluation strictly on a comparison of soil capacity to seismic loads, the current approach would be to confirm that the factor of safety is greater than 1.1 to 1.2 for an acceleration coefficient of 0.5 times the peak ground acceleration (PGA) at the ground surface. (Many applications in geotechnical engineering are based on factors of safety—where the resistance of the soil is compared to the forces causing failure. When using LRFD methods for the same design, it is often more meaningful to refer to the capacity to demand (C/D) ratio rather than the factor of safety. The use of C/D ratio also is consistent with terminology used by bridge engineers. Discussions in this report will refer to C/D ratio and factor of safety interchangeably.) This same approach can be taken in the context of LRFD design, but in this case the resistance factor is defined by the reciprocal of the factor of safety used, assuming that the load factor is equal to 1.0 for the reasons stated above.

With this in mind the thrust of the work was to formulate the LRFD specifications in terms of the following three considerations:

1. Identifying the limit states to be considered during the earthquake load case.
2. Defining the expected performance of the designed system for each of the limit states defined in item (1) above.
3. Outlining the design analysis procedure and capacity criteria.

The various limit states to be examined were categorized into three areas. The first involved the evaluation of the global stability of the overall site, which includes requirements for slope stability and similar mechanisms. The next dealt with the design of the foundation system for external stability (that is, sliding, overturning, and bearing) to ensure that the size of the foundation and the implied geotechnical (that is, overall soil) capacity was sufficient. The last involved the design for internal structural stability to ensure that structural components functioned properly under the increased dynamic load from the earthquake. Depending on whether a design project involved a retaining wall, a slope or embankment, or a buried structure, an assessment of one or more of these limit states may not be required. For example, the limit state for seismic design of slopes and embankments only involves global stability, while the buried structure only considers internal stability.

1.2.1.2 Relationship to Design Process

From past earthquake experience, most cases of observed or postulated failures relate to intolerable structural damage, as opposed to excessive overall movement, especially for retaining walls and buried structures. These structures are inherently more sensitive to movement relative to aboveground structures. Also, most freestanding retaining walls (that is, other than bridge abutments) can undergo a significant degree of movement without adversely impacting their intended functions.

Therefore, the most germane LRFD design issue was to assure structural integrity, commonly referred to as designing for the internal stability of the earth retaining system. When designing for structural integrity, the geotechnical engineer will define the seismic loading criteria and conducts soil-structure interaction analyses, as needed, for characterizing foundation stiffness and damping parameters. The responsibility of actual design usually falls to the structural designer. The structural engineer typically will bear the responsibility for conducting the structural response analyses and will make use of the recommendations regarding seismic loading and foundation stiffness in a global model. The structural designer would be the one who actually goes through the LRFD design process in checking the structural capacity versus demand, and eventually will sign the structural drawings. Requirements in other sections of the AASHTO *LRFD Bridge Design Specifications* are followed when conducting structural analyses and design checks.

Note that this general approach is not always the case. For some wall types, such as the Mechanically Stabilize Earth (MSE) or soil nail walls, the geotechnical engineer also may be responsible for the internal stability as well. In this case the geotechnical engineer would select reinforcing or soil nail size, and confirm that the stresses imposed by seismic loading are acceptable relative to LRFD requirements.

Understanding the role of the geotechnical and structural engineers is rather important, and this Project needed to clarify these roles in the process of preparing the LRFD specifications. These roles also need to be understood in the definition of load and resistance factors to use during design. Since independent groups often are responsible for the design elements, each group needs to have a basic understanding of what is being conveyed by the load or resistance factor that is being used for seismic design.

1.2.1.3 Example of LRFD Reserve Capacity Concept

In formulating the LRFD guidelines, consideration needs to be given to a prevalent consensus among practitioners, especially in state highway departments, that retaining walls, slopes and embankments, and buried structures generally have performed very well during seismic events—even though many constructed structures have not been designed for the earthquake load case. The main reason for this relates to the fact that the capacity of most retaining walls, slopes and embankments, and buried structures provides sufficient reserve to resist some level of earthquake loading when they are designed for static loading. This observation needed to be kept in mind when formulating the LRFD specifications in order that the proposed approach was determined to be reasonable to engineers using the methodology.

As an illustration of this point, Dr. Lee Marsh, who served on the Technical Advisory Panel for the NCHRP 12-70 Project, quantified the level of reserve structural capacity for a hypothetical wall, to put the design process in perspective. In the course of a design, retaining walls are designed for global and external stability (that is, the process of checking for sufficient soil capacity for the global system), as well as for internal stress in the structural components. Dr. Marsh conducted a set of analyses to determine the reserve structural capacity for a standard wall that had been designed for a static load condition. For simplicity, Dr. Marsh conducted the analyses for a nongravity cantilever sheet pile wall to focus on structural integrity issues, rather than involving additional complexity associated with other nonstructural failure modes such as sliding failure through the soil at the base of a semi-gravity wall. Such mechanisms introduce an additional load fuse which might further reduce the earthquake design load to a lower value than the case associated with sheet pile walls. Results of these analyses are included in Appendix B.

The sensitivity study conducted by Dr. Marsh indicates the following:

1. Most existing retaining walls, even when they only are designed for static loading, have sufficient reserve structural capacity to withstand an appreciable level of earthquake load.
2. If a retaining wall has been designed to satisfy typical requirements for static loading, the inherent capacity will withstand about 0.12g pseudo-static loading, based on a very conservative capacity associated with first yield, with the most conservative assumption on wave scattering (that is, 1.0 as discussed in Chapter 6), and the most conservative nonyielding structural performance criteria.
3. Under a less conservative interpretation, more suitable for correlating to historical structural damage from past earthquakes, the inherent capacity is likely to be much higher, to a PGA at the ground surface as high as 0.68g. This case corresponds to a scattering factor (see Chapter 6) equal to 0.5, and nominal yielding is allowed.
4. Even for a nonyielding limit state, a scattering factor equal to 0.5 can be justified for most design situations, especially for much of the central and eastern United States (CEUS), where the characteristic ground shaking has lower, long-period ground motion content. In this situation the retaining wall can withstand a site-adjusted PGA of 0.24g.

For the 1,000-year return period ground motion criterion that was adopted by AASHTO in July of 2007, most regions in the CEUS, other than the New Madrid and the Charleston regions, will be required to design for a PGA at the ground surface of about 0.1g or lower. For much of the Western United States (WUS), outside of California, Alaska, and the Pacific Northwest, design would be for a PGA at the ground surface of about 0.2g. Based on the above cited reserve structural capacity study, along with results from dynamic analyses of retaining walls, many of the regions in the CEUS and WUS can use simplifying screening criteria to eliminate the need for overly complicated seismic analyses.

1.2.2 Overview of Conclusions from Initial Phase of Work

The initial phase of work involved Tasks 1 through 5 of the Working Plan. A number of conclusions were reached in this early work, and these conclusions formed the framework for the work plan that was implemented in Task 6 and reported in the 1st Interim Report. Highlights from Tasks 1 through 4 are summarized here:

- **Task 1: Data Collection and Review.** The conclusions from this task were that the methodologies available to design professionals within departments of transportation (DOTs) and consultants for the DOTs are primarily limited either to pseudo-static methods, such as the Mononobe-Okabe (M-O) method for the design of retaining structures and the limit equilibrium method of slope stability analysis, or to simplified deformation methods (for example, Newmark charts or analyses). Although these methods have limitations, as discussed in later chapters of this Draft Final Report, improvements in these methodologies still offer

the most practical approaches to seismic design. A growing trend towards the use of more rigorous modeling methods, such as the computer code FLAC (Itasca, 2007), for the evaluation of retaining structures, slopes and embankments, and buried structures has occurred recently. While FLAC and similar software appear to provide a more rigorous modeling of various soil and soil-structure problems, these more numerically intensive procedures do not appear to be suitable for development of day-to-day design methodologies required by this Project.

- **Task 2: Problems and Knowledge Gaps.** On the basis of the work carried out for this task, primary development needs were identified. These needs included common needs that applied to all three of the Project areas (retaining walls, slopes and embankments, and buried structures) and area-specific developments, as summarized here:
  - Common Needs
    - Better definition of the ground motions that should be used during design, including appropriate adjustments for ground motion incoherency, strain amplitude, and ground motion amplification/deamplification.
    - Development of screening procedures that advise the designer when sufficient margin exists within the static design to preclude the need for seismic analyses.
    - Guidance on the selection of soil strength properties that should be used during seismic design.
  - Retaining Walls
    - Numerical procedure that avoided deficiencies in the M-O procedure at high acceleration levels and high back slope angles and that handled mixed soil (c-ϕ) conditions. The recommendation was to use either wedge-based equations or a limit-equilibrium stability program to determine the forces needed for seismic design.
    - Charts for estimating wall displacement for representative areas of the United States (for example, CEUS versus WUS).
    - Guidance on the selection of the seismic coefficient for limit-equilibrium and displacement-based design and the variation of this coefficient with wall height.
  - Slopes and Embankments
    - Procedures for determining the appropriate seismic coefficient and its variation with slope height.
    - Charts for estimating displacement for representative areas of the United States (for example, CEUS versus WUS). (These charts are the same as those used for estimating the displacement of conventional rigid gravity walls.)
    - Procedures for introducing the effects of liquefaction.
    - Procedures for treating rock slopes.
  - Buried Structures
    - Simple-to-use design methods for medium-to-large-size culverts and pipes under the effect of transverse seismic racking deformations, taking into account soil-structure interaction effects.
    - Guidance on how to select transient ground deformation (or strain) parameters for design and analysis purposes.
    - Development of a consistent and rational procedure for buried structures subject to various forms of permanent ground displacement (PGD), including lateral spreading, embankment slope movements or flow, and faulting.
- **Task 3: Work Plan—Analytical Methodologies.** Information from Tasks 1 and 2 was used to identify types of analytical methodology developments required. These developments resulted in work product elements shown in Table 1-1. This summary is a modified version of Exhibit 6 of the Working Plan for the NCHRP 12-70 Project.
- **Task 4: Work Plan—Performance Strategy.** A strategy for accomplishing the Development of Analytical Methodologies was provided in Task 4. As noted in the NCHRP research project statement, Task 4 also included the identification of example applications and parametric studies that were to be performed, including the comparison with existing methods. The performance strategy that was identified served as a basis for the work that was conducted in Task 6, as reported in the second Interim Report.

1.2.3 Overview of Conclusions from Second Phase of Work

The second phase of the work covered Tasks 6 through 8 of the Working Plan. This work was documented in the 2nd Interim Report.

Work on Task 6 involved developments in the four areas summarized below. The discussions in the following chapters provide details in each of these four areas of development.

- **Ground Motion Parameters.** Procedures for selecting ground motion parameters for use in seismic design were evaluated, and recommendations for the selection of ground motions to use in the seismic response studies were developed. Ground motion conditions characteristic of both WUS and CEUS were considered during this development.
- **Retaining Walls.** An approach for evaluating the behavior of retaining walls during seismic events was identified, and evaluations of this approach were carried out. This approach considered the global stability of walls, as well as the forces to be used in structural design. Various types of retaining walls were considered during this evaluation, including semi-gravity, nongravity cantilever (for example, sheet pile and soldier pile), MSE, anchored, and soil nail walls.

Table 1-1. Proposal for work product elements.

Type of Investigation	Purpose	Methods or Concepts
Evaluate Suitability of Limit Equilibrium Computer Program based on Method of Slices for Determination of Lateral Earth Pressures	Offer to end users the means for improved methodology for establishing design seismic earth pressure magnitudes for mixed soil conditions, steep backslopes, and high ground motions.	Examples showing evaluation of seismic earth pressures based on readily available limit equilibrium computer programs for representative wall types (gravity, nongravity, anchored, MSE, nail), including comparisons to existing chart solutions.
Analyses of MSE Walls	Develop revised design methodology for MSE walls	A single integrated design method based on limit equilibrium computer programs is envisaged
Analyses to Develop Design Charts for Estimating Height-Dependent Seismic Coefficient	Provide a rational basis for selecting seismic coefficient as a function of both wall height and slope height for different soil conditions	Separate charts or equations for WUS and CEUS earthquakes
Analyses to Update Design Charts for Estimating Slope and Wall Movement Displacements	This design chart will provide end users the means of estimating slope and wall movements as a function of yield acceleration, PGA, and PGV.	Methodology that accounts for differences in WUS and CEUS earthquakes
Analyses to Develop Design Approaches for Permanent and Transient Ground Deformation for Culverts and Pipelines	Provide design guidance and specifications	Design approaches for rigid culverts/pipelines and one for flexible culverts/pipelines

- **Slopes and Embankments.** Methods for evaluating the seismic stability of natural slopes and constructed embankments were identified and reviewed. A deformation-based approach for evaluating the seismic performance of slopes and embankments was developed based on the ground motion parameters established for the Project.
- **Buried Structures.** Procedures for evaluating the response of buried pipelines and culverts during seismic loading also were identified and evaluated. These procedures were extended from an approach used to evaluate the seismic performance of large-diameter, vehicular tunnels. Both the transient and permanent movements of the ground were considered in these evaluations. The types of buried pipelines ranged from flexible materials to rigid pipelines. Vehicle tunnels are not considered.

Results of the work on Task 6 constituted the majority of work completed in this phase. However, the work also included an outline for the LRFD specifications, designated as Task 7 within the Working Plan. The objective of Task 7 was to outline a methodology for implementing the recommended approach to seismic design in a format similar to that used within the current LRFD specifications. This outline built on the then current (2005 and 2006) AASHTO *LRFD Bridge Design Specifications* where possible. However, some of the topics addressed during this Project were not covered within the existing LRFD specifications. For these cases suggestions were made on how the information might be incorporated within the context of the existing LRFD specifications.

Task 8, which involved preparation of the second Interim Report, completed the second phase of the work. The second Interim Report was submitted to NCHRP for review by the NCHRP Oversight Panel. Comments and suggestions from the NCHRP Oversight Panel were subsequently discussed during a meeting between the Oversight Panel and the Project Team in May of 2006.

The levels of effort for the four areas of development were not equal. More priority was placed on topics where the risk was considered highest during seismic events, as summarized below:

- **Retaining Walls.** This topic was assigned the highest priority, as problems associated with the design of retaining walls, and in particular the use of the Mononobe-Okabe equations, is a continued source of uncertainty for designers. Part of the reason for assigning this topic the highest priority is the potential consequences of retaining wall failures during a seismic event. Retaining wall damage and occasionally failures after earthquakes have been observed, and the repair of these walls can be time consuming and costly. Finally, the category of retaining walls involves a number of different cases, ranging from gravity to anchored walls. The seismic response of these cases differs in the way that seismic demands develop within the wall, as well as the manner that these demands are resisted.

- **Slopes and Embankments.** This topic was assigned a lower priority for several reasons. First, many times the seismic design of slopes and embankments is ignored, as the cost of mitigating potential problems is often far more than the cost of repairing damage after an earthquake. A second reason is the factor of safety (FS) used for the static design of slopes (for example, FS = 1.3 to 1.5 for permanent slopes) is often observed to be sufficient to cover stability during small to medium seismic events (where liquefaction is not an issue). Finally, failure of a slope often involves minimal risk to the highway users and the failed slope can usually be quickly repaired.
- **Buried Structures.** This topic is given a lower priority primarily because the consequences of failure are often limited. Nevertheless, the current AASHTO *LRFD Bridge Design Specifications* is deficient in that no guidelines are provided, even for those designers who might want to consider seismic loading.

One of the other important considerations during the second phase of work was developments that were occurring in the area of ground motions. At the time of the work, current AASHTO *LRFD Bridge Design Specifications* (2006) provided guidance on the determination of ground motions required for design; however, the guidance was being modified as part of a separate NCHRP project to update the current LRFD seismic provisions. This work was being performed within NCHRP 20-07 Project being conducted by Imbsen & Associates (Imbsen, 2006). Part of the recommended update involved changing from the then current 500-year earthquake (that is, 10 percent probability of occurrence in 50 years) to a 1,000 year design basis (approximately 7 percent in 75 years). (Various probabilities of occurrence are associated with the nominal 1,000-year return period. For a 75-year exposure period, the exceedance probability is approximately 7 percent. This exceedance probability is also approximately 5 percent for a 50-year exposure period.) Included within the proposed update was a focus on using the spectral acceleration at 1 second (S_1) as a basic proxy for ground motion. Realizing the plans within the NCHRP 20-07 Project, as well as a fundamental need for velocity information for some of the methodologies being proposed as part of the NCHRP 12-70 Project, a significant focus was given to the development of a set of rational ground motion parameters to use during the seismic design and analysis of retaining walls, slopes and embankments, and buried structures.

1.2.4 Overview of Conclusions from Third Phase of Work

The third phase of work involved Tasks 9 and 10: the development of specifications, commentaries, and example problems. Results of this work were summarized in the third Interim Report.

Specifications and commentaries were presented in three sections:

- **Section X: Retaining Walls.** This section provided proposed specifications and commentaries for six types of retaining walls: (1) rigid gravity and semi-gravity (conventional) walls, (2) nongravity cantilever walls, (3) anchored walls, (4) mechanically stabilized earth (MSE) walls, (5) prefabricated modular walls, and (6) soil nail walls. With the exception of soil nail walls, design methods for gravity loads for each of these wall types were covered within the current AASHTO *LRFD Bridge Design Specifications.*
- **Section Y: Slopes and Embankments.** This section provided proposed specifications and commentaries for the seismic design of slopes and embankments. The specifications covered natural slopes and engineered fills. A methodology for addressing sites with liquefaction potential was included in the specifications. Current AASHTO *LRFD Bridge Design Specifications* do not provide specific guidance on the methods used to evaluate the stability of slopes under gravity and live loads. In this case the specifications and commentaries used the standard of geotechnical practice as the starting point for design.
- **Section Z: Buried Structures.** This section covered the seismic design of culverts and drainage pipes. The discussion focused on the design for transient ground displacements (TGD) and included mention of the requirements for design for PGD. Generally, the ability of the culvert or drainage pipe to withstand PGD depends on the amount of permanent ground movement that occurs during the seismic event. Procedures given in Section Y provide a means for estimating these displacements. Culverts and drainage pipes will generally move with the ground; therefore, movement of more than a few inches to a foot will often damage the pipe or culvert.

Also included within the third Interim Report were (1) an appendix presenting charts for estimating seismic active and passive earth pressure coefficients that included the contributions from cohesion and (2) an appendix summarizing the design of nongravity cantilever walls using a beam-column displacement method.

Contents of the third Interim Report were reviewed with the NCHRP 12-70 Oversight Panel. The focus of the panel discussions was on the organization of the specifications and the example problems that needed to be completed to support the development of the specifications. This feedback was used to modify the specifications and commentaries and to update the example problems. A fourth Interim Report was prepared to document this information. The NCHRP Oversight Panel

provided comments on the fourth Interim Report, and these comments have been addressed where possible in this Final Report.

1.3 Organization of Final Report

This Final Report is organized into two volumes. The first volume, titled Final Report, is a compilation of information presented previously in the first, second, third, and fourth Interim Reports; it is published as NCHRP Report 611. The second volume, titled Recommended Specifications, Commentaries, and Example Problems, presents the proposed specifications, commentaries, and example problems for the retaining walls, slopes and embankments, and buried structures.

1.3.1 Volume 1—Final Project Report

This volume has 10 chapters following Chapter 1 Introduction. These chapters were taken from interim reports prepared as the Project was completed. The Draft Final Report serves as documentation for the work as it was being performed during the Project and provides the basis for information presented in the recommended specifications, commentaries, and example problems.

- Chapter 2—Data Collection and Review summarizes results from the literature review for the three principal areas of development (that is, retaining walls, slopes and embankments, and buried structures). This summary includes conclusions reached from discussions with individuals representing selected DOTs, vendors, and consultants regarding the availability of seismic design guidelines for each of the three principal areas of development.
- Chapter 3—Problems and Knowledge Gaps involves a discussion of knowledge gaps and problems associated with current design methodologies for each of the three areas. These knowledge gaps and problems were identified on the basis of the literature review and discussions with representatives from DOTs, vendors, and other consultants summarized in Chapter 2, as well as the Project Team's experience on related retaining wall, slope and embankment, and buried structure projects in seismically active areas.
- Chapter 4—Work Plan: Analytical Methodologies describes the work plan for developing analytical methodologies that was recommended for addressing the knowledge gaps and problems outlined in Chapter 3. The proposed analytical methodologies included development of methods for quantifying the determination of seismic demand, as well as the methods used to determine the capacity during seismic loading for each area of development.
- Chapter 5—Seismic Ground Motions summarizes results from the ground motion studies. These results include a review of the seismic loading criteria developed for the Project. This discussion also covers information on the ground motion revisions being proposed at the time (and since adopted) to the current AASHTO *LRFD Bridge Design Specifications,* the range of ground shaking levels that new seismic maps show, and the variation in response spectra between WUS and CEUS. The review of seismic loading criteria is followed by summaries of (1) the Newmark displacement correlations that were developed and (2) the correlation between peak ground velocity (PGV) and spectral acceleration at one second (S_1). Information in this chapter serves as basic input data for the following studies.
- Chapter 6—Height-Dependent Seismic Coefficient involves a summary of the results of the height-dependent seismic coefficient that was developed for use in the analysis of retaining walls, as well as slopes and embankments. This summary covers effects of ground motion incoherency, referred to as wave scattering analyses, for slopes and for retaining walls, and it provides guidance on the intended application of the scattering solutions.
- Chapter 7—Retaining Walls describes the current design process, including the use of the Mononobe-Okabe equations and the limitations of this approach. This discussion is followed by a summary of the potential effects of cohesive soil content on seismic earth pressures estimated by the Mononobe-Okabe method and a generalized limit-equilibrium approach for determining seismic active earth pressures. The next discussions cover results of a study of impedance contrasts and nonlinear effects on seismic design coefficients and the use of a displacement-based design approach for gravity, semi-gravity, and MSE walls. The chapter concludes with specific comments on the design of gravity and MSE walls and some general guidance on the design of nongravity cantilever, anchored, and soil nail walls.
- Chapter 8—Slopes and Embankments reviews the current approach used for the seismic design of slopes and embankments. This review is followed by a recommended displacement-based approach for evaluating seismic stability. The recommended approach provided a basis for developing screening methods where no analysis is required or where a factor of safety approach is preferred.
- Chapter 9—Buried Structures covers the recommended approach for the TGD design of buried pipes and culverts. The discussions in this chapter review the general effects of earthquake loading and the potential failure modes. A brief summary of the seismic design practice is given, and then the proposed methodology is defined. This methodology covers ovaling of circular conduits, racking of rectangular conduits, and then results of a series of parametric and verification studies.
- Chapter 10—Recommendations for Future Work summarizes a number of topics not resolved during the Project

and are believed to warrant further study. These topics range from identification of methods for quantifying the amount of cohesion that can be counted on during design to methods for describing the liquefaction strength of soils located beneath embankments.
- Chapter 11—References lists the references used during the Project.

This report also includes a number of appendices with supporting documentation for the work presented in Chapters 2 through 9.

1.3.2 Volume 2—Recommended Specifications, Commentaries, and Example Problems

This volume includes recommended specifications, commentaries, and example problems as summarized below. The background for some, but not all, of the methods described in Volume 2 is included in Volume 1. Some methods outlined in the specifications and commentaries and used in the example problems were developed as the specifications, commentaries, and example problems were being completed. This work occurred after the completion of work described in Volume 1.

- Specifications and Commentaries summarize the recommended specifications and commentaries after revisions to address (1) the NCHRP Oversight Panel's comments on drafts of the specifications and commentaries and (2) modifications made by the Project Team after completing example problems. Some topics such as slope stability did not currently have an independent section or subsection within the AASHTO *LRFD Bridge Design Specifications*, but rather were scattered within the various sections. The approach for including the work developed during the NCHRP 12-70 Project became, therefore, more of a challenge.
- Example Problems show the steps necessary to complete a seismic design following the methods proposed for this Project.

CHAPTER 2

Data Collection and Review

The goal of Task 1 of the NCHRP 12-70 Project was to collect, review, and interpret relevant practice, performance data, research findings, and other information needed to establish a starting point for subsequent phases of the Project. The work performed within this task included review of the current status the NCHRP 20-07 Project; literature searches; and contacts with individuals involved in the seismic design of retaining walls, slopes and embankments, and buried structures. Realizing that the final product for the Project needed to be a set of specifications that can be implemented by practicing engineers, the focus of this task was on the identification of approaches or ideas that could be implemented on a day-to-day basis by practicing engineers, rather than highly rigorous or numerically intensive methods that would be more suited for special studies. The results of this data collection and review task are summarized in four sections consisting of discussion of the earthquake design basis, key observations from the literature review, results of contacts with various individuals engaged in design, and a summary of conclusions reached from this phase of the Project. Although this task was largely complete early in the Project, limited data collection and review continued throughout the duration of the Project.

2.1 Earthquake Design Basis

One of the key requirements for this Project was the determination of an earthquake design basis. The earthquake design basis was important because it defined the level of ground motion that will occur at a site. The level of ground motion creates the "demand" side of the basic LRFD equation. As the earthquake design basis increases, the demand (or load) increases; and the capacity of the foundation needs to be proportionately larger to limit displacements and forces to acceptable levels. The earthquake design basis also established the performance expectations—for example, the amount of displacement that was acceptable. These performance expectations will vary depending on the function of the retaining wall, slope and embankment, or buried structure.

With the exception of California, the standard approach within AASHTO at the time of the NCHRP 12-70 Project involved use of a 500-year design earthquake (that is, approximately 10 percent chance of exceedance in a 50-year period). Individual states could adopt more stringent requirements for critical bridges. For example, the design basis used by the Washington Department of Transportation (WSDOT) for the new Tacoma Narrows Bridge was 2,500 years (that is, approximately 2 percent probability of exceedance in 50 years), as this bridge was considered a critical structure. Under the standard design approach, the structure (normally a bridge and its related abutment and wing walls) was designed to withstand the forces from the design earthquake without collapse, albeit damage could require demolition following the design event.

The NCHRP 12-49 Project (NCHRP Report 472, 2003) attempted to increase the minimum design basis within AASHTO *LRFD Bridge Design Specifications* to a 2,500-year return period for the collapse-level event. The 2,500-year return period event has approximately a 2 percent probability of exceedance in 50 years. However, the recommended increase was not adopted for several reasons, including the potential cost of designing for the longer return period and a concern about the complexity of the recommended design process. A follow-up effort was undertaken by Dr. Roy Imbsen of Imbsen & Associates to modify the previous NCHRP 12-49 work, referred to as the NCHRP 20-07 Project (Imbsen, 2006). As part of this effort, the design return period was reconsidered. A consensus was reached by Dr. Imbsen and the AASHTO Highway Subcommittee on Bridges and Structures on the earthquake design basis for both new and retrofitted structures. This consensus involved a single level design with a return period of 1,000 years.

The decision on the design return period established a basis for determining the approach to seismic design for the NCHRP

12-70 Project. Specifically, ground motions associated with the 1,000-year return period could be used to identify the following:

- Geographic areas that will *not* require special seismic design studies. For these areas there will be enough margin in the static design of retaining walls, slopes and embankments, and buried structures to accommodate seismic loading, unless special conditions (such as liquefaction) occur.
- The type of analyses that will be required in more seismically active areas. For example, the decrease from the 2,500-year return period proposed in the NCHRP 12-49 Project to the 1,000-year return period resulted in smaller increases in ground motions. This meant that nonlinear behavior of soil was not as significant in any proposed design methodology as it would have been for the original NCHRP 12-49 Project recommendations.

Another important recommendation made as part of the NCHRP 20-07 Project was to follow an NCHRP 12-49 recommendation to use the spectral acceleration from a response spectrum at 1 second (S_1), rather than the PGA, as the parameter for defining the seismic performance category. The spectral acceleration at 1 second was used for determining both the level of and the requirement for design analyses. Part of the motivation for this change was the observation that damage during earthquakes was better correlated to S_1 than to PGA. By adopting S_1 as the parameter for determining the level of and the requirements for design, the region where the threshold of seismic demand would be sufficiently low to avoid the need for specialized seismic demand analyses increased. There have been significant developments in the seismological community in the past 10 years which concluded that the seismological environment in CEUS differs from WUS in regards to the long-period content of earthquake ground shaking. For the same PGA, ground motion records from CEUS have much lower shaking intensity at longer periods of ground motion. The choice of using spectral acceleration at 1 second held the potential for minimizing the need for dynamic response analyses for many transportation structures.

In order to simplify integration of the results of the NCHRP 12-70 Project with future editions of the AASHTO *LRFD Bridge Design Specifications,* developments resulting from the NCHRP 20-07 Project served as the basis when formulating analysis requirements for retaining walls, slopes and embankments, and buried structures. The relevant analysis requirements included typical levels of ground shaking and spectral shapes for WUS and CEUS, which then defined the demand requirements for completing the design of retaining walls, slopes and embankments, and buried structures.

While the preliminary decision on return period addressed one critical design need for the NCHRP 12-70 Project, the following additional changes regarding the earthquake design basis also needed to be considered by the NCHRP 12-70 Project or at least be coordinated with future work being done to implement the NCHRP 20-07 Project recommendations:

- The shape of the spectrum to be used for design. Significant differences in spectral shapes occur between CEUS and WUS. These differences in spectral shape affect soil response in terms of either peak spectral acceleration or time histories from which design computations or response analyses are conducted. The previous AASHTO *LRFD Bridge Design Specifications* made no distinction between spectral shapes within the CEUS and WUS. The updated maps use the USGS Seismic Hazard Maps for a 1,000-year return period, thereby accounting for differences in spectral shape of characteristic earthquakes in CEUS versus WUS.
- The method of introducing site effects on the rock motions developed for the 1,000-year earthquake return periods. The former site categories in the AASHTO *LRFD Bridge Design Specifications* were too qualitative in description to allow consistent use. The new site factors followed recommendations given in the Federal Emergency Management Agency's (FEMA) National Earthquake Hazards Reduction Program (NEHRP) reports and the International Building Code (IBC) documents, similar to what was recommended by the NCHRP 12-49 Project and consistent with South Carolina Department of Transportation (SCDOT) guidelines prepared by Imbsen & Associates.
- Performance expectation for the retaining walls, embankments and slopes, and buried structures under the 1,000-year event. For this event the amount of acceptable deformation depended on factors such as the potential consequences of the deformation (that is, to the retaining wall, roadway embankment or cut slope, or culvert), the potential need for and cost of repair, and the additional design requirements associated with the performance evaluation. A single set of design guidelines that captured all of these factors was not easily developed.

2.2 Literature Search

Literature reviews were conducted for the three primary technical areas of the Project: retaining walls, slopes and embankments, and buried structures. The goal of the literature review was to do the following:

- Identify the state-of-the practice in each of the areas of consideration,
- Understand the basis for the methods being applied, including their assumptions and limitations,
- Investigate alternative approaches that might be adopted during the development of analytical methodologies,
- Establish some of the desirable features of analytical methods that should be considered for development, and

- Develop a list of potential example problems that could be used during validation studies and preparation of design examples.

2.2.1 Key References

The literature review consisted of collecting and evaluating information already available to the Project Team, as well as electronic literature searches. One of the most effective search mechanisms was through use of Quakeline®, the search mechanism identified in the Multidisciplinary Center for Earthquake Engineering Research (MCEER) Center's website (http://mceer.buffalo.edu/utilities/quakeline.asp).

More than 140 abstracts have been downloaded and reviewed in the area of retaining walls dating from the past 10 years, more than 130 for seismic response of slopes and embankments, and more than 50 references for seismic response of pipelines and culverts. Copies of papers and reports were obtained for those references that appeared to contain unique information or results that are particularly relevant to the Project objectives. As noted in the introductory paragraph to this chapter, this phase of the Project focused on references that could be used directly or indirectly to develop methodologies that could be implemented by practicing engineers.

Some of the representative relevant articles and reports identified are summarized below.

- **Retaining Walls**
  - "Analysis and Design of Retaining Structures Against Earthquakes." Geotechnical Special Publication No. 80, ASCE, November, 1996.
  - Ausilio, E., E. Conte, and G. Dente. "Seismic Stability Analysis of Reinforced Slopes." *Soil Dynamics and Earthquake Engineering,* Vol. 19, No. 3, pp. 159–172, April 2000.
  - Bathurst, R. J., M. C. Alfaro, and K. Hatami. "Pseudo-Static Seismic Design of Geosynthetic Reinforced Soil Retaining Structures." Asia Conference on Earthquake Engineering, Manila, Philippines, Vol. 2, pp. 149–160, March 2004.
  - Bathurst, R. J. and Z. Cai. "Pseudo-Static Seismic Analysis of Geosynthetic-Reinforced Segmental Retaining Walls." *Geosynthetics International,* Vol. 2, No. 5, pp. 787–830, 1995.
  - Bathurst, R. J. and K. Hatami. "Seismic Response Analysis of a Geosynthetic Reinforced Soil Retaining Wall." *Geosynthetics International,* Vol. 5, Nos. 1&2, pp. 127–166, 1998.
  - Bathurst, R. J., K. Harami, and M. C. Alfaro. "Geosynthetic Reinforced Soil Walls and Slopes: Seismic Aspects." (S. K. Shukla Ed.): *Geosynthetics and Their Applications,* (2002) Thomas Telford Ltd., London, UK, pp. 327–392, November 2004.
  - Caltabiano, S., E. Cascone, and M. Maugeri. "Sliding Response of Rigid Retaining Walls." In *Earthquake Geotechnical Engineering: Proceedings of the Second International Conference on Earthquake Geotechnical Engineering;* Lisbon, Portugal, 21–25 June 1999, Rotterdam: A. A. Balkema, 1999.
  - Cardosa, A. S., M. Matos Fernandes, and J. A. Mateus de Brito. "Application of Structural Eurocodes to Gravity Retaining Wall Seismic Design Conditioned by Base Sliding." In *Earthquake Geotechnical Engineering: Proceedings of the Second International Conference on Earthquake Geotechnical Engineering;* Lisbon, Portugal, 21–25 June 1999, Rotterdam: A. A. Balkema, 1999.
  - Cascone, E. and M. Maugeri. "On the Seismic Behavior of Cantilever Retaining Walls." In Proceedings of the 10th European Conference on Earthquake Engineering; Vienna, Austria, 28 August-2 September 1994, Rotterdam: A. A. Balkema, 1995.
  - Choukeir, M., I. Juran, and S. Hanna. "Seismic Design of Reinforced-Earth and Soil Nailed Structures." *Ground Improvement,* Vol. 1, pp. 223–238, 1997.
  - Chugh, A. K. "A Unified Procedure for Earth Pressure Calculations." In Proceedings of the 3rd International Conference on Recent Advances in Geotechnical Earthquake Engineering and Soil Dynamics, St. Louis, 1995.
  - FHWA. "Manual for Design & Construction Monitoring of Soil Nail Walls." U.S. Department of Transportation, Federal Highway Administration, Publication No. FHWA-SA-96-069R, Revised October, 1998.
  - FHWA. "Mechanically Stabilized Earth Walls and Reinforced Soil Slopes Design & Construction Guidelines." U.S. Department of Transportation Federal Highway Administration, National Highway Institute, Office of Bridge Technology, Publication No. FHWA-NHI-00-043, March 2001.
  - Green, R. A., C. G. Olgun, R. M. Ebeling, and W. I. Cameron. "Seismically Induced Lateral Earthquake Pressures on a Cantilever Retaining Wall." In *Advancing Mitigation Technologies and Disaster Response for Lifeline Systems: Proceedings of the Sixth U.S. Conference and Workshop on Lifeline Earthquake Engineering* (TCLEE 2003), ASCE, Reston, VA, 2003.
  - Lazarte, C. A., V. Elias, D. Espinoza, and P. Sabatini. "Soil Nail Walls." *Geotechnical Engineering,* Circular No. 7, March 2003.
  - Ling, H. I. "Recent Applications of Sliding Block Theory to Geotechnical Design." *Soil Dynamics and Earthquake Engineering,* Vol. 21, No. 3, pp. 189–197, April 2001.
  - Ling, H. I., D. Leschinsky, and N. S. C. Nelson. "Post-Earthquake Investigation on Several Geosynthetic-Reinforced Soil Retaining Walls and Slopes during the

Ji-Ji Earthquake of Taiwan." *Soil Dynamics and Earthquake Engineering,* Vol. 21, pp. 297–313, 2001.
– Ling, H. I., D. Leschinsky, and E. B. Perry. "Seismic Design and Performance of Geosynthetic-Reinforced Soil Structures." *Geotechnique,* Vol. 47, No. 5, pp. 933–952, 1997, Earthquake Engineering and Soil Dynamics, St. Louis, 1997.
– Michalowski, R. L. and L. You. "Displacements of Reinforced Slopes Subjected to Seismic Loads." *Journal of Geotechnical and Geoenvironmental Engineering,* ASCE, Vol. 126, No. 8, pp. 685–694, August 2000.
– Nova-Roessig, L. and N. Sitar. "Centrifuge Studies of the Seismic Response of Reinforced Soil Slopes." Proceedings of the 3rd Geotechnical Earthquake Engineering and Soil Dynamics Conference, Special Publication No. 75, ASCE, Vol. 1, pp. 458–468, 1998.
– Peng, J. "Seismic Sliding and Tilting of Retaining Walls in Kobe Earthquake." M.S. Thesis, State University of New York at Buffalo, August 1998.
– Prakash, S. and Y. M. Wei. "On Seismic Displacement of Rigid Retaining Walls." Proceedings of the 3rd International Conference on Recent Advances in Geotechnical Earthquake Engineering and Soil Dynamics, St. Louis, 1995.
– Sakaguchi, M. "A Study of the Seismic Behavior of Geosynthetic Walls in Japan." *Geosynthetic International,* Vol. 3, No. 1, pp. 13–30, 1996.
– Sarma, S. K. "Seismic Slope Stability—The Critical Acceleration." Proceedings of the 2nd International Conference on Earthquake Geotechnical Engineering, Lisbon, Vol. 3, pp. 1077–1082, 1999.
– Seco e Pinto, P. S. "Seismic Behavior of Gravity Retaining Structures." In *Earthquake Geotechnical Engineering:* Proceedings of IS-Tokyo '95, The First International Conference on Earthquake Geotechnical Engineering; Tokyo, 14–16 November 1995, Rotterdam: A. A. Balkema, 1995.
– Simonelli, A. L. "Earth Retaining Wall Displacement Analysis under Seismic Conditions." Proceedings of the 10th European Conference on Earthquake Engineering; Vienna, Austria, 28 August-2 September 1994, Rotterdam: A. A. Balkema, 1995.
– Tatsuoka, F., M. Tateyama, and J. Koseki. "Behavior of Geogrid-Reinforced Soil Retaining Walls During the Great Hanshin-Awaji Earthquake." Proceedings of the 1st International Symposium on Earthquake Geotechnical Engineering, K. Ishihara, ed., Tokyo, pp. 55–60, 1995.
– Tufenkjian, M. R. and M. Vucetic. "Seismic Stability of Soil Nailed Excavations." Civil Engineering Department, UCLA School of Engineering and Applied Science, June 1993.

- **Slopes and Embankments**
  – ASCE/SCEC. "Recommended Procedures for Implementation of DMG Special Publication 117 Guidelines for Analyzing Landslide Hazards in California." February 2002.
  – Ashford, S. A. and N. Sitar. "Seismic Coefficients for Steep Slopes." Proceedings of the 7th International Conference on Soil Dynamics and Earthquake Engineering, pp. 441–448, 1995.
  – Dickenson, S. E., N. J. McCullough, M. G. Barkau, and B. J. Wavra. "Assessment and Mitigation of Liquefaction Hazards to Bridge Approach Embankments in Oregon." Prepared for the Oregon Department of Transportation and Federal Highways Administration, November 2002.
  – Leshchinsky, D. and K. San. "Pseudo-Static Seismic Stability of Slopes: Design Charts." *Journal of Geotechnical Engineering,* ASCE, Vol. 120, No. 9, pp. 1514–1532, September 1994.
  – Ling, H. I. "Recent Applications of Sliding Block Theory to Geotechnical Design." *Soil Dynamics and Earthquake Engineering,* Vol. 21, No. 3, pp. 189–197, April 2001.
  – Loukidis, D., P. Bandini, and R. Salgado. "Stability of Seismically Loaded Slopes Using Limit Analysis." *Geotechnique,* Vol. 53, No. 5, pp. 463–479, June 2003.
  – Martin, G. "Evaluation of Soil Properties for Seismic Stability Analyses of Slopes." *Stability and Performance of Slopes and Embankments II:* Proceedings of a Specialty Conference Sponsored by the Geotechnical Division of the American Society of Civil Engineers, Vol. 1, pp. 116–142, 1992.
  – Munfakh, G. and E. Kavazanjian. "Geotechnical Earthquake Engineering, Reference Manual." Federal Highway Administration, National Highway Institute, 1998.
  – Rogers, J. D. "Seismic Response of Highway Embankments." In *Transportation Research Record 1343,* TRB, National Research Council, Washington, D.C., 1992, pp. 52–62.
  – Sarma, S. K. "Seismic Slope Stability—The Critical Acceleration." Proceedings of the 2nd International Conference on Earthquake Geotechnical Engineering, Lisbon, Vol. 3, pp. 1077–1082, 1999.
  – Simonelli, A. "Displacement Analysis in Earth Slope Design Under Seismic Conditions." *Soil Dynamics and Earthquake Engineering VI,* pp. 493–505, 1993.
  – Simonelli, A. and E. Fortunato. "Effects of Earth Slope Characteristics on Displacement Based Seismic Design." Proceedings of the 11th World Conference on Earthquake Engineering, CD-ROM-1017, 1996.
  – Simonelli, A. and C. Viggiano. "Effects of Seismic Motion Characteristics on Earth Slope Behavior." 1st Inter-

national Conference on Earthquake Geotechnical Engineering, pp. 1097–1102, 1995.
– Stewart, J. P., T. F. Blake, and R. A. Hollingsworthe. "A Screen Analysis Procedure for Seismic Slope Stability." *Earthquake Spectra,* Vol. 19, Issue 3, pp. 697–712, August 2003.
– Wahab, R. M. and G. B. Heckel. "Static Stability, Pseudo-Static Seismic Stability and Deformation Analysis of End Slopes." Proceedings of the 2nd International Conference on Earthquake Geotechnical Engineering, Lisbon, Portugal, Vol. 2, pp. 667–672, 1999.
– Wartman, J. et al. "Laboratory Evaluation of the Newmark Procedure for Assessing Seismically-Induced Slope Deformations." Proceedings of the 2nd International Conference on Earthquake Geotechnical Engineering, Lisbon, Portugal, Vol. 2, pp. 673–678, 1999.

• **Buried Structures**
– American Lifelines Alliance. "Seismic Fragility Formulations for Water System." Part 1—Guidelines and Part 2—Appendices, April 2001.
– ASCE. "Guidelines for the Seismic Design of Oil and Gas Pipeline Systems." American Society of Civil Engineers, Committee on Gas and Liquid Fuel Lifelines of the ASCE Technical Council on Lifeline Earthquake Engineering, 1994.
– Hamada, M., R. Isoyama, and K. Wakamatsu. "Liquefaction-Induced Ground Displacement and Its Related Damage to Lifeline Facilities." *Soils and Foundations,* Special Issue, 1996.
– Holzer, et al. "Causes of Ground Failure in Alluvium during the Northridge, California, Earthquake of January 17, 1994." Technical Report NCEER-96-0012, 1996.
– Johnson, E. R., M. C. Metz, and D. A. Hackney. "Assessment of the Below-Ground Trans-Alaska Pipeline Following the Magnitude 7.9 Denali Fault Earthquake." TCLEE, Monograph 25, 2003.
– MCEER. "Response of Buried Pipelines Subject to Earthquake Effects." MCEER Monograph Series No. 3, 1999.
– NCEER. "Highway Culvert Performance during Earthquakes." NCEER Technical Report NCEER-96-0015, November 1996.
– NCEER. "Case Studies of Liquefaction and Lifeline Performance during Past Earthquakes." Technical Report NCEER-92-0001, Volume 1, M. Hamada, and T. D. O'Rourke Eds., 1992.
– O'Rourke, M. J. and X. Liu. "Continuous Pipeline Subjected to Transient PGD: A Comparison of Solutions." Technical Report NCEER-96-0012, 1996.
– O'Rourke, M. J. and C. Nordberg. "Longitudinal Permanent Ground Deformation Effects on Buried Continuous Pipelines." Technical Report NCEER-92-0014, 1996.
– O'Rourke, T. D. "An Overview of Geotechnical and Lifeline Earthquake Engineering." *Geotechnical Special Publication No. 75—Geotechnical Earthquake Engineering and Soil Dynamics III,* ASCE, Vol. 2, 1999.
– O'Rourke, T. D., S. Toprak, and Y. Sano. "Factors Affecting Water Supply Damage Caused by the Northridge Earthquake." *Proceedings, 6th US National Conference on Earthquake Engineering,* Seattle, WA, 1998.
– Pease, J. W. and T. D. O'Rourke. "Seismic Response of Liquefaction Sites." Journal of Geotechnical and Geoenvironmental Engineering, ASCE, Vol. 123, No. 1, pp. 37–45, January 1997.
– Shastid, T., J. Prospero, and J. Eidinger. "Southern Loop Pipeline—Seismic Installation in Today's Urban Environment." TCLEE, Monograph 25, 2003.
– Youd, T. L. and C. J. Beckman. "Performance of Corrugated Metal Pipe (CMP) Culverts during Past Earthquakes." TCLEE, Monograph 25, 2003.

2.2.2 General Observations

Results of this literature review determined that a significant amount of information has and continues to be published on the topics of seismic design and performance of retaining walls, slopes and embankments, and buried structures. These publications cover all facets of seismic design and performance from simplified to highly rigorous numerical methods, laboratory testing with shake tables and centrifuges, and case histories, though the number falling into this last category is relatively limited.

Whereas the amount of literature is significant, the advances in design methodology have been relatively limited over the past 10 to 20 years. New methodologies often have been refinements of procedures suggested many years before. What might be considered the only significant advance is the common application of various numerical methods to investigate seismic response.

- Limit-equilibrium computer codes are available from various vendors for evaluation of global stability of retaining walls, slopes and embankments, and the permanent displacement component of buried structures. These codes allow the designer to consider various internal and external forces, with seismic forces included as a horizontal force coefficient. Results from these analyses include critical failure surfaces and factors of safety for global stability.
- A more limited number of finite element and finite difference codes also are being used now to estimate the displacement of soils or soil-structure systems during seismic loading. These more rigorous numerical procedures allow consideration of various geometries, time-dependent loads, and soil properties whose strength changes with cycles of loading.

A number of observations relative to the overall goals of this Project can be made from the results of the literature review. Further discussion is provided in Chapter 3.

- **Retaining Walls**
  - M-O equations are used almost exclusively to estimate seismic active and passive earth pressure. Little attention seems to be given to the assumptions inherent to the use of the M-O equations. The seismic coefficient used in the M-O equation is assumed to be some percent of the free field ground acceleration—typically from 50 to 70 percent—and the soils behind the retaining structure are assumed to be uniform.
  - There is widespread acceptance, particularly in Europe, of displacement-based methods of design, although it is recognized that displacements are sensitive to the nature of earthquake time histories.
  - Only limited experimental data exist to validate the forces estimated for the design of retaining walls. These data are from shake tables and centrifuge tests. In most cases they represent highly idealized conditions relative to normal conditions encountered during the design of retaining walls for transportation projects.
  - The overall performance of walls during seismic events has generally been very good, particularly for MSE walls. This good performance can be attributed in some cases to inherent conservatism in the design methods currently being used for static loads.
- **Slopes and Embankments**
  - Except in special cases the seismic stability analysis for slopes and embankments is carried out with commercially available limit-equilibrium computer codes. These codes have become very user friendly and are able to handle a variety of boundary conditions and internal and external forces.
  - Limited numbers of laboratory and field experiments have been conducted to calibrate methods used to estimate seismic stability or displacements. These experiments have used centrifuges to replicate very idealized conditions existing in the field. Usually the numerical method is found to give reasonable performance estimates, most likely because of the well-known boundary conditions and soil properties.
  - Slope and embankment performance during earthquakes has varied. Most often slopes designed for seismic loading have performed well. The exception has been where liquefaction has occurred. The most dramatic evidence of seismically induced slope instability has occurred for oversteepened slopes, where the static stability of the slope was marginal before the earthquake.
- **Buried Structures**
  - A number of procedures have been suggested for the design of culverts and pipelines. Most often these procedures have been based on post-earthquake evaluations of damage to water and sewer pipelines. The procedures consider both the TGD and PGD. Most examples of damage are associated with PGD. Pressures on the walls of buried structures are typically estimated using conventional earth pressure equations, including the M-O equations for seismic loading.
  - Experimental studies have been conducted with centrifuges and shake tables to estimate the forces on culverts and pipes that result from seismically induced PGD. Only limited attention has been given to experimental studies involving the effects of TGD on pipelines and culverts.
  - Observations from past earthquakes suggest that performance of culverts and pipe structures located beneath highway embankments has generally been good. This good performance is most likely associated with the design procedures used to construct the embankment and backfill specifications for the culverts and pipes. Typical specifications require strict control on backfill placement to assure acceptable performance of the culvert or pipe under gravity loads and to avoid settlement of fill located above the pipeline or culvert, and these strict requirements for static design lead to good seismic performance.
  - The most common instances of culvert or pipe structure damage during past earthquakes is where lateral flow or spreading associated with liquefaction has occurred. In these situations the culvert or pipe has moved with the moving ground.

2.3 DOT, Vendor, and Consultant Contacts

Contacts were made with staff on the Project Team, staff in geotechnical groups of DOTs, vendors, and other consultants to determine the availability of design guidelines to handle seismic design of retaining walls, slopes and embankments, and buried structures. During these contacts, an effort also was made to determine the normal approach followed when performing seismic design and analyses of retaining walls, slopes and embankments, and buried structures. This was viewed as a key step in the data collection and review process, as the procedures used by this group of practitioners represent the current state-of-the practice and should form the starting point for the development of any new methodology.

Some of the key design guides and references identified from these contacts are summarized here:

- Caltrans: Contacts with California Department of Transportation (Caltrans) personnel focused on the design

requirements for retaining walls and the approach used to evaluate seismic slope stability. Caltrans personnel confirmed that the retaining wall design requirements are documented in the Caltrans Bridge Design Specifications dated August 2003. Specifications include a 14-page Part-A on General Requirements and Materials and 106-page Part-B on Service Load Design Method, Allowable Stress Design. Some of the key design requirements for retaining walls include the following:

  - A minimum factor of safety of 1.3 for static loads on overall global stability.
  - A minimum factor of safety of 1.0 for design of retaining walls for seismic loads.
  - Seismic forces applied to the mass of the slope based on a horizontal seismic acceleration coefficient (k_h) equal to one third of the site-adjusted PGA, the expected peak acceleration produced by the maximum credible earthquake. Generally, the vertical seismic coefficient (k_v) is considered to equal zero.

  Caltrans specifications go on to indicate that if the factor of safety for the slope is less than 1.0 using one-third of the site-adjusted PGA, procedures for estimating earthquake-induced deformations, such as the Newmark Method, may be used provided the retaining wall and any supported structure can tolerate the resulting deformations.

- WSDOT: Initial contacts with WSDOT's geotechnical staff focused on WSDOT's involvement in developing technical support for load and resistance factors used in geotechnical design. While this work was not specifically directed at seismic loading, both the methodology and the ongoing work through the AASHTO T-3 group appeared to be particularly relevant to Phase 2 of this Project. WSDOT efforts included evaluation of load and resistance factors through Monte Carlo simulations. Subsequent discussions took place with WSDOT on seismic design methods for retaining walls in general and MSE walls in particular. One key concern on the part of WSDOT was how to incorporate load and resistant factors in the seismic design process. This concern was particularly critical in the use of the M-O procedure for determining seismic earth pressures. WSDOT found that if no resistance factors were applied to the dynamic case, as suggested in NCHRP 12-49 Project report and other similar documents, it was possible that the seismic earth pressure will be lower than the static earth pressure determined using load and resistance factors in the AASHTO *LRFD Bridge Design Specifications.* WSDOT also provided a preliminary copy of their draft seismic design requirements for retaining walls, slopes, and embankments.
  - For pseudo-static analyses, WSDOT proposed using a horizontal seismic coefficient equal to 0.5 times the site-adjusted PGA with a target factor of safety of 1.1. Newmark-type analyses were allowed where an estimate of deformations was needed.
  - Seismic earth pressures on walls were determined using the M-O equations. WSDOT staff specifically pointed out the difficulties that they have had in dealing with high acceleration values and steep back slopes when using the M-O equations.
- ODOT and ADOT&PF: Both the Oregon Department of Transportation (ODOT) and the Alaska Department of Transportation and Public Facilities (ADOT & PF) have recently worked on developing guidelines for addressing the effects of liquefaction on embankment stability. Some of this information is useful for addressing the response of slopes in liquefiable soils.
- Vendors: Design methods used by several vendors of MSE walls (for example, Keystone, Hilfiker, and Mesa) were reviewed. Generally, these vendors followed methods recommended by FHWA. Both the inertial force within the reinforced zone and the dynamic earth pressure from M-O earth pressure calculations were used in external stability evaluations. Guidelines also were provided for evaluation of internal stability in the approach used by some vendors.
- Consultants: Contacts also were made with geotechnical engineers and structural designers to determine what they perceived as the important issues for seismic design of retaining walls, slopes and embankments, and buried structures. Below is a list of some of the issues identified from this limited survey:
  - There was consensus that there needs to be clarification on the responsibility between geotechnical engineers and structural engineers in the overall design process. The view was that a lack of communication occurs between the two parties resulting in much confusion at times.
  - The design practice varied tremendously from state to state and from project to project on many fundamental requirements, including whether retaining walls need to be designed for the seismic load case at all. A common practice was to design retaining walls for static loading only with its inherent factor of safety, and many designers believed that retaining walls have performed well in past earthquakes and traditional static design practice and its inherent conservatism were adequate.
  - A major objective in future effort should be to devote some effort to clarifying basic steps involved in designing retaining walls.
  - Pseudo-static methods are typically used to evaluate stability of slopes and embankments during seismic loading. There seems to be a divergence of opinion on the

seismic coefficient to use during these analyses and an acceptable factor of safety.
– Design of buried structures (that is, pipelines and culverts) is normally limited to a check on liquefaction potential, on the potential for flotation, and an evaluation of slope stability or lateral flow. Where lateral soil movement was expected, the buried structure was either considered expendable or ground treatment methods were used to mitigate the potential for lateral ground movement.

An interesting observation from these contacts was that the approach used by transportation agencies, specifically DOTs, seemed to lag the methodologies being used by many consultants. This is particularly the case for the seismic design of slopes, where the common practice was to limit the seismic stability analyses to the abutment fill using pseudo-static methods. With the possible exception of some DOTs, such as Caltrans and WSDOT, there was some hesitation towards using deformation methods. It also seemed that free-standing retaining walls and buried structures most often were not designed for seismic loading. This was due in part to the lack of generally accepted design guidelines and the general costs associated with the implementation of additional design requirements.

As a final note, it was commonly accepted by most practitioners involved in designing retaining walls and underground structures that earth structures have performed well in past earthquakes, even for the higher ground shaking levels in WUS. These observations suggested that the seismic design requirement for earth structures should not burden the designer with overly complex and often over costly designed systems. A very important part of the NCHRP 12-70 Project was to take advantage of recent seismological studies and seismic performance observations to avoid unwarranted conservatism and to reduce the region of the country requiring seismic loading analyses.

2.4 Conclusions

Conclusions from this task were that the methodologies available to design professionals within DOTs and consultants for the DOTs are primarily limited either to pseudo-static methods, such as the M-O equations for estimating seismic earth pressures on retaining structures and the limit-equilibrium method of slope stability analysis, or to simplified deformation methods (for example, Newmark charts or analyses). Although these methods have limitations, improvements in these methodologies still offer the most practical approaches to seismic design.

A growing trend towards the use of more rigorous modeling methods, such as the computer code FLAC (Itasca, 2007), for the evaluation of retaining structures, slopes and embankments, and buried structures has occurred recently. While FLAC and similar software provide a more rigorous modeling of these problems and can be a very powerful method of analysis, these more numerically intensive procedures do not appear to be suitable for development of design methodologies required by this Project. Rather they offer methodologies either to check the simplified procedures appropriate for conventional design or to evaluate special loading conditions and special geometries. Even in these special cases, these more rigorous procedures can be prone to significant inaccuracies when the person using the software does not have a good understanding of conditions that could affect results.

As discussed in the next chapter, it also was apparent from the review of the literature that some areas of seismic design were relatively mature, with design methods provided and generally accepted. The design of slopes and embankments is an example of this. But other areas were less well understood even for static loading. Design of geosynthetic walls falls into this category. This difference in "design maturity" added to the complexity of the NCHRP 12-70 Project, as the intent of the NCHRP 12-70 Project was to have design guides consistent with and build upon static design methods.

CHAPTER 3

Problems and Knowledge Gaps

The goal of Task 2 of the NCHRP 12-70 Project was to identify, illustrate, and document problems and knowledge gaps in current seismic analysis and design of retaining wall, slopes and embankments, and buried structures. This objective was based on the Task 1 data collection and review, as well as the Project Team's experience gained from conducting seismic design studies for retaining walls, slopes and embankments, and buried structures in seismically active areas. The discussion of knowledge gaps and problems is organized in four subsections. The first three summarize knowledge gaps and problems for retaining walls, slopes and embankments, and buried structures, respectively. The final section provides key conclusions about knowledge gaps and problems. As with the previous chapter, the primary focus of this effort was to identify practical problems and knowledge gaps commonly encountered by design engineers when conducting seismic design studies.

3.1 Retaining Walls

The discussion of problems and knowledge gaps for retaining walls focused on three primary types of retaining walls: gravity and semi-gravity walls, MSE walls, and soil nail walls. Various other categories of walls exist, such as nongravity cantilever walls and anchored walls. The discussions for gravity and semi-gravity walls are generally relevant to these other walls as well, though additional complexity is introduced from the constraints on deformation resulting from the structural system and the need to meet structural capacity requirements.

3.1.1 Gravity and Semi-Gravity Walls

Current AASHTO Specifications use the well-established M-O equations developed in the 1920s for determining pseudo-static seismic active earth pressures behind conventional gravity or semi-gravity retaining walls (that is, cast-in-place gravity walls or cast-in-place concrete cantilever or counterfort walls), where the maximum inertial forces acting on the wall and backfill soil are computed from the peak ground acceleration coefficient at ground level. This approach is still widely used in general geotechnical practice since being suggested as a standard method by Seed and Whitman (1970). A number of problems and related knowledge gaps with the above approach have been identified, as discussed in the following subsections.

3.1.1.1 Use of M-O Approach for Seismic Earth Pressures

The following problems are encountered when using the M-O equations for the determination of seismic earth pressures:

- How to use the M-O equations for a backfill that is predominantly clayey, for a soil involving a combination of shear strength derived from both c (cohesion of the soil) and ϕ (friction angle of the soil), or where backfill conditions are not homogenous.
- How to use the M-O equations for sloping ground behind the wall where an unrealistically large seismic active earth pressure coefficient can result.
- How to use the M-O equations when high values of the selected seismic coefficient cause the M-O equation to degenerate into an infinite earth pressure.

These concerns reflect the limitations of the M-O equations as discussed in the Commentary within the NCHRP Project 12-49 Guidelines (NCHRP Report 472, 2002). As noted in the commentary, these limitations in the M-O approach are the result of basic assumptions used in the derivation of the M-O methodology. For the case of seismic active earth pressures, the M-O equation is based on the Coulomb failure wedge assumption and a cohesionless backfill. For high accelerations or for steep backslopes, the equation leads to excessively high pressures that asymptote to infinity at critical accelera-

tion levels or backslope angles. For the latter conditions, no real solutions to the equation exist implying equilibrium is not possible. A horizontal backfill with a friction angle for sand of 40 degrees, a wall friction angle of 20 degrees, and a peak acceleration coefficient of 0.4 has a failure surface angle of 20 degrees to the horizontal. It will lead to very large seismic earth pressures due to the size of the failure wedge. For a peak acceleration coefficient of 0.84, the active pressure becomes infinite, implying a horizontal failure surface. Since many areas along the West Coast and Alaska involve peak ground accelerations in excess of 0.3g and it is common to have a backslope above the retaining wall, it is not uncommon for the designers to compute what appear to be unrealistically high earth pressures.

In practical situations cohesionless soil is unlikely to be present for a great distance behind a wall and encompass the entire critical failure wedge under seismic conditions. In some cases, free-draining cohesionless soil may only be placed in the static active wedge (say at a 60 degrees angle) with the remainder of the soil being cohesive embankment fill ($c - \phi$ soil), natural soil, or even rock. Under these circumstances, the maximum earthquake-induced active pressure could be determined using trial wedges as shown in Figure 3-1, with the strength on the failure planes determined from the strength parameters for the soils through which the failure plane passes. This approach (in effect the Culmann method identified for use with noncohesionless backfill in the 2007 AASHTO *LRFD Bridge Design Specifications* for static wall design) will provide more realistic estimates of seismic active pressure. The above problem becomes further unrealistic in the case of a sloping backfill, where earthquake active pressures become rapidly infinite for small seismic coefficients and relatively shallow slope angles, as illustrated in Figure 3-2.

As discussed in Chapter 4, these problems with the M-O active earth pressure equation appear to be avoidable through the use of commercially available computer programs based on the method slices—the same as conventionally used for slope stability analyses. This approach can be used to compute earthquake active earth pressures for generalized and nonhomogeneous soil conditions behind a retaining wall.

The determination of seismic passive earth pressures using the M-O equation for passive earth pressure also suffers limitations. In many cases the soil is not a homogeneous cohesionless soil. However, more importantly, the use of the Coulomb failure wedge is not necessarily conservative, potentially resulting in an underestimation of passive pressures. For some cases (for example, where the wall height is shallow), a sufficient approach for the computation of seismic passive earth pressures can be the use of the static passive earth pressure equations, as discussed in the NCHRP 12-49 guidelines (NCHRP Report 472, 2002). However, this approach fails to consider the earthquake inertial effects of the soil within the passive pressure zone. A preferred approach involves use of a log spiral method that incorporates seismic effects, as described by

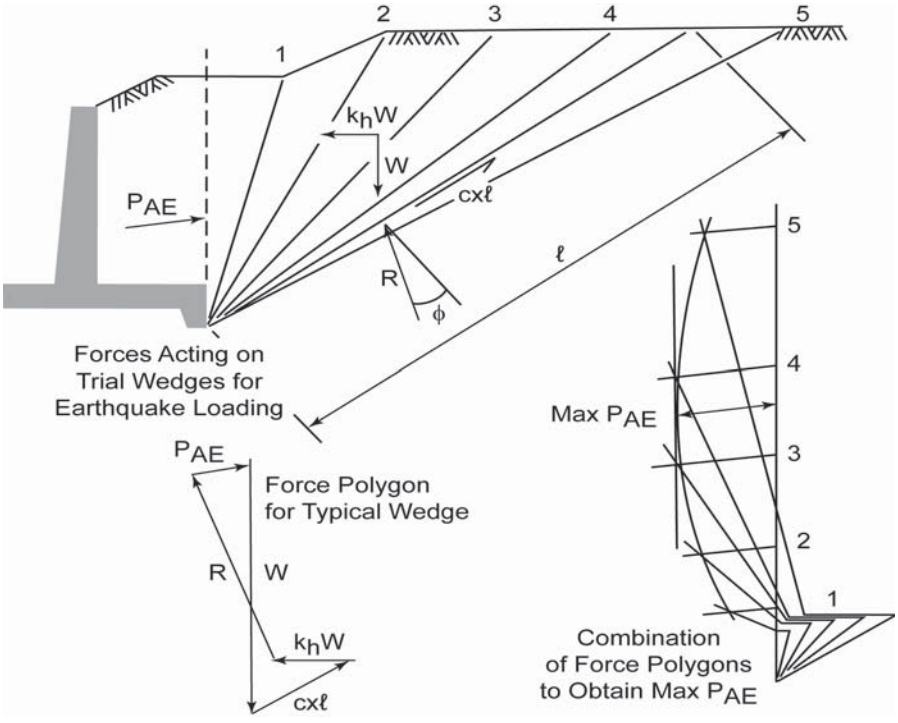

Figure 3-1. Trial wedge method for determining critical earthquake induced active forces.

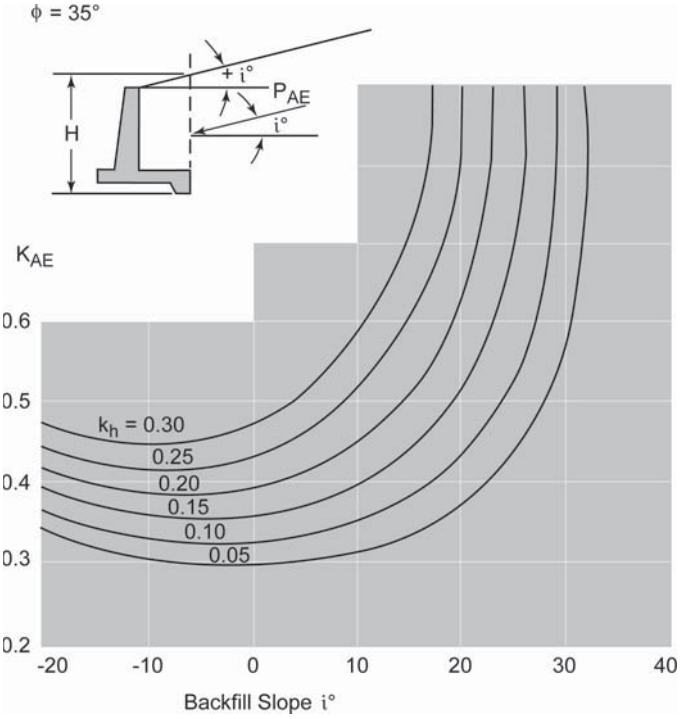

Figure 3-2. Effect of backfill slope on the seismic active earth pressure coefficient using M-O equations.

Shamsabadi et al. (2007). The passive case is important for establishing the resisting force at the toe of semi-gravity walls or for the face of a sheet pile wall or a cantilever wall comprised of tangent or secant piles.

3.1.1.2 Wall Sliding Assumption

The concept of allowing walls to slide during earthquake loading and displacement-based design (that is, assuming a Newmark sliding block analysis to compute displacements when accelerations exceed the horizontal limit equilibrium yield acceleration) was introduced by Richards and Elms (1979). Based on this concept, Elms and Martin (1979) suggested that a design acceleration coefficient of 0.5A in M-O analyses would be adequate for a limit equilibrium pseudo-static design, provided allowance be made for a horizontal wall displacement of 10A inches. The coefficient "A" used in this method was the peak ground acceleration (in gravitational units, g) at the base of the sliding soil wedge behind the retaining wall. This concept was adopted by AASHTO in 1992, and is reflected in current AASHTO *LRFD Bridge Design Specifications.* However, the concept is not well understood in the design community, as designers often use values of 33 to 70 percent of the peak ground acceleration for pseudo-static design without a full understanding of the rationale for the reduction.

Observations of the performance of conventional semi-gravity cantilever retaining walls in past earthquakes, and in particular during the Hyogoken-Nambu (Kobe) earthquake in 1995, have found significant tilting or rotation of walls in addition to horizontal deformations, reflecting cyclic bearing capacity failures of wall foundations during earthquake loading. To represent permanent wall deformation from mixed sliding and rotational modes of deformation using Newmark block failure assumptions, it is necessary to formulate more complex coupled equations of motions as described, for example, by Siddharthen et al. (1992) and Peng (1998). A coupled deformation approach also has been documented in the MCEER report *Seismic Retrofitting Manual for Highway Structures: Part 2—Retaining Walls, Slopes, Tunnels, Culverts, and Roadways* (MCEER, 2006). Peng (1998) indicates that such an analytical approach (including P-Δ effects) appears to provide a reasonable simulation of observed rotational and sliding wall deformations in the Kobe earthquake.

From the standpoint of performance criteria for the seismic design of new conventional retaining walls, the preferred design approach is to limit tilting or a rotational failure mode by ensuring adequate factors of safety against foundation bearing capacity failures and to place the design focus on performance criteria that ensures acceptable sliding displacements. For weaker foundation materials, this rotational failure requirement may result in the use of pile or pier foundations, where lateral seismic loads would of necessity be larger than those for a sliding wall. For retrofit design, the potential for wall rotation may have to be studied, but retrofit design is not within the scope of the proposed AASHTO specifications for this Project.

3.1.1.3 Rigid Block Sliding Assumption

Much of the recent literature on the seismic analysis of conventional retaining walls, including the European codes of practice, focuses on the use of Newmark sliding block analysis methods. The basic assumption with this approach is the soil in the failure wedge behind the retaining wall responds as a rigid mass. Intuitively, for short walls, the concept of a backfill failure zone deforming as a rigid block would seem reasonable. However, for very high walls, the dynamic response of the soil in the failure zone could lead to nonuniform accelerations with height and negate the rigid block assumption. Wall flexibility also could influence the nature of soil-wall interaction.

A number of finite element or finite difference numerical response analyses have been published in recent years, modeling the dynamic earthquake response of cantilever walls. Unfortunately, many of these analyses are based on walls founded on soil layers leading to wall rotation. In addition, numerical difficulties in modeling interface elements between structural and soil elements, along with problems modeling boundary conditions, tend to cloud the results. Many of the analyses use only one wall height, usually relatively high—greater than 30 feet, for example.

Many conventional gravity retaining wall designs involve heights between 5 and 30 feet for economic reasons, with MSE walls being favored for greater wall heights. For this range of heights, and considering the frequency range of likely input ground accelerations, the rigid block assumption is probably adequate; however, as discussed in the next chapter additional studies were required to confirm this expectation.

3.1.1.4 Earthquake Time Histories for Wall Displacement Analyses

The existing AASHTO Specifications use an empirical equation based on peak ground acceleration to compute wall displacements for a given wall yield acceleration. This equation was derived from studies of a limited number of earthquake accelerograms. However, recent studies including publications related to the seismic response of retaining walls have clearly indicated the sensitivity of displacement computations (based on Newmark sliding block analyses) to the frequency and duration characteristics of earthquake acceleration records. Studies by Martin and Qiu (1994) showed sensitivity to both peak accelerations and peak ground velocity.

Whereas site-specific design time histories could be developed for projects, the approach identified in Chapter 4 involved developing new design charts reflecting differences between WUS and CEUS time histories. To develop these charts, it was necessary to have separate sets of time histories representative of WUS and CEUS characteristic earthquakes. As will be discussed in the next chapter, a database of these records was available for use on this Project for developing the proposed charts.

3.1.2 MSE Retaining Walls

MSE walls generally have performed well in past earthquakes, based on case histories reported in the Northridge, Kobe, and Nisqually earthquakes. Minor damage patterns included tension cracks on soil behind reinforced zones and cracking of concrete facing panels. In some cases significant wall displacements were observed. For example, roughly 12 and 6 inches of lateral displacements at the top and bottom of a 20-foot-high wall in Kobe were noted, where ground accelerations were 0.7g. Such minor damage did not affect the integrity or stability of wall, and the wall continued to function.

Based on the above evidence, it could be argued that current seismic design methods for MSE walls are adequate. However, the lack of monitoring data and the lack of case histories for wall heights greater than 30 to 50 feet, together with the limitations and uncertainties of current design methodologies, suggest that improvements in design approaches are still needed. As an extreme example of this need, an MSE wall with a height of over 100 feet was designed and constructed for the third runway extension at the Seattle–Tacoma International Airport. The firm-ground PGA value for this site will vary from approximately 0.3g to 0.6g for return periods ranging from 500 to 2,500 years. The combination of large PGA and very high wall height poses questions as to the appropriate seismic coefficient to use for design.

Whereas model studies using centrifuge or large shaking tables, together with numerical analyses using finite element of finite difference programs, are providing insight on the complex physical behavior of MSE walls under seismic loading, current practical design approaches described in the literature rely on pseudo-static, limit-equilibrium analyses, such as those used for conventional gravity walls. Data from such models or numerical studies often are used to calibrate pseudo-static approaches, which have been developed over the past 20 years.

Based on the literature survey carried out for Task 1 of this Project, the following general observations summarize the data gaps and uncertainties related to aspects of published design approaches using limit equilibrium analyses of MSE walls.

- Limit equilibrium approaches to the seismic design of MSE walls entail consideration of the following two stability modes:
  - Internal or local stability, which considers the potential for rupture or pullout of tensile reinforcement; and
  - External or global stability, which considers the overturning or sliding stability of the reinforced fill, assumed a coherent mass.
- Existing design guidelines or procedures use different assumptions in addressing internal stability. Current AASHTO guidelines assume inertial forces act only on the static active pressure zone, leading to additional tensile forces in reinforcement strips. A horizontal acceleration coefficient k_h = (1.45-A) A is used to determine inertial loading, where A is the peak ground acceleration coefficient. This empirical equation reflects potential amplification of low ground accelerations in the reinforced zone. A maximum acceleration of 0.45g is assumed reflecting a potential sliding failure mode at this acceleration level. Choukeir et al. (1997) describe a procedure where k_h is a function of the natural frequency of the reinforced soil mass and the dominant earthquake input frequency. To improve design guidelines, a better understanding of the influence of reinforced fill height and stiffness and the frequency characteristics of input motions on design acceleration levels is needed. It is also clear that the geometry of the earthquake-induced active pressure zone will be influenced by the level of acceleration. The Bathhurst and Cai (1995) analysis method adopted in the 2006 MCEER report *Seismic Retrofit Guidelines for Highway Structures* (MCEER, 2006) assumes a seismic active pressure zone defined by the M-O Coulomb

failure surface and is used in conjunction with maximum ground accelerations. Other analytical approaches search for a critical active pressure zone defined by a bi-linear failure surface.

- External stability is addressed in most guidelines by assuming the M-O method for determining the earthquake-induced active earth pressures in the fill behind the reinforced soil mass. To evaluate the potential for sliding, the AASHTO *LRFD Bridge Design Specifications* assume only 50 percent of the earthquake active pressure acts in conjunction with the reinforced soil mass inertial load on the assumption that the two components would not be in phase, which is questionable and requires further evaluation. In addition, the limitations and problems with the use of the M-O equations for external stability assessments are similar to those previously described for conventional semi-gravity retaining walls, and along with performance criteria based on allowable wall displacements, can be addressed in a similar manner to approaches described for semi-gravity walls.

As discussed in the next chapter, studies related to wall height/stiffness and ground motion dependent seismic coefficients for design, along with improved approaches for evaluation of internal and external seismic stability, are clearly needed.

3.1.3 Soil Nail Walls

Soil nail walls act in a similar manner to MSE walls, but are typically a ground reinforcement technique used for cut slopes as opposed to fill slopes in the case of MSE walls. As described in an FHWA Geotechnical Engineering Circular No. 7 *Soil Nail Walls* (FHWA, 2003), soil nail walls have performed remarkably well during strong earthquakes, with no sign of distress or permanent deflection.

Choukeir et al. (1997) note a seismic design methodology similar to that previously described for MSE walls. Caltrans have developed a computer program SNAIL for the design of soil nail walls based on a limit equilibrium approach using a two-wedge or bilinear failure surface for both internal and external stability considerations, including the specification of horizontal and vertical seismic coefficients. The computer program GOLDNAIL also is widely used in practice during the design of soil nails. This software also can be used to evaluate the performance of anchored walls by replacing the nail with a tendon having a specified strength and pullout capacity

As the design issues for MSE and soil nail walls are generally similar, analysis methods for development were also somewhat similar, with potential applications of the SNAIL and GOLDNAIL programs also requiring review.

3.2 Slopes and Embankments

The dominant theme in the literature on the topic of evaluating the seismic stability or performance of slopes and embankments was the use of either pseudo-static or the Newmark sliding block methods of analysis. Whereas dynamic response analyses (particularly of large earth structures such as dams) using computer programs such as FLAC were finding increasing use, for routine seismic design of slopes and embankments related to highways, the pseudo-static method has found wide acceptance, while the use of Newmark sliding block deformation method was gaining favor, particularly where pseudo-static methods resulted in low factors of safety. Often results of the deformation analysis indicated that the amount of deformation for a slope or embankment was tolerable, say less than 1 to 2 feet, even when the factor of safety from the pseudo-static analysis is less than 1.0.

3.2.1 Seismic Considerations for Soil Slopes

A number of considerations relative to the seismic analysis of slopes and embankments are summarized below.

- As described in both the MCEER (2006) *Seismic Retrofitting Manual for Highway Structures* and the SCEC (2002) *Guidelines for Analyzing and Mitigating Landslide Hazards in California,* recommended practice for the analysis of seismic slope or embankment performance is a displacement-based analysis using a Newmark sliding block approach. This approach also was adopted by the NCHRP 12-49 Project for evaluating liquefaction-induced lateral spread displacement at bridge approach fills or slopes.
- Newmark displacements provide an index of probable seismic slope performance. As a general guideline, a Newmark displacement of less than 4 inches often is considered to represent a "stable" slope, whereas more than 12 inches is considered unstable from a serviceability standpoint. Several design charts correlating Newmark displacement with the ratio of yield acceleration (defined as the acceleration required to bring the factor of safety 1.0) to the peak acceleration exist. The approach identified in Chapter 4 involved review of the existing data for the purpose of developing improved design charts applicable to nationwide seismic hazard conditions—with different charts produced for WUS versus CEUS sites.
- As previously discussed for retaining wall design, studies described in the literature suggest that displacement-based analyses are very sensitive to the frequency and amplitude characteristics of earthquake acceleration time histories and to earthquake duration, together with the earthquake response characteristics of higher walls, slopes, or embank-

ments. Whereas design charts or simplified expressions are available to provide design guidance, improvements were needed to better reflect the above variables and to provide a basis for nationwide application and to use as a screening tool to establish "no seismic analysis" criteria based on appropriate serviceability criteria. Caltrans guidelines, for example, use a "no analysis" screening criteria based on pseudo-static factors of safety greater than 1.1 when a seismic coefficient of ⅓ of the maximum ground acceleration was used.

- For slopes and embankments of limited height, say less than about 30 to 40 feet, the assumption of a rigid sliding block and the use of ground acceleration parameters to define inertial lateral forces was thought to be a reasonable approximation. For higher slopes and embankments, however, where the dynamic response of the sliding mass may influence displacement magnitudes, modifications to computed Newmark displacements were required, depending on the comparative natural period characteristics of the earthquake ground motion and the slope. Such modifications are included, for example, in the design methods documented in the SCEC (2002) recommended procedures. An approach for analytical development is described in Chapter 4 to address this issue.

3.2.2 Seismic Considerations for Rock Slopes

Rock slopes are encountered in many situations—both urban and mountainous terrain. Some considerations related to these types of slopes are summarized below.

- In regularly bedded or foliated rock, cut by joints, there are many possibilities for block movement along weak planes. Where there are multiple sets of discontinuous planes intersecting at oblique angles, three failure modes must be examined: plane sliding, wedge sliding, and toppling. A plane slide can form where a block of rock rests on an inclined plane that dips downward and intersects the face of the slope. A wedge slide can occur where two planes of weakness intersect to define a tetrahedral block. Toppling failure can develop from overturning of certain types of rock, such as slates and schists, that have bedding planes inclined steeply into the hillside.
- In practical solutions, the plane failure is examined using a two-dimensional limit equilibrium approach treating the seismic inertial load as a constant horizontal acceleration acting on the potential failure block. For the wedge failure, three-dimensional limit equilibrium wedge analyses using stereographic projection of joints and open free surface orientations are used for gravity loading. While the consideration of seismic loads in terms of pseudo-static acceleration can readily be implemented for the plane failure which can be carried out with most two-dimensional slope stability programs, a wedge failure under seismic excitation is not widely analyzed. Analyses for the toppling failure, which generally involves moment equilibrium, rarely are used in practice due to the complexity of the problem and lack of adequate rock properties for carrying out meaningful solutions.
- Often the seismic performance of the rock slope is expressed in terms of a pseudo-static factor of safety. The challenge faced by the practicing engineer involves assigning appropriate shear strength parameters on the weakness plane where sliding is anticipated. Some engineers may be reluctant to assign cohesion to the joint surface due to lack of 'stickiness' as found in a clayey soil. In fact, this assumed cohesive strength is defined by the intercept on the shear strength axis, of a tangent of a curvilinear Mohr envelope. This curvature is the result of the interlocking of aspirates on the matching surface of the joints. Furthermore, laboratory direct shear tests are generally conducted on small rock specimens, and thus dilation due to waviness (undulatory nature) of the joint that has a wave length longer than the specimen size is not captured in the test. These conditions would increase the gross shear strength properties of the joint planes when a large failure surface is considered. When a large block failure is considered, the potential failure plane is likely to go through the existing discontinuities and to shear the intact rock that bridges the joint planes. In this case, the shear strength parameters assigned to the potential failure plane in a limit equilibrium analysis should include some portion of the intact rock strength. These increases in shear strength play a crucial role in the stability of rock slope.
- The seismic design of the rock slope can be further improved by a deformation analysis involving a Newmark sliding block analysis on the failure plane. The Newmark sliding analysis for a plane failure is relatively simple to perform; however, for the wedge failure, it requires modification to deal with sliding on two planes under three-directional loading. The resultant vector of the inertial body forces acting onto each joint plane due to the three-component acceleration is checked against the yield acceleration of the joint. Sliding can take place on either plane or along the interception of the two planes depending on the direction of the loads at any given instance of time. This type of analysis provides a rational basis for deformation analysis of the wedge failure.

Although these seismic performance considerations can be identified, it was also apparent that a transparent approach for evaluating the seismic response of rock slopes could not be developed into a guideline consistent with the simplified approaches needed for these AASHTO *LRFD Bridge Design*

Specifications, at least within the scope of this Project. Rather, the seismic design of rock slopes would be more accurately treated on a case-by-case basis.

For rock slope stability evaluations, geologists and geotechnical engineers will be required to define the potential mechanisms of failure, the strength parameters representing the failure mechanisms, and the seismic loads. With this information an assessment of available computer software is required to investigate seismic stability. In some cases where two-dimensional conditions are predominant, conventional stability software similar to programs used for soil slopes could be used. Otherwise, more complete or specialized programs, involving two- and three-dimensional wedge-failure surfaces would be needed.

3.3 Buried Structures

Almost all highway culverts and buried pipes have been designed and built without regard to seismic effects. Currently, there are no seismic provisions in AASHTO *LRFD Bridge Design Specifications* for culverts and buried structures, except for a general requirement stating that "earthquake loads should be considered only where buried structures cross active faults." Unless there is a global slope stability problem within the embankment through which the culvert of pipeline passes, it is unlikely that existing highway culverts or buried structures (other than tunnels) have been designed and built with the consideration of fault displacements. While this approach may be acceptable for drainage culverts and most pipelines, it may not be an acceptable approach for a well-used pedestrian tunnel.

In recent years, a great deal of attention has been given to the study of seismic performance of underground structures to improve the understanding of factors influencing the seismic behavior of underground structures. Design and analysis procedures also have been proposed by some researchers and design engineers, but they are generally developed either for pipelines (for example, gas and water) or tunnels (that is, transportation or water) systems. These procedures have not been directly applied to culvert installations.

The potential problems and knowledge gaps associated with the current seismic design and evaluation procedures for buried structures were considered.

- Culverts and buried pipes have performed much better than other highway structural components (for example, bridges and foundations). The "no-analysis required" criterion proposed for the bridge structures may not be applicable to the culvert structures. A separate and less stringent screening criterion, taking into account both the ground shaking intensity and the project geological site conditions, was needed.
- Current design and analysis methodologies for pipeline and tunnel systems were developed typically for long, linear structures. For most highway applications, the culvert or pipe, however, is typically with limited length. The effect of the short length of the culvert or pipe on seismic response, as well as on the analysis procedure, had to be evaluated.
- Current design and analysis methodologies for pipeline and tunnel systems were developed typically for level-ground conditions. Culverts and pipes, however, are typically constructed within a built-up embankment. There was a lack of data of how to determine the appropriate TGD parameters for culverts and pipes embedded in embankments, especially in high embankments.
- The effect of soil overburden thickness (or embedment depth) and the effect of vertical components of the ground shaking on culvert or pipe performance was not well understood. Further studies in these aspects were required.
- When subjected to the TGD effect, the response of a buried linear structure can be described in terms of three principal types of deformations: (1) axial deformations, (2) curvature deformations, and (3) ovaling (for circular cross section) or racking (for rectangular cross section) deformations. The first two types, axial and curvature deformations, are induced by components of seismic waves that propagate along the culvert/pipe axis. The ovaling/racking deformations are induced along the transverse cross section when seismic waves propagate perpendicularly to the culvert/pipe axis. Previous observations have suggested that smaller diameter pipes (or small diameter highway culverts) are more resistant to ovaling deformations than the tunnel structures (and large diameter/size culverts). On the other hand, tunnels and large-size highway culverts have performed better than small diameter pipes under the effects of axial/curvature deformations. A further understanding of the factors resulting in this different performance between large and small buried structures was important. Once identified, these factors were considered in the design and analysis procedures.
- Simplified ovaling and racking analysis procedures developed for tunnel structures (for example, mined circular tunnels and box type cut-and-cover tunnels) can be applied to large-span circular and rectangular culverts, respectively. Simplified procedures for noncircular and nonrectangular sections (for example, ellipse, arch, arch top 3-sided, etc.) were nonexistent. Numerical analysis was required in this case and specific procedures related to performing this type of analysis were needed.
- Various approaches for analysis or design of pipeline systems (for gas and water) have been proposed, particularly under the effect of PGD, including fault displacements, lateral spread, and slope deformations (slump). Significant disparity exists among these approaches. There are also

different performance requirements and loading criteria being used or proposed from different studies. A consistent methodology and design criteria compatible with the other components of the highway facilities have yet to be developed for the culvert structures.

3.4 Conclusions

Knowledge gaps and problems identified in the literature review, through discussions with various individuals at DOTs and those conducting research in the area, and through the completion of Task 2 have not identified any additional or new knowledge gaps or problems; the ones cited above are relatively well-known and documented. It appeared that in most cases, existing simplified methodologies with appropriate improvements and documentation could be used to address these knowledge gaps and problems.

While many problems could be handled by existing simplified methodologies, the complexity of some topics, such as the seismic design of geosynthetic MSE walls, was seen as more complex than originally anticipated. This complexity resulted in part from the changing approach to the static design of this wall type. It also appeared that the seismic design of other wall types, such as soil nail walls, still lacked the rigor needed to be considered state-of-the-practice. As noted in the discussion of earthquake design basis, current practice with some of these wall types involved sufficient conservatism in the ground motion specification, as well as the inherent conservatism in static design, that these shortcomings were not a serious design issue. In fact, overall current design methods have worked surprisingly well.

On the basis of the work carried out for this task, the primary development needs were identified as follows:

- Retaining walls
  - Numerical procedure that avoided deficiencies in the M-O procedure at high acceleration levels and steep backslopes and that handled mixed soil (c-ϕ) conditions. The recommendation was to use either a wedge-equilibrium equation or a limit-equilibrium stability program to determine the forces needed for stability.
  - Charts for estimating wall displacement for representative areas of the United States (for example, CEUS versus WUS).
  - Guidance on the selection of the seismic coefficient for limit-equilibrium and displacement-based design and its variation with wall height.
- Slopes and embankments
  - Procedures for determining the appropriate seismic coefficient and its variation with slope height.
  - Charts for estimating displacement for representative areas of the United States (for example, CEUS versus WUS). (These charts are the same as those used for estimating the displacement of conventional rigid gravity walls.)
  - Procedures for introducing the effects of liquefaction.
  - Procedures for treating rock slopes.
- Buried structures
  - Simple-to-use design charts for medium-to-large-size culverts and pipes under the effect of transverse seismic racking deformations, taking into account soil-structure interaction effect.
  - Guidance on how to select transient ground deformation (or strain) parameters for design and analysis purposes.
  - Development of a consistent and rational procedure for buried structures subject to various forms of PGD, including lateral spread, embankment slope movements or flow, and faulting.

An overall need for the three areas was a screening procedure that would provide guidance to the designer as to when a seismic analysis could be neglected, because the reserve capacity for static design was sufficient to meet seismic demands during the design seismic event. Further, guidance was needed on the selection of appropriate ground motions to use for seismic design and the determination of appropriate soil strengths to use in the capacity estimate.

CHAPTER 4

Work Plan: Analytical Methodologies

The goal of Task 3 for the NCHRP 12-70 Project was to identify analytical methodologies that would be developed to address the knowledge gaps and problems presented in the previous chapters. The discussion of the work plan for analytical methodology developments is presented under four major headings:

- Seismic ground motions
- Retaining walls
- Slopes and embankments
- Buried structures

The discussion of seismic ground motion follows earlier discussions about the importance of the ground motions to the overall Project. As noted previously, decisions on seismic ground motion levels depended to a certain extent on conclusions reached during the NCHRP 20-07 Project, which was conducted as a separate contract. One of the principal investigators for the NCHRP 12-70 Project served as a technical advisor to the NCHRP 20-07 Project, enabling the NCHRP 12-70 Project to keep abreast of the ground motion recommendations and other components of the NCHRP 20-07 Project that could affect the NCHRP 12-70 Project.

4.1 Developments for Seismic Ground Motions

The first area of development involved the ground motions used during the seismic design of retaining walls, slopes and embankments, and buried structures. The LRFD design procedure involves comparing the capacity of the design element to the seismic demand for various limit states (that is, strength, service, and extreme). Establishing the seismic ground motion was a necessary step when defining the expected demand during seismic loading.

The Project followed the recommendations from the NCHRP 20-07 Project in the definition of the seismic ground motion demand. The NCHRP 20-07 Project recommended adoption of the 1,000-year return period for the extreme limit state (that is, an event having a 7 percent probability of exceedance in 75 years). The NCHRP 20-07 guideline also focused its approach on the spectral acceleration at 1–second period (S_1). This was an important development prompted by the observation that PGA is not a good parameter to correlate with historical damage to structures. Measures of ground shaking at some intermediate period range (say spectral accelerations around 1 to 2 seconds) are a better indicator of displacement demand related to historical damage and hence more important for characterizing ground shaking for design. This is also true for designing retaining walls, slopes and embankments, and buried structures.

In general, PGV is closely related to spectral accelerations at intermediate periods and, therefore, is a more appropriate measure of ground motion displacement demand than PGA, especially for cross correlation to the amplitude of ground deformations or permanent slope displacements. Also, recent seismological research suggested that lower levels of spectral acceleration at intermediate periods for CEUS compared to WUS, and these reductions are relevant to Project requirements.

Historically, due to the absence of strong motion data from CEUS sites, seismic design criteria for projects in CEUS have generally been developed by applying the small PGA values from the CEUS sites to empirical WUS spectral shapes to define the target design spectrum for CEUS conditions. However, studies such as NUREG/CR-6728 conducted by the Nuclear Regulatory Commission (NRC) for nuclear power plant applications (NUREG, 2001) have shown that the differences in CEUS seismological conditions not only result in lower shaking levels (that is, lower PGA), but also result in much lower long-period content for CEUS sites. The NUREG/CR-6728 studies have been adopted by the NRC in recognition of the fundamental difference between requirements for seismological studies in CEUS versus historical WUS

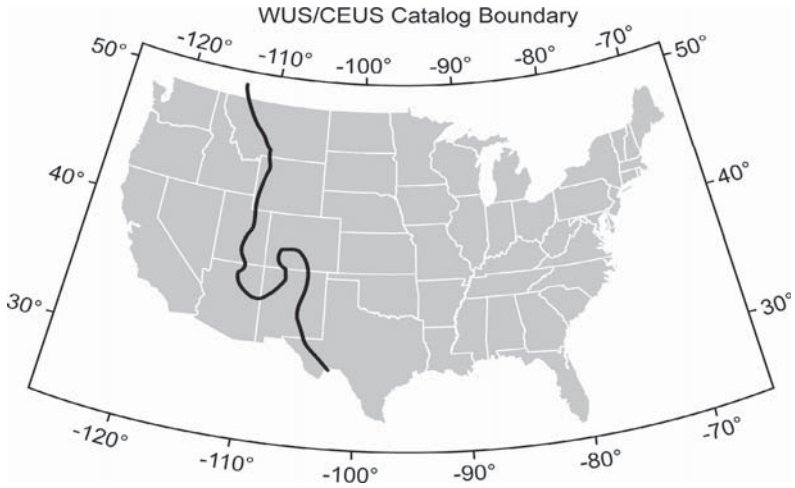

Figure 4-1. Boundary between WUS and CEUS.

practice. Figure 4-1 presents the WUS and CEUS geographical boundary following the USGS seismic-hazard mapping program. The boundary basically follows the Rocky Mountains passing through Montana, Wyoming, Utah, Arizona, then bending east through southern Colorado, New Mexico, and western Texas.

Figure 4-2 presents results from a major study funded by NRC to identify differences in ground motion characteristics between WUS and CEUS for horizontal motions representative of magnitude 6.5 events for generic soil sites. The NUREG/CR-0098 spectral shape shown in Figure 4-2 is based on Newmark's recommendation using historical strong motion data from WUS, while the spectral shape for CEUS was developed using procedures described in the NUREG/CR-6728 report based on up-to-date techniques for CEUS endorsed by NRC. The Regulatory Guide 1.60 is the historical design spectral shape originally used for designing nuclear power plants, now considered overly conservative. In this figure both spectral displacement (RD) and peak spectral acceleration (PSA) at 1 second are normalized by PGA.

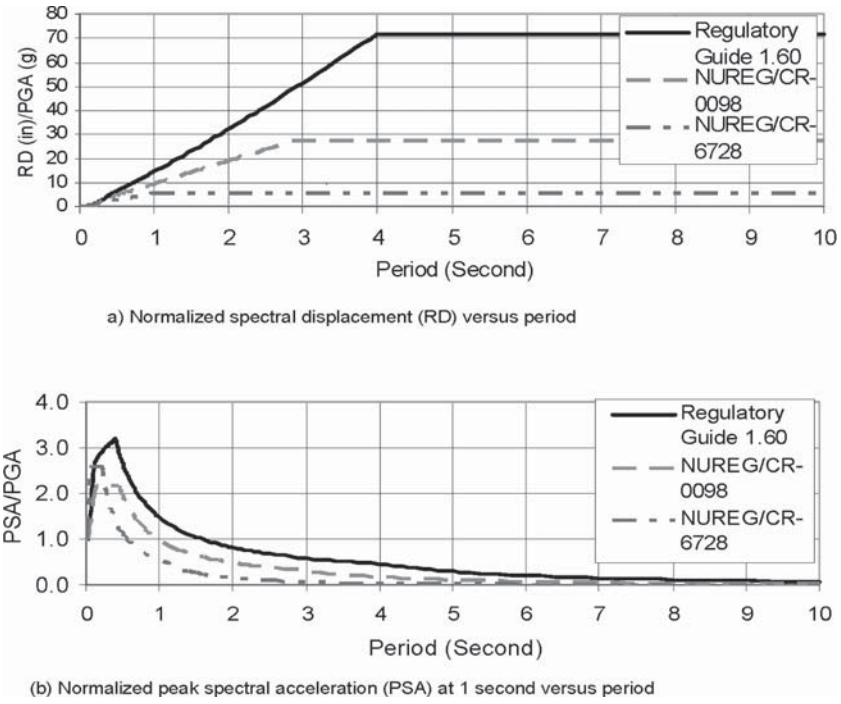

Figure 4-2. Spectral curve shapes for generic sites covering both WUS and CEUS (Sandia, 2004).

Along with the difference in the PGA between WUS and CEUS sites, these figures show the drastic difference in the shaking hazard as measured by the peak spectral acceleration at 1 second (S_1) or PGV between a WUS and a CEUS site. Such changes between the WUS and CEUS are also reflected in AASHTO 1,000-year maps.

In view of the differences in ground motion characteristics, hence response spectra, between CEUS and WUS, as well as the NCHRP 20-07 Project recommendation to use the spectral acceleration at a 1-second period as the parameter for defining the level and requirements for bridge design, a focused ground motion study was conducted during the NCHRP 12-70 Project to establish a consistent approach for both projects. The NCHRP 12-70 ground motion study involved development of an analytical methodology that relates PGV and spectral acceleration at 1-second period (S_1) and between PGV and PGA for CEUS and WUS. Effects of local soil conditions on the relationship between these ground motion parameters were avoided by developing the relationships for NEHRP Site Class B conditions (that is, rock with a shear wave velocity between 2,500 and 5,000 feet per second), and then applying site coefficients to correct for soil conditions. This development was accomplished using an available ground motion database, including spectrum-compatible time history development reflecting differences in WUS and CEUS conditions.

4.2 Developments for Retaining Walls

The next major area of development involved improved methods for estimating the forces on and the displacement response of retaining walls. The approach for evaluating the seismic displacement response of retaining walls consisted of using a limit equilibrium stability analysis in combination with the results of the seismic demand (ground motion) studies described above. Analytical developments were required in three areas, as discussed in the following subsections. The focus of these developments was on rational methods for estimating forces on and deformation of retaining walls located in CEUS and WUS.

4.2.1 Generalized Limit Equilibrium Analyses

The problems and knowledge gaps associated with existing AASHTO Specifications for seismic earth pressure determination have been summarized in the Chapter 3 discussion. Many problems are associated with the M-O equations used to compute seismic active and passive earth pressures for wall design. These problems include the inability of the M-O equations to handle complex wall profiles, soil stratigraphies, and high seismic coefficients. With a few exceptions, these problems preclude practical modification of the M-O equations for general use. The problem for seismic active earth pressures can be overcome by the use of commercially available, limit-equilibrium computer programs—the same as used for the analysis of seismic slope stability. Current versions of many of these programs have the versatility to analyze conventional semi-gravity walls, as well as MSE, soil nail, or anchored walls. These analyses can be performed for complex wall profiles, soil stratigraphy, surcharge loading, and pseudo-static lateral earthquake loading.

In the case of semi-gravity walls, values of earthquake-induced wall loads (P_{AE}) induced by retained soils can be computed from a limit equilibrium stability analysis by calculating the maximum equivalent external load on a wall face (Figure 4-3) corresponding to a safety factor of 1.0. This concept, referred to as the generalized limit equilibrium (GLE) method, can be calibrated back to an idealized M-O solution for uniform cohesionless backfill, and has been used in practice to replace M-O solutions for complex wall designs. The line of action of the external load can reasonably be assumed at the mid-height of the wall acting at an appropriate friction angle. In the case of MSE or soil nail walls, internal and external stability evaluations may be undertaken using limit equilibrium computer programs without the empiricism presently associated with AASHTO Specifications. Such an approach has been described by Ling et al. (1997).

Potential computer programs for evaluating the GLE methodology were reviewed. One of the most valuable documents for this review was a study by Pockoski and Duncan (2000) comparing 10 available computer programs for limit equilibrium analysis. Programs included in the study were UTEXAS4, SLOPE/W, SLIDE, XSTABLE, WINSTABL, RSS,

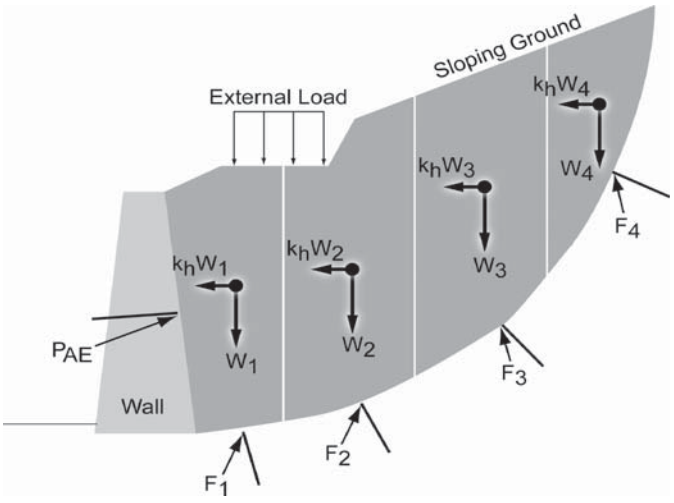

Figure 4-3. Limit equilibrium method for estimating seismic active earth pressures.

SNAIL, and GOLDNAIL. Example problems in the Pockoski and Duncan report addressed design and analysis of MSE, soil nail and anchored (tieback) walls, and examined issues such as ease of use, accuracy, and efficiency. However, the Pockoski and Duncan study considered only static loading conditions. The programs MSEW (based on AASHTO Specifications for MSE walls) and ReSSA (a limit equilibrium program for reinforced soil slopes), both developed by ADAMA Engineering Inc. (ADAMA, 2005a and b) and licensed to the FHWA, also were considered in this review. An application of the latest version of ReSSA has been illustrated in a paper by Leshchinsky and Han (2004) and compared to FLAC analyses.

Based on the review of the above report by Pockoski and Duncan, information from some of the software suppliers, and discussions with various researchers and practitioners, the programs SLIDE, MSEW, and ReSSA (2.0) appeared to be the best suited for use in the analytical methodology development of the Project. Checks with an alternate program were also performed to confirm the flexibility of the methodology being recommended for development. Application examples are further discussed in Chapter 7.

In the case of semi-gravity walls validation of the GLE approach with the closed-form M-O solutions is discussed in Chapter 7. Parametric studies and examples of design applications to representative walls including wall-height effects and deformation analyses (discussed in Sections 4.2.2 and 4.2.3, respectively), along with comparative examples using existing AASHTO design methods, also are discussed in Chapter 5 and 6.

4.2.2 Wall Height-Dependent Seismic Coefficient

The next area of analytical methodology development involved a sound technical procedure for selecting the seismic coefficient to be used in the limit equilibrium approach. The current practice in selecting the seismic coefficient assumes rigid body soil backfill response where the seismic coefficient is defined by the peak ground acceleration occurring at a point in the free field. For wall heights in excess of approximately 30 feet, this rigid-body assumption can be questioned.

Figure 4-4 presents two schematic diagrams illustrating the issues pertaining to the seismic coefficient used for wall pressure determination compared to the free-field motion at a point on the ground surface. For simplicity, a massless retaining wall is used to eliminate the inertial response of the retaining wall, thereby resulting in a relatively simple problem involving inertial response of the retained fill acting on the wall. For this problem the soil mass behind the retaining wall is governed by incoherency in the ground motion at different points of the soil mass.

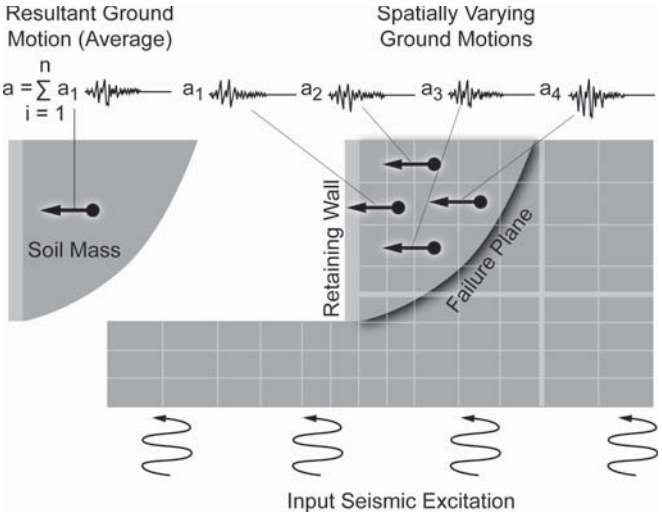

Figure 4-4. Effects of spatially varying ground motions on seismic coefficient.

The acceleration time history response at different points in the soil mass will be different from each other. Total force acting when normalized by the soil mass within the failure plane gives rise to an equivalent seismic coefficient for wall design. As the retaining wall height and the lateral dimension of the mass increase, an increasing degree of the high frequency content of the ground motion will be eliminated. Hence, the seismic coefficient for earth pressure determination should be a function of wall height, as well as a function of the frequency content of the ground motion record. High frequency-rich ground motions tend to be more incoherent and result in a lower seismic coefficient. This observation also means that the seismic coefficient should decrease for the low, long-period content of CEUS motion records as compared to WUS, or for rock motion records as opposed to soft soil site records.

This analytical development to quantify the effects of incoherency (also referred to as scattering or wave scattering in this Final Report) involved use of a library of spectrum-compatible time histories representing a range of conditions, including earthquake magnitudes, soil versus rock sites, and CEUS versus WUS locations. This information was used to evaluate the dependence of the seismic coefficient on wall height. Coherency (wave-scattering) analyses were conducted, and then the acceleration time histories for various failure mechanisms were integrated to evaluate the relation of seismic coefficient versus the original reference PGA and spectral acceleration at 1 second (S_1). The wave scattering analyses were conducted for multiple wall heights (for example, 30-foot, 60-foot, and 100-foot heights). The variation in seismic coefficient was established as a function of time, thereby defining "seismic coefficient time histories" for different locations behind the retaining wall.

The resultant seismic coefficient time histories were used for conducting Newmark sliding block analyses for wall deformation studies. More meaningful seismic coefficients for pseudo-static earth pressure design were established by relating the acceleration ratio in the Newmark analysis to a limiting permanent displacement value (say at 6 inches) from the conducted analyses. The resultant product of this effort was charts of seismic coefficient versus PGA for different wall heights. Charts of wall height-dependent seismic coefficient versus 5 percent damped spectral acceleration at 1 second (S_1) also were developed. The latter charts might have better technical merit as discussed earlier regarding fundamental differences between PGA versus S_1.

4.2.3 Deformation Analyses

As part of this effort, an updated analytical methodology was developed for estimating wall deformations during seismic loading as a function of yield acceleration. This approach was allowed within the then current (2006) AASHTO Specifications; however, the equation used for estimating displacements was based on a limited database.

The following approach was taken from the updated analytical methodology:

1. Semi-gravity walls: Using the computed time histories associated with the wall height seismic coefficient studies, Newmark sliding block charts showing displacements versus the ratio of yield acceleration to the peak ground acceleration (k_y/k_{max}) were determined. (Note that k_y is the acceleration that results in a factor of safety of 1.0; k_{max} is the PGA adjusted for local site effects. The k_{max} term is equivalent to A_s in the current AASHTO *LRFD Bridge Design Specifications.* The seismic coefficient for retaining wall design is commonly defined in terms of k rather than PGA to indicate a dimensionless seismic coefficient. The use of *k* to define seismic coefficient during wall design is followed in this Project.) These charts are a function of S_1, which relates strongly to PGV. The charts in turn were used to reassess the suitability of the 50 percent reduction factor in peak acceleration included within AASHTO for pseudo-static wall design. As noted previously, the 50 percent reduction is based on acceptable horizontal displacement criteria, where walls are free to slide. For walls supported by piles, displacement limits need to be integrated with pile performance criteria associated with pile capacity. In such cases, questions related to pile pinning forces and their influence on yield accelerations of the wall-pile system also need to be considered.
2. MSE walls: Deformation analyses to assess performance criteria for MSE walls are clearly more complex than for semi-gravity walls due to the flexibility of the wall system. A valuable source of reference material on this topic has been documented in a University of Washington Master of Science thesis by Paulsen (2002), where an equivalent Newmark sliding block analysis was developed to accommodate the additional deformations arising from reinforcing strip deformation and slip. However, parameter selection for the model was empirical and based on calibrations from centrifuge and shake table tests. Whereas the model was promising, it was insufficiently mature for practical application at this time. FLAC analyses also have been performed to evaluate deformation behavior under seismic loading, and may be applicable for analysis of special cases. However, with respect to AASHTO Specifications, the analytical methodology attempted to relate the proposed pseudo-static limit equilibrium analyses to deformation performance criteria in an empirical way, based on existing case histories and model tests, and the approach described by Ling et. al. (1997).

4.3 Developments for Slopes and Embankments

The next major area of development involved methods for evaluating the seismic performance of cut slopes and fill embankments. Relative to the development needs for retaining walls, these needs were not as significant. In most cases suitable analytical methodologies already existed for evaluating the seismic response of slopes and embankments, but these methods were not documented in the AASHTO *LRFD Bridge Design Specifications,* suggesting that much of the work related to slopes and embankments involved adapting current methodologies into an LRFD specification and commentary.

Although development needs for slopes and embankments were less than for the other two areas, three developments were required, as summarized below:

- Develop a robust set of Newmark displacement charts for slope displacement evaluations, reflecting both differences between WUS and CEUS and the influence of slope height. In this respect, the analysis approach was similar to that previously described for walls. However, additional parameters were needed in examining the coherence of inertial loads over potential sliding masses, including slope angle and shear wave velocities of slope material, and strength parameters ranging from those for cut slopes to fills. The analysis program used for wave scattering analyses involved QUAD-4M (1994).
- Develop a screening method for determining areas requiring no seismic analysis. The screening method depended on a combination of the level and duration of ground shaking, the geometry of the slope, and the reserve capacity that the slope has under static loading. A critical consideration in

the development of a screening method was the identification of potentially liquefiable soils and how these conditions would be handled in the evaluation. Guidelines were developed for the NCHRP 12-49 Project for treating the stability of approach fills located on liquefiable soils; these methods served as a starting point for this Project as well.
- As no LRFD approach for the static design of slopes exists, a commentary that addressed strength parameter selection for static and seismic design and was consistent with approaches to retaining wall design was developed as part of this Project.

Based on the literature review and identification of knowledge gaps summarized in Chapters 2 and 3, the work on slopes and embankments was limited to soil conditions and did not include rock slopes. The stability of rock slopes during seismic loading is controlled by the specific fracturing patterns of the rock, making a generic approach for the evaluation of the seismic stability of rock slopes beyond what could be accomplished by this Project. For this reason it was concluded that the topic of rock slope stability during seismic loading should be addressed by site-specific evaluations.

4.4 Developments for Buried Structures

The final area of development involved a methodology for dealing with buried culverts and pipe structures. It was recognized that the seismic hazard to buried culverts and pipes can be classified as being caused by either peak ground displacement or TGD resulting from wave propagation. However, there was no existing seismic design methodology or guidelines for the design of culvert or pipe structures in Section 12 of the AASHTO *LRFD Bridge Design Specifications.*

Design and analysis procedures have been proposed by some researchers and design engineers for pipelines (for example, gas and water) or tunnel (that is, transportation or water) systems. While some of these procedures can be used for the design and analysis of culvert and pipes (for example, the transverse racking/ovaling deformation of the section), others cannot be directly applied because (1) culverts and pipes are typically of limited length, (2) culverts and pipe structures are typically constructed within a built-up embankment, and (3) the characteristics of peak ground displacement and its effects on culvert and pipes are phenomenologically complex.

The analytical methodology development for buried structures involved the following main elements:

- Develop analysis procedures for TGD.
  - Guidelines on the selection of design TGD parameters.
  - Methods for estimating transverse racking/ovaling deformations (provide design charts as well as recommended step-by-step procedure).
  - Validation of design charts by numerical analysis.
  - Apply procedures to an established range of problems.
  - Develop screening guidelines to provide a basis for screening culverts and pipelines relative to their need for further seismic evaluation (that is, define the "no-analysis required" criteria).
- Identify analysis procedures for peak ground displacement.
  - Guidelines on the selection of design peak ground displacement parameters (for example, spatial distribution of ground motions and soil stiffness parameters).
  - Effects of soil slope slumping, liquefaction-induced lateral spread and settlements, and fault rupture.

4.4.1 Analysis Procedures for TGD

The response of a buried linear structure can be described in three principal types of deformations: (a) axial deformations, (b) curvature deformations, and (c) ovaling (for circular cross section) or racking (for rectangular cross section) deformations as shown in Figures 4-5 and 4-6.

The axial and curvature deformations are induced by components of seismic waves that propagate along the culvert/pipe axis. Current design and analysis methodologies for pipelines and tunnel systems were developed typically for long, linear structures. Culverts and pipe structures for transportation applications, however, are typically of limited length. For this condition the transient axial/curvature deformations should generally have little adverse effects on culvert/pipe structures and, therefore, design and analysis provisions may not be required for these two modes of TGD effects. This preliminary assumption, however, was further evaluated during the completion of the initial phase of this study and verified by numerical analysis.

The ovaling/racking deformations are induced along the transverse cross section when seismic waves propagate perpendicularly to the culvert/pipe axis. The design and analysis methodology develop by Wang (1993) can be readily applied for culverts with circular or rectangular cross sections. For example, the simple design chart shown in Figure 4-7 allows quick determinations of induced culvert/pipe racking/ovaling deformations.

Previous observations have suggested that smaller diameter pipes (or small diameter highway culverts) are more resistant to ovaling deformations than the larger culvert structures. A further investigation of the factors resulting in this different performance between large and small buried structures was evaluated. Once identified, these factors were reflected in the screening guidelines discussed above. In addition, the proposed analytical methodology development attempted to identify simplified procedures for noncircular and nonrectangular sections. It was anticipated that parametric numerical analyses would be required for developing these simplified procedures.

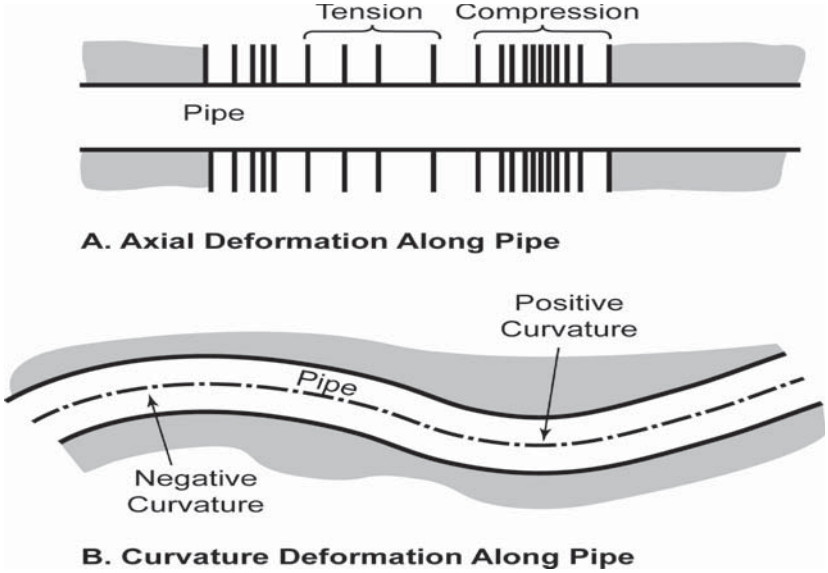

Figure 4-5. Axial/curvature deformations.

Another important aspect for evaluating the TGD effects on culvert/pipe structures was to determine the appropriate design ground motion parameters to characterize the ground motion effects. It has long been recognized that PGA is not a good parameter for buried underground structures. Instead, PGV is a good indicator for ground deformations (strains) induced during ground shaking. This is particularly important because given the same PGA value, the anticipated PGV for CEUS would typically be much smaller than that for the WUS. Results based on the PGA versus PGV study presented earlier in the work plan for the retaining walls, slopes, and embankments were used for the culvert structures.

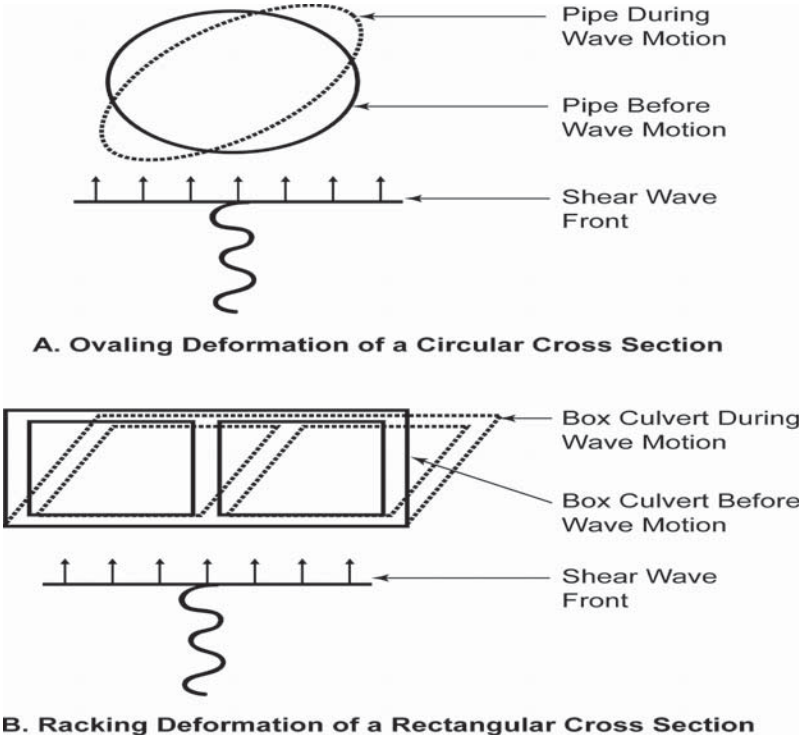

Figure 4-6. Ovaling/racking deformations.

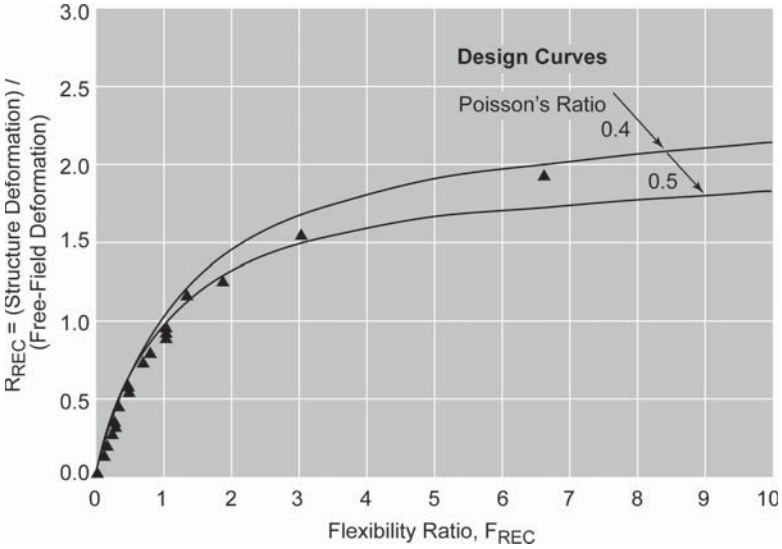

Figure 4-7. Earthquake-induced structural transient racking/ovaling deformations.

As a final consideration, there is an on-going proposal (NCHRP Project 15-28) to upgrade the computer program CANDE-89 to incorporate the LRFD design methodology. CANDE-89 is a comprehensive design/analysis tool for the cross section design and analysis (in two-dimensional plane-strain domain) of buried structures, particularly culverts. The seismic effects of transient racking/ovaling deformations on culverts and pipe structures must be considered additional to the normal load effects and preferably could be incorporated into the updated CANDE analysis. In Chapter 10 recommendations on proposed seismic design methodologies to be incorporated into the CANDE program are made. It is anticipated that an option would be required in the CANDE program to allow ground displacement profile as a loading input to the CANDE analysis.

4.4.2 Analysis Procedures for Permanent Ground Deformations (PGD)

Various approaches for analysis or design of pipeline systems (for gas and water) have been proposed under the effect of PGD including those to account for the effects of liquefaction-induced lateral spread, slope deformations (slump), post-liquefaction settlements, and fault displacements. Significant disparity exists among these approaches. There are also different performance requirements and loading criteria being used or proposed for different studies. A consistent methodology and design criteria compatible with other components of the highway facilities are yet to be developed for the culvert and pipe structures.

In general, there are three major steps for evaluating the PGD effects: (1) determine the PGD patterns (that is, spatial distributions) using the site-specific subsurface conditions encountered at the culvert location; (2) derive the suitable soil stiffness accounting for the dynamic as well as cyclic effects (for example, softening due to liquefaction and repeated loading cycles; and hardening due to increased strain rates); and (3) evaluate the structural response to the PGD taking into consideration soil-structure interaction effects.

In estimating the PGD patterns for liquefaction-induced lateral spread, slopes/embankment slumping, and post-liquefaction settlements, the procedures developed for retaining walls, slopes, and embankments can be used. Fault rupture has a relatively low occurrence frequency. It is generally difficult to design for the effects of fault rupture unless the fault displacement is small or the backfill within the soil envelope consists primarily of properly designed compressible material to accommodate the fault displacement. As part of this study, general guidelines on design strategy for coping with large PGD, based on various previous project experiences gained from tunnel and pipeline design, were identified.

4.5 Summary

In summary, the proposed analytical methodology development plan resulted in work product elements shown in Table 4-1. This summary is a modified version of Exhibit 6 of the Working Plan for the NCHRP 12-70 Project.

Table 4-1. Work product elements.

Type of Investigation	Purpose
Establish Basis for Determining Ground Motions Suitable for CEUS and WUS	Identifies consistent approach for defining ground motions to use for seismic evaluation of retaining walls, slopes and embankments, and buried structures, including modifications that account for permanent displacements.
Develop Design Charts for Estimating Height-Dependent Seismic Coefficient	Provides a rational basis for selecting seismic coefficient as a function of both wall height and slope height for different soil conditions.
Update Design Charts for Estimating Slope and Wall Movement Displacements	Provides end users the means of estimating slope and wall movements as a function of yield acceleration, PGA, and PGV.
Evaluate Suitability of Limit Equilibrium Computer Program based on Method of Slices for Determination of Lateral Earth Pressures	Offers end users the means for improved methodology for establishing design seismic earth pressure magnitudes for mixed soil conditions, steep backslopes, and high ground motions.
Identify Method for Designing Nongravity Cantilever Walls and Anchored Walls Using Limit Equilibrium and Displacement-Based Methods	Establishes a basis for estimating seismic earth pressures to use for wall design and provides a simplified approach for conducting displacement-based analyses.
Review Basis for Estimating Seismic Performance of MSE Walls	Proposes revisions to design methodology based on conclusions from evaluations carried out for this Project, as appropriate.
Document Approach for Evaluating Seismic Stability of Slopes and Embankments	Provides documentation for limit equilibrium and displacement-based approach for evaluating seismic stability of slopes.
Develop Design Approaches for Permanent and Transient Ground Deformation for Culverts and Pipelines	Provides design guidance and specifications.

CHAPTER 5

Seismic Ground Motions

This chapter summarizes the results of ground motion studies completed for the Project. The primary objectives of the ground motion studies were to

- Provide a consistent basis for establishing ground motion to use during the seismic analysis of retaining walls, slopes and embankments, and buried structures;
- Update Newmark charts for estimating permanent ground displacements of retaining walls and slopes to be consistent with the results of ground motion studies for CEUS and WUS; and
- Establish correlations between PGV and spectral acceleration at a period of 1 second (S_1) for use in the seismic analyses of retaining walls, slopes and embankments, and buried structures.

Information in this chapter serves as input for the seismic response studies discussed in Chapters 6 through 9. These results also form the basis of sections in Volume 2 containing recommended specifications and commentaries in the AASHTO *LRFD Bridge Design Specifications.*

5.1 Seismic Loading Criteria

The seismic design of bridges in the then current (2006) AASHTO *LRFD Bridge Design Specifications* was based on the peak ground accelerations and an appropriate response spectrum for the site. This same general approach was reviewed during the NCHRP 12-70 Project for the seismic analyses of retaining walls, slopes and embankments, and buried structures. However, criteria in the AASHTO *LRFD Bridge Design Specifications* were expected to change based on recommendations from the NCHRP 20-07 Project. Key changes recommended by the NCHRP 20-07 Project included (1) a change in the return period of the ground motion used for bridge design from the existing 10 percent probability of exceedance in a 50-year period (that is, 475-year return period) to a 7 percent probability of exceedance in 75 years, which corresponded approximately to a 1,000-year return period; and (2) a change in the shape of the 5 percent damped response spectrum in the longer period range. The discussion of these seismic loading criteria in this section begins with a review of the update to the current AASHTO *LRFD Bridge Design Specifications.* This review is followed by a summary of the ranges of ground motions that can be expected in various regions of the United States and then the variation in response spectra for CEUS versus WUS based on approaches recommended by the NCHRP 20-07 Project.

5.1.1 Update to AASHTO Seismic Ground Motion Criteria

Seismic loading criteria used by the NCHRP 12-70 Project were taken from the criteria being developed for the seismic design of bridges within the NCHRP 20-07 Project *Recommended LRFD Guidelines for the Seismic Design of Highway Bridges* (Imbsen, 2006). At the time the NCHRP 12-70 Project work was being performed, preliminary feedback from the AASHTO T3 subcommittee was very favorable towards use of the 1,000 year return period and the NEHRP spectral shape concept. Rather than taking a separate approach or conducting a dual development, the NCHRP 12-70 Project assumed that the NCHRP 20-07 recommendations would be adopted at the AASHTO meeting in 2007. AASHTO members later adopted the ground motion changes during a vote in July of 2007.

There were several good reasons for using the criteria developed for the NCHRP 20-07 Project for the seismic design of retaining walls, slopes and embankments, and buried structures. First, it would be consistent with the approach being used by most transportation agencies and already used in part within the current AASHTO *LRFD Bridge Design Specifications.* Secondly, by using the same criteria as developed for the NCHRP 20-07 Project, there was less chance for

confusion between guidelines being used for different parts of a project. Lastly, retaining walls, slopes and embankments, and buried structures are all components of the transportation network and by using the same criteria used by bridges, there was a common basis for judging risk to the transportation system.

Key aspects of the NCHRP 20-07 Project related to ground motion criteria are summarized below:

1. The safety level earthquake was based on the USGS/AASHTO seismic hazard mapping program. The recommended ground motion hazard level was a 7 percent probability of exceedance in 75 years, corresponding roughly to a 1,000-year return period. The USGS was contracted by AASHTO to provide 1,000-year hazard maps and an implementation CD.
2. The map and implementation CD, with the proposed specifications developed by the NCHRP 20-07 Project team, were used by various state bridge departments for trial designs. These trials were carried out in 2006 and balloting for adoption by AASHTO was held in July of 2007. As noted above, this meant that much of the NCHRP 12-70 Project had to proceed on the basis that the NCHRP 20-07 recommendations would be adopted by AASHTO.
3. The approach recommended in the NCHRP 20-07 Project report involved developing a free-field ground surface design spectrum that served as the basic benchmark ground shaking criteria. The spectrum was defined on the basis of spectral acceleration (S_a) at three periods: 0.0, 0.2 and 1.0 seconds corresponding to the 1,000-year uniform-risk spectrum for a referenced soft rock condition. The three periods defined the PGA, short-period spectral acceleration (S_s), and the spectral acceleration at 1 second (S_1), respectively. These spectral values are for soft rock site conditions where the average shear wave velocity within the upper 100 feet of geologic profile ranges from 2,500 to 5,000 feet per second (ft/sec), which is referred as Site Class B.
4. The above three spectral ordinates (that is, at 0.0, 0.2 and 1.0 seconds) are used to anchor a spectral curve shape. Figure 5-1 shows the resultant design acceleration response spectrum after adjusting the referenced soft rock spectrum for site soil effects. The adjustments for site effects account for amplification or deamplification of the referenced rock motion for soil conditions at the site. This method of determining the spectrum is generally the same as that proposed earlier in the NCHRP 12-49 Project (NCHRP Report 472, 2002) and has been used in both the 2003 and 2006 International Building Code (IBC) for regulating the design of new buildings. The primary difference with the new approach adopted by AASHTO in July of 2007 from a ground motion standpoint is that it is using the 1,000-year return period, versus the 2,475-year return period recommended in NCHRP 12-49 and IBC 2003 and IBC 2006. (The IBC

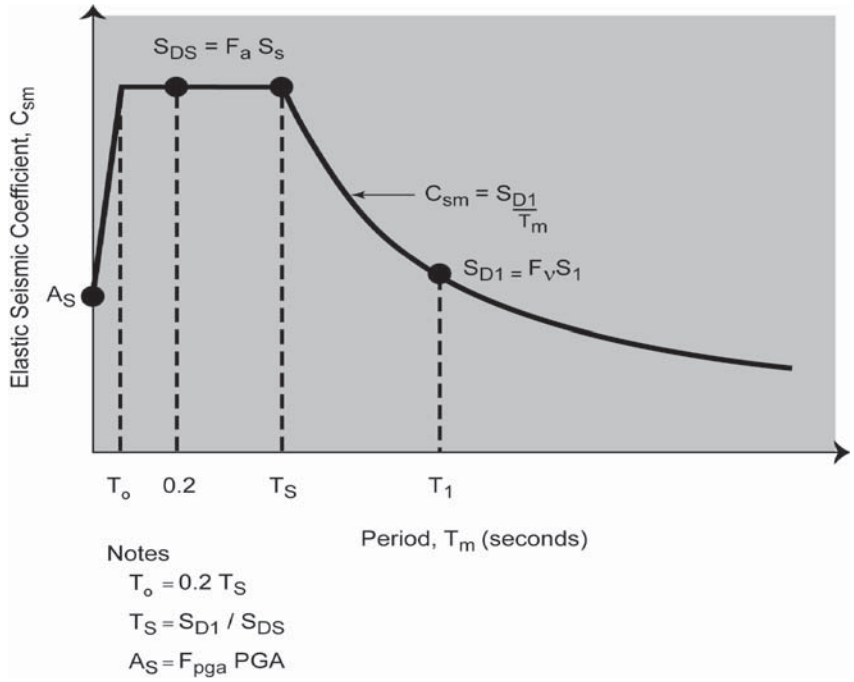

Figure 5-1. Design response spectrum constructed with the three-point method.

Table 5-1. Values of F_a as a function of site class and mapped short-period spectral acceleration.

Site Class	Mapped Spectral Response Acceleration at Short Periods				
	$S_s \leq 0.25$ g	$S_s = 0.50$ g	$S_s = 0.75$ g	$S_s = 1.00$ g	$S_s \geq 1.25$ g
A	0.8	0.8	0.8	0.8	0.8
B	1.0	1.0	1.0	1.0	1.0
C	1.2	1.2	1.1	1.0	1.0
D	1.6	1.4	1.2	1.1	1.0
E	2.5	1.7	1.2	0.9	0.9
F	*a*	*a*	*a*	*a*	*a*

Table notes: Use straight line interpolation for intermediate values of S_s, where S_s is the spectral acceleration at 0.2 second obtained from the ground motion maps.

a Site-specific geotechnical investigation and dynamic site response analyses shall be performed (Article 3.4.3).

design approach also multiplies the resulting spectrum by a 2/3rd factor to account for the "reserve capacity" against collapse within most buildings.) The AASHTO procedure also involves anchoring the design spectrum at zero period (PGA) based on a 1,000-year return period hazard level. This approach compares to the IBC which assumes that the PGA is equal to 0.4 times the spectral acceleration at 0.2 seconds (that is, the short period spectral acceleration, S_s). The site coefficient used by AASHTO to adjust the PGA value (F_{pga}) for various soil classifications is identical to the coefficient used for the 0.2-second, short period site factor (F_a) recommended by the NCHRP 12-49 Project and used by IBC.

5. Similar to NCHRP 12-49 and IBC 2006, the NCHRP 20-07 document provided two tables for site modification factors to be applied to the two spectral ordinates for other site soil/rock categories. Table 5-1 tabulates site coefficients (F_a) at the short period range (that is, at 0.0-second and 0.2-second periods), and Table 5-2 tabulates site coefficients (F_v) at the 1-second period. (AASHTO subsequently adopted a separate table for F_{pga} to be applied to PGA. Values of F_{pga} are the same as F_a. Note also that AASHTO normalizes PGA to be dimensionless. The current version of AASHTO shows the same F_a and F_v values but without the units of gravitational acceleration (g).) The two site coefficient factors are applied to the three spectral ordinates from the new AASHTO 1,000-year maps and implementation CD for various site categories in relation to the reference USGS Site Class B condition.

Table 5-2. Values of F_v as a function of site class and mapped 1 second period spectral acceleration.

Site Class	Mapped Spectral Response Acceleration at 1 Second Periods				
	$S_1 \leq 0.1$ g	$S_1 = 0.2$ g	$S_1 = 0.3$ g	$S_1 = 0.4$ g	$S_1 \geq 0.5$ g
A	0.8	0.8	0.8	0.8	0.8
B	1.0	1.0	1.0	1.0	1.0
C	1.7	1.6	1.5	1.4	1.3
D	2.4	2.0	1.8	1.6	1.5
E	3.5	3.2	2.8	2.4	2.4
F	*a*	*a*	*a*	*a*	*a*

Table notes: Use straight line interpolation for intermediate values of S_1, where S_1 is the spectral acceleration at 1.0 second obtained from the ground motion maps.

a Site-specific geotechnical investigation and dynamic site response analyses shall be performed (Article 3.4.3).

– The spectral ordinate at 0.2 second defines a flat plateau with a constant spectral acceleration. This constant acceleration branch of the spectral curve starts at 0.2 T_s where T_s is defined by the ratio of S_a at 0.2 seconds to S_a at 1 second. The long-period limit of the spectrum is governed by the intersection of the constant acceleration branch of the curve and the decreasing spectral acceleration branch of the response spectrum curve anchored at the 1-second ordinate.
– The long-period range (decreasing spectral acceleration) is defined by the spectral ordinate at 1 second along with the assumption that the curve shape is inversely proportional to period (T); that is, $S_a \propto 1/T$. This $1/T$ decrease is consistent with an assumption of constant spectral velocity. It also corresponds with a spectral displacement that increases linearly with the period of motion. (Note that the current IBC 2006 has a further provision where the $1/T$ decrease changes to a $1/T^2$ decrease. The period of this change differs across the United States, ranging from 4 seconds to 16 seconds. The change from $1/T$ to $1/T^2$ was introduced for the design of long-period structures, such as multistory buildings, and for sloshing of large-diameter water reservoirs. A similar approach has not been taken by AASHTO for the design of long-period bridges. The maps in IBC 2006 are not applicable because they represent a return period of 2,475 years as opposed to the 1,000-year return period being recommended within the new AASHTO maps. It is presumed that the seismic design of long-span bridges would use site-specific evaluation methods in the absence of maps similar to those in IBC 2006.)

5.1.2 Range of Ground Shaking Levels in the United States for Referenced Soft Rock

A sensitivity analysis was conducted during the NCHRP 12-70 Project to determine the ground shaking levels for the 1,000-year return period at various locations in the United States. Site Class B soft rock reference condition was used for conducting this analysis. The purpose of the study was to establish the range in ground shaking levels that must be considered during the seismic design of retaining walls, slopes and embankments, and buried structures—based on the recommendations given in the NCHRP 20-07 Project.

The 1,000-year hazard spectra used in this sensitivity study were generated by making use of the USGS interactive website, rather than the results of the USGS 1,000-Year Mapping Program. Although the USGS program was very close to completion at the time of this work, the results of the 1,000-year data were not available at the time the analyses were conducted (Fall 2005). Appendix C provides background information on the USGS interactive website.

Figure 5-2 shows the results from this analysis; Table 5-3 tabulates these results. The figure shows the distinctly different shapes of the response spectra in CEUS versus the WUS. In this figure, spectral curves for sites located in the more active WUS are shown by continuous lines, and sites for the less active CEUS are denoted by dashed lines. The difference between WUS and CEUS occurs along a distinctive boundary (see Figure 4-1) along the US Rocky Mountains. West of this boundary is referred to as the more seismically active WUS, and east is the less active CEUS. In general, ground shaking is higher in WUS as compared to CEUS, especially at longer periods (for example, 0.5 seconds or more).

Other observations regarding the variation in ground motion intensity between CEUS and WUS also were made from the sensitivity study, as summarized here. These observations are keyed to the spectral demand at the 1-second period, following the approach taken in the NCHRP 20-07 Project, which makes use of spectral demand at 1 second for quantification of the seismic design category.

1. In general, the expected ground motion shaking level at 1-second period (S_1), as measured by the 5 percent damped spectral acceleration for WUS typically ranges from 0.3 to 0.6g. In contrast for CEUS, the shaking level is much lower for S_1—typically no more than 0.2g, even for relative active seismic areas near the cities of Memphis and Charleston. For many of the population centers, including New York and Boston, S_1 is well below 0.1g—often being 0.05g or less.
2. There appears to be a larger range in ground shaking for CEUS sites as compared to WUS. For example, the design S_1 for Seattle or Salt Lake City is approximately 50 percent of San Francisco and Los Angeles, the most active regions. In contrast for CEUS, the population centers in the Northeast

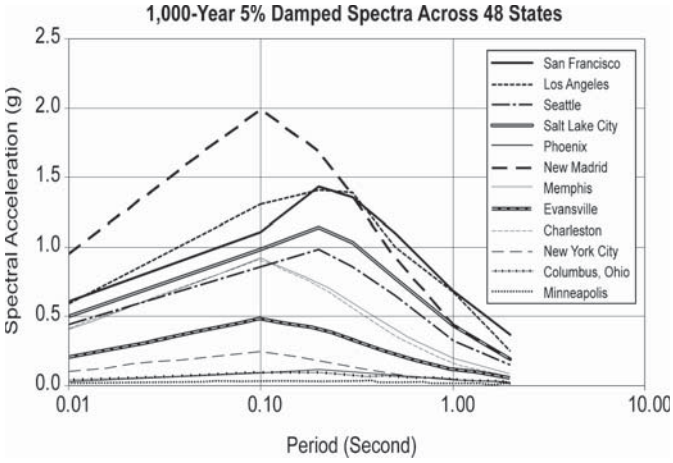

Figure 5-2. Variation in the 1,000-year benchmark soft rock spectra over the United States.

Table 5-3. 1000-year soft rock spectral ordinates.

Period (Second)	5% Damped Spectral Acceleration (g)											
	WUS Sites					EUS Sites						
	San Francisco	Los Angeles	Seattle	Salt Lake City	Phoenix	New Madrid	Memphis	Evansville	Charleston	New York	Columbus	Minneapolis
0.01	0.607	0.593	0.443	0.492	0.051	0.952	0.397	0.200	0.406	0.101	0.040	0.015
0.10	1.107	1.306	0.861	0.986	0.091	1.995	0.916	0.474	0.910	0.240	0.094	0.031
0.20	**1.431**	**1.405**	**0.985**	**1.139**	**0.116**	**1.687**	**0.746**	**0.407**	**0.713**	**0.184**	**0.090**	**0.033**
0.30	1.361	1.393	0.856	1.034	0.102	1.368	0.588	0.326	0.547	0.132	0.077	0.030
0.50	1.102	0.998	0.647	0.776	0.071	0.920	0.391	0.220	0.348	0.078	0.059	0.024
1.00	**0.686**	**0.671**	**0.328**	**0.433**	**0.039**	**0.437**	**0.191**	**0.113**	**0.158**	**0.038**	**0.038**	**0.016**
2.00	0.363	0.247	0.149	0.194	0.021	0.190	0.085	0.052	0.066	0.017	0.021	0.010
Deag Magnitude at 1-Sec	7.9	7.9	7.2	7.0	6.6	7.7	7.7	7.7	7.3	7.0	7.7	7.7
Deag Distance (Km)	11.5	12.0	7.0	1.7	171.0	17.2	59.7	164.2	23.5	413.9	616.6	939.3

Note: Spectral values shown in bold correspond to points S_{DS} and S_{D1} in Figure 5-1.

are less than 25 percent of what would be expected for Memphis and Charleston (without considering the much higher shaking at the epicenter location at New Madrid).

The relationship between spectral accelerations at 1 second and the PGA also is observed to differ between the CEUS and the WUS. A good rule-of-thumb is to assume that for the Class B soft rock ground shaking, PGA is related to S_1 by the following relationship: (1) WUS Class B Rock Sites, PGA $\approx S_1$; and (2) CEUS Class B Rock Sites, PGA $\approx 2S_1$.

5.1.3 Variation in Spectral Shapes for Soil and Rock Sites in WUS versus CEUS

The design response spectra shown in the previous section were developed from the USGS Hazard Mapping website for the referenced soft rock conditions. Figure 5-3 presents the normalized spectral curve shapes for the spectra shown in Figure 5-2.

The differences between the spectral curve shapes for CEUS (shown in dashed lines) versus WUS (shown in continuous lines) is quite evident in this figure. Beyond approximately 0.3 seconds, the ordinates for CEUS sites are generally about half of the ordinates from WUS sites for the same period, with the exception of the Columbus, Ohio and the Minneapolis, Minnesota sites. These sites are extremely far from known seismic sources and are of extremely low design shaking levels.

The spectral shapes shown in Figure 5-3 reflect the variations in spectral shapes (that is, response spectra after normalizing by the design PGA) across the United States for a referenced soft rock condition classified as Site Class B by the USGS. However, for sites where deposits of soil occur, the soft rock spectra need to be modified to local site soil conditions. For typical soil sites (commonly encountered in practical design conditions), there tends to be a higher level of amplification for the intermediate period of response around 1 second.

The effects of local soil amplification on the spectral shapes shown in Figure 5-3 also were evaluated. Following the NCHRP 20-07 Project guidelines, adjustments were made to the spectral ordinates at 0.2 (short) and 1-second (long) periods. For this evaluation an adjustment factor for Site Class E site conditions (loose sand or soft clays with $V_s < 650$ ft/sec.) was used to evaluate the maximum potential effects of soil amplification on the spectral shapes. At lower shaking levels where maximum site amplification occurs, the site adjustment factors were 3.5 and 2.5, respectively, for the short-period and long-period adjustment factors.

Figure 5-4 shows three spectral curve shapes developed from the above discussed sensitivity studies. These three curves are used to illustrate variations in the spectral curve shapes after allowing for differences between CEUS and WUS ground motions, as well as between rock and soil site effects. The three spectral curve shapes define an upper bound (UB), lower bound (LB), and intermediate (Mid) spectral shape—representing the combination of seismological variations

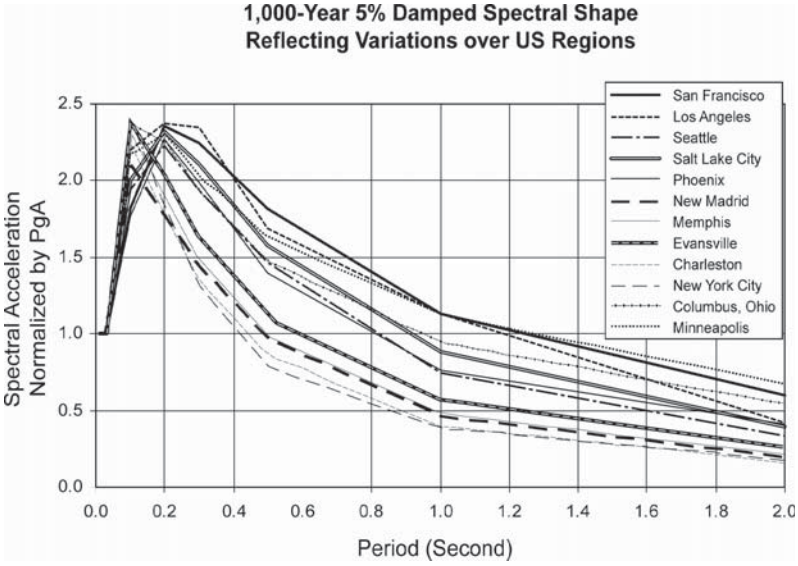

Figure 5-3. Spectral curve shapes from spectra presented in Figure 5-2.

(that is, between WUS and CEUS) and potential soil conditions variations (that is, Category B, C, D, and E sites).

The physical representation of the three shapes shown in Figure 5-4 is:

- The LB spectral curve shape was developed from the soft rock spectrum for the New York City site, a CEUS site.
- The UB spectral curve shape was developed for a San Francisco site, a WUS site, after applying the Site Class D soil factor to the San Francisco reference soft rock spectrum.
- The Mid spectral curve shape is the soft rock spectrum directly developed for San Francisco

The spectral curve ordinates at 1-second period now reflect about a factor of 4.5 variation between the UB versus the LB shaking conditions reflecting amplification of the intermediate period (that is, about 1 second) motion due to site soil response effects. As discussed later, spectrum-compatible motions will be generated for the three spectral curve shapes that then will be used for slope and retaining wall scattering

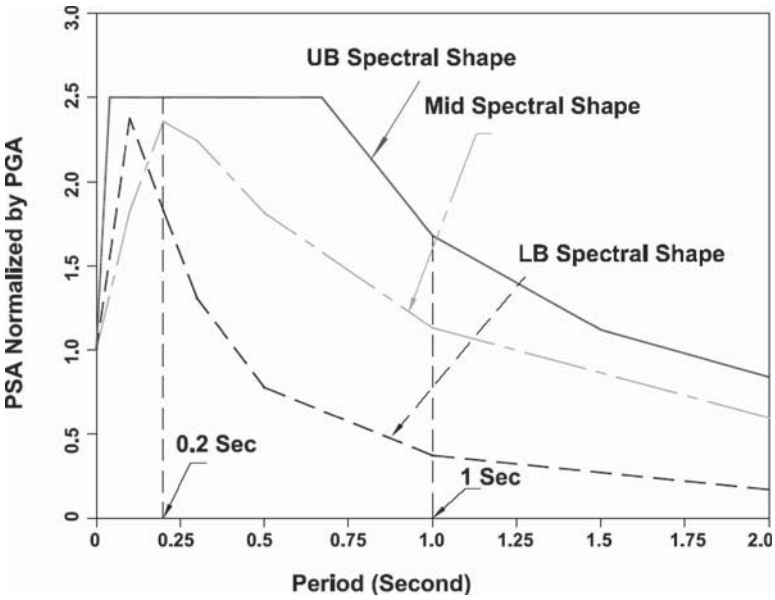

Figure 5-4. Spectral curve shapes adopted for further ground motion studies.

(coherency) analyses. The scattering analyses will be used to examine height-dependent average acceleration factors.

5.2 Newmark Displacement Correlations

The following section provides a summary of work done to refine Newmark-displacement correlations that will be used in the retaining wall, slopes and embankments, and buried structures analyses discussed in later chapters. These correlations often are presented in the form of charts or equations that can be used by the designer to estimate the amount of displacement based on an acceleration ratio at a site. The acceleration ratio is defined as the ratio of the acceleration at which a slope or retaining wall starts to slide to the peak ground acceleration. The current AASHTO *LRFD Bridge Design Specifications* has a discussion of the Newmark method in Appendix A of Section 11. Various updates of the Newmark relationship have been made. One of the more recent relationships was developed as part of the NCHRP 12-49 Project (NCHRP Report 472, 2002). The following subsections present refinements to the NCHRP 12-49 work based on a strong motion database that covers CEUS, as well as WUS.

5.2.1 Approach for Updating Newmark Charts

One major step in establishing performance criteria for design purposes is to estimate the displacement of a retaining structure or slope due to the design earthquake. When a time history of the design earthquake is available, earthquake-induced displacements can be calculated using the Newmark's sliding block method. This approach involves integrating the earthquake record twice for the region above the yield acceleration, where the yield acceleration is the point where the factor of safety in sliding is 1.0. For routine retaining structures or slope designs, however, a design motion time history is often not available, and the designer relies on design motion parameters such as PGA and PGV.

Research has shown there is a reasonable correlation between these ground motion parameters and calculated permanent displacement from the Newmark method. A relationship that was developed for the NCHRP 12-49 Project was updated using the records from recent earthquakes. To establish a nationwide relationship for permanent displacement, it was necessary to use ground motions with characteristics representative of CEUS and WUS earthquake records in the analyses.

A database of strong ground motion records was used to study the design ground motion criteria for the NCHRP 12-70 Project. The main characteristics of this database:

- Include over 1,800 strong motion records (horizontal and vertical components);
- Contain records from recent (before 2001) large-magnitude earthquakes around the world (events in Japan, Turkey, and Taiwan);
- Represent earthquake records in WUS and CEUS; and
- Contain earthquake records for rock and soil site conditions.

This strong motion database has been used to update the correlations between permanent seismic displacement (Newmark Sliding Block Method) and strong motion record characteristics developed during the NCHRP 12-49 Project. The update involved accounting for the much larger database compared to the limited database used by Martin and Qiu (1994) in developing the charts shown in the NCHRP 12-49 Project report. The database also was used to check relationships for PGV based on S_1, as described later in this chapter.

5.2.2 Description of Ground Motion Database

The ground motion database was developed from the strong motion catalog compiled as part of the United States Nuclear Regulatory Commission (USNRC) publication NUREG/CR-6728 *Technical Basis for Revision of Regulatory Guidance on Design Ground Motions: Hazard- and Risk-Consistent Ground Motion Spectra Guidelines* (McGuire et al., 2001). The catalog is available on two CDs, one for WUS and the other one for CEUS. Data are compiled in terms of magnitude, distance, and soil type bins, as follows:

- Two regions: WUS and CEUS;
- Two site conditions: rock and soil;
- Three magnitude bins: 4.5–6, 6–7, and 7–8; and
- Four distance bins: 0–10 km, 10–50 km, 50–100 km, and 100–200 km.

The earthquake records are reasonably distributed in the range of practical interest. Figure 5-5 shows the distribution of the strong motion records in the catalog.

Each record includes the following data:

- Acceleration, velocity, and displacement time histories;
- Relative displacement, relative velocity, pseudo relative velocity, absolute acceleration, and pseudo absolute acceleration spectra (5 percent damped); and
- Time interval and duration of Arias intensity for various ranges.

It should be noted that due to the limited number of recordings east of the Rocky Mountains, a majority of CEUS records are based on WUS records with a scaling factor.

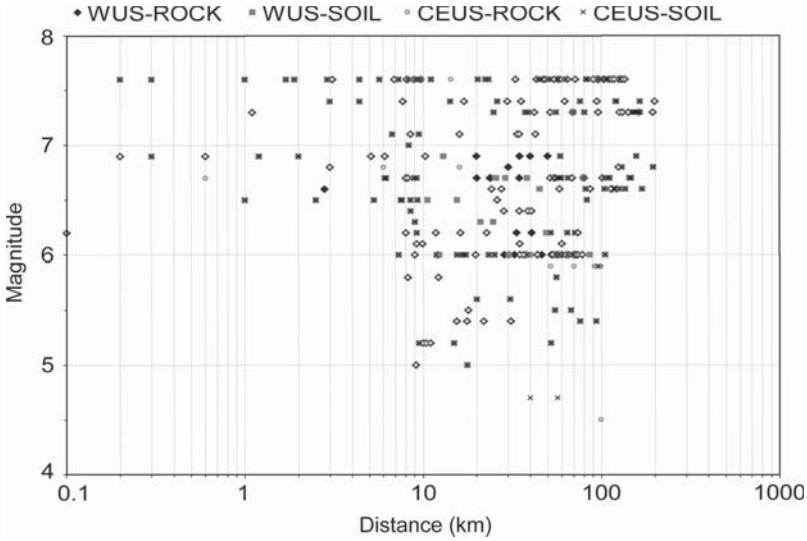

Figure 5-5. Distribution of the magnitude and distance from source for the records in the USNRC Earthquake Catalog.

5.2.3 Permanent Displacement Data

Permanent displacement is a characteristic of the strong motion record, as well as the ratio of the structure yield acceleration to peak ground acceleration in the sliding mass (k_y/k_{max}) of the subject structure. Using the strong motion records in the USNRC catalog, permanent displacements have been calculated for k_y/k_{max} values in the range of 0.01 to 1. A nonsymmetrical displacement scheme was assumed in these analyses, meaning that the displacement occurs in one direction and is not reversible. Figure 5-6 shows the concept of the Newmark sliding block method for calculation of permanent displacements due to earthquake time histories.

5.2.4 Microsoft Access Database

To evaluate the correlations between different parameters in the USNRC earthquake catalog, an Access database has been developed. The database comprises two tables, one for storage of basic record information (INFOTAB), and a second table (NEWMARK) for storage of permanent displacement data. Figure 5-7 shows a schematic diagram for the ground motion

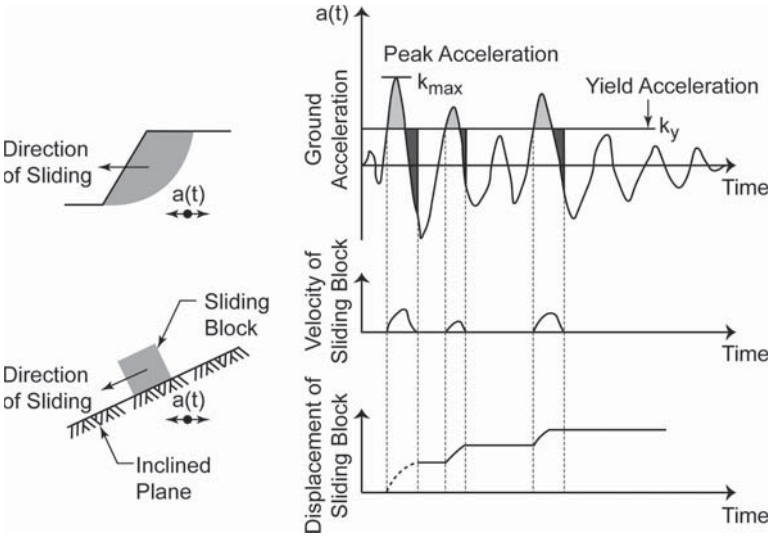

Figure 5-6. Illustration of Newmark's sliding block method for estimation of permanent displacement due to earthquake.

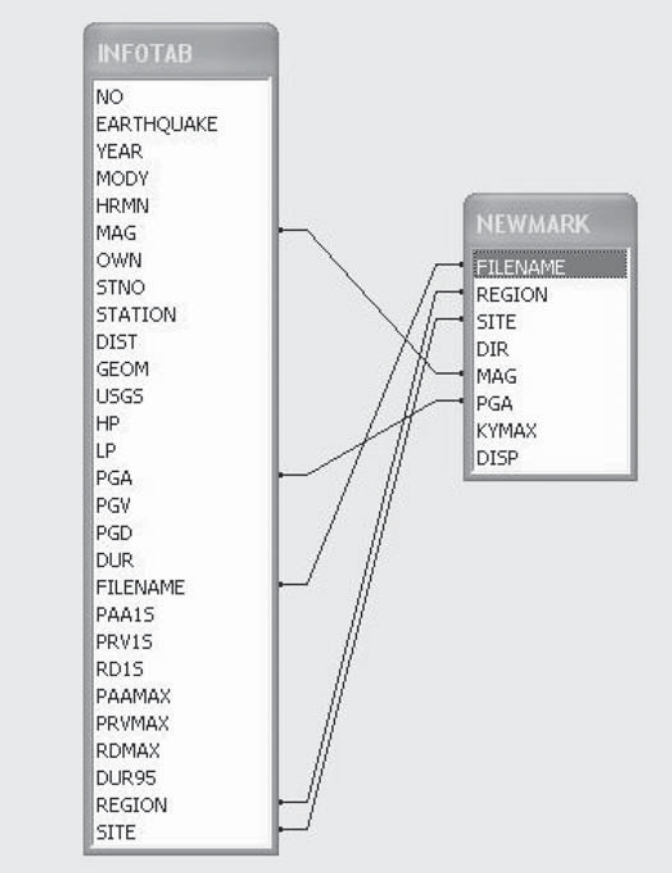

Figure 5-7. Strong motion information database model.

information database, and Table 5-4 gives a description of each field in the Access database. The developed database can be used to efficiently explore correlations between different record characteristics. It also can be used to prepare data sets required for various statistical analyses.

5.2.5 Spectral Acceleration Characteristics

To compare strong motion records from different region, magnitude, and soil type bins, the normalized spectral acceleration and normalized relative density graphs are plotted for each bin. The average spectrum for each region-site condition for different magnitude ranges was calculated. The average normalized spectra are presented in Figures 5-8 and 5-9.

Results in Figures 5-8 and 5-9 show the following trends:

- Records with higher magnitudes generally have higher amplitude in the long-period range.
- Records for WUS and CEUS generally have different spectral shapes. WUS records have higher normalized amplitudes in lower frequency (long-period) ranges, while CEUS records have higher amplitudes in high frequency (low-period) ranges.
- The difference in spectral shape between WUS and CEUS records is more evident for the rock records.
- Having larger amplitudes at long periods implies that for the same PGA, the earthquake records in WUS will have larger PGV, therefore inducing larger displacements in the structure.

5.2.6 Correlation between PGV and S_1, PGA and M

Several correlations between PGV and other ground motion parameters such as S_1, PGA, and M were developed during this study. After reviewing recent publications related to this subject, a revised form of a PGV correlation suggested by Abrahamson (2005) for the estimation of PGV from spectral acceleration at one second (S_1) was selected for use, as discussed in Section 5.3.

It is expected that in the future, USGS will publish recommended PGV values for different locations nationwide. In that case the S_1-PGV correlation will be replaced in favor of design PGV values, and the designers can use Newmark displacement correlations directly using the USGS-recommended PGV values.

5.2.7 Newmark Sliding Block Displacement Correlations

Various researchers have proposed different correlations for predicting the permanent displacement of earth structures subjected to seismic loading. A summary and comparison of some of these correlations can be found in a paper by Cai and Bathurst (1996). The majority of these correlations are based on the results of direct Newmark sliding block analyses on a set of strong motion records.

Martin and Qiu (1994) used the following general form for estimation of Newmark displacement:

$$d = C\left(k_y/k_{\max}\right)^{a1}\left(1-k_y/k_{\max}\right)^{a2} A^{a3} V^{a4} M^{a5} \qquad (5\text{-}1)$$

Using a database of earthquake records with a magnitude range between 6.0 and 7.5, published by Hynes and Franklin (1984), Martin and Qiu concluded that the correlation with *M* (magnitude) is negligible. The following simplified equation was proposed by Martin and Qiu and adopted in NCHRP 12-49 Project:

$$d = 6.82\left(k_y/k_{\max}\right)^{-0.55}\left(1-k_y/k_{\max}\right)^{5.08} A^{-0.86} V^{-0.86} M^{1.66} \qquad (5\text{-}2)$$

where

d = permanent displacement in inches,
k_y = yield acceleration,

Table 5-4. Description of different fields in the access ground motion database.

Table	Field	Description
INFOTAB	NO	Earthquake event number
INFOTAB	EARTHQUAKE	Earthquake event name
INFOTAB	YEAR	Event year
INFOTAB	MODY	Event date
INFOTAB	HRMN	Event time
INFOTAB	MAG	Earthquake magnitude
INFOTAB	OWN	Station owner
INFOTAB	STNO	Station number
INFOTAB	STATION	Station name
INFOTAB	DIST	Closest distance from source
INFOTAB	GEOM	Geomatrix site classification code
INFOTAB	USGS	USGS site classification code
INFOTAB	HP	Filter corner frequency, high
INFOTAB	LP	Filter corner frequency, low
INFOTAB	PGA	Peak ground acceleration
INFOTAB	PGV	Peak ground velocity
INFOTAB	PGD	Peak ground displacement
INFOTAB	DUR	Duration
INFOTAB	FILENAME	Record file name
INFOTAB	PAA1S	Pseudo spectral acceleration at 1 second
INFOTAB	PRV1S	Pseudo relative velocity at 1 second
INFOTAB	RD1S	Relative displacement at 1 second
INFOTAB	PAAMAX	Peak pseudo spectral acceleration
INFOTAB	PRVMAX	Peak pseudo relative velocity
INFOTAB	RDMAX	Peak relative displacement
INFOTAB	DUR95	5%-95% Arias intensity duration
INFOTAB	REGION	Region (WUS or CEUS)
INFOTAB	SITE	Site type (Soil/Rock)
NEWMARK	FILENAME	Record file name
NEWMARK	REGION	Region (WUS or CEUS)
NEWMARK	SITE	Site type (Soil/Rock)
NEWMARK	DIR	Record direction (horizontal/vertical)
NEWMARK	MAG	Earthquake magnitude
NEWMARK	PGA	Peak ground acceleration
NEWMARK	KYMAX	k_y/k_{max} (ratio of yield acceleration to PGA)
NEWMARK	DISP	Calculated permanent (Newmark) displacement

Note: Rock/Soil Definitions ≈A and B for rock, C, D and E for soil based on NEHRP classification.

k_{max} = the maximum seismic acceleration in the sliding block,
A = peak ground acceleration (in/sec^2), and
V = peak ground velocity (in/sec).

A correlation based on Equation (5-2), but in logarithmic form, was used for estimation of Newmark displacement from peak ground acceleration and peak ground velocity. Writing Equation (5-2) in logarithmic form resulted in the following equation:

$$\log(d) = b_0 + b_1 \log(k_y/k_{max}) + b_2 \log(1 - k_y/k_{max}) + b_3 \log(k_{max}) + b_4 \log(PGV) \quad (5\text{-}3)$$

Using a logarithmic transformation of the data helped to stabilize the variance of residuals and normalize the variables, hence improving the correlation in the entire range of the parameters.

The coefficients for Equation (5-3) were estimated using regression analysis. The permanent displacement data from

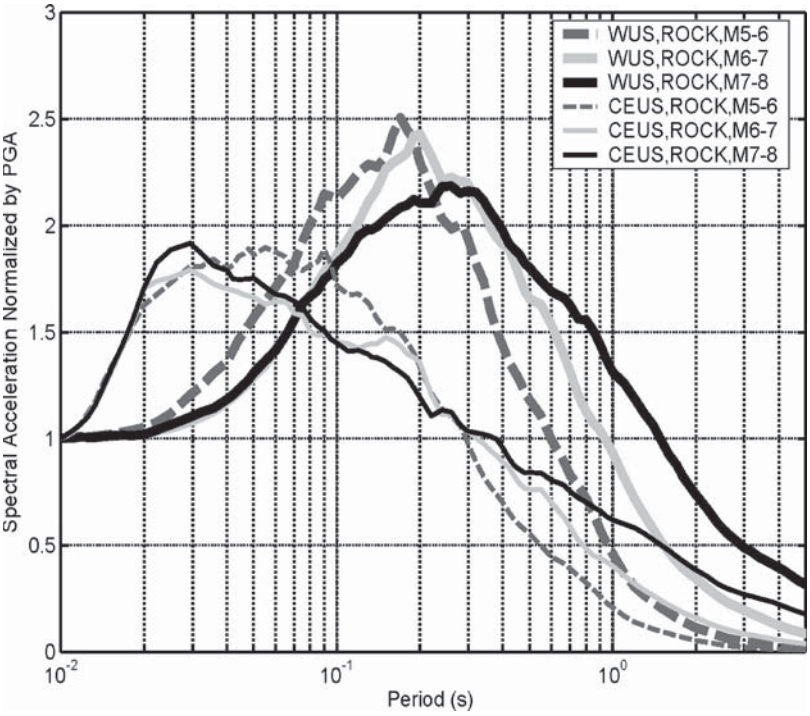

Figure 5-8. Average normalized spectral acceleration for rock records.

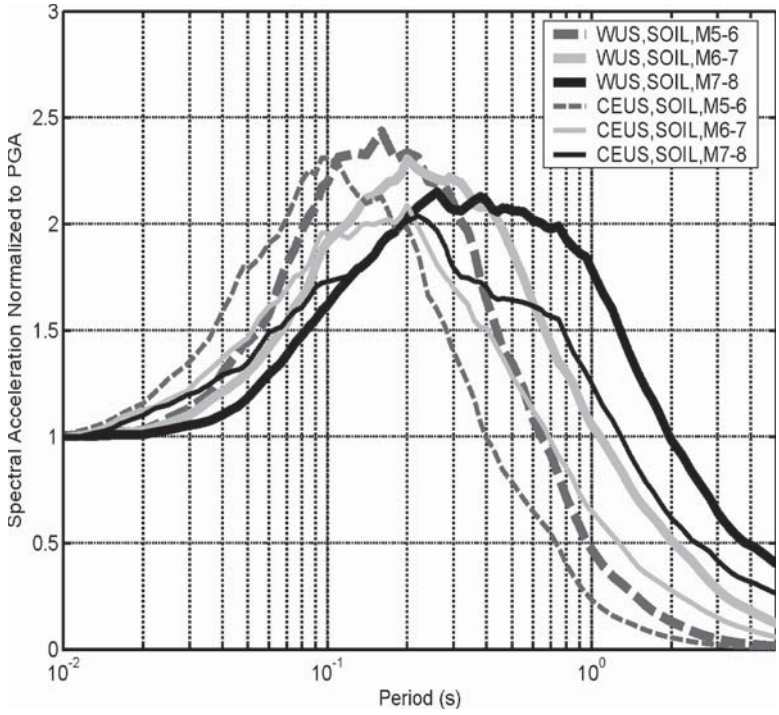

Figure 5-9. Average normalized spectral acceleration for soil records.

the previously mentioned database were used in the regression analysis. The regression analyses were performed for different regions (WUS/CEUS) and site conditions (rock/soil), resulting in four different correlations. The correlations are presented in Equations (5-4) to (5-7). The units in Equations (5-4) to (5-7) are displacement (d) in inches, PGA in g, and PGV in in/sec.

WUS-Rock:

$$\log(d) = -1.55 - 0.75\log\left(k_y/k_{\max}\right) + 3.05\log\left(1 - k_y/k_{\max}\right) - 0.76\log\left(k_{\max}\right) + 1.56\log(\text{PGV}) \quad (5\text{-}4)$$

with a standard error of 0.22 $\log_{10}$ units.

WUS-Soil:

$$\log(d) = -1.56 - 0.72\log\left(k_y/k_{\max}\right) + 3.21\log\left(1 - k_y/k_{\max}\right) - 0.87\log\left(k_{\max}\right) + 1.62\log(\text{PGV}) \quad (5\text{-}5)$$

with a standard error of 0.22 $\log_{10}$ units.

CEUS-Rock:

$$\log(d) = -1.31 - 0.93\log\left(k_y/k_{\max}\right) + 4.52\log\left(1 - k_y/k_{\max}\right) - 0.46\log\left(k_{\max}\right) + 1.12\log(\text{PGV}) \quad (5\text{-}6)$$

with a standard error of 0.31 $\log_{10}$ units.

CEUS-Soil:

$$\log(d) = -1.49 - 0.75\log\left(k_y/k_{\max}\right) + 3.62\log\left(1 - k_y/k_{\max}\right) - 0.85\log\left(k_{\max}\right) + 1.61\log(\text{PGV}) \quad (5\text{-}7)$$

with a standard error of 0.23 $\log_{10}$ units.

When using the above equations, the term $k_{\max}$ is the peak ground acceleration coefficient (PGA) at the ground surface modified by the Site Class factor for peak ground acceleration (F_{pga}). The current AASHTO *LRFD Bridge Design Specifications* define the site-adjusted PGA as A_s. For this Project $k_{\max}$ is used rather than A_s to be consistent with the common practice in geotechnical earthquake engineering of using k as the seismic coefficient during seismic earth pressure and slope stability evaluations.

5.2.8 Comparison Between Correlations

A comparison between correlations for different regions and site conditions has been performed. The comparison was carried out for two cases, assuming PGV (in/sec) = 30 × PGA (in/sec^2) and PGV (in/sec) = 60 × PGA (in/sec^2), respectively. These comparisons are shown in Figures 5-10 through 5-17. The results from these comparisons are summarized as follows:

- Figures 5-10 and 5-11 show the comparison between rock and soil correlations for WUS region [Equations (5-4) and (5-5)] for PGV = 30 × $k_{\max}$ and PGV = 60 × $k_{\max}$, respectively.
- Figures 5-12 and 5-13 show the comparison between the rock and soil correlations for CEUS region [Equations (5-6) and (5-7)] for PGV = 30 × $k_{\max}$ and PGV = 60 × $k_{\max}$, respectively.
- Figures 5-14 and 5-15 compare WUS-Rock and CEUS-Rock correlations [Equations (5-4) and (5-6)].
- Figures 5-16 and 5-17 show the comparison between Martin-Qiu correlation and WUS-Rock correlation [Equations (5-2) and (5-4)].

These comparisons show that the CEUS-Rock correlation results in smaller displacements in comparison to other correlations, including the Martin-Qiu correlation. It should be

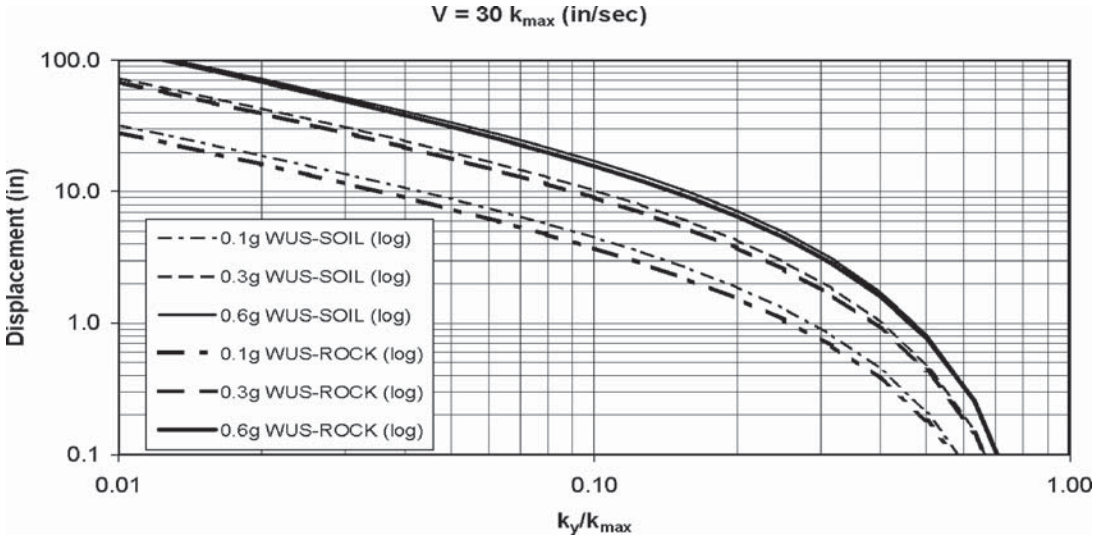

Figure 5-10. Comparison between WUS-Rock and WUS-Soil correlations for PGV = 30 × k_{max}.

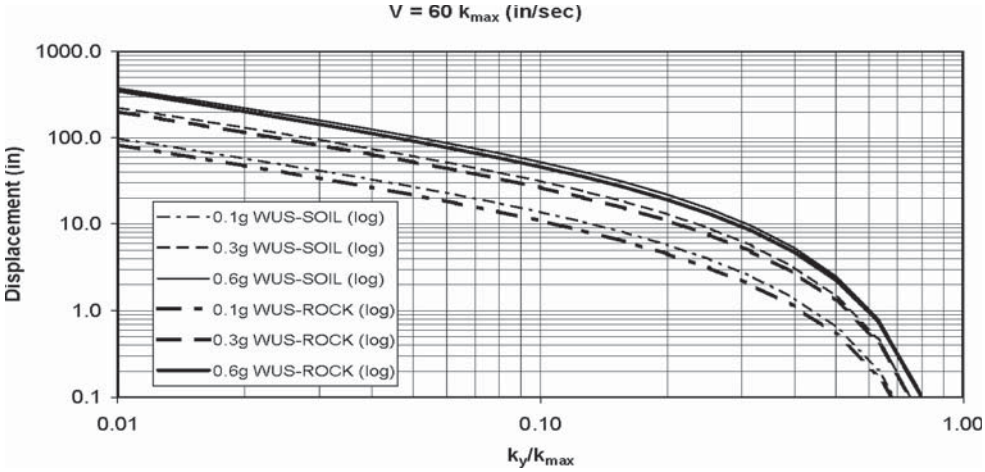

Figure 5-11. Comparison between WUS-Rock and WUS-Soil correlations for PGV = 60 × k_{max}.

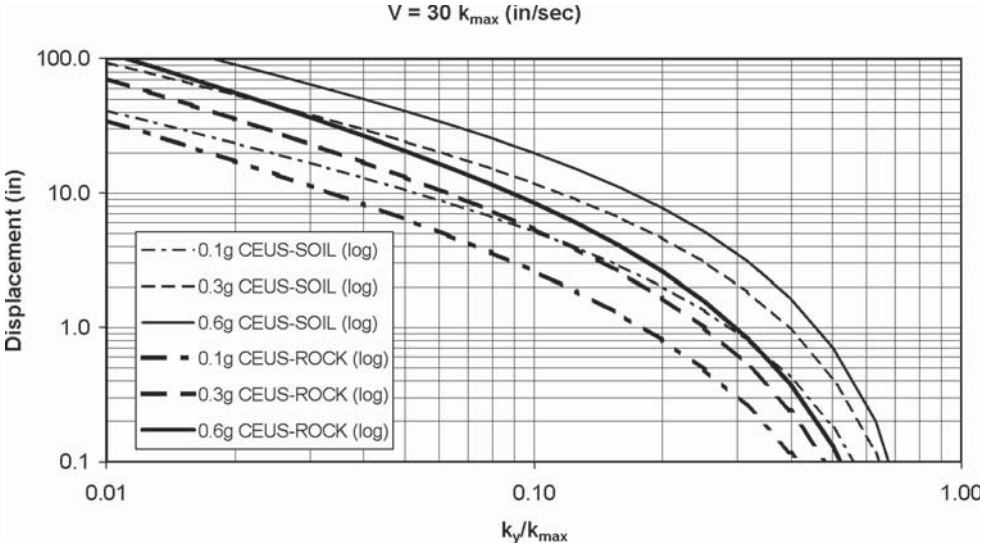

Figure 5-12. Comparison between CEUS-Rock and CEUS-Soil correlations for PGV = 30 × k_{max}.

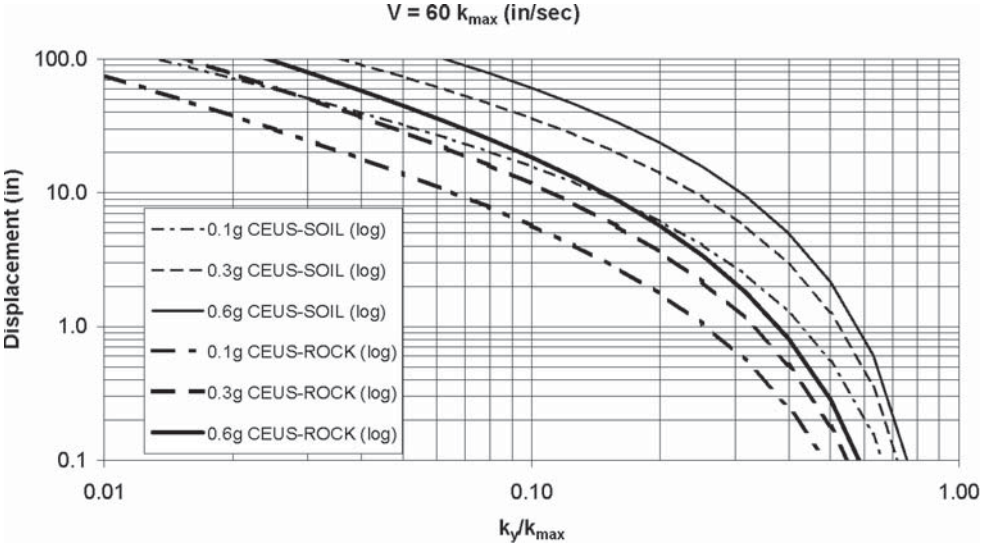

Figure 5-13. Comparison between CEUS-Rock and CEUS-Soil correlations for PGV = 60 × k_{max}.

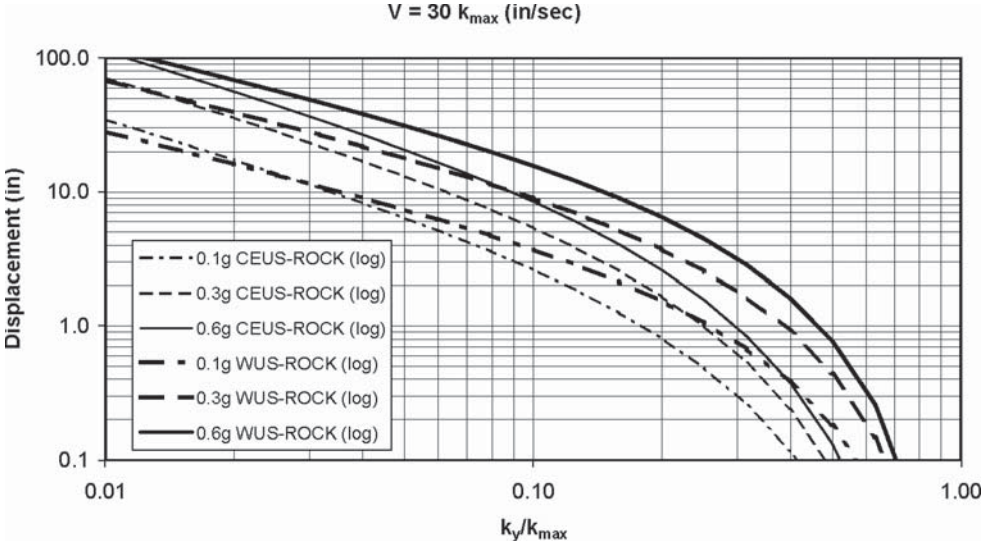

Figure 5-14. Comparison between WUS-Rock and CEUS-Rock correlations for PGV = 30 × k_{max}.

noted that the correlations for other regions (that is, CEUS-Soil, WUS-Rock, and WUS-Soil) result in relatively similar displacement levels slightly greater than the Martin-Qiu correlation.

Consequently correlations were combined for these data leading to a mean displacement correlation given by:

All data except CEUS-Rock:

$$\log(d) = -1.51 - 0.74\log\left(k_y/k_{\max}\right) + 3.27\log\left(1 - k_y/k_{\max}\right) - 0.80\log\left(k_{\max}\right) + 1.59\log(\mathrm{PGV}) \quad (5\text{-}8)$$

with a standard error of 0.23 $\log_{10}$ units.

5.2.9 Confidence Level

The displacement correlations discussed in previous sections were based on a mean regression curve on the observed data. For design purposes a higher confidence level than the mean curve (the mean curve corresponds to 50 percent confidence level) is often selected. A common practice is to use the mean curve plus one standard deviation, which approximately corresponds to a confidence level of 84 percent. Figures 5-18 and 5-19 show the 84 percent confidence intervals for permanent displacement based on site-adjusted peak ground acceleration coefficient of 0.3 and PGV = 30 × k_{max} and

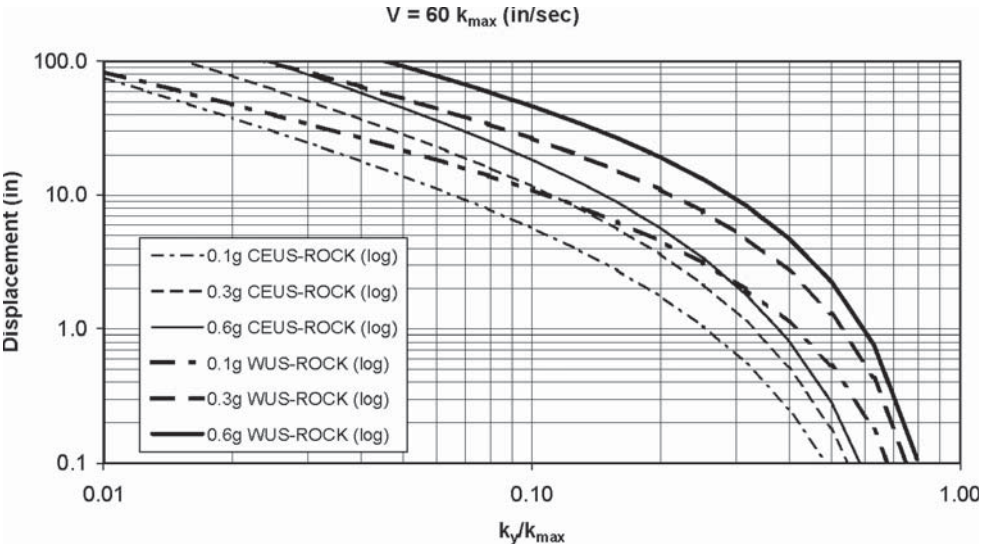

Figure 5-15. Comparison between WUS-Rock and CEUS-Rock correlations for PGV = 60 × k_{max}.

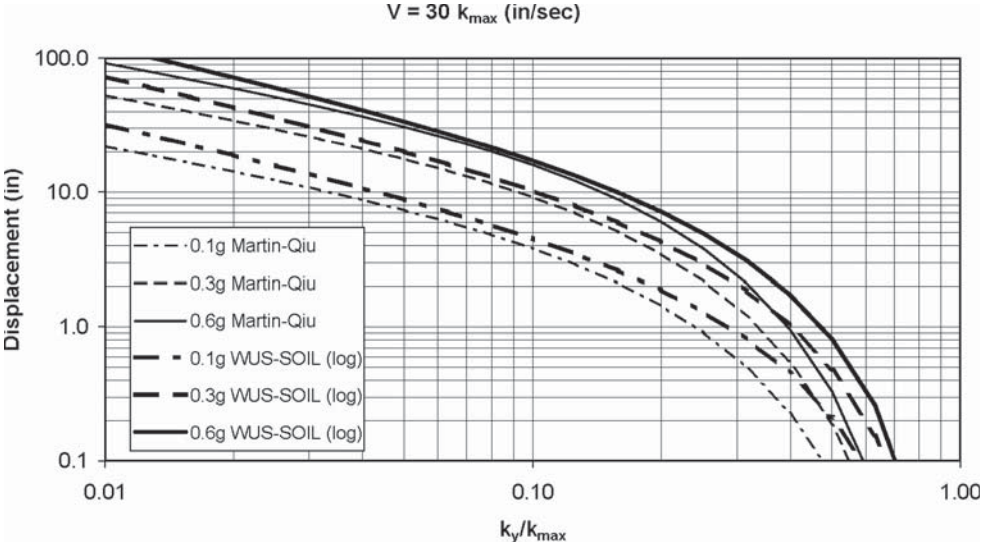

Figure 5-16. Comparison between Martin-Qiu and WUS-Soil correlations for PGV = 30 × k_{max}.

PGV = 60 × k_{max}, respectively, with respect to the mean design curve given by Equation (5-8).

5.2.10 Design Recommendations

For design applications, Equation (5-8) for soil and rock sites for WUS and CEUS and Equation (5-6) for CEUS rock sites are recommended. The regression curves shown on Figure 5-18 and Figure 5-19 suggest that 84 percent confidence levels in displacement evaluations could be reasonably approximated by multiplying the mean curve by a factor of 2.

5.3 Correlation of PGV with S_1

A procedure for establishing the PGV for design from the spectral acceleration at one second (S_1) also was developed for the Project. For earth and buried structures, PGV provides a direct measure of the ground deformation (as opposed to ground shaking parameters represented by the spectral amplitude) and is a more meaningful parameter than PGA or spectral accelerations for designing against kinematic loading induced by ground deformation. Also PGV is a key parameter used for Newmark deformation analysis, as described in Section 5.2.

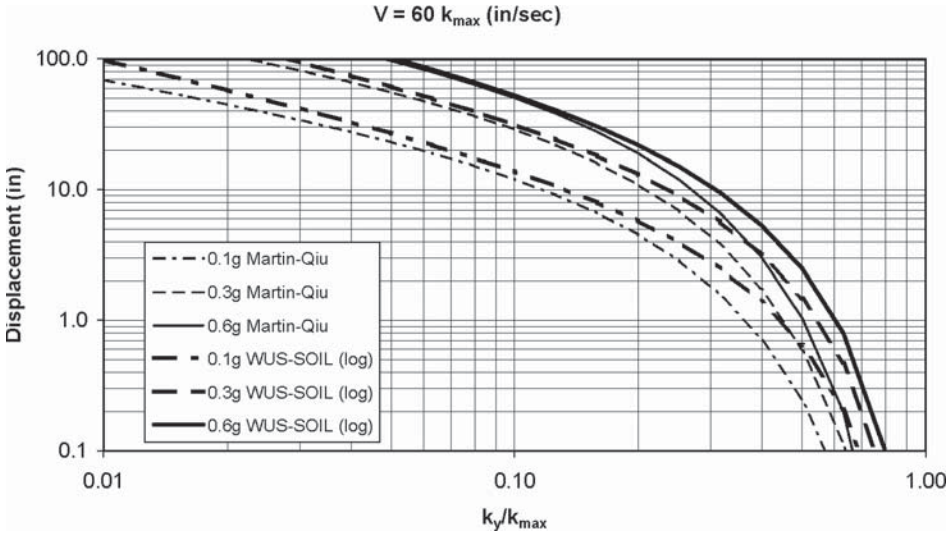

Figure 5-17. Comparison between Martin-Qiu and WUS-Soil correlations for PGV = 60 × k_{max}.

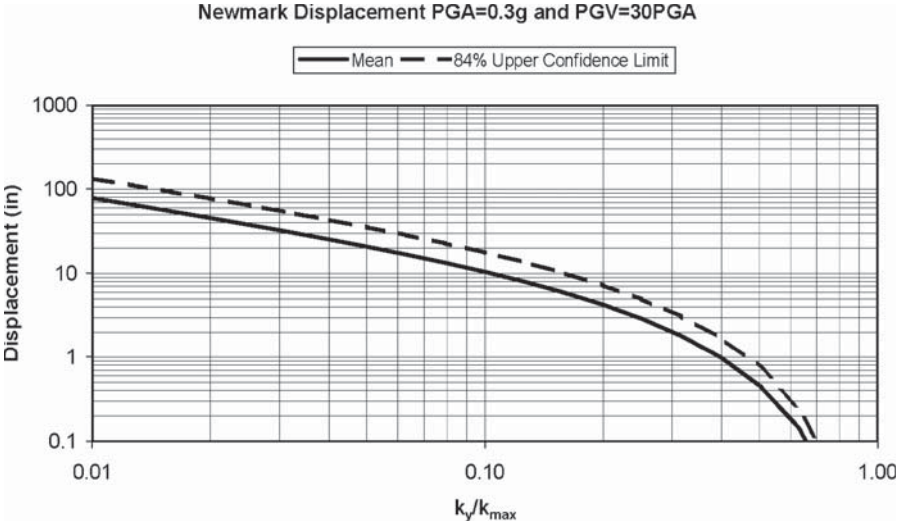

Figure 5-18. Mean Newmark displacement and 84% confidence level, PGA = 0.3g, PGV = 30 × k_{max}.

The initial approach taken to develop the PGV-S_1 correlation involved performing statistical studies of the USNRC database. However, the resulting correlation exhibited considerable scatter. Subsequently a correlation being developed by Dr. Norm Abrahamson of the Pacific Gas and Electric Group in San Francisco was identified through discussions with seismologists involved in ground motion studies. Dr. Abrahamson forwarded a draft paper that he was writing on the topic. (A copy of the draft paper was originally included in Appendix D. Copyright restrictions prevented including this draft as part of the Final Report for the NCHRP 12-70 Project.)

In the draft of the Abrahamson's paper, the following regression equation was recommended for determining PGV based on the spectral acceleration at 1 second (S_1) and the magnitude (M) of the earthquake.

$$\ln(\mathrm{PGV}) = 3.97 + 0.94\ln(S_1) + 0.013\left(\ln(S_1) + 2.93\right)^2 + 0.063M \qquad (5\text{-}9)$$

where PGV is in units of cm/sec, S_1 is spectral acceleration at $T = 1$ sec in units of g, and M is magnitude. Dr. Abrahamson reported that this equation has a standard deviation of 0.38 natural log units.

Because the strong motion database used in Dr. Abrahamson's regression analyses consists of exclusively the WUS database, an evaluation was performed to determine whether the above regression equation would be valid for representative

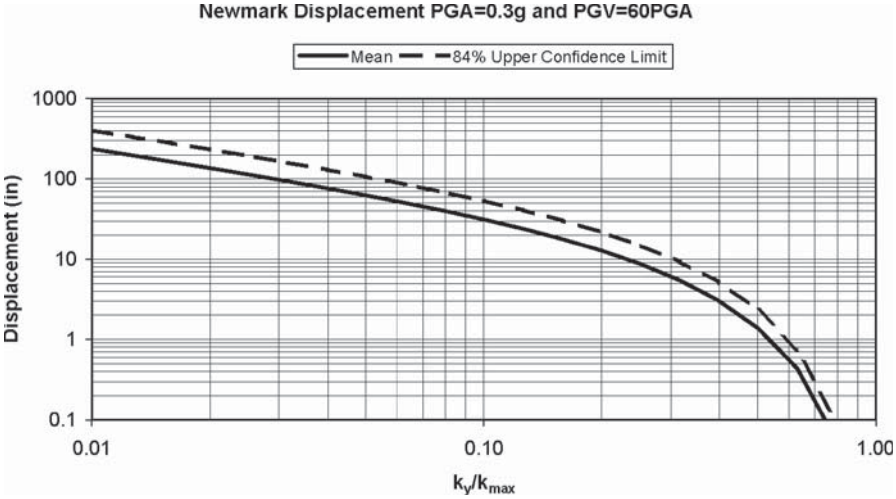

Figure 5-19. Mean Newmark displacement and 84% confidence level, PGA = 0.3g, PGV = 60 × k_{max}.

CEUS records. The NUREG/CR-6728 strong motion data, as discussed in Section 5.2.4, was used to evaluate the validity of the Abrahamson PGV equation shown above. Figures 5-20 through 5-24 present comparisons between the results of the Abrahamson PGV equation and the strong motion database from NUREG/CR-6728.

The following conclusions can be made from Figures 5-20 through 5-24:

1. The Abrahamson PGV equation gives reasonable predictions using the NUREG/CR-6728 database, even though the strong motion database from CEUS is characterized by much lower long-period ground motion content. Part of the reason is that the spectral acceleration at 1 second has been used as a dependent variable in the regression equation. The reasonableness of the comparisons occurs when rock and soil conditions are separated for the CEUS and the WUS.
2. Magnitude (M) appears to play a very small role in affecting the predicted PGV result. For example, there is very little change (that is, barely 10 percent) in the resultant PGV value as the magnitude M changes from 5.5 to 7.5. The insensitivity of magnitude, as well as the potential difficulty and/or ambiguity in establishing the deaggregated magnitude parameter for many CEUS sites where the seismic sources are not well defined, was discussed with Dr. Abrahamson (2005). From a practical perspective, it was concluded that the PGV correlation could be significantly simplified by eliminating the parameter M from Equation (5-9). Dr. Abrahamson concurred with this suggestion.
3. During discussions with Dr. Abrahamson, various other versions of the PGV predictive equation were discussed. Other versions involve using spectral acceleration at the 3-second period. These equations are more suitable for capturing peak ground velocity if there is a strong velocity pulse from near-fault earthquake records. However, for applications involving the entire United States, especially for CEUS, these near-fault attenuation equations are not believed to be relevant or appropriate at this time.

Dr. Abrahamson reported that his research found that PGV is strongly correlated with the spectral acceleration at 1 second (S_1); therefore, the attenuation equation used S_1 to anchor the regression equation. Dr. Abrahamson commented that besides the 1-second spectral acceleration ordinate, other spectral values around 1 second might be used to improve the PGV prediction; however, from his experience, the PGA (that is, peak ground acceleration or spectral acceleration at zero-second period) has a frequency too far off for correlating with PGV, and this difference tends to increase the error in the regression equation. From these comments, a decision was made to use the PGV equation based solely on the 1-second spectral acceleration ordinate (S_1). In all the presented figures, the PGA amplitudes are depicted in four different categories.

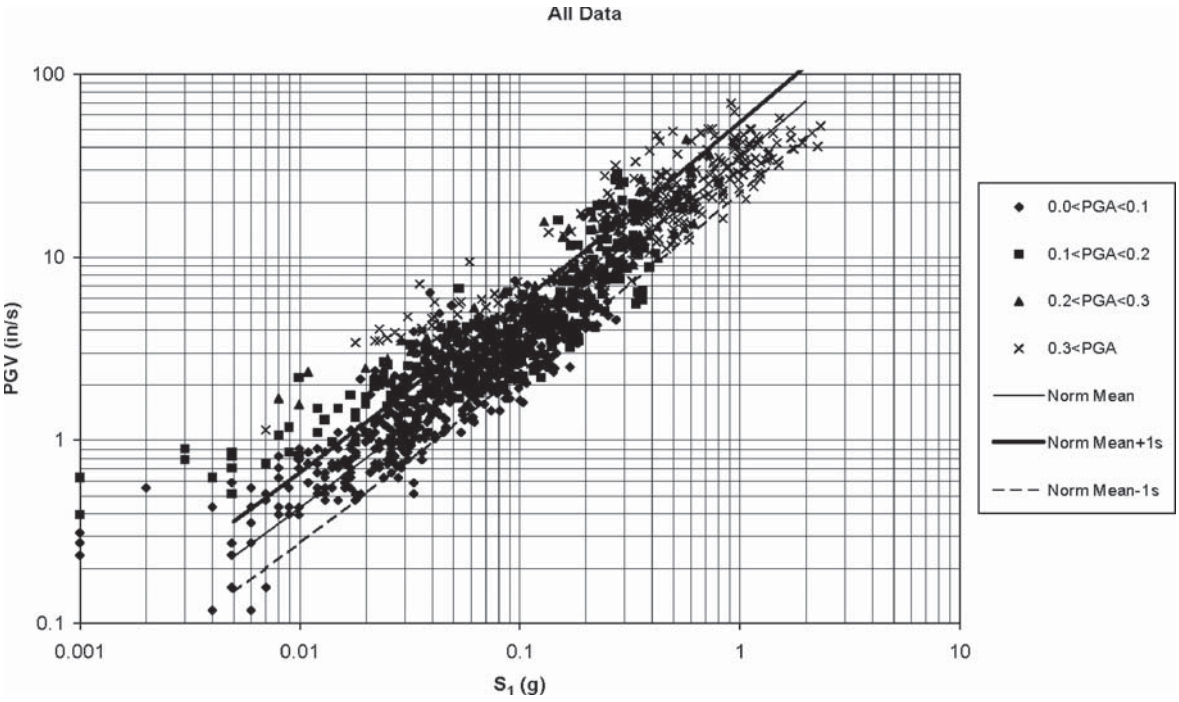

Figure 5-20. Comparison between Abrahamson PGV equation with all data in NUREG/CR-6728.

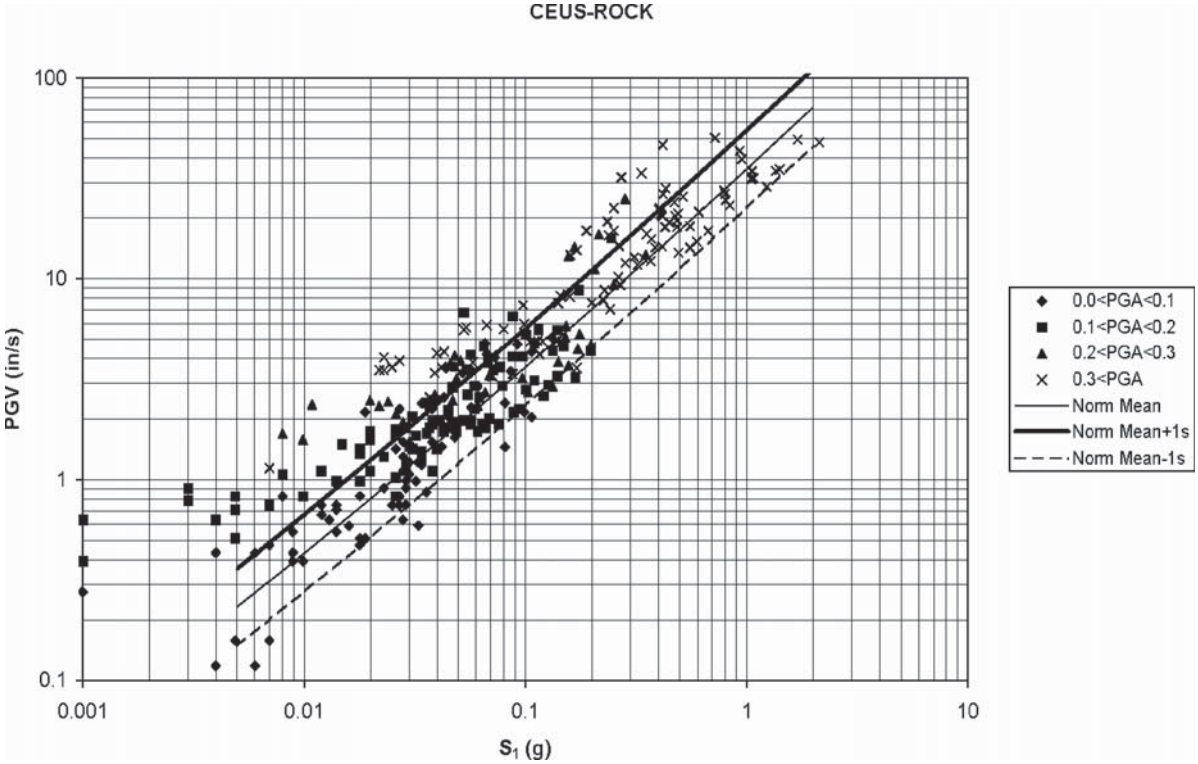

Figure 5-21. Comparison between Abrahamson PGV equation with only NUREG/CR-6728 CEUS rock data.

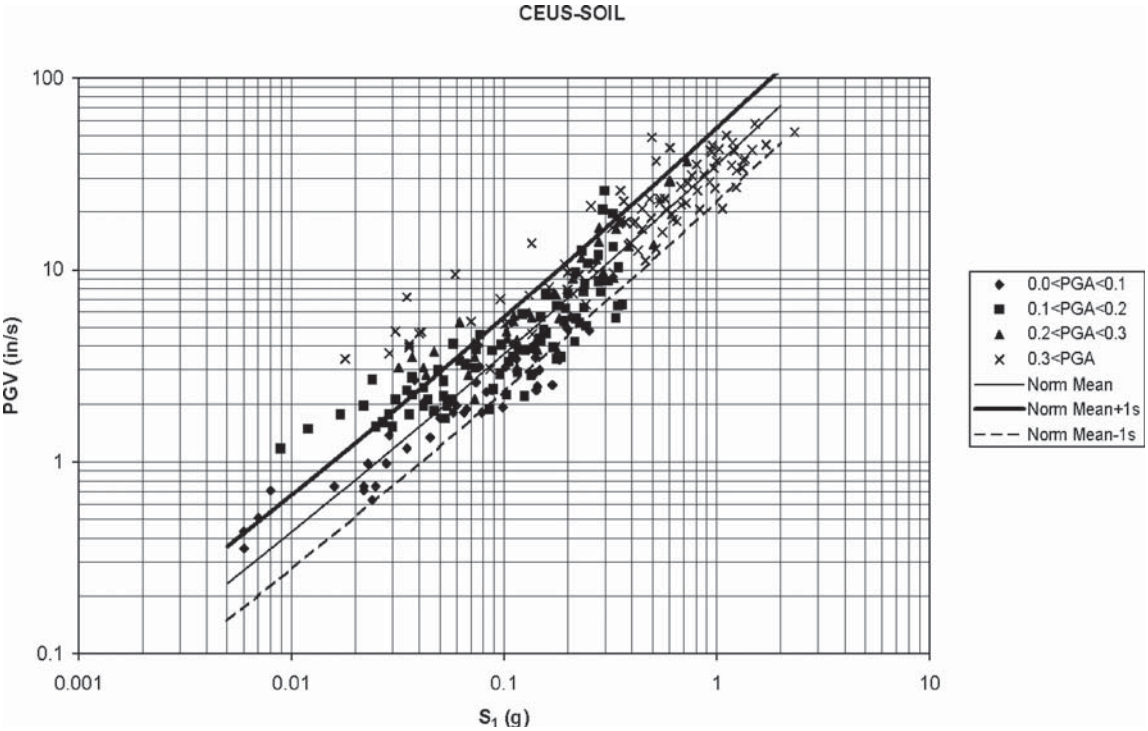

Figure 5-22. Comparison between Abrahamson PGV equation with only NUREG/CR-6728 CEUS soil data.

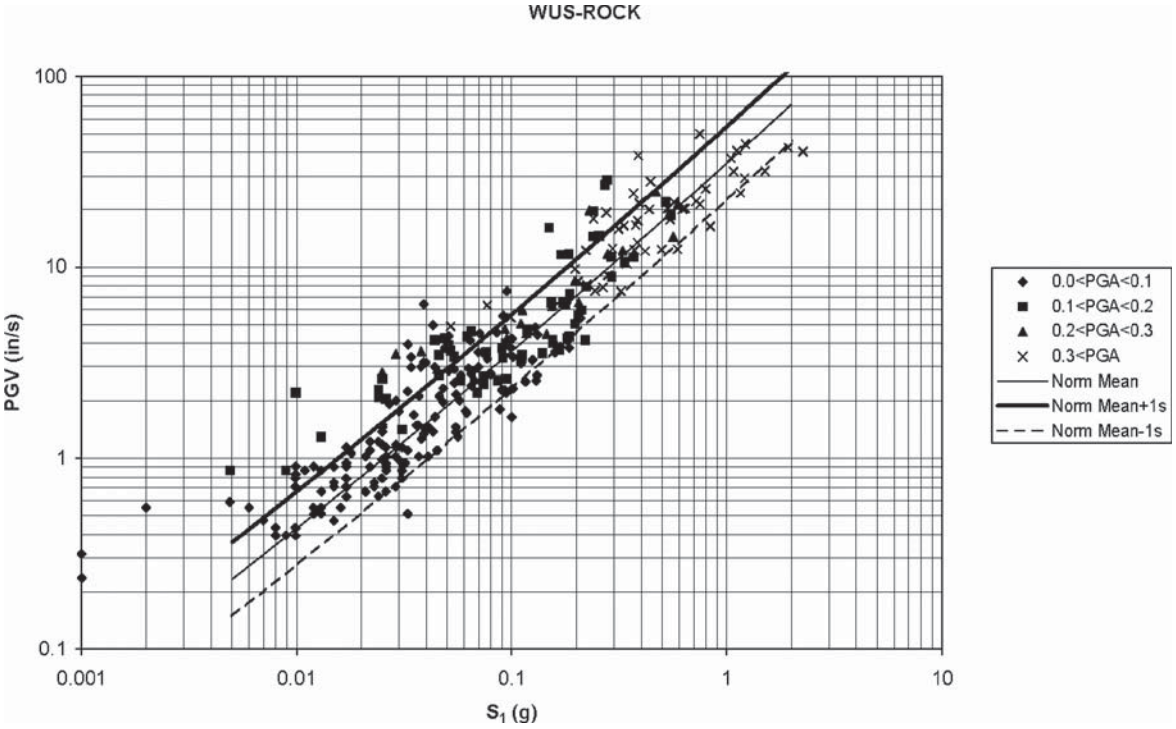

Figure 5-23. Comparison between Abrahamson PGV equation with only NUREG/CR-6728 WUS rock data.

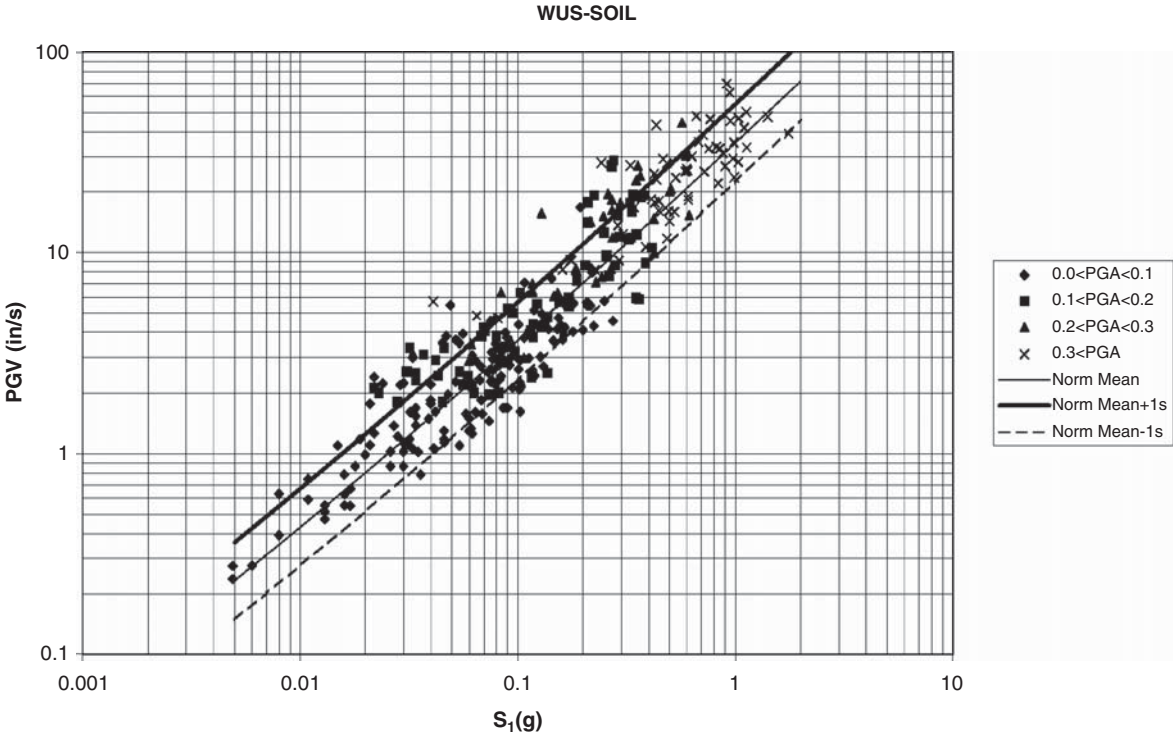

Figure 5-24. Comparison between Abrahamson PGV equation with only NUREG/CR-6728 WUS soil data.

From these plots, the trend of increasing PGV with S_1 is very evident; however, there is no discernible trend for PGA.

In addition to presenting the median PGV equation, Figures 5-20 through 5-24 show the mean-plus and the mean-minus one standard deviations. These lines use the standard deviation coefficient of 0.38 as suggested by the Abrahamson PGV equation. The use of the standard deviation coefficient of 0.38 implies that the mean-plus one standard deviation and the mean-minus one standard deviation will be 1.46 and 0.68 of the median PGV values.

From the five figures presented in this section, the following relationship was selected for estimating PGV for design analyses, with the equation reduced to the following expression in $\log_{10}$ units rather than natural log basis:

$$\mathrm{PGV} = 0.3937 \times 10^{0.434C_1} \tag{5-10}$$

where

PGV = inches/sec and

$$C_1 = 4.82 + 2.16 \log_{10} S_1 + 0.013\left[2.30 \log_{10} S_1 + 2.93\right]^2$$

For design purposes Equation (5-10) was later simplified to the following equation.

$$\mathrm{PGV}\left(\mathrm{in}/\mathrm{sec}\right) = 55 F_v S_1 \tag{5-11}$$

Equation (5-10) was developed by using the mean-plus one standard deviation prediction (shown in heavy thick lines in the five figures for an $M = 7.5$ event).

5.4 Conclusions

The work presented in this chapter forms the basis of the ground motion determination used during the seismic analysis and design of retaining walls, slopes and embankments, and buried structures. The results of the ground motion studies were developed by interpreting existing strong motion data relative to recommendations that were made for the update of the AASHTO *LRFD Bridge Design Specifications.*

Earthquake ground motion studies described in this chapter are based on an earthquake with a 7 percent probability of exceedance in 75 years (that is, the 1,000-year return period), consistent with the recommendations adopted by AASHTO in July of 2007. The 1,000-year earthquake ground motions are available in maps and from an implementation CD developed by the USGS for AASHTO. As shown in this chapter, the recommended 1,000-year return period is a significant change from the existing AASHTO Specifications, in terms of PGA and spectral shape for WUS and CEUS locations. These differences need to be considered when conducting seismic analysis and design for retaining walls, slopes and embankments, and buried structures, and therefore these ground motion discussions form an important component of the overall NCHRP 12-70 Project.

The information from ground motion review also was used to update Newmark displacement correlations, as also described in this chapter. Newmark displacement correlations will be used for estimating the displacement of retaining walls, slopes and embankments, and buried structures, as discussed in later chapters. The update in the displacement correlations considered ground motions that will typically occur in CEUS as well as WUS. Again both the PGA and spectral shape were important considerations during the development of these correlations. Results of the Newmark displacement studies led to two equations [Equation (5-6) for CEUS rock sites and Equation (5-8) for WUS soil and rock sites and CEUS soil sites] and two charts (Figures 5-18 and 5-19) for use in design.

As a final component of the ground motion studies, a correlation between PGV and spectral acceleration at 1 second (S_1) was developed. This information is needed within the Newmark displacement correlations developed for this Project, as well as for evaluating the transient response of buried structures. Equation (5-10) presents the correlation. Results of the equation are compared with records from the USNRC strong motion database to show the reasonableness of the recommended equation. For design purposes Equation (5-10) was later simplified to Equation (5-11). The simplified equation provided a reasonable approximation of the data.

CHAPTER 6

Height-Dependent Seismic Coefficients

This chapter summarizes the results of seismic wave incoherence or scattering studies. These scattering studies were conducted to evaluate the variation in average ground acceleration behind retaining walls and within slopes, as a function of height. The primary objectives of these studies were to

- Evaluate the changes in ground motion within the soil mass that occur with height and lateral distance from a reference point. The consequence of this variation is that the average ground motion within a soil mass behind a retaining wall or within a slope, which results in the inertial force on the wall or within the slope, is less than the instantaneous peak value within the zone.
- Develop a method for determining the average ground motion that could be used in the seismic design of retaining structures, embankments and slopes, and buried structures based on the results of the scattering evaluations.

The wave scattering analyses resulted in the development of a height-dependent seismic coefficient. These results are described in the following sections of this chapter. The discussions provide background for the scattering studies, the results of the scattering analyses for a slope and for retaining walls, and recommendations on the application of the scattering effects. These results also will form the basis of discussion in sections proposed for use in the AASHTO *LRFD Bridge Design Specifications.*

6.1 Wave Scattering Evaluations

Current practice in selecting the seismic coefficient for retaining walls normally assumes rigid body soil response in the backfill behind a retaining wall. In this approach the seismic coefficient is defined by the PGA or some percentage of the PGA. A limit equilibrium concept, such as the M-O equation, is used to determine the force on the retaining wall. A similar approach often is taken when assessing the response of a slope to seismic loading. In this case the soil above the critical failure surface is assumed to be a rigid mass. By assuming a rigid body response, the ground motions within the rigid body are equal throughout. For wall or slope heights in excess of about 20 to 30 feet, this assumption can be questioned. The following sections of this chapter summarize the results of the wave scattering analyses. This summary starts with a case study for a 30-foot high slope to illustrate the wave scattering process. This is followed by a more detailed evaluation of the scattering effects for retaining walls.

6.1.1 Scattering Analyses for a Slope

Wave propagation analyses were conducted for an embankment slope that was 30 feet in height and had a 3H:1V (horizontal to vertical) slope face. A slope height of 30 feet was selected as being representative of a case that might be encountered during a typical design. The objective of the analysis was to determine the equivalent average seismic coefficient that would be used in a limit equilibrium slope stability evaluation, taking into consideration wave scattering. Figure 6-1 depicts the slope model employed in the wave propagation study.

6.1.1.1 Slope Model

The wave propagation analysis was carried out for a two-dimensional (2-D) slope using the computer program QUAD-4M (1994). For these analyses the seismic coefficient was integrated over predetermined blocks of soil. The seismic coefficient is essentially the ratio of the seismic force induced by the earthquake in the block of soil divided by the weight of that block. Since the summation of forces acting on the block is computed as a function of time, the seismic coefficient is computed for each time step, yielding a time history of the seismic coefficient for the block. In this study, three soil blocks bounded by potential failure surfaces shown in Figure 6-1 were evaluated.

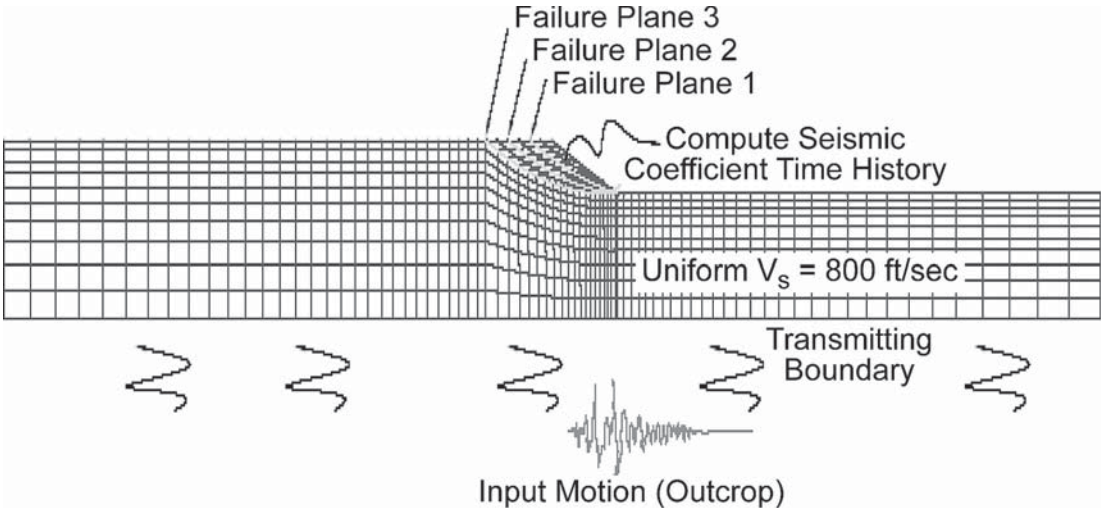

Figure 6-1. QUAD-4M model for 30-feet high wall.

The model used for these analyses had the following characteristics:

- Soil properties assigned for the finite element mesh are shown in Figure 6-1. These properties reflect typical compacted fill properties with a uniform shear wave velocity of 800 feet per second (ft/sec).
- Ground motions in the form of acceleration time histories were assigned as outcrop motions at the base of the model where a transmitting boundary was provided.
- The half-space property beneath the transmitting boundary was assigned a shear wave velocity of 800 ft/sec, identical to the soil mesh above the transmitting boundary.

The velocity of the half-space was assigned the same velocity as the embankment to avoid introduction of an impedance contrast in the finite-element model (hence an artificial natural frequency defined for the system). Assigning a uniform soil property above and below the half-space transmitting boundary meant that the resultant ground shaking would implicitly be compatible to the intended free-field ground surface condition, as defined by a given design response spectrum.

To further explain this aspect, reference is made to the left and the right side boundaries of the finite element mesh shown in Figure 6-1. These boundaries are specifically established as being sufficiently far from the slope face to avoid boundary effects. With the half-space and soil mesh properties as discussed earlier, it is observed that at the left and right edge soil columns, the response should approach the theoretical semi-infinite half-space problem of a vertically propagating shear wave (as modeled by the one-dimensional computer program SHAKE—Schnaebel et al., 1972). Therefore, the overall problem at the free-field ground surface, with the exception of the region locally adjacent to the slope face in the middle, should approach a level ground reference outcrop benchmark condition.

Rigorously speaking, free-field response at the left side (top of slope) versus the right side (bottom of slope) will be of little difference in amplitude of shaking, reflecting a slight time delay due to wave passage over a 30-foot difference in soil column height in the model. Introduction of any impedance contrast in either the soil mesh or what is implied by the transmitting boundary effectively introduces a boundary condition into the problem and results in a natural frequency in the boundary value problem. This will result in a free-field ground surface shaking condition deviating from the intended level-ground outcrop response spectrum design basis. Likewise, introduction of an impedance contrast would introduce complexities to the ground motion design definitions. Solutions involving such impedance contrast will, however, be relevant for site-specific cases, as discussed in Chapters 7 and 8 of this Final Report.

6.1.1.2 Earthquake Records Used In Slope Studies

Several earthquake time histories were used for input excitation; each one was spectrum matched to lower bound, mid, or upper bound spectra, as discussed in Chapter 5. Further documentation of the input motions used for the analyses can be found in Appendix E.

Prior to presenting results of the equivalent seismic coefficient evaluations, Figure 6-2 shows a representative acceleration time history extracted from a node on the free-field surface at the left side boundary (that is, at the top of the slope). The time history is for the Imperial Valley input motion that was used to match the mid target spectrum. This time history can be compared to the reference outcrop motion shown in the same figure. As can be seen from the comparison, the two

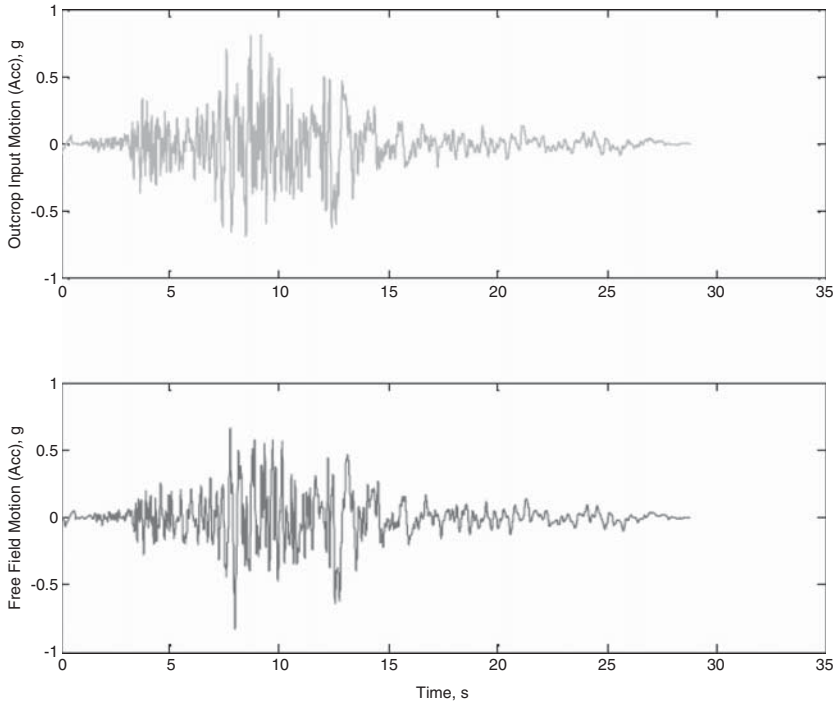

Figure 6-2. Comparison QUAD 4M input outcrop motion (top figure) versus free field ground surface response motion (bottom figure).

motions are rather similar as intended by the use of the transmitting boundary and a uniform set of soil properties. The Rayleigh damping parameters are intentionally chosen to be sufficiently low to avoid unintended material damping that would lower the resultant shaking at the free-field surface from wave propagation over the small height in soil column used for analysis.

6.1.1.3 Results of Scattering Analyses for Slopes

Figures 6-3 through 6-5 show comparisons of seismic coefficient time histories (dark lines) against the input outcrop motion (light lines) for three acceleration time histories fitted for the lower bound spectral shape. Figures 6-6 through 6-8 and Figures 6-9 through 6-11 present the corresponding comparisons for the mid and upper bound spectrum, respectively. In each figure, three traces of seismic coefficient were computed for the three blocks as compared to the light colored reference outcrop motion.

6.1.1.4 Observations from Evaluations

It can be observed from Figures 6-2 through 6-11 that the variation in the seismic coefficient amongst the three blocks for a given earthquake motion is rather small. However, there is a clear reduction in seismic coefficient from the integrated seismic coefficient time history (dark lines) as compared to the input outcrop motion (light lines). From the comparison, it is also clear that the reduction in shaking in the seismic coefficient time history as compared to the reference input design time history is highly frequency dependent.

The reduction in shaking is much more apparent for the lower bound spectrum records (see Figures 6-3 through 6-5) relative to the mid and upper bound cases. The reduction in shaking for the analyses associated with the mid and the upper bound spectra indicates that the reduction in shaking is justified for the several relative peaks at the time of strong ground shaking, but the reduction becomes much less apparent for other portions of the response time history, especially toward the end of the time history. The scattering phenomenon results from the fact that several relative peaks at the time of peak earthquake loading will be chopped off, as opposed to a uniformly scaling down of the overall time history motion record.

As observed from time-history comparisons for the average seismic coefficients resulting for the three failure blocks in each of the figures, the high frequency cancellation effect, or variation in seismic coefficient among the three failure blocks, appears to be relatively small in the lateral dimension. As discussed more fully in the summary of wave scattering analyses for retaining walls, it appears that the resultant ratio decreases with increasing lateral dimension in the failure

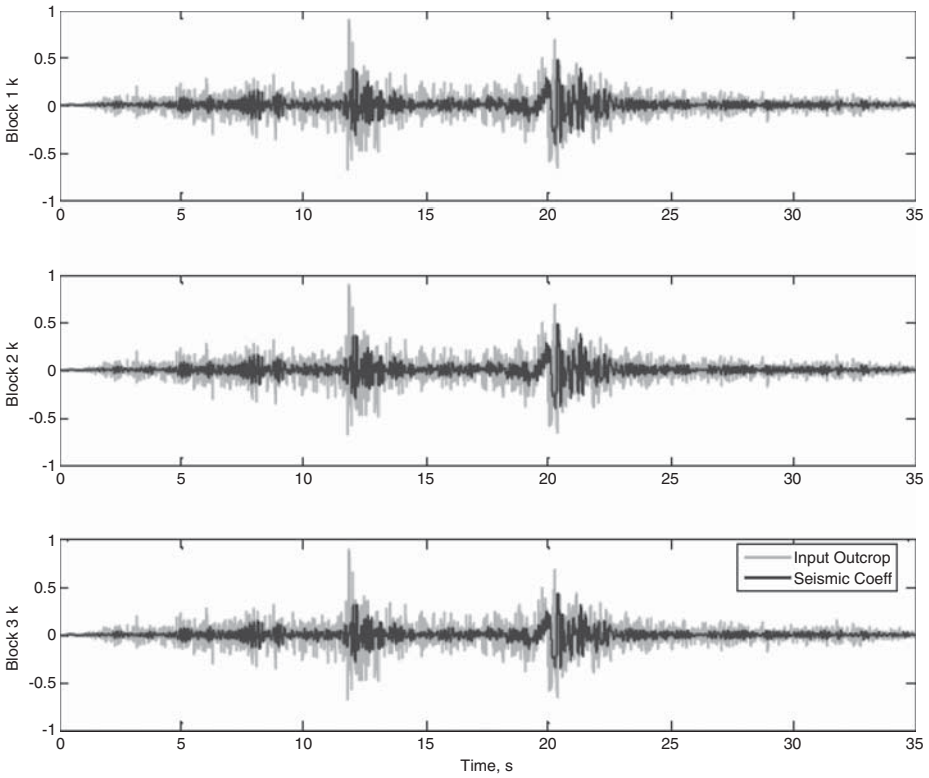

Figure 6-3. Scattering results for lower bound spectral shape, Cape Mendocino record.

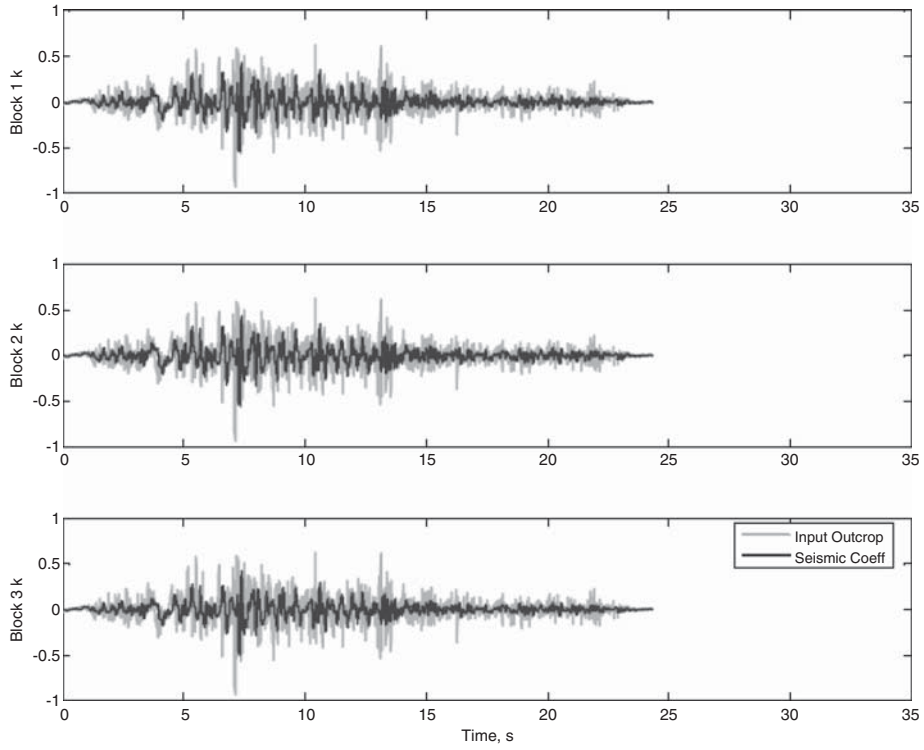

Figure 6-4. Scattering results for lower bound spectral shape, Dayhook record.

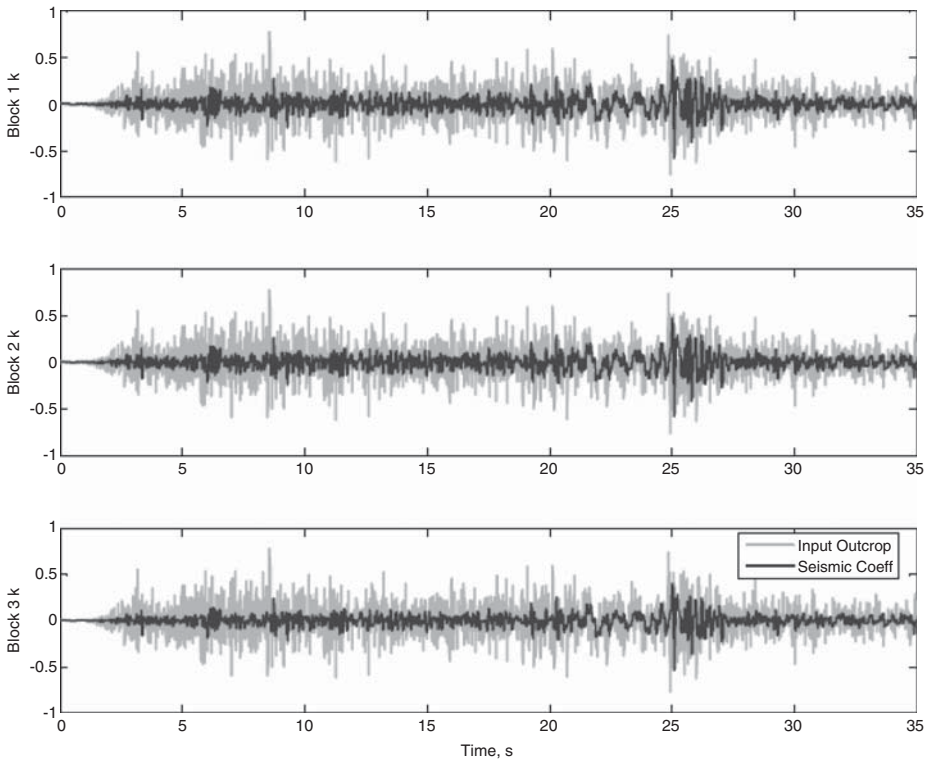

Figure 6-5. Scattering results for lower bound spectral shape, Landers EQ record.

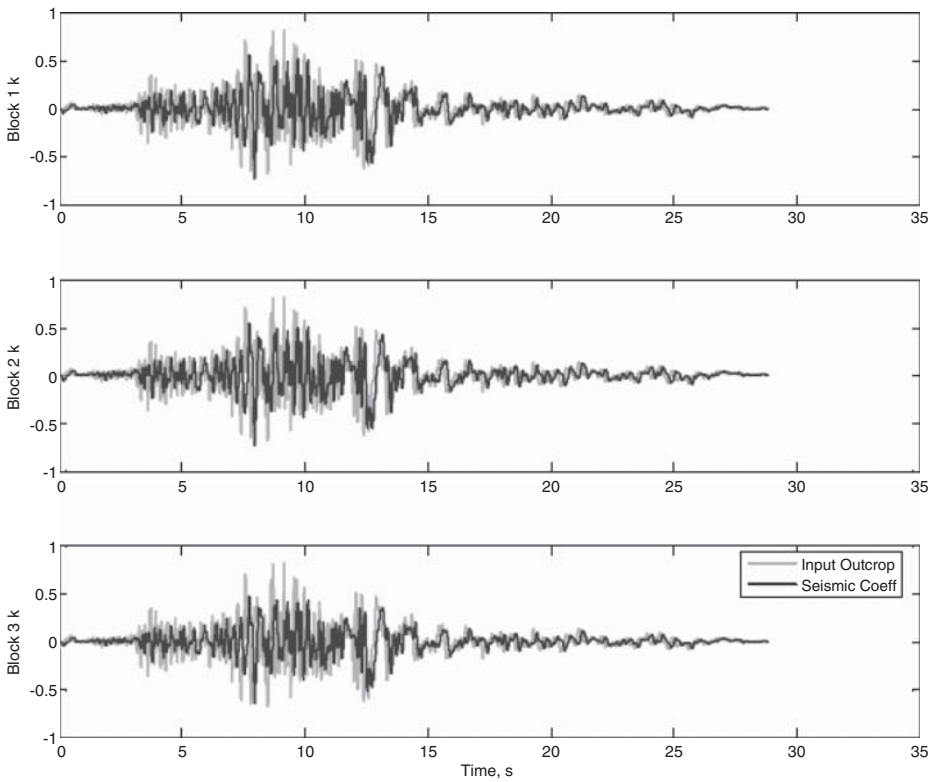

Figure 6-6. Scattering results for mid spectral shape, Imperial Valley EQ record.

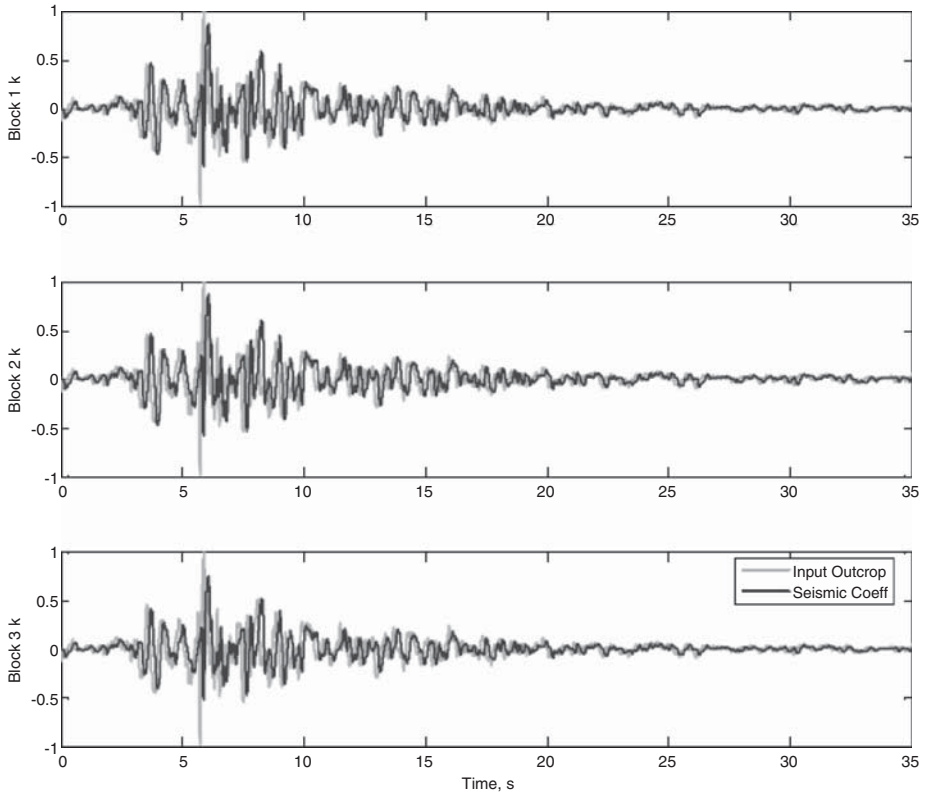

Figure 6-7. Scattering results for mid spectral shape, Loma Prieta EQ record.

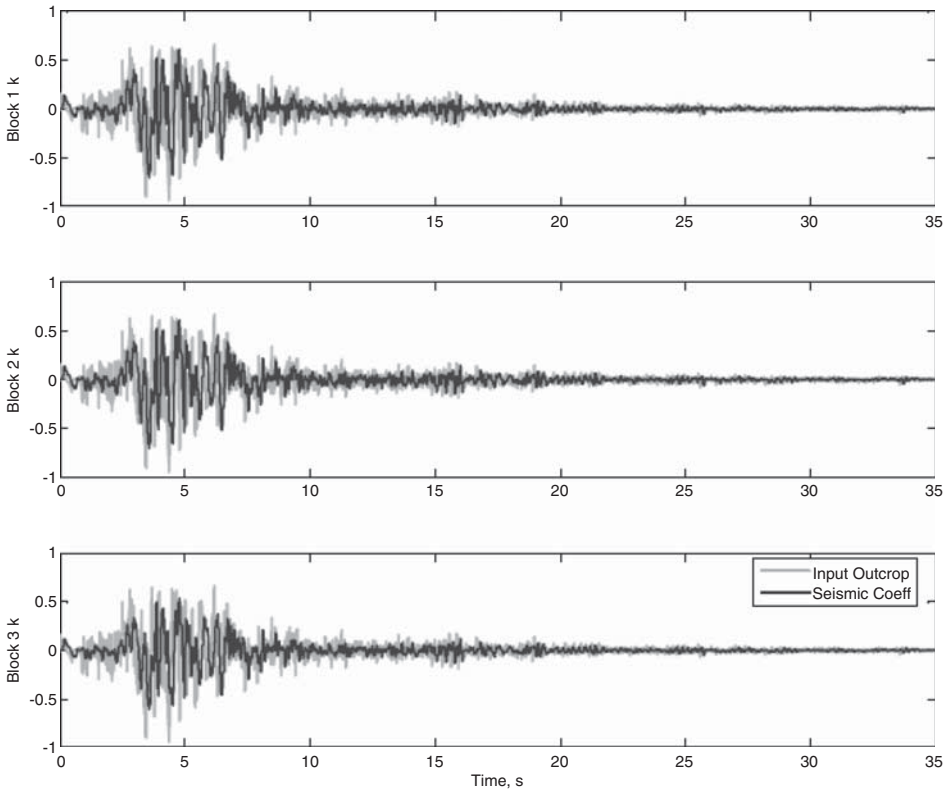

Figure 6-8. Scattering results for mid spectral shape, San Fernando EQ record.

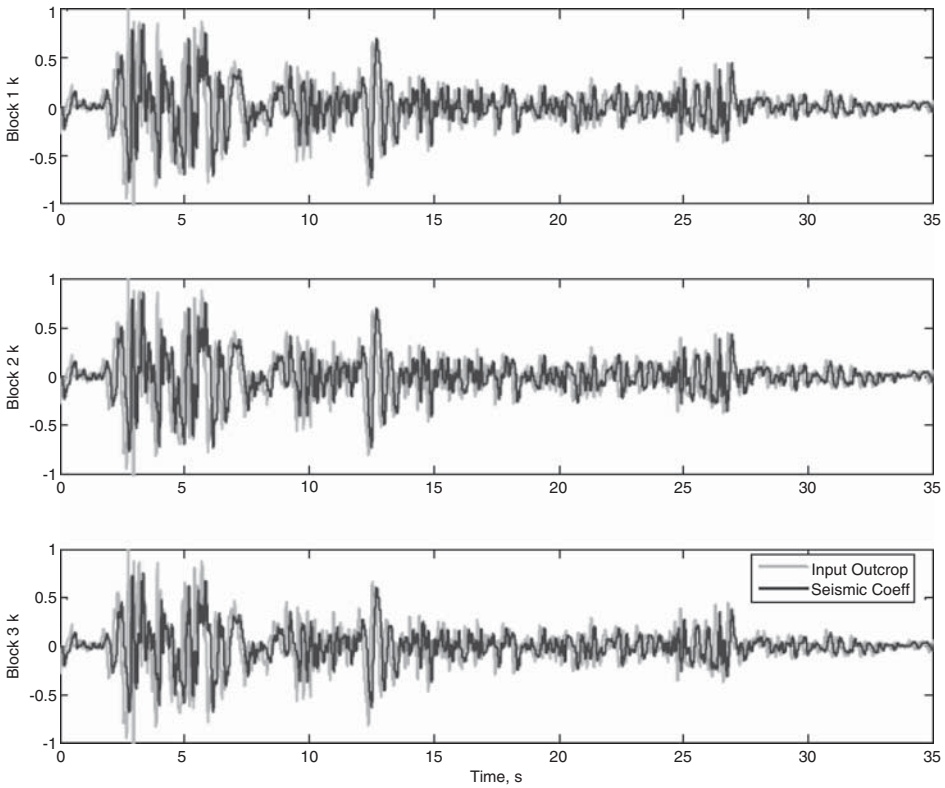

Figure 6-9. Scattering results for upper bound spectral shape, Imperial Valley EQ record.

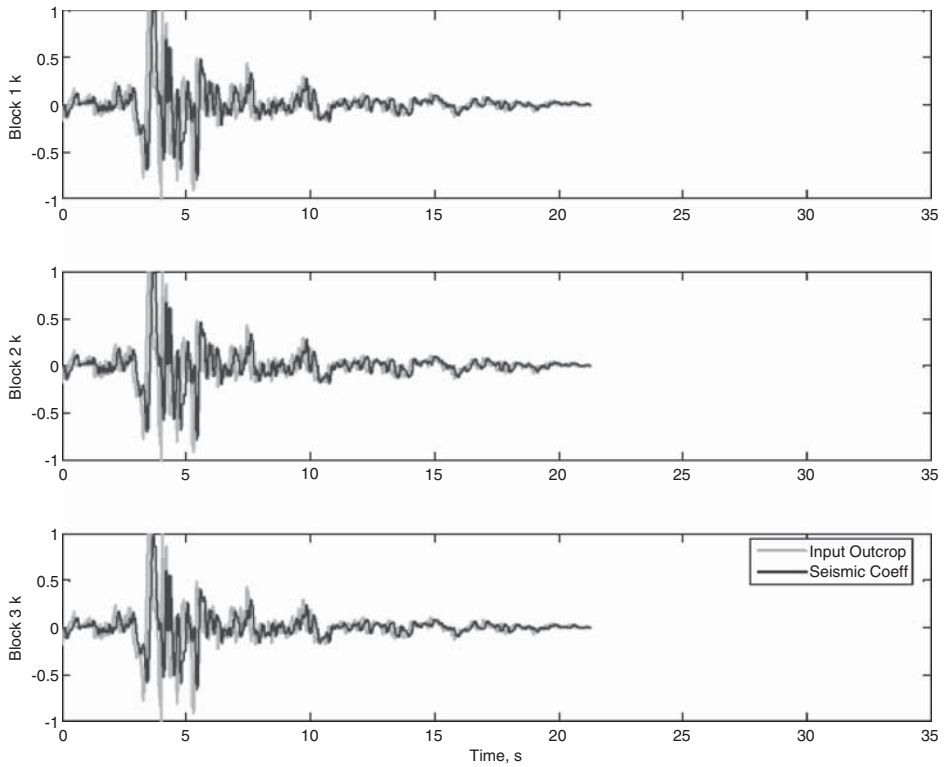

Figure 6-10. Scattering results for upper bound spectral shape, Turkey EQ record.

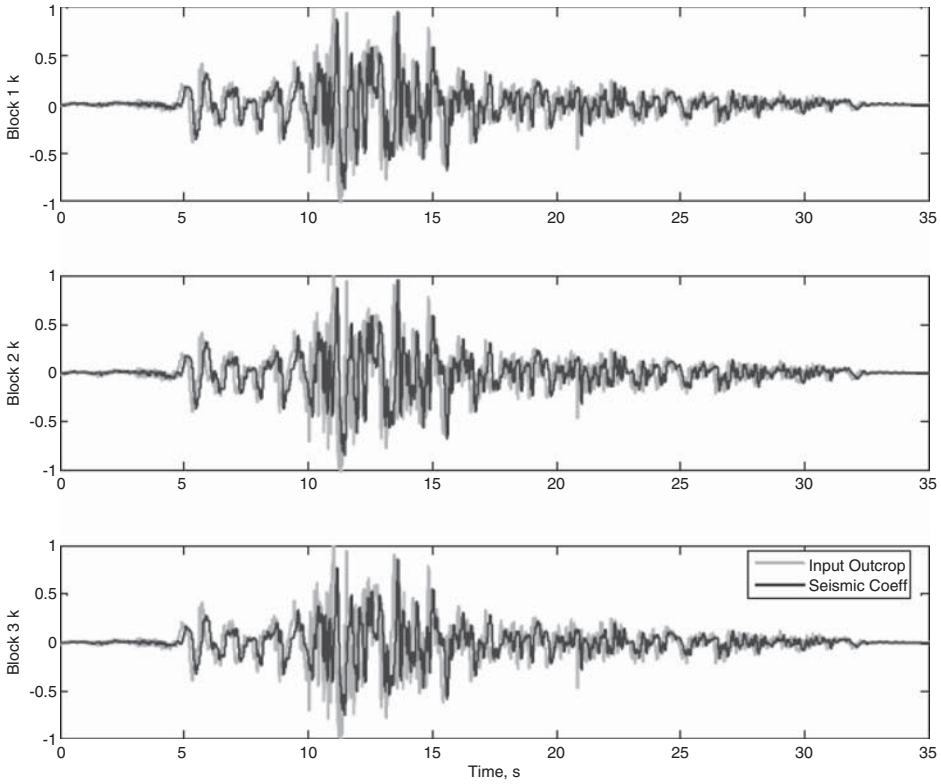

Figure 6-11. Scattering results for upper bound spectral shape, El Centro EQ record.

block. However, the change appears to be much smaller (on the order of 10 percent among the three blocks).

Such variations seem insignificant compared to scattering analyses involving the vertical dimensions of the soil mass. This observation can be explained by prevalent assumptions in wave propagation phenomena interpreted from strong motion data. For example, data from closely spaced strong motion arrays indicate that the wave passage effect in the lateral direction in space tends to be correlated to a very high apparent wave speed (say 2.0 to 3.5 km/sec) range, whereas the apparent wave speed in the vertical direction (for example, from downhole arrays) is related to shear wave velocity at the site. The apparent wave speed in the horizontal direction would typically be 10 to 20 times the apparent wave speed in the vertical direction. This would imply that the wave length in the vertical direction would be much smaller than the horizontal direction. Consistent with this observation, the wave scattering analyses used an identical input motion at all the nodes across the base of the finite-element mesh. Given the uniform motion input at the base, along with the side boundary conditions chosen to create a vertically propagating shear wave, a relatively minor variation in the motion in the horizontal direction should be expected.

Wave scattering analyses presented in this section for slopes provide a qualitative illustration of the wave scattering phenomena. A more comprehensive set of wave scattering analyses is presented for retaining walls. The retaining wall was used to evaluate wave scattering reduction factors (termed an α factor) which could be applied to a site-adjusted PGA to determine an equivalent maximum average seismic coefficient. This equivalent seismic coefficient was than applied to the soil mass for force-based design.

6.1.1.5 Conclusions from Scattering Analyses for Slopes

From these studies using the three sets of time histories for each spectral shape (lower bound, mid, and upper bound), reduction factors that can be applied to the peak ground acceleration were estimated. For the 30-foot slope, these scattering factors will be on the order of 0.5 for the lower bound spectral shape, 0.6 for the mid spectral shape, and 0.7 for the upper bound spectral shape. For slopes higher than 30 feet, further reductions due to canceling of high frequency motions in the vertical dimension due to incoherency effects from the wave scattering phenomenon could be anticipated, as shown in the wall height study.

The primary parameter controlling the scaling factor for a height-dependent seismic coefficient is related to the frequency content of the input motion with a lower seismic coefficient associated with the high, frequency-rich lower bound spectrum

input motion. Hence a smaller scaling factor (less than unity) should be expected for a CEUS seismological condition and for rock sites. In typical design applications, both the seismological and geotechnical conditions should be implicit in the adopted reference ground surface outcrop design response spectrum following seismic loading criteria defined by the NCHRP 20-07 Project.

The second parameter controlling the scaling factor for seismic coefficients is related to the height of the soil mass (that is, slope height in the context of the presented slope response analysis) or the height of a retaining wall as discussed below. In general, the scattering analyses show that the effect of height on PGV (a parameter of interest for Newmark sliding block analyses) is relatively small.

6.1.2 Scattering Analyses for Retaining Walls

The wave scattering analyses discussed in the previous section have been extended from a slope configuration to configurations commonly encountered for retaining wall designs. Wave scattering analyses were conducted to establish the relationship between peak ground acceleration at a given point in the ground to the equivalent seismic coefficient. In this context the equivalent seismic coefficient was the coefficient that should be applied to a soil mass to determine the peak force amplitude used in pseudo-static, force-based design of a retaining wall. The product of the equivalent seismic coefficient and soil mass defined the inertial load that would be applied to wall surface from the retained backfill.

6.1.2.1 Retaining Wall Model

Figure 6-12 provides a schematic description of the wave scattering analyses performed for the retaining wall problem. Similar to the slope scattering study described in the previous subsection, the QUAD-4M program was used during these analyses.

Nine input motions were used for the analyses. Features of these records are described in Appendix E. These records were used as input motion at the base of the finite-element mesh. The analyses included use of a transmitting boundary element available within the QUAD-4M program. A free boundary at the wall face was assumed.

6.1.2.2 Results of Wave Scattering Analyses for Retaining Walls

Table 6-1 summarizes the results from the wave scattering analyses for the retaining structure. Data presented in Table 6-1 are from 36 QUAD-4M runs covering four wall heights, three spectral shapes, and three time histories for each spectral shape. Ratios of peak average seismic coefficient response versus input motion (as measured by PGA) tabulated in the third column from right in the table were used to develop the scaling factors (defined as α) applied to the PGA to determine the peak average seismic coefficients acting on a block of soil for pseudo-static seismic analyses of the retaining walls.

Results in Table 6-1 are based on the average ground motions within each set of analyses. The time-dependent change in PGA, PGV, and S_1 is not considered. Use of the scaling factor does not, therefore, account for changes in inertial loading with time. In other words the scaled PGA is the peak loading and will be less for most of the earthquake duration. The average inertial force over the duration of shaking can vary from less than one-third to two-thirds of the peak value, depending on the magnitude, location, and other characteristics of the earthquake.

Similar to the observation made earlier from the slope scattering analyses, the variation in the α coefficient was not very significant among the three failure blocks evaluated, and therefore, results from the three failure blocks were averaged. Also, results from the three time histories each matched to the same response spectrum were averaged. The resultant solutions for the α coefficients categorized by wall height and the spectral shapes (that is, upper bound, mid and lower bound spectral shapes) are summarized in Figure 6-13.

The reduction in PGA shown in the above figure arises from a wave scattering reduction in the peak PGA for design analyses. There are other factors that provide further justification for reducing the PGA value, as discussed here:

1. Average versus peak response. As noted previously, a pseudo-static analysis treats the seismic coefficient as a constant horizontal static force applied to the soil mass. However, the peak earthquake load from a dynamic response analysis occurs for a very short time—with the average seismic force typically ranging from 30 to 70 percent of the peak depending on the characteristics of the specific earthquake event. Hence further reduction in the force demand reflecting the overall average cyclic loading condition might be justified, where a structural system is designed for some degree of ductile yielding. The acceptability of an additional time-related reduction should be decided by the structural design, since it will depend on the method of analysis and the design philosophy. The Project Team decided that a-priori reduction in the PGA after adjustment for wave scattering by time-related factor was not appropriate, and therefore this additional reduction has not been introduced into the design approach. This decision also means that it is very important for the geotechnical engineer to very clearly define whether the resulting seismic coefficient is the instantaneous peak or an average peak corrected for the duration of ground shaking.

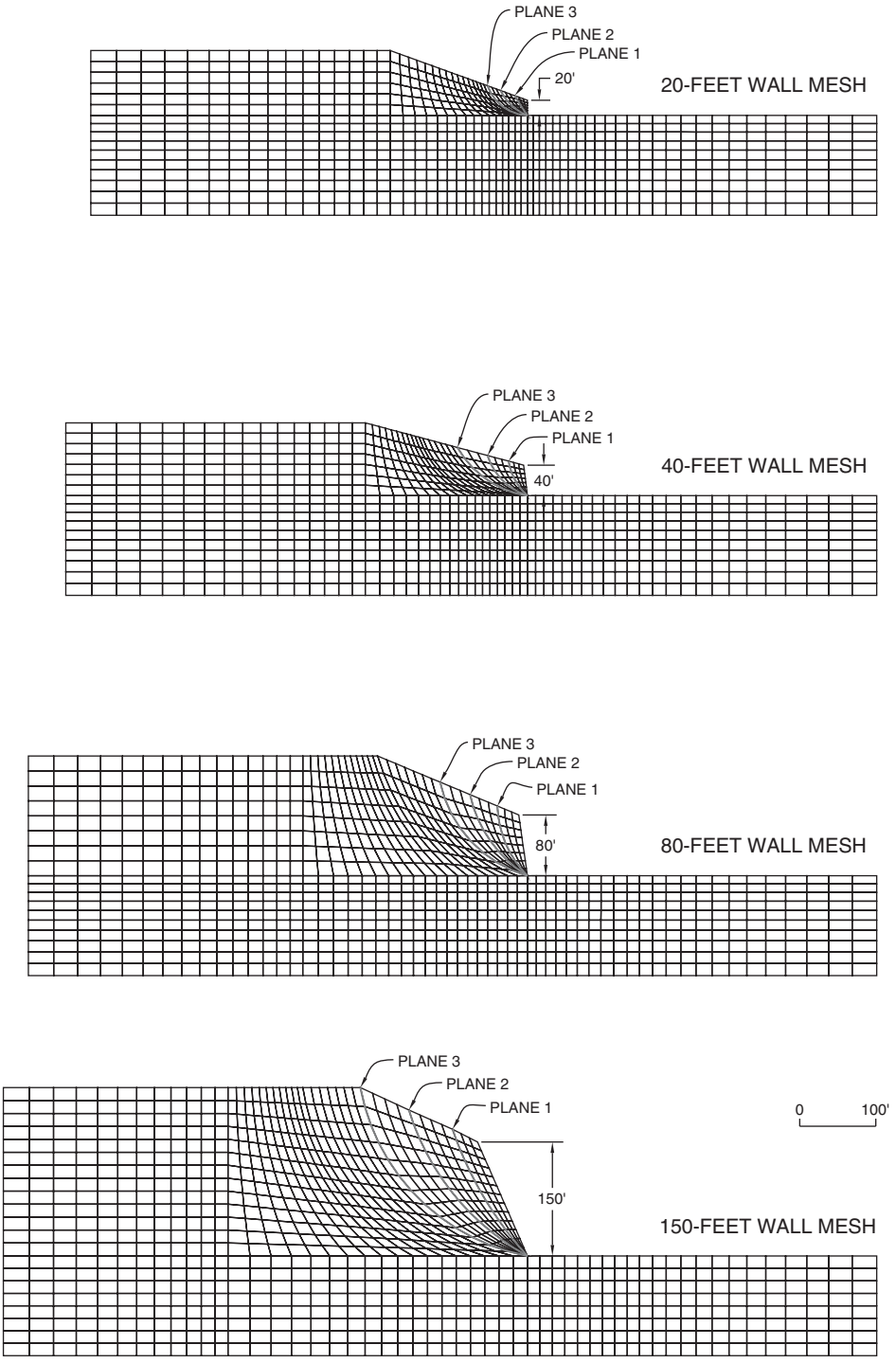

Figure 6-12. Models used in scattering analyses.

2. Load fuse from wall movements. Another justification for designing to a value less than the PGA arises from the fact that many retaining walls are implicitly designed for wall movements when the wall is designed for an active earth pressure condition. The wave scattering analyses in this evaluation were based on linear elastic analyses and further reduction in the force demand is justified when the retaining wall is designed to slide at a specific threshold load level as discussed in Chapter 7.

From Table 6-1 it can be observed that the ratio of equivalent seismic coefficient (for a block of soil) to the PGA (at a single point on the ground surface) did not change drastically for the three failure planes studied in the analyses. However,

Table 6-1. Results of scattering analyses.

			Seismic Coefficient Response				Input Motion				Ratio of Seismic Coefficient Response vs. Input Motion		
I	Model	File Name	Block	PGV (max)	PGV (max)	Sa1	File Name	PGV (max)	PGV (max)	Sa1	PGA	PGV	Sa1
				g	in/s	g		g	in/s	g	g	in/s	g
1	20 ft wall	w20-cap-.Q4K	1	0.579	13.506	0.33	CAP-L.acc	0.894	15.370	0.39	0.65	0.88	0.85
2	20 ft wall	w20-cap-.Q4K	2	0.590	13.862	0.34	CAP-L.acc	0.894	15.370	0.39	0.66	0.90	0.87
3	20 ft wall	w20-cap-.Q4K	3	0.518	12.344	0.30	CAP-L.acc	0.894	15.370	0.39	0.58	0.80	0.77
4	20 ft wall	w20-day-.Q4K	1	0.740	10.486	0.34	DAY-L.acc	0.936	11.684	0.39	0.79	0.90	0.87
5	20 ft wall	w20-day-.Q4K	2	0.730	10.705	0.35	DAY-L.acc	0.936	11.684	0.39	0.78	0.92	0.90
6	20 ft wall	w20-day-.Q4K	3	0.670	9.286	0.31	DAY-L.acc	0.936	11.684	0.39	0.72	0.79	0.79
7	20 ft wall	w20-lan-.Q4K	1	0.759	12.033	0.31	LAN-L.acc	0.771	15.173	0.36	0.98	0.79	0.86
8	20 ft wall	w20-lan-.Q4K	2	0.761	12.297	0.32	LAN-L.acc	0.771	15.173	0.36	0.99	0.81	0.89
9	20 ft wall	w20-lan-.Q4K	3	0.699	10.173	0.28	LAN-L.acc	0.771	15.173	0.36	0.91	0.67	0.78
Average of Above 9				0.672	11.632	0.320	**L.B. Spectrum**	0.867	14.076	0.380	**0.783**	**0.830**	**0.842**
10	20 ft wall	w20-imp-.Q4K	1	0.670	31.047	0.97	IMP-M.acc	0.812	37.054	1.12	0.83	0.84	0.87
11	20 ft wall	w20-imp-.Q4K	2	0.685	31.884	1.00	IMP-M.acc	0.812	37.054	1.12	0.84	0.86	0.89
12	20 ft wall	w20-imp-.Q4K	3	0.602	28.298	0.87	IMP-M.acc	0.812	37.054	1.12	0.74	0.76	0.78
13	20 ft wall	w20-lom-.Q4K	1	0.992	31.034	1.06	LOM-M.acc	1.026	32.275	1.20	0.97	0.96	0.88
14	20 ft wall	w20-lom-.Q4K	2	1.010	31.719	1.08	LOM-M.acc	1.026	32.275	1.20	0.98	0.98	0.90
15	20 ft wall	w20-lom-.Q4K	3	0.855	27.454	0.94	LOM-M.acc	1.026	32.275	1.20	0.83	0.85	0.78
16	20 ft wall	w20-san-.Q4K	1	0.742	40.453	1.03	SAN-M.acc	0.948	42.312	1.18	0.78	0.96	0.87
17	20 ft wall	w20-san-.Q4K	2	0.758	41.297	1.06	SAN-M.acc	0.948	42.312	1.18	0.80	0.98	0.90
18	20 ft wall	w20-san-.Q4K	3	0.655	33.340	0.92	SAN-M.acc	0.948	42.312	1.18	0.69	0.79	0.78
Average of above 9				0.774	32.947	0.992	**Mid Spectrum**	0.929	37.214	1.167	**0.830**	**0.886**	**0.850**
19	20 ft wall	w20-elc-.Q4K	1	0.986	40.725	1.56	ELC-U.acc	1.083	45.320	1.78	0.91	0.90	0.88
20	20 ft wall	w20-elc-.Q4K	2	0.981	41.631	1.60	ELC-U.acc	1.083	45.320	1.78	0.91	0.92	0.90
21	20 ft wall	w20-elc-.Q4K	3	0.890	35.655	1.37	ELC-U.acc	1.083	45.320	1.78	0.82	0.79	0.77
22	20 ft wall	w20-erz-.Q4K	1	1.068	43.290	1.43	ERZ-U.acc	1.089	52.950	1.69	0.98	0.82	0.85
23	20 ft wall	w20-erz-.Q4K	2	1.094	44.468	1.47	ERZ-U.acc	1.089	52.950	1.69	1.00	0.84	0.87
24	20 ft wall	w20-erz-.Q4K	3	0.978	39.040	1.26	ERZ-U.acc	1.089	52.950	1.69	0.90	0.74	0.75
25	20 ft wall	w20-tab-.Q4K	1	1.091	41.827	1.54	TAB-U.acc	1.060	46.922	1.76	1.03	0.89	0.88
26	20 ft wall	w20-tab-.Q4K	2	1.103	42.756	1.58	TAB-U.acc	1.060	46.922	1.76	1.04	0.91	0.90
27	20 ft wall	w20-tab-.Q4K	3	0.938	37.597	1.38	TAB-U.acc	1.060	46.922	1.76	0.88	0.80	0.78
Average of Above 9				1.014	40.777	1.466	**U.B. Spectrum**	1.077	48.397	1.743	**0.942**	**0.845**	**0.840**
28	40 ft wall	w40-cap-.Q4K	1	0.543	14.021	0.32	CAP-L.acc	0.894	15.370	0.39	0.61	0.91	0.82
29	40 ft wall	w40-cap-.Q4K	2	0.530	14.543	0.34	CAP-L.acc	0.894	15.370	0.39	0.59	0.95	0.87
30	40 ft wall	w40-cap-.Q4K	3	0.470	13.677	0.33	CAP-L.acc	0.894	15.370	0.39	0.53	0.89	0.85
31	40 ft wall	w40-day-.Q4K	1	0.441	12.190	0.36	DAY-L.acc	0.936	11.684	0.39	0.47	1.04	0.92
32	40 ft wall	w40-day-.Q4K	2	0.410	12.414	0.38	DAY-L.acc	0.936	11.684	0.39	0.44	1.06	0.97
33	40 ft wall	w40-day-.Q4K	3	0.385	11.284	0.36	DAY-L.acc	0.936	11.684	0.39	0.41	0.97	0.92
34	40 ft wall	w40-lan-.Q4K	1	0.449	11.961	0.33	LAN-L.acc	0.771	15.173	0.36	0.58	0.79	0.92
35	40 ft wall	w40-lan-.Q4K	2	0.427	12.771	0.34	LAN-L.acc	0.771	15.173	0.36	0.55	0.84	0.94
36	40 ft wall	w40-lan-.Q4K	3	0.411	12.045	0.33	LAN-L.acc	0.771	15.173	0.36	0.53	0.79	0.92
Average of Above 9				0.452	12.767	0.343	**L.B. Spectrum**	0.867	14.076	0.380	**0.524**	**0.916**	**0.904**
37	40 ft wall	w40-imp-.Q4K	1	0.734	31.666	0.99	IMP-M.acc	0.812	37.054	1.12	0.90	0.85	0.88
38	40 ft wall	w40-imp-.Q4K	2	0.745	33.017	1.05	IMP-M.acc	0.812	37.054	1.12	0.92	0.89	0.94
39	40 ft wall	w40-imp-.Q4K	3	0.696	31.165	0.99	IMP-M.acc	0.812	37.054	1.12	0.86	0.84	0.88
40	40 ft wall	w40-lom-.Q4K	1	0.968	35.371	1.09	LOM-M.acc	1.026	32.275	1.20	0.94	1.10	0.91
41	40 ft wall	w40-lom-.Q4K	2	0.993	37.374	1.15	LOM-M.acc	1.026	32.275	1.20	0.97	1.16	0.96
42	40 ft wall	w40-lom-.Q4K	3	0.903	35.285	1.09	LOM-M.acc	1.026	32.275	1.20	0.88	1.09	0.91
43	40 ft wall	w40-san-.Q4K	1	0.804	40.479	1.07	SAN-M.acc	0.948	42.312	1.18	0.85	0.96	0.91
44	40 ft wall	w40-san-.Q4K	2	0.839	42.883	1.13	SAN-M.acc	0.948	42.312	1.18	0.89	1.01	0.96
45	40 ft wall	w40-san-.Q4K	3	0.772	39.551	1.06	SAN-M.acc	0.948	42.312	1.18	0.81	0.93	0.90
Average of Above 9				0.828	36.310	1.069	**Mid Spectrum**	0.929	37.214	1.167	**0.891**	**0.982**	**0.916**
46	40 ft wall	w40-elc-.Q4K	1	0.785	43.411	1.60	ELC-U.acc	1.083	45.320	1.78	0.72	0.96	0.90
47	40 ft wall	w40-elc-.Q4K	2	0.814	45.795	1.69	ELC-U.acc	1.083	45.320	1.78	0.75	1.01	0.95
48	40 ft wall	w40-elc-.Q4K	3	0.766	43.155	1.60	ELC-U.acc	1.083	45.320	1.78	0.71	0.95	0.90
49	40 ft wall	w40-erz-.Q4K	1	1.229	45.744	1.48	ERZ-U.acc	1.089	52.950	1.69	1.13	0.86	0.88
50	40 ft wall	w40-erz-.Q4K	2	1.267	48.699	1.56	ERZ-U.acc	1.089	52.950	1.69	1.16	0.92	0.92
51	40 ft wall	w40-erz-.Q4K	3	1.179	45.240	1.47	ERZ-U.acc	1.089	52.950	1.69	1.08	0.85	0.87
52	40 ft wall	w40-tab-.Q4K	1	1.017	44.276	1.55	TAB-U.acc	1.060	46.922	1.76	0.96	0.94	0.88
53	40 ft wall	w40-tab-.Q4K	2	1.020	46.188	1.63	TAB-U.acc	1.060	46.922	1.76	0.96	0.98	0.93
54	40 ft wall	w40-tab-.Q4K	3	0.913	43.438	1.55	TAB-U.acc	1.060	46.922	1.76	0.86	0.93	0.88
Average of Above 9				0.999	45.105	1.570	**U.B. Spectrum**	1.077	48.397	1.743	**0.927**	**0.935**	**0.900**
55	80 ft wall	w80-cap-.Q4K	1	0.380	14.464	0.43	CAP-L.acc	0.894	15.370	0.39	0.43	0.94	1.10
56	80 ft wall	w80-cap-.Q4K	2	0.371	14.270	0.43	CAP-L.acc	0.894	15.370	0.39	0.41	0.93	1.10
57	80 ft wall	w80-cap-.Q4K	3	0.340	13.829	0.42	CAP-L.acc	0.894	15.370	0.39	0.38	0.90	1.08
58	80 ft wall	w80-day-.Q4K	1	0.240	9.725	0.41	DAY-L.acc	0.936	11.684	0.39	0.26	0.83	1.05

(continued on next page)

Table 6-1. (Continued).

			Seismic Coefficient Response				Input Motion				Ratio of Seismic Coefficient Response vs. Input Motion		
I	Model	File Name	Block	PGV (max)	PGV (max)	Sa1	File Name	PGV (max)	PGV (max)	Sa1	PGA	PGV	Sa1
				g	in/s	g		g	in/s	g	g	in/s	g
59	80 ft wall	w80-day-.Q4K	2	0.224	9.800	0.41	DAY-L.acc	0.936	11.684	0.39	0.24	0.84	1.05
60	80 ft wall	w80-day-.Q4K	3	0.202	9.545	0.40	DAY-L.acc	0.936	11.684	0.39	0.22	0.82	1.03
61	80 ft wall	w80-lan-.Q4K	1	0.257	14.593	0.38	LAN-L.acc	0.771	15.173	0.36	0.33	0.96	1.06
62	80 ft wall	w80-lan-.Q4K	2	0.243	14.504	0.38	LAN-L.acc	0.771	15.173	0.36	0.32	0.96	1.06
63	80 ft wall	w80-lan-.Q4K	3	0.221	13.858	0.37	LAN-L.acc	0.771	15.173	0.36	0.29	0.91	1.03
Average of Above 9				0.275	12.732	0.403	**L.B. Spectrum**	0.867	14.076	0.380	**0.319**	**0.899**	**1.061**
64	80 ft wall	w80-imp-.Q4K	1	0.607	37.264	1.12	IMP-M.acc	0.812	37.054	1.12	0.75	1.01	1.00
65	80 ft wall	w80-imp-.Q4K	2	0.599	37.154	1.13	IMP-M.acc	0.812	37.054	1.12	0.74	1.00	1.01
66	80 ft wall	w80-imp-.Q4K	3	0.550	36.002	1.10	IMP-M.acc	0.812	37.054	1.12	0.68	0.97	0.98
67	80 ft wall	w80-lom-.Q4K	1	0.672	41.988	1.22	LOM-M.acc	1.026	32.275	1.20	0.65	1.30	1.02
68	80 ft wall	w80-lom-.Q4K	2	0.635	41.563	1.22	LOM-M.acc	1.026	32.275	1.20	0.62	1.29	1.02
69	80 ft wall	w80-lom-.Q4K	3	0.569	39.643	1.19	LOM-M.acc	1.026	32.275	1.20	0.55	1.23	0.99
70	80 ft wall	w80-san-.Q4K	1	0.762	45.732	1.24	SAN-M.acc	0.948	42.312	1.18	0.80	1.08	1.05
71	80 ft wall	w80-san-.Q4K	2	0.732	44.796	1.23	SAN-M.acc	0.948	42.312	1.18	0.77	1.06	1.04
72	80 ft wall	w80-san-.Q4K	3	0.669	42.321	1.18	SAN-M.acc	0.948	42.312	1.18	0.71	1.00	1.00
Average of Above 9				0.644	40.718	1.181	**Mid Spectrum**	0.929	37.214	1.167	**0.697**	**1.104**	**1.012**
73	80 ft wall	w80-elc-.Q4K	1	0.895	42.781	1.76	ELC-U.acc	1.083	45.320	1.78	0.83	0.94	0.99
74	80 ft wall	w80-elc-.Q4K	2	0.878	43.230	1.77	ELC-U.acc	1.083	45.320	1.78	0.81	0.95	0.99
75	80 ft wall	w80-elc-.Q4K	3	0.828	42.279	1.73	ELC-U.acc	1.083	45.320	1.78	0.76	0.93	0.97
76	80 ft wall	w80-erz-.Q4K	1	1.181	52.435	1.77	ERZ-U.acc	1.089	52.950	1.69	1.08	0.99	1.05
77	80 ft wall	w80-erz-.Q4K	2	1.135	52.091	1.77	ERZ-U.acc	1.089	52.950	1.69	1.04	0.98	1.05
78	80 ft wall	w80-erz-.Q4K	3	1.055	49.750	1.70	ERZ-U.acc	1.089	52.950	1.69	0.97	0.94	1.01
79	80 ft wall	w80-tab-.Q4K	1	1.025	43.980	1.83	TAB-U.acc	1.060	46.922	1.76	0.97	0.94	1.04
80	80 ft wall	w80-tab-.Q4K	2	1.011	42.697	1.83	TAB-U.acc	1.060	46.922	1.76	0.95	0.91	1.04
81	80 ft wall	w80-tab-.Q4K	3	0.936	40.261	1.78	TAB-U.acc	1.060	46.922	1.76	0.88	0.86	1.01
Average of Above 9				0.994	45.500	1.771	**U.B. Spectrum**	1.077	48.397	1.743	**0.922**	**0.939**	**1.016**
82	120 ft wall	w12-cap-.Q4K	1	0.221	12.815	0.47	CAP-L.acc	0.894	15.370	0.39	0.25	0.83	1.21
83	120 ft wall	w12-cap-.Q4K	2	0.202	12.610	0.46	CAP-L.acc	0.894	15.370	0.39	0.23	0.82	1.18
84	120 ft wall	w12-cap-.Q4K	3	0.199	12.263	0.43	CAP-L.acc	0.894	15.370	0.39	0.22	0.80	1.10
85	120 ft wall	w12-day-.Q4K	1	0.195	10.675	0.45	DAY-L.acc	0.936	11.684	0.39	0.21	0.91	1.15
86	120 ft wall	w12-day-.Q4K	2	0.176	10.497	0.44	DAY-L.acc	0.936	11.684	0.39	0.19	0.90	1.13
87	120 ft wall	w12-day-.Q4K	3	0.189	10.159	0.42	DAY-L.acc	0.936	11.684	0.39	0.20	0.87	1.08
88	120 ft wall	w12-lan-.Q4K	1	0.241	14.801	0.44	LAN-L.acc	0.771	15.173	0.36	0.31	0.98	1.22
89	120 ft wall	w12-lan-.Q4K	2	0.224	14.223	0.43	LAN-L.acc	0.771	15.173	0.36	0.29	0.94	1.19
90	120 ft wall	w12-lan-.Q4K	3	0.203	13.376	0.41	LAN-L.acc	0.771	15.173	0.36	0.26	0.88	1.14
Average of Above 9				0.206	12.380	0.439	**L.B. Spectrum**	0.867	14.076	0.380	**0.240**	**0.881**	**1.156**
91	120 ft wall	w12-imp-.Q4K	1	0.625	40.256	1.24	IMP-M.acc	0.812	37.054	1.12	0.77	1.09	1.11
92	120 ft wall	w12-imp-.Q4K	2	0.574	39.312	1.21	IMP-M.acc	0.812	37.054	1.12	0.71	1.06	1.08
93	120 ft wall	w12-imp-.Q4K	3	0.516	37.327	1.16	IMP-M.acc	0.812	37.054	1.12	0.64	1.01	1.04
94	120 ft wall	w12-lom-.Q4K	1	0.486	39.153	1.33	LOM-M.acc	1.026	32.275	1.20	0.47	1.21	1.11
95	120 ft wall	w12-lom-.Q4K	2	0.435	38.141	1.30	LOM-M.acc	1.026	32.275	1.20	0.42	1.18	1.08
96	120 ft wall	w12-lom-.Q4K	3	0.450	36.063	1.26	LOM-M.acc	1.026	32.275	1.20	0.44	1.12	1.05
97	120 ft wall	w12-san-.Q4K	1	0.521	40.379	1.45	SAN-M.acc	0.948	42.312	1.18	0.55	0.95	1.23
98	120 ft wall	w12-san-.Q4K	2	0.504	38.840	1.41	SAN-M.acc	0.948	42.312	1.18	0.53	0.92	1.19
99	120 ft wall	w12-san-.Q4K	3	0.449	37.336	1.33	SAN-M.acc	0.948	42.312	1.18	0.47	0.88	1.13
Average of Above 9				0.507	38.534	1.299	**Mid Spectrum**	0.929	37.214	1.167	**0.556**	**1.047**	**1.113**
100	120 ft wall	w12-elc-.Q4K	1	0.863	55.709	1.93	ELC-U.acc	1.083	45.320	1.78	0.80	1.23	1.08
101	120 ft wall	w12-elc-.Q4K	2	0.843	53.682	1.90	ELC-U.acc	1.083	45.320	1.78	0.78	1.18	1.07
102	120 ft wall	w12-elc-.Q4K	3	0.774	50.337	1.83	ELC-U.acc	1.083	45.320	1.78	0.71	1.11	1.03
103	120 ft wall	w12-erz-.Q4K	1	0.921	55.895	1.81	ERZ-U.acc	1.089	52.950	1.69	0.85	1.06	1.07
104	120 ft wall	w12-erz-.Q4K	2	0.860	54.019	1.77	ERZ-U.acc	1.089	52.950	1.69	0.79	1.02	1.05
105	120 ft wall	w12-erz-.Q4K	3	0.820	50.339	1.68	ERZ-U.acc	1.089	52.950	1.69	0.75	0.95	0.99
106	120 ft wall	w12-tab-.Q4K	1	0.874	43.529	2.09	TAB-U.acc	1.060	46.922	1.76	0.82	0.93	1.19
107	120 ft wall	w12-tab-.Q4K	2	0.825	41.913	2.03	TAB-U.acc	1.060	46.922	1.76	0.78	0.89	1.15
108	120 ft wall	w12-tab-.Q4K	3	0.738	40.690	1.93	TAB-U.acc	1.060	46.922	1.76	0.70	0.87	1.10
Average of Above 9				0.835	49.568	1.886	**U.B. Spectrum**	1.077	48.397	1.743	**0.775**	**1.027**	**1.081**

this ratio systematically decreased for increasing wall height and lowering of the spectral shape at long periods. Therefore, averaging the ratios (shown in the right-most column) from the three failure mechanisms evaluated in this study would seem to be reasonable. Cursory review of the data supports to some degree, the presumptive historical practice of adopting about ½ to ⅔ of PGA for pseudo-static design analysis. However, as noted above, rather than the prevalent view that the reduction is to account for the time variation in PGA, the reduction being introduced in this discussion is for wave scattering. Any further reduction for the duration of earthquake loading should be determined by the structural designer.

6.2 Conclusions

Figure 6-13 provides a basis for determining a reduction factor (that is, the α factor) to be applied to the peak ground acceleration used when determining the pseudo-static force

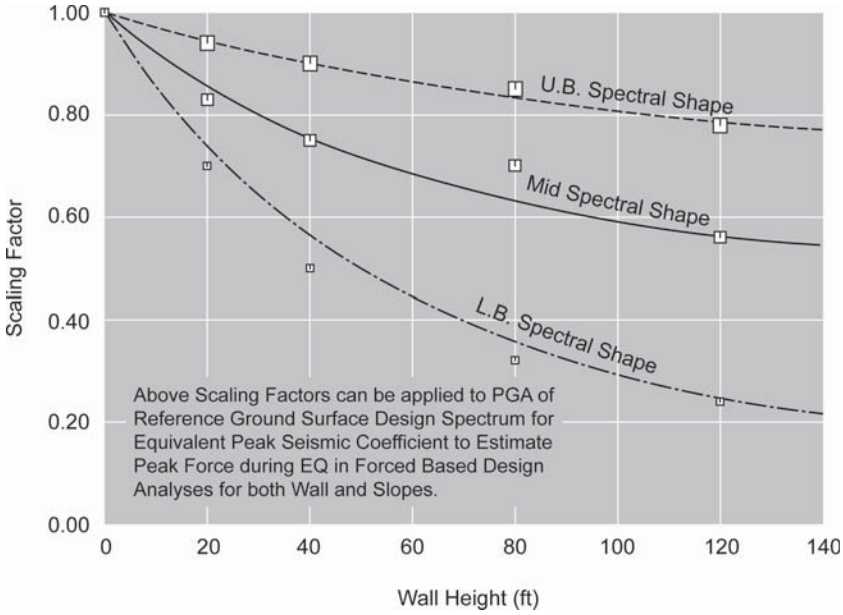

Figure 6-13. Resultant wave scattering α coefficients for retaining wall design.

in the design of retaining walls and slopes. Further discussion of the use of the α factor is provided in Chapter 7.

Results of these height-dependent seismic coefficient studies are general enough that they can be applied to either the seismic design of retaining walls, embankments and slopes, or buried structures. The design process involves first determining the response spectra for the site. This determination is made using either guidance in the 2008 AASHTO *LRFD Bridge Design Specifications* or from site-specific seismic hazard studies. Note that spectra in the 2007 AASHTO *LRFD Bridge Design Specifications* do not distinguish between CEUS and WUS shapes and are not consistent with this recommended approach; however, the newly adopted AASHTO ground motion maps will account for this difference. The only assumption made is that the ground motion design criteria should be defined by a 5 percent damped design response spectrum for the referenced free-field ground surface condition at the project site.

Once the design ground motion is established for a site, the analyses could proceed following the methodology outlined in this chapter. This methodology involves defining the seismic coefficient for the evaluation of retaining walls, slopes and embankments, or buried structures, as follows:

- The design ground motion demand is characterized by a design response spectrum that takes into account the seismic hazard and site response issues for the site. This requirement is rather standard, and should not present undue difficulties for the designer. The selection of the appropriate spectra shape should focus on the 1-second ordinate.
- Starting from the design response spectrum, the designer would normalize the response spectrum by the peak ground acceleration to develop the normalized spectral shape for the specific project site. This spectrum is then overlaid on the spectral shape shown on Figure 5-4 to determine the most appropriate spectral curve shape for the design condition.
- After selecting the appropriate spectral shape (that is, in terms of UB, Mid, and LB spectral shapes), Figure 6-13 is used to select the appropriate reduction factor (the α factor).

The approach described above was further simplified for use in the proposed Specifications by relating the α factor to height, PGA, and S_1 in a simple equation, as discussed in Chapter 7. Either the approach discussed in this chapter or the equation given in Chapter 7 is an acceptable method of determining the α factor.

As discussed earlier, wave scattering theory represents one of the several justifications for selecting a pseudo-static seismic coefficient lower than the peak ground acceleration. In addition to the wave scattering α factor, additional reduction factors may be applied as appropriate, including that some permanent movement is allowed in the design, as discussed in Chapter 7. Consideration also can be given to the use of a time-averaged seismic coefficient based on the average level of ground shaking, rather than the peak, as long as the structural designer confirms that the average inertial force is permissible for design.

CHAPTER 7

Retaining Walls

This chapter summarizes results of studies conducted for the seismic analysis and design of retaining walls. The primary objectives of these studies were to:

- Address limitations with current methods used to estimate seismic earth pressures on retaining walls. These limitations include difficulties in using the M-O equations for certain combinations of seismic coefficient and backslope above the retaining structure or for backfill conditions where soils are not cohesionless or are not uniform.
- Develop guidance on the selection of the seismic coefficient used to conduct either a force-based or displacement-based evaluation of the seismic performance of retaining walls. There is considerable confusion in current practice on the selection of the seismic coefficient, particularly for different wall types.
- Provide recommendations on methodologies to use for the seismic analysis and design of alternate wall types that can be used to develop LRFD specifications.

The approach taken to meet these objectives involved using results from the ground motion and wave scattering studies discussed in the previous two chapters. Specifically, the approach for determining ground motions and displacements summarized in Chapter 5 provides the information needed for a force-based design and for determining retaining wall displacements. The information in Chapter 6 is used for modifying the site-adjusted PGA to account for wave scattering effects. With this information two methodologies are provided for the seismic analysis and design of retaining walls. The first involves use of the classic M-O equations, and the second uses a more GLE methodology for cases where the M-O procedure is not applicable or where an estimate of retaining wall displacements is desired.

7.1 Current Design Practice

Various wall types are commonly used for transportation systems. A useful classification of these wall types is shown in Figure 7-1 (FHWA 1996), which uses terminology adopted in the AASHTO *LRFD Bridge Design Specifications.* The cut and fill designations refer to how the wall is constructed, not necessarily the nature of the earthwork (cut or fill) associated with the wall. For example, a fill wall, such as a MSE wall or a nongravity cantilever wall, may be used to retain earth fill for a major highway cut as illustrated in the representative Figures 7-2 to 7-5 showing wall types. This becomes an important factor in the subsequent discussions related to external seismic stability of such walls.

Current AASHTO *LRFD Bridge Design Specifications* address seismic design of retaining wall types as summarized in the following paragraphs:

1. Conventional gravity and semi-gravity cantilever walls (Article 11.6.5). The seismic design provisions cite the use of the M-O method (specified in Appendix A, Article A11.1.1.1) to estimate equivalent static forces for seismic loads. Reductions due to lateral wall movements are permitted as described in Appendix A (A11.1.1.1).
2. Nongravity cantilever walls (Article 11.8.6). Seismic design provisions are not explicit. Rather reference is made to an accepted methodology, albeit the M-O equations are suggested as a means to compute active and passive pressures provided a seismic coefficient of 0.5 times the site-adjusted PGA is used.
3. Anchored walls (Article 11.9.6). Seismic design provisions are not explicit, and reference is made to M-O method for cantilever walls. However, Article A11.1.1.3 indicates that,

   > For abutments restrained against lateral movement by tiebacks or batter piles, lateral pressures induced by inertia forces in the backfill will be greater than those given by the Mononobe-Okabe analysis.

   The discussion goes on to suggest using a factor of 1.5 in conjunction with site-adjusted PGA for design "where doubt exists that an abutment can yield sufficiently to mobilize soil strength."

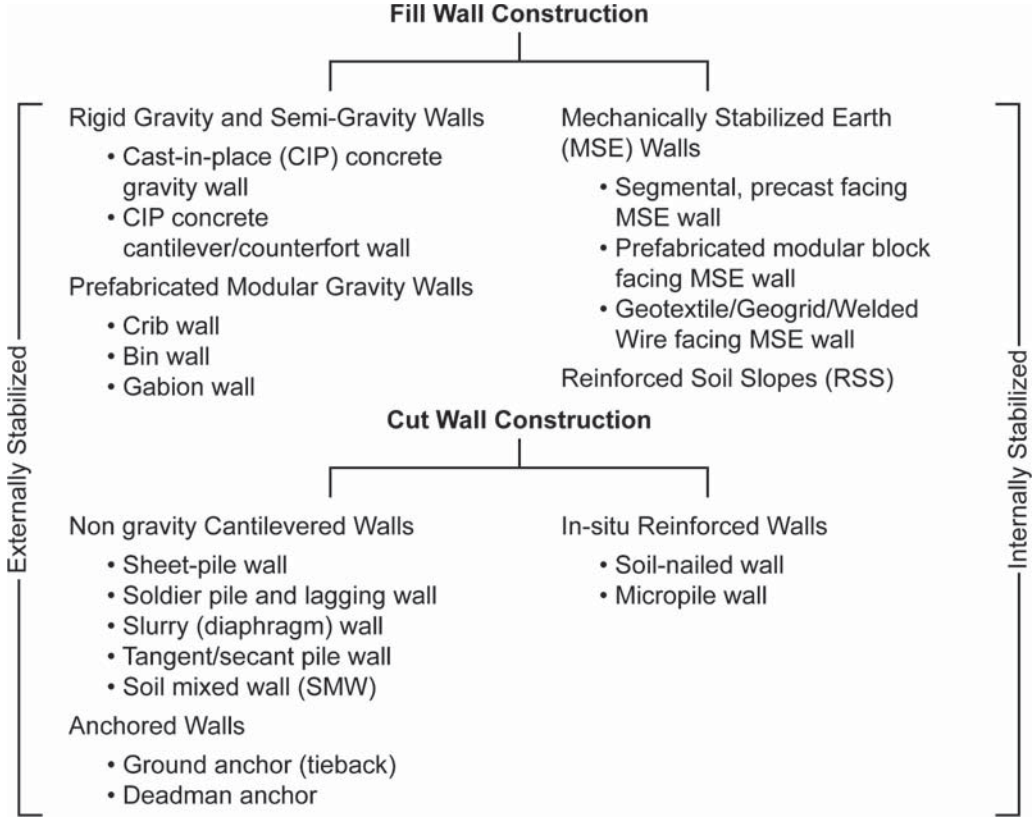

Figure 7-1. Earth retaining system classification (after FHWA, 1996).

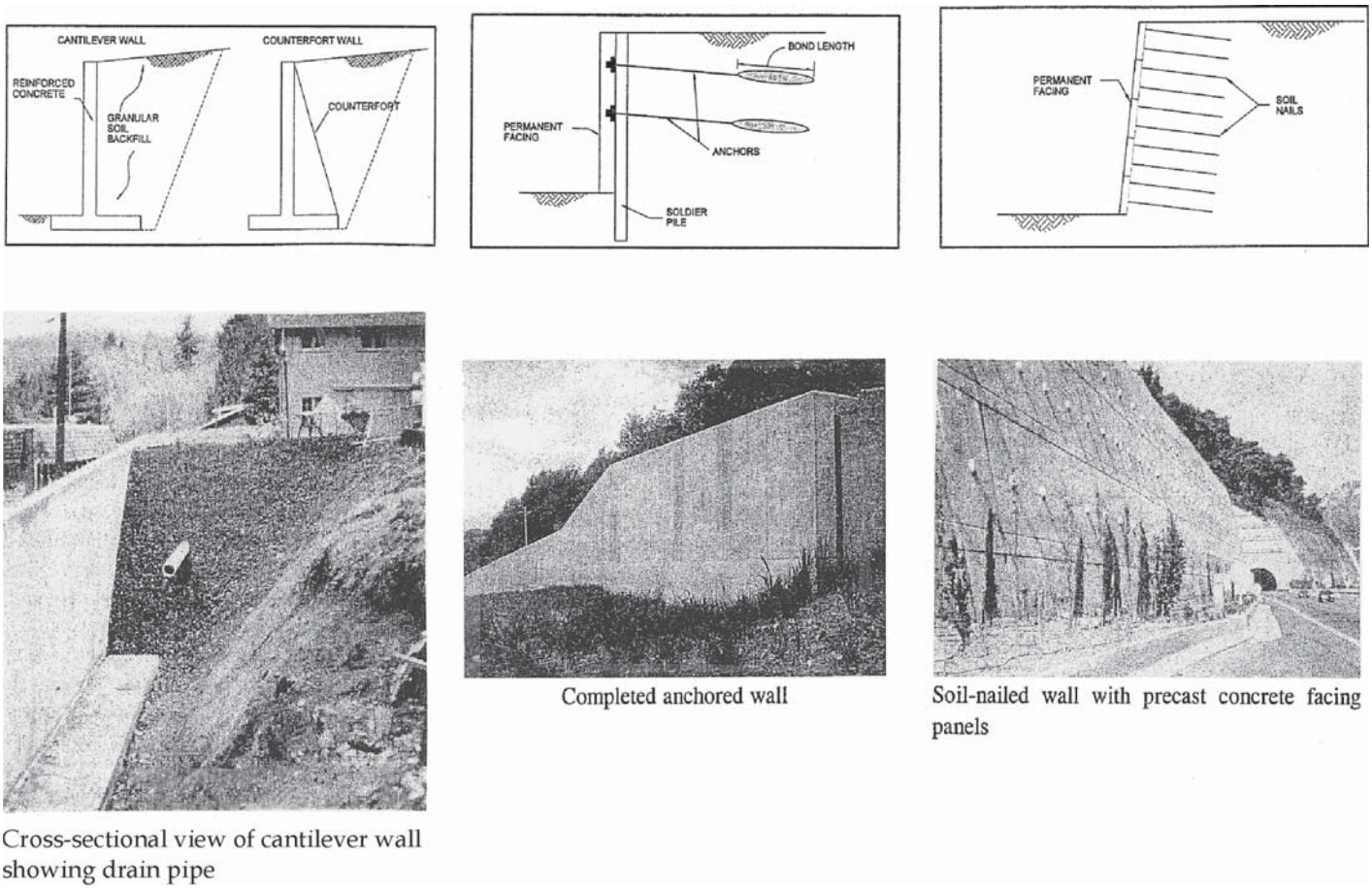

Figure 7-2. Wall types (after FHWA, 1996).

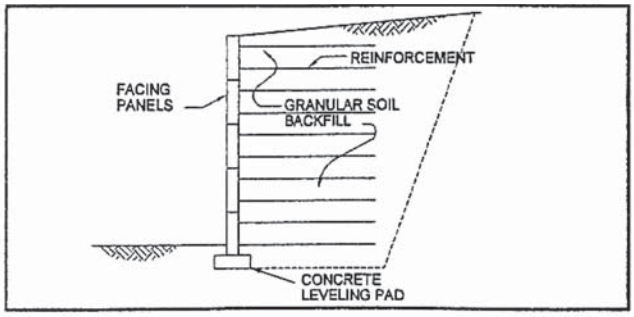

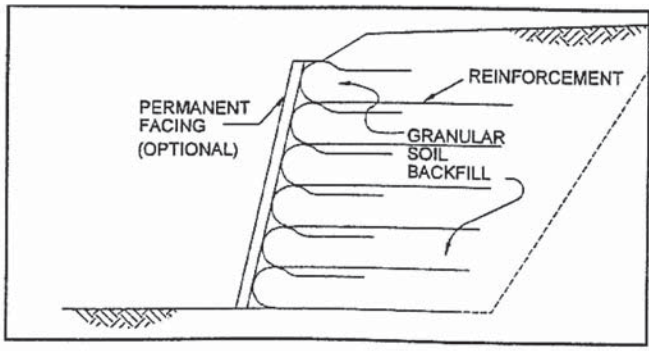

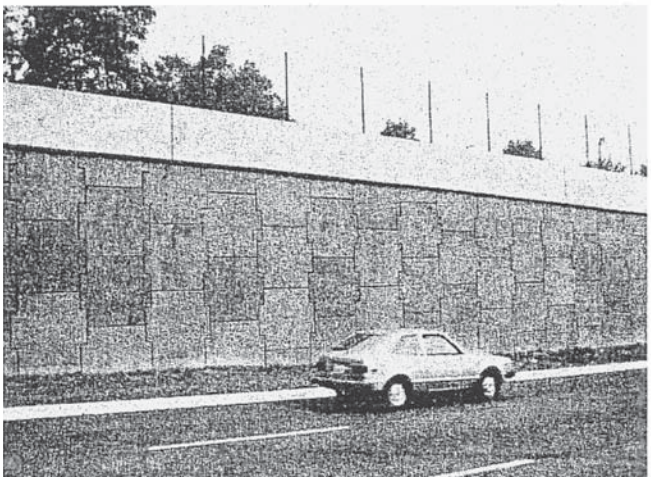

Completed MSE wall

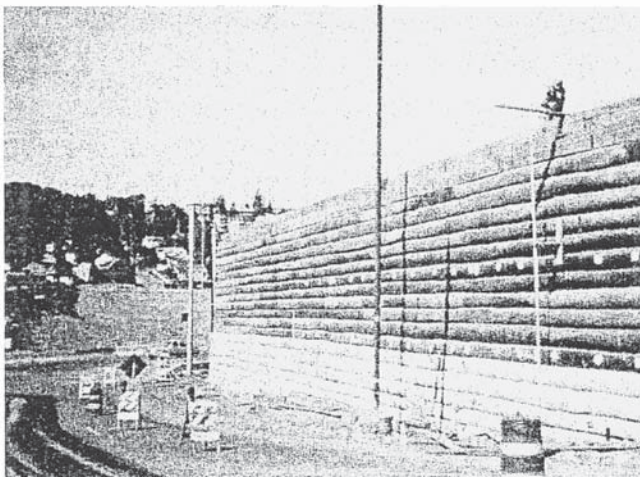

Geotextile wall

Figure 7-3. MSE wall types (after FHWA, 1996).

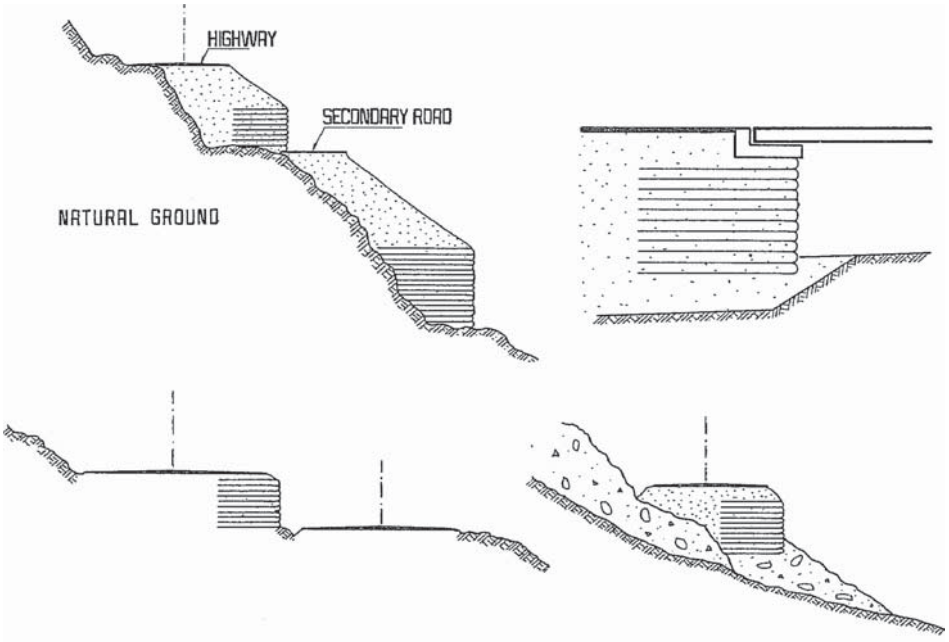

Figure 7-4. MSE walls—construction configurations.

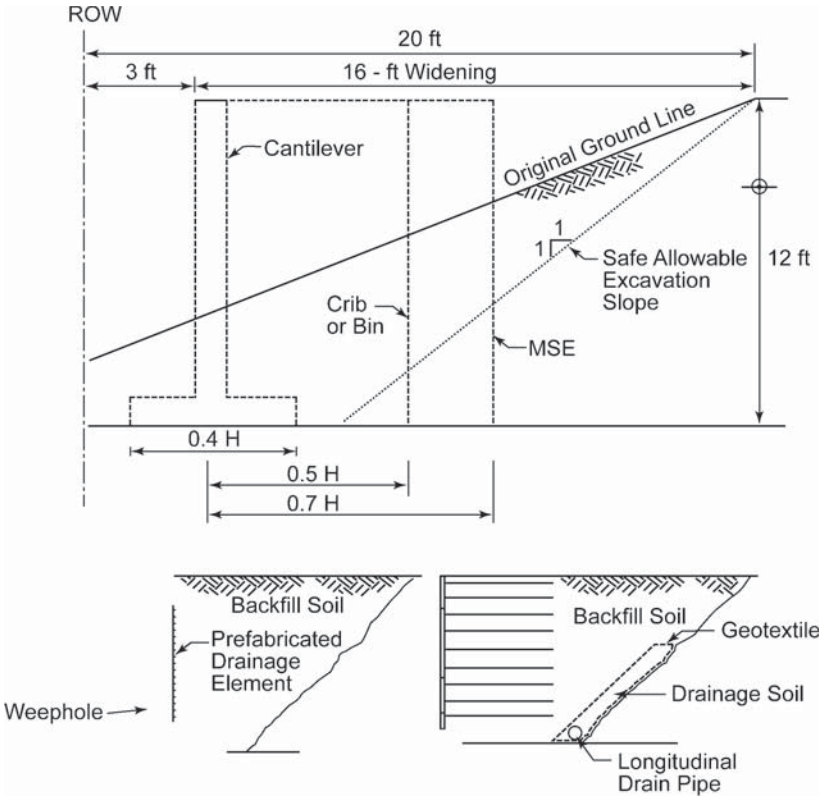

Figure 7-5. Cut slope construction.

4. MSE walls (Article 11.10.7). Seismic design provisions are very explicit and are defined for both external and internal stability. For external stability the dynamic component of the active earth pressure is computed using the M-O equation. Reductions due to lateral wall movement are permitted for gravity walls. Fifty percent of the dynamic earth pressure is combined with a wall inertial load to evaluate stability, with the acceleration coefficient modified to account for potential amplification of ground accelerations. In the case of internal stability, reinforcement elements are designed for horizontal internal inertial forces acting on the static active pressure zone.
5. Prefabricated modular walls (Article 11.11.6). Seismic design provisions are similar to those for gravity walls.
6. Soil-nail walls. No static or seismic provisions are currently provided in AASHTO *LRFD Bridge Design Specifications.* However, an FHWA manual for the design of nail walls (FHWA, 2003) suggests following the same general procedures as used for the design of MSE walls, which involves the use of the M-O equation with modifications for inertial effects.

The use of the M-O equations to compute seismic active and passive earth pressures is a dominant factor in wall design. Limitations and design issues are summarized in the following sections.

7.2 The M-O Method and Limitations

The analytical basis for the M-O solution for calculating seismic active earth pressure is shown in Figure 7-6 (taken from Appendix A11.1.1.1 of the AASHTO *LRFD Bridge Design Specifications*). This figure identifies the equations for seismic active earth pressures (P_{AE}), the seismic active earth pressure coefficient (K_{AE}), the seismic passive earth pressure (P_{PE}), and the seismic active pressure coefficient (K_{PE}). Implicit to these equations is that the soil within the soil is a homogeneous, cohesionless material within the active or passive pressure wedges.

7.2.1 Seismic Active Earth Pressures

In effect, the solution for seismic active earth pressures is analogous to that for the conventional Coulomb active pressure solution for cohesionless backfill, with the addition of a horizontal seismic load. Representative graphs showing the effect of seismic loading on the active pressure coefficient K_{AE} are shown in Figure 7-7. The effect of vertical seismic loading is traditionally neglected. The rationale for neglecting vertical loading is generally attributed to the fact that the higher frequency vertical accelerations will be out of phase with the horizontal accelerations and will have positive and negative contributions to wall pressures, which on average can reasonably be neglected for design.

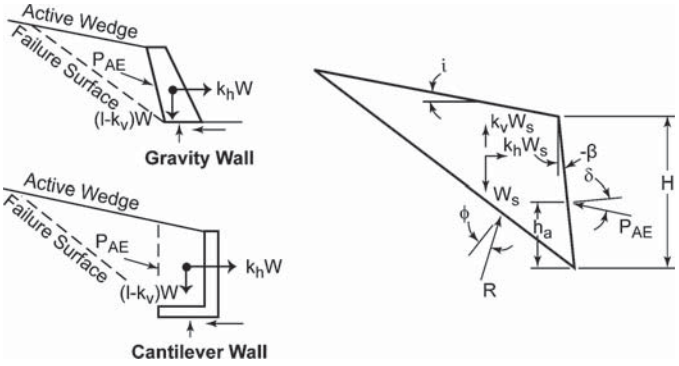

Seismic Active Earth Pressure

$$P_{AE} = 0.5\,\gamma\,H^2\left(1-k_v\right)K_{AE}$$

Seismic Passive Earth Pressure

$$P_{PE} = 0.5\,\gamma\,H^2\left(1-k_v\right)K_{PE}$$

where

$$K_{AE} = \frac{\cos^2(\phi-\theta-\beta)}{\cos\theta\cos^2\beta\cos(\delta+\beta+\theta)} \times\left[1-\sqrt{\frac{\sin(\phi+\delta)\sin(\phi-\theta-i)}{\cos(\delta+\beta+\theta)\cos(i-\beta)}}\right]^{-2}$$

$$K_{PE} = \frac{\cos^2(\phi-\theta+\beta)}{\cos\theta\cos^2\beta\cos(\delta-\beta+\theta)} \times\left[1-\sqrt{\frac{\sin(\phi+\delta)\sin(\phi-\theta+i)}{\cos(\delta-\beta+\theta)\cos(i-\beta)}}\right]^{-2}$$

γ = unit weight of soil (ksf)
H = height of wall (ft)
ϕ = friction angle of soil (°)
θ = arc tan $(k_h/(1-k_v))$(°)
δ = angle of friction between soil and wall (°)
k_h = horizontal acceleration coefficient (dim.)
k_v = vertical acceleration coefficient (dim.)
i = backfill slope angle (°)
β = slope of wall to the vertical, negative as shown (°)

Figure 7-6. M-O solution.

Figure 7-8 shows the effect of backfill slope angle on K_{AE} as a function of seismic coefficient, and illustrates the design dilemma commonly encountered of rapidly increasing earth pressure values with modest increases in slope angles. Figure 7-9 indicates the underlying reason, namely the fact that the failure plane angle α approaches that of the backfill slope angle ω, resulting in an infinite mass of the active failure wedge. For example, for a slope angle of 18.43° (3H:1V slope) and a seismic coefficient of 0.2, the failure plane is at an angle

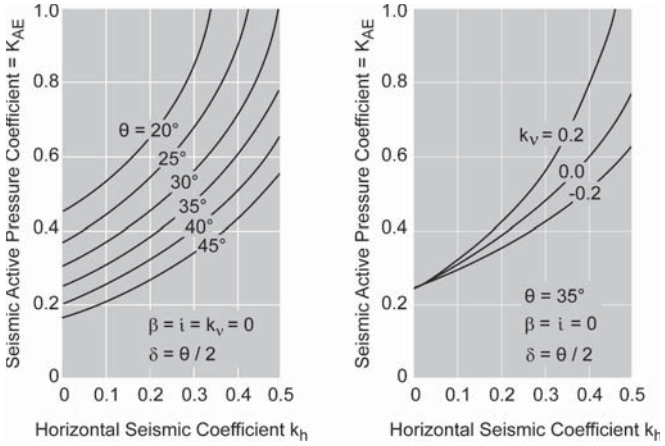

Figure 7-7. Effect of seismic coefficient and soil friction angle on active pressure coefficient.

of 38° in a $\phi = 35°$ material. The M-O solution increases significantly if the seismic coefficient increases to 0.25 for the same case, as the failure plane angle decreases to 31°. In practice, however, as shown in Figures 7-3 to 7-5, the failure plane would usually intersect firm soils or rock in the cut slope behind the backfill rather than the slope angle defined by a purely cohesionless soil, as normally assumed during the M-O analyses. Consequently, in this situation the M-O solution is not valid.

A designer could utilize an M-O approach for simple non-homogeneous cases such as shown in Figure 7-10 using the following procedure, assuming $\phi_1 < \phi_2$:

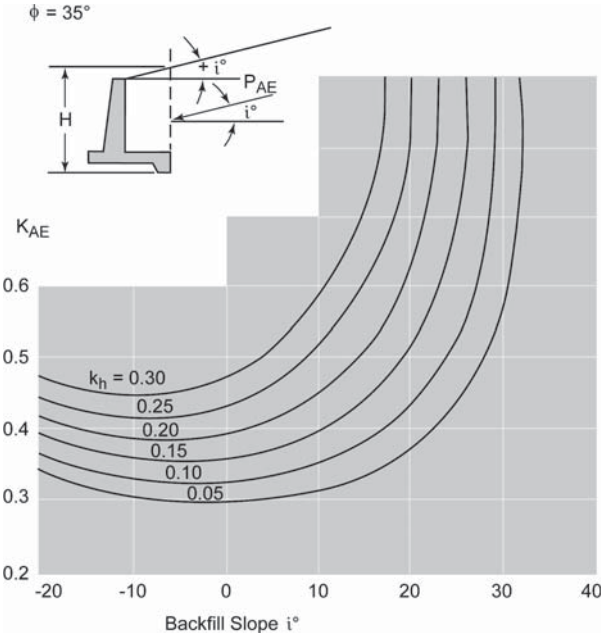

Figure 7-8. Effect of backfill slope on the seismic active earth pressure coefficient using M-O equation, where CF = seismic coefficient.

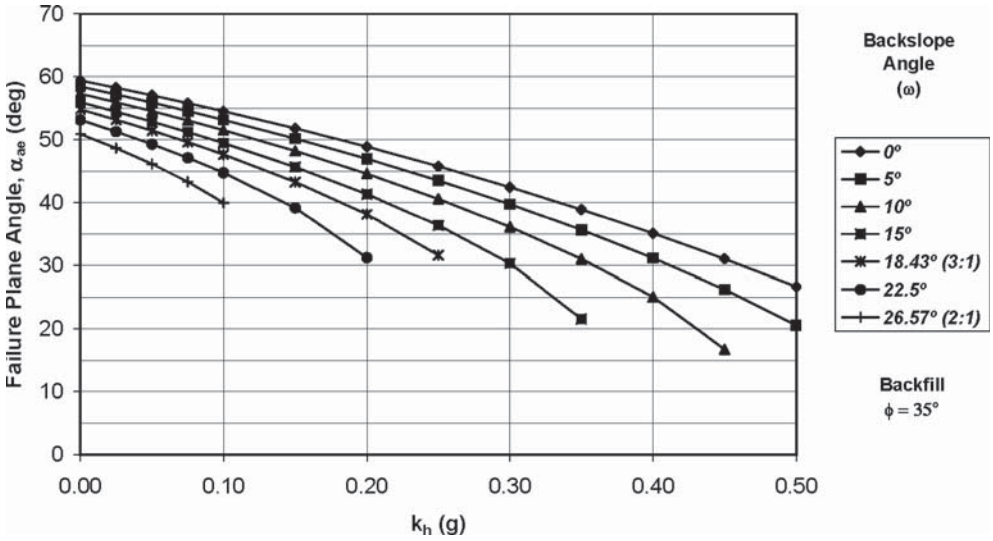

Figure 7-9. Active failure plane angle based on M-O equation.

1. Calculate the active pressure P_{AE1} and active failure plane angle (α_{AE1}) for the backfill material. Graphs such as Figures 7-8 and 7-9 may be used for simple cases.
2. If $\alpha_{AE1} < \alpha_{1/2}$, the solution stands and P_{AE1} gives the correct seismic active pressure on the wall.
3. If $\alpha_{AE1} > \alpha_{1/2}$, calculate the active pressure (P_{AE2}) and active failure plane angle (α_{AE2}) for the native soil material. For cohesive (c-ϕ) soils, solutions described in Section 7.3 may be used. Also, calculate the active pressure (P_{AEi}) for the given interface between two soils from limit equilibrium equations. The larger of P_{AEi} and P_{AE2} gives the seismic active pressure on the wall.

In most cases, the native soil cut will be stable, in which case it will be clear that the active pressure corresponding to the cut angle $\alpha_{1/2}$ will govern. For more complex cases involving nonuniform backslope profiles and backfill/cut slope soils, numerical procedures using the same principles of the M-O method may be used, such as the well-known, graphical Culmann method illustrated in Figure 3-1. The principles of the Culmann wedge method have been incorporated in the Caltrans' computer program CT-FLEX (Shamsabadi, 2006). This program will search for the critical failure surface corresponding to the maximum value of P_{AE} for nonuniform slopes and backfills, including surcharge pressures.

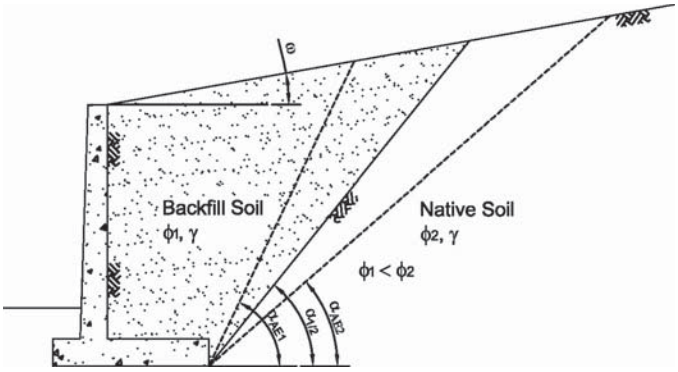

Figure 7-10. Application of M-O method for nonhomogeneous soil.

For uniform cohesive backfill soils with c and ϕ strength parameters, solutions using M-O analysis assumptions have been developed, as discussed in Section 7.3. However, the most versatile approach for complex backfill and cut slope geometries is to utilize conventional slope stability programs, as described in Section 7.4.

7.2.2 Seismic Passive Earth Pressures

The M-O equation for passive earth pressures also is shown in Figure 7-6. The seismic passive pressure becomes important for some wall types that develop resistance from loading of the embedded portion of the wall. If the depth of embedment is limited, as in the case of many gravity, semi-gravity, and MSE walls, the importance of the passive earth pressure to overall equilibrium is small, and therefore, using the static passive earth pressure is often acceptable.

In the case of nongravity cantilever walls and anchored walls the structural members below the excavation depth depend on the passive earth pressure for stability and therefore the effects of seismic loading on passive earth pressures can be an important contribution. Work by Davies et al. (1986) shows that the seismic passive earth pressure can decrease by 25 percent relative to the static passive earth pressure for a seismic coefficient of 0.4. This decrease is for a $\phi = 35$ degree material and no backslope or wall friction.

Although the reduction in passive earth pressure during seismic loading is accounted for in the M-O equation for passive pressures (Equation A11.1.1.1-4 in AASHTO *LRFD Bridge Design Specifications*), the M-O equation for passive earth pressures is based on a granular soil and Coulomb failure theory. Various studies have shown that Coulomb theory is unconservative in certain situations. Similar to the M-O equation for active earth pressure, the M-O equation for passive earth pressure also does not include the contributions of any cohesive content in the soil. The preferred approach for passive earth pressure determination is to use log spiral procedures, similar to the preferred approach for gravity loading. Shamsabadi et al. (2007) have published a generalized approach that follows the log spiral procedure, while accounting both for the inertial forces within the soil wedge and the cohesive content within the soil.

A key consideration during the determination of static passive pressures is the wall friction that occurs at the soil-wall interface. Common practice is to assume that some wall friction will occur for static loading. The amount of interface friction for static loading is often assumed to range from 50 to 80 percent of the soil friction angle. Similar guidance is not available for seismic loading. In the absence of any guidance, the static interface friction value often is used for seismic design.

Another important consideration when using the seismic passive earth pressure is the amount of deformation required to mobilize this force. The deformation to mobilize the passive earth pressure during static loading is usually assumed to be large, say 2 to 5 percent of the embedded wall height, depending on the type of soil (that is, granular soils will be closer to the lower limit while cohesive soils are closer to the upper limit). Only limited guidance is available for seismic loading (for example, see Shamsabadi et al., 2007), and therefore the displacement to mobilize the seismic passive earth pressure is often assumed to be the same as for static loading.

7.3 M-O Earth Pressures for Cohesive Soils

The M-O equation has been used to establish the appropriate earth pressure coefficient (K_{AE}) for a given seismic coefficient k_h. Although it is possible to use the Coulomb method to develop earth pressure equations or charts that include the contribution of any cohesive content, the available M-O earth pressure coefficient equations and charts have been derived for a purely cohesionless (frictional) soil where the soil failure criteria would be the Mohr-Coulomb failure criterion, parameterized by the soil friction angle, ϕ. However, experience from limit equilibrium slope stability analyses shows that the stability of a given slope is very sensitive to the soil cohesion, even for a very small cohesion.

7.3.1 Evaluation of the Contribution from Cohesion

Most natural cohesionless soils have some fines content that often contributes to cohesion, particularly for short-term loading conditions. Similarly, cohesionless backfills are rarely fully saturated, and partial saturation would provide for some apparent cohesion, even for clean sands. In addition, it appears to be common practice in some states, to allow use of backfill soils with 30 percent or more fines content (possibly containing some clay fraction), particularly for MSE walls. Hence the likelihood in these cases of some cohesion is very high. The effect of cohesion, whether actual or apparent, is an important issue to be considered in practical design problems.

The M-O equations have been extended to c-ϕ soils by Prakash and Saran (1966), where solutions were obtained for cases including the effect of tension cracks and wall adhesion. Similar solutions also have been discussed by Richards and Shi (1994) and by Chen and Liu (1990).

To further illustrate this issue, analyses were conducted by deriving the M-O equations for active earth pressures and extending it from only a ϕ soil failure criterion to a generalized c-ϕ soil failure criterion. Essentially, limit equilibrium analyses were conducted using trial wedges. The active earth pressure value (P_{AE}) was computed to satisfy the condition of moment equilibrium of each of the combinations of the assumed trial wedge and soil shear strength values over the failure surface. The configurations of the trial wedges were varied until the relative maximum P_{AE} value was obtained for various horizontal seismic coefficient k_h. The planar failure mechanism is retained in the analyses and is a reasonable assumption for the active earth pressure problem. Zero wall cohesion was assumed and tension cracks were not included.

7.3.2 Results of M-O Analyses for Soils with Cohesion

Figure 7-11 and Figure 7-12 present active earth pressure coefficient charts for two different soil friction angles with different values of cohesion for horizontal backfill, assuming no tension cracks and wall adhesion. Within each chart, earth pressure coefficients are presented as a function of the seismic coefficient (k_h,) and various values of cohesion (c). The c value was normalized by the product $\gamma * H$ where γ is the unit weight of soil and H is the wall height in the presented design charts.

The following illustrates both the use and the importance of the cohesive contribution:

1. For a typical compacted backfill friction angle of 40 degrees, the $c/\gamma * H$ would be about 0.083 and 0.167 for a slope height (H) of 20 feet and 10 feet, respectively (for a $\gamma = 120$ pcf in combination of a small cohesion value $c = 200$ psf).
2. From Figure 7-12 (for $\phi = 40$ degrees), it can seen that the resultant design force coefficients K_{ae} for a seismic coefficient

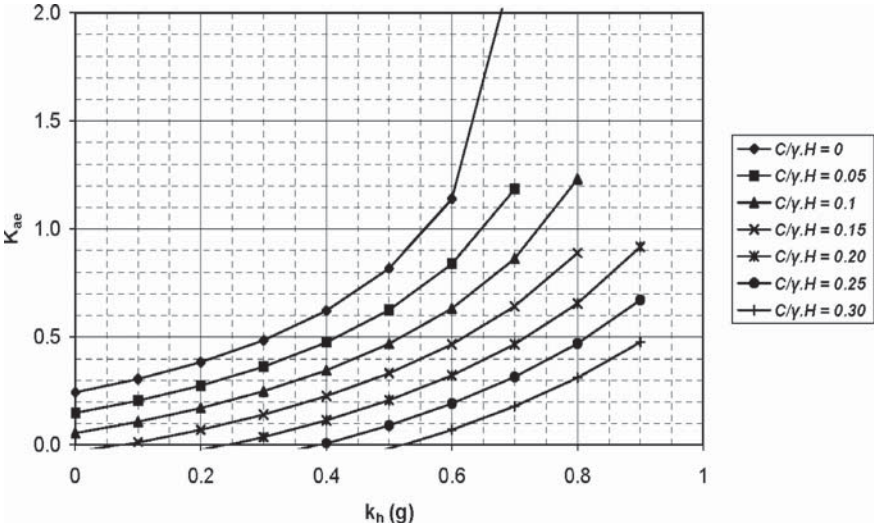

Figure 7-11. Seismic coefficient charts for c-ϕ soils for ϕ = 35°.

$k_h = 0.3$ would be (i) 0.4 for no cohesion; (ii) 0.25 for a wall height 20 feet with 200 psf cohesion, and (iii) be 0.1 for a wall height at 10 feet with 200 psf cohesion.

7.3.3 Implication to Design

From this example, it can be observed that a small amount of cohesion would have a significant effect in reducing the dynamic active earth pressure for design. The reduction for typical design situations could be on the order of about 50 percent to 75 percent. For many combinations of smaller k_h conditions (which would be very prevalent for CEUS conditions) and also shorter wall heights, a rather small cohesion value would imply that the slope is stable and the soil capacity, in itself, would have inherent shear strength to resist the inertial soil loading leading to the situation of zero additional earth pressure imparted to the retaining wall during a seismic event. This phenomenon could be a factor in explaining the good performance of retaining walls in past earthquakes.

To illustration this, traditionally reduction factors on the order of about 0.5 have been applied to the site-adjusted PGA to determine the seismic coefficient used in wall design. Wall movement is a recognized justification for the reduction factor as previously discussed. However, the wall movement concept may not be correct for retaining walls supported on piles, particularly if battered piles are used to limit the movement of the wall. In this case the contributions of a small amount of cohesion (for example, 200 psf) could effectively reduce the seismic coefficient of a 20-foot tall wall by a factor of 0.5, thereby achieving the same effects as would occur for a wall that is able to move.

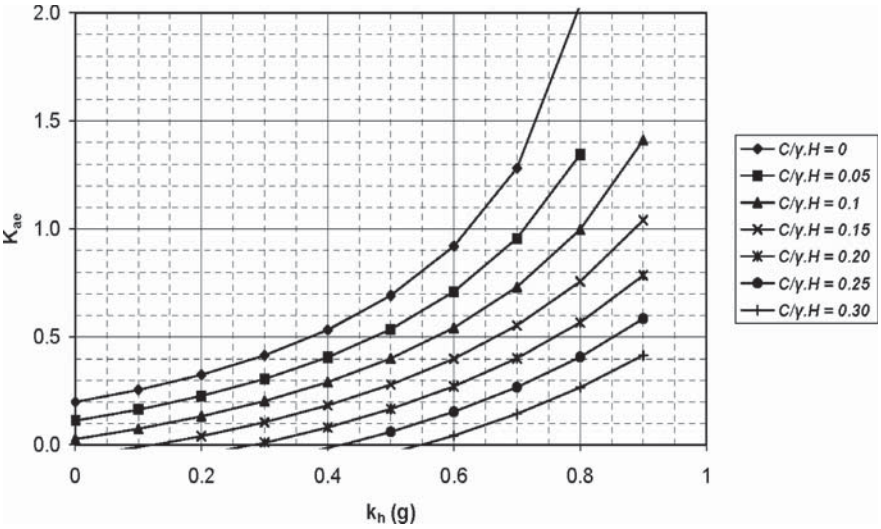

Figure 7-12. Seismic coefficient charts for c-ϕ soils for ϕ = 40°.

Mobilization of cohesion could significantly reduce seismic earth pressures to include such reductions in design practice is not always straight forward due to uncertainties in establishing the magnitude of the cohesion for compacted fills where mixed *c*-ϕ conditions exist under field conditions. This is particularly the case for cohesionless fills, where the degree of saturation has a significant effect on the apparent cohesion from capillarity.

From a design perspective, uncertainties in the amount of cohesion or apparent cohesion makes it difficult to incorporate the contributions of cohesion in many situations, particularly in cases where clean backfill materials are being used, regardless of the potential benefits of partial saturation. However, where cohesive soils are being used for backfill or where native soils have a clear cohesive content, then the designer should give consideration to incorporating some effects of cohesion in the determination of the seismic coefficient.

7.4 GLE Approach for Determining Seismic Active Pressures

To overcome the limitations of the M-O method for cases involving nonhomogeneous soils and complex backslope geometry, conventional limit-equilibrium slope stability computer programs may be used. The concept has been illustrated, in a paper by Chugh (1995). For the purpose of both evaluation of this approach and application to examples used for the recommended methodology (Appendix F), the computer program SLIDE (RocScience, 2005), a program widely used by geotechnical consultants, was used.

The basic principle in using such programs for earth pressure computations is illustrated in Figure 7-13. Steps in the analysis are as follows:

1. Setup the model geometry, ground water profile, and design soil properties. The internal face of the wall, or the plane where the earth pressure needs to be calculated, should be modeled as a free boundary.
2. Choose an appropriate slope stability analysis method. Spencer's method generally yields good results because it satisfies the equilibrium of forces and moments.

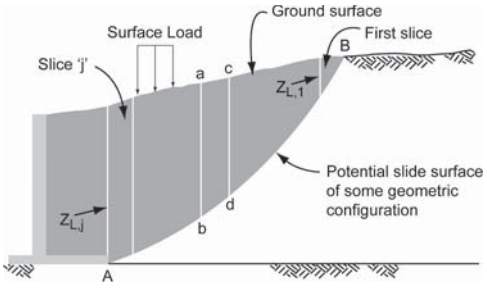

Figure 7-13. Adoption of slope stability programs to compute seismic earth pressure (Chugh, 1995).

3. Choose an appropriate sliding surface search scheme. Circular, linear, multi-linear, or random surfaces can be examined by SLIDE and other commercial slope stability analysis programs.
4. Apply the earth pressure as a boundary force on the face of the retained soil. The location of the force is assumed at one-third from the base (⅓ H, where H is retained soil height) for static cases. For seismic cases the location can be reasonably assumed at mid height (0.5 H) of the retained soil. However, different application points between ⅓ H and ⅔ H from the base can be examined to determine the maximum seismic earth pressure. The angle of applied force depends on assumed friction angle between wall and soil. A horizontal load simulates a smooth wall, whereas a load inclined at ϕ degrees indicates that the friction angle between wall and soil is equal or greater than internal friction angle of the soil.
5. Change the magnitude of the applied load until a minimum ratio of C/D of 1.0 is obtained. The C/D ratio is equivalent to the factor of safety for the analyses. The force corresponding to a C/D ratio of 1.0 is equal to total earth pressure on the retaining structure.
6. Verify design assumptions and material properties by examining the loads on individual slices in the output.

The program SLIDE was calibrated against M-O solutions by considering examples shown on Figures 7-14 and 7-15. The first set of figures shows the application of SLIDE for computing active earth pressure on a wall with horizontal backfill. The two analyses in Figure 7-14A show the computation of the active earth pressure for a homogeneous backfill and seismic acceleration of 0.2g and 0.4g. The calculated results are identical to results from the M-O equation. The two analyses in Figure 7-14B show computation of the active earth pressure for a case with nonhomogenous backfill. Figures 7-15A and 7-15B show the similar analyses for a wall with sloping backfill.

7.5 Height-Dependent Seismic Design Coefficients

Current AASHTO *LRFD Bridge Design Specifications* use peak ground acceleration in conjunction with M-O analysis to compute seismic earth pressures for retaining walls. Except for MSE walls where amplification factors as a function of peak ground acceleration are used, based on studies by Segrestin and Bastick (1988), the current approach makes no adjustments in assigned ground acceleration for wall height. Chapter 6 provides a fundamental approach for making these adjustments based on scattering analyses for elastic soils. To confirm that the recommendations in Chapter 6 apply for situations where there is an impedance contrast between foundation and fills, and the possible influence of nonlinear soil behavior, an additional set of analyses was performed. Results

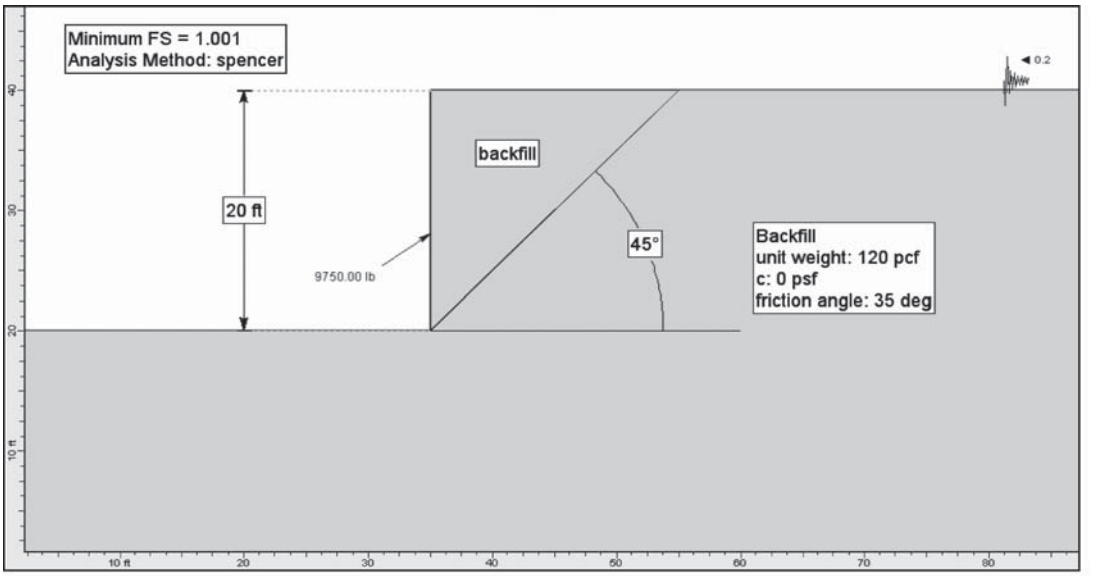

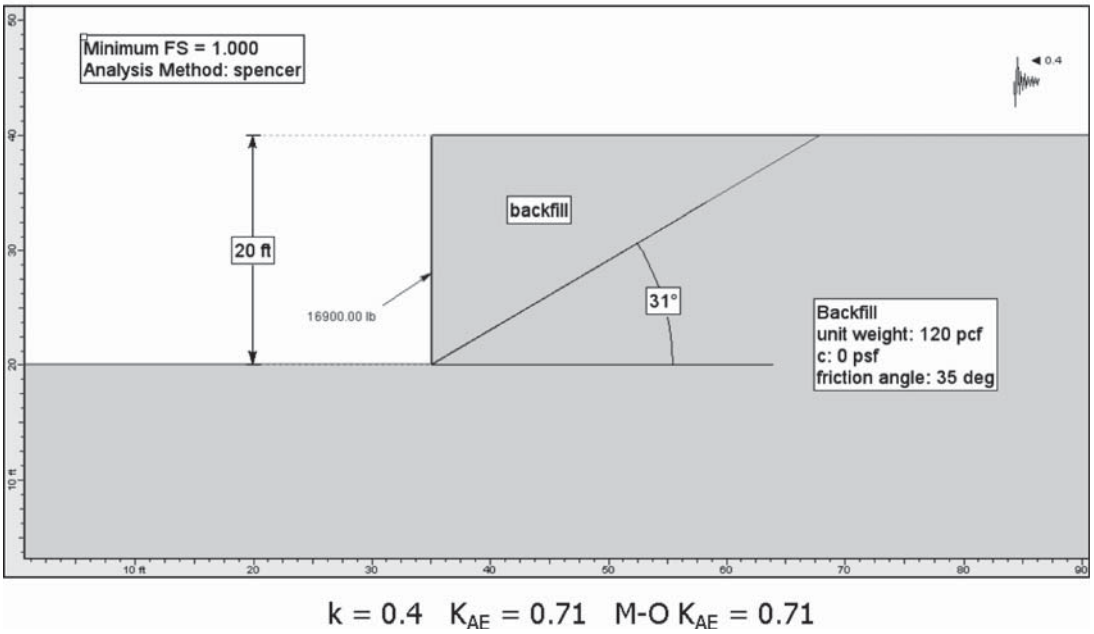

Figure 7-14A. SLIDE calibration analyses for horizontal backfill (homogeneous soil conditions).

of these analyses are used with the results of the analyses in Chapter 6 to develop recommendations for height-dependent seismic design coefficients.

7.5.1 Evaluation of Impedance Contrasts and Soil Behavior

To examine the effects of impedance contrasts and nonlinear soil behavior on height effects, one-dimensional SHAKE91 (1992) analyses were undertaken and are documented in detail in Appendix G. The initial set of SHAKE analyses repeated many of the parameters originally evaluated by Segrestin and Bastick:

- 20-foot wall height.
- Three different shear wave velocities for soil supporting the wall (820 ft/sec; 1,200 ft/sec; and 3,300 ft/sec). Idriss modulus and damping versus shearing strain curves for rock.
- Compacted backfill within wall with $\phi = 30$ degrees and maximum shear modulus (G_{max}) equal to 70 $(\sigma'_m)^{0.5}$. The

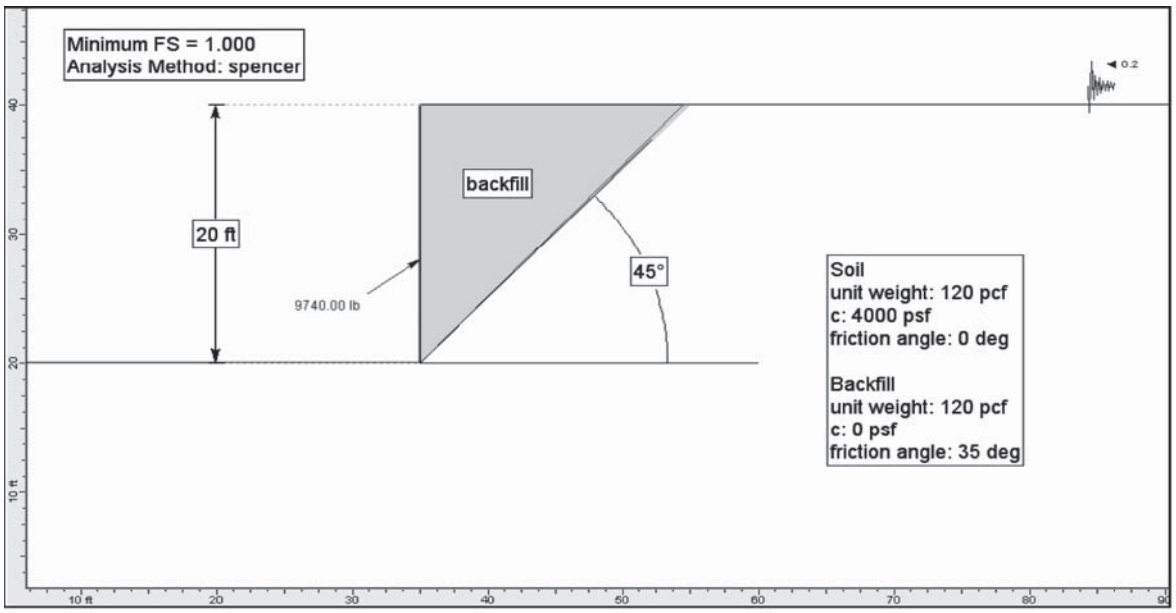

$k = 0.2 \qquad K_{AE} = 0.41$

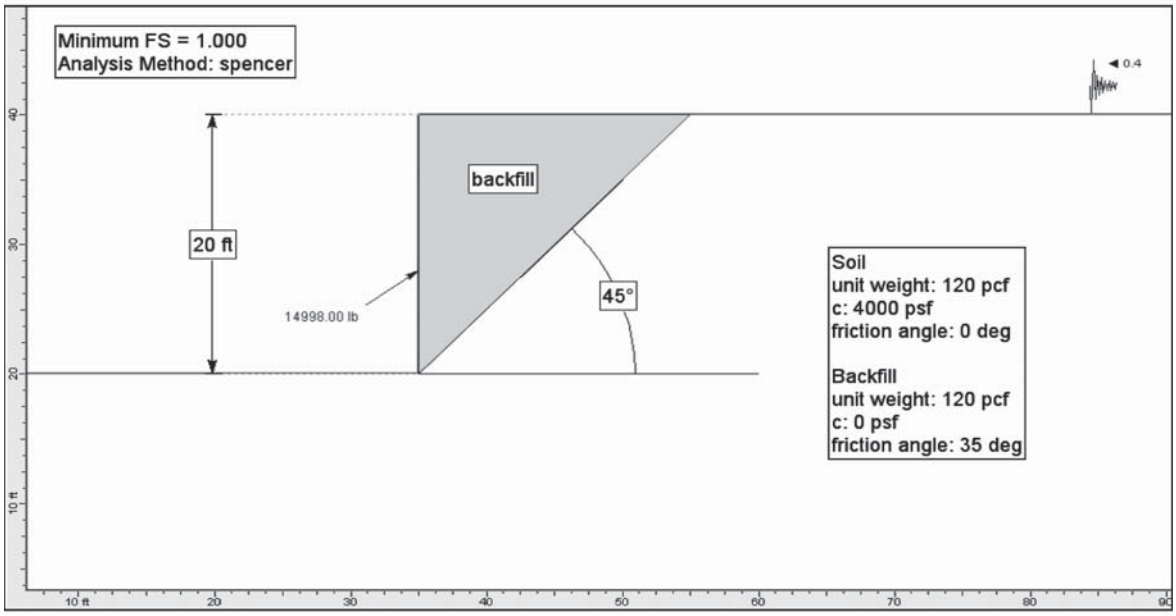

$k = 0.4 \quad K_{AE} = 0.63$

Figure 7-14B. SLIDE calibration analyses for horizontal backfill (nonhomogeneous soil conditions).

Seed and Idriss modulus and damping curves were used to represent shearing strain effects.

- Nine ground motions consistent with the discussions in Chapter 5, including the two used by Segrestin and Bastick.

These studies were successfully calibrated against studies undertaken by Segrestin and Bastick (1988) for MSE walls, which forms the basis for MSE wall backfill seismic coefficients and external stability evaluations in the AASHTO *LRFD Bridge Design Specifications.* Plots showing these comparisons are provided in Appendix G. These results show amplification at the top of the wall, as well as maximum average acceleration along the wall height, similar to results from Segrestin and Bastick. However, the latter studies were limited to 20-foot high (6 meter) walls.

Additional parametric studies were subsequently conducted to evaluate the effects of wall heights, impedance

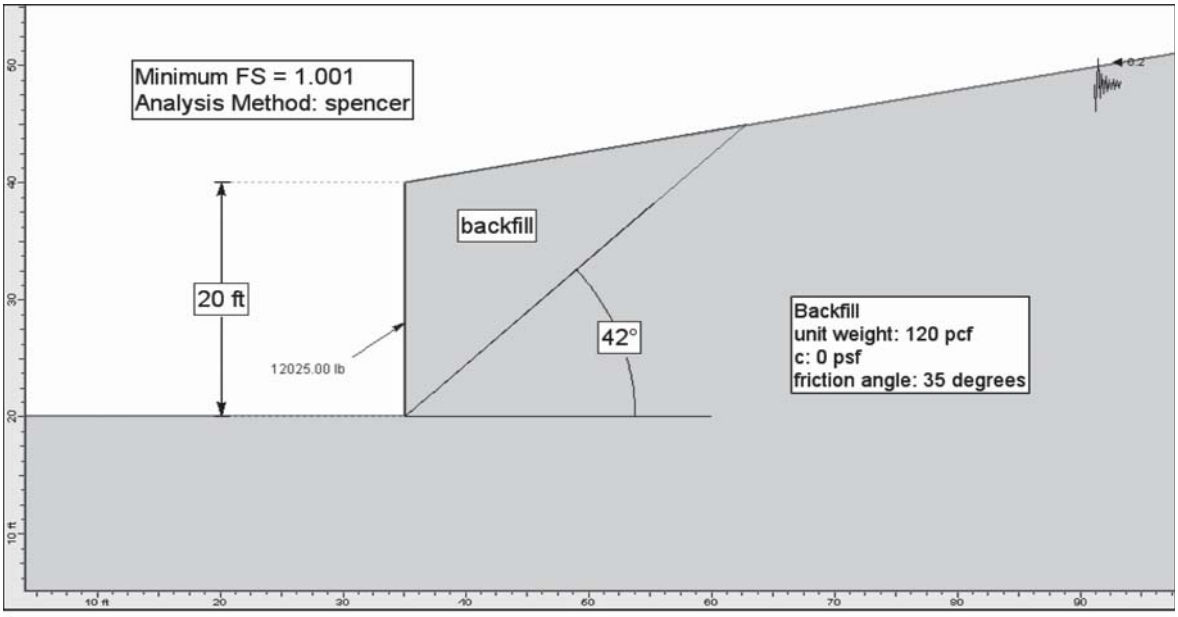

Figure 7-15A. SLIDE calibration analyses for sloping backfill (homogeneous soil conditions).

contrasts, and accelerations levels, using the same SHAKE models:

- Response evaluated at wall heights of 20, 50, and 100 feet.
- The low-strain shear modulus changed to $G_{max} = 59\ (\sigma'_m)^{0.5}$ to correspond to a relative density of 75 percent, which was judged to be more realistic.
- Nine ground motions used as noted above.

7.5.2 Results of Impedance Contrast and Nonlinearity Evaluations

Results of the studies summarized above and described in Appendix G generally follow trends similar to the wave scattering studies described in Chapter 6. However, based on a study of the results and to simplify the results for the development of recommended specifications and commen-

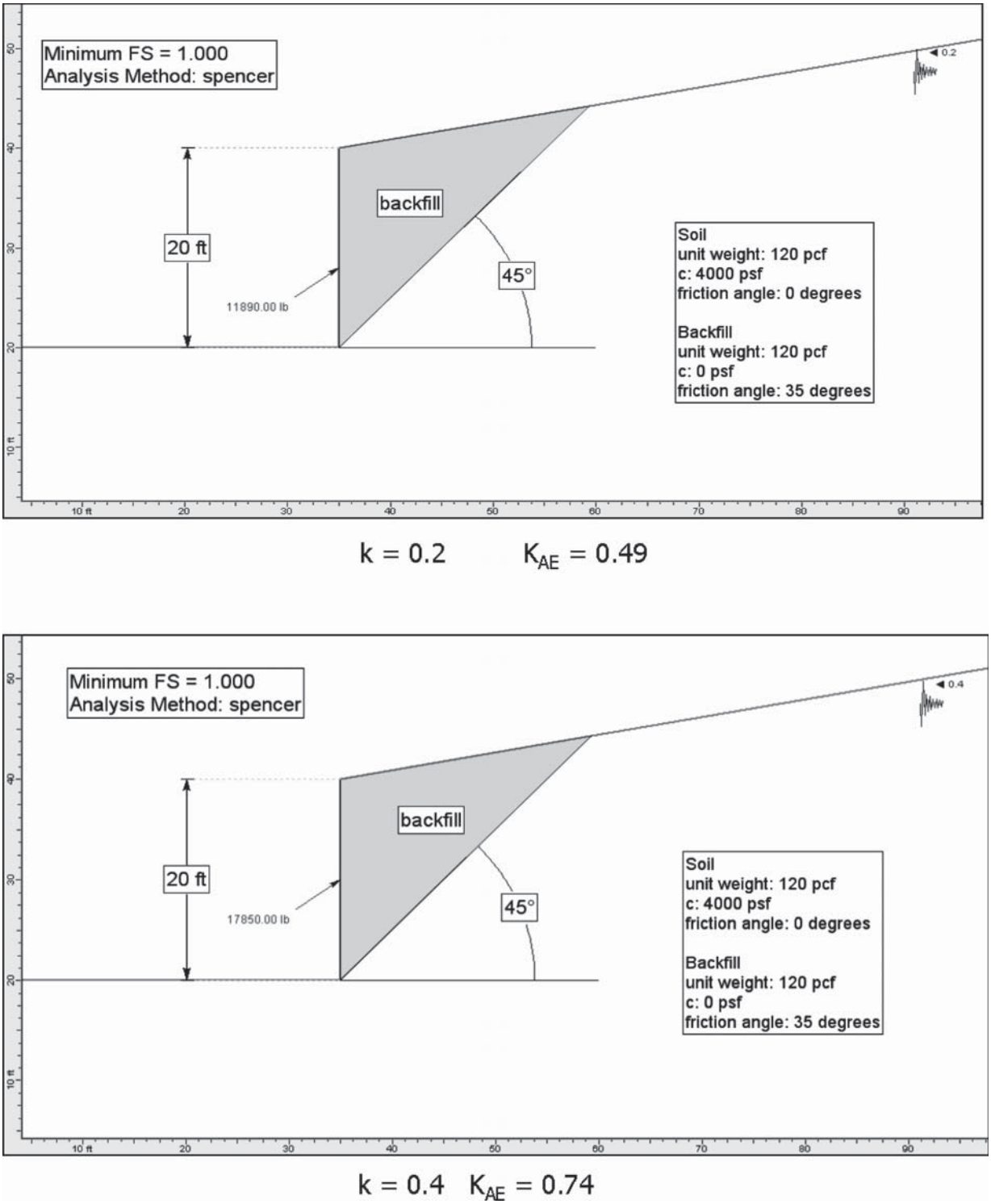

Figure 7-15B. SLIDE calibration analyses for sloping backfill (nonhomogeneous soil conditions).

taries for the AASHTO *LRFD Bridge Design Specifications,* the use of a simple linear function to describe reductions in average height-dependent seismic coefficients, as shown in Figure 7-16, is recommended. Comparisons with the curves resulting from the height-dependent scattering studies also are noted in Figure 7-16.

Curves in Figure 7-16 from Chapter 6 are for slightly different equivalent β values than shown for the simplified approach. These values are 1.7, 1.1, and 0.4 for UB, mid, and LB spectral response, respectively. The differences in the β values explain the difference between the locations of the lines for the curves from Chapter 6 versus the simplified straight-line functions.

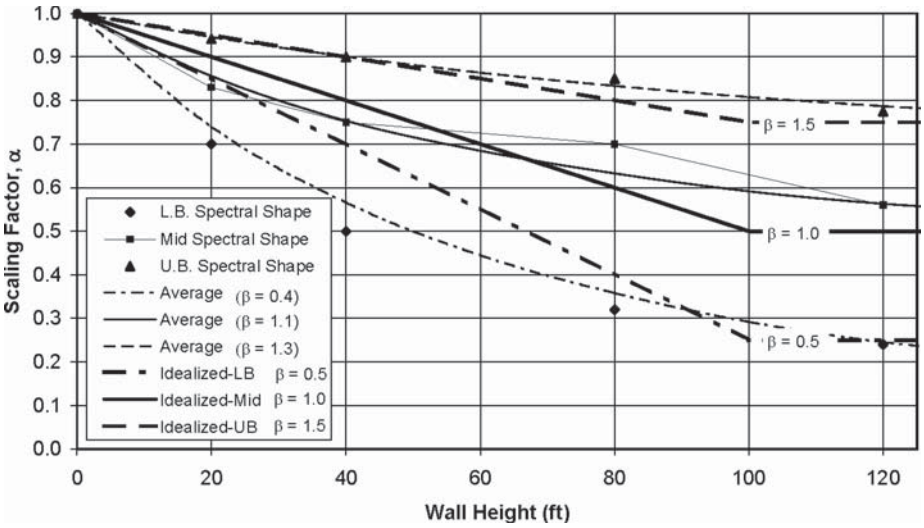

Figure 7-16. Simplified height-dependent scaling factor recommended for design.

Recommendations for seismic coefficients to be used for earth pressure evaluations based on the simplified straight line functions shown can be expressed by the following equations:

$$k_{av} = \alpha\, k_{\max} \tag{7-1}$$

where

$k_{\max}$ = peak seismic coefficient at the ground surface = F_{pga} PGA; and

α = fill height-dependent reduction factor.

For C, D, and E foundations soils

$$\alpha = 1 + 0.01H\left[(0.5\beta) - 1\right] \tag{7-2}$$

where

H = fill height in feet; and

$\beta = F_v S_1 / k_{\max}$.

For Site Class A and B foundation conditions (that is, hard and soft rock conditions) the above values of α should be increased by 20 percent. For wall heights greater than 100 feet, α coefficients may be assumed to be the 100-foot value. Note also for practical purposes, walls less than say 20 feet in height and on very firm ground conditions (B/C foundations), $k_{av} \approx k_{\max}$ which has been the traditional assumption for design.

7.6 Displacement-Based Design for Gravity, Semi Gravity, and MSE Walls

The concept of allowing walls to slide during earthquake loading and displacement-based design (that is, assuming a Newmark sliding block analysis to compute displacements when accelerations exceed the horizontal limiting equilibrium yield acceleration) was introduced by Richards and Elms (1979). Based on this concept (as illustrated in Figure 7-17), Elms and Martin (1979) suggested that a design acceleration coefficient of 0.5A in M-O analyses would be adequate for limit equilibrium pseudo-static design, provided allowance be made for a horizontal wall displacement of 10A (in inches). The design acceleration coefficient (A) is the peak ground acceleration at the base of the sliding wedge behind the wall in gravitational units (that is, g). This concept was adopted by AASHTO in 1992, and is reflected in following paragraph taken from Article 11.6.5 of the 2007 AASHTO *LRFD Bridge Design Specifications.*

> Where all of the following conditions are met, seismic lateral loads may be reduced as provided in Article C11.6.5, as a result of lateral wall movement due to sliding, from values determined

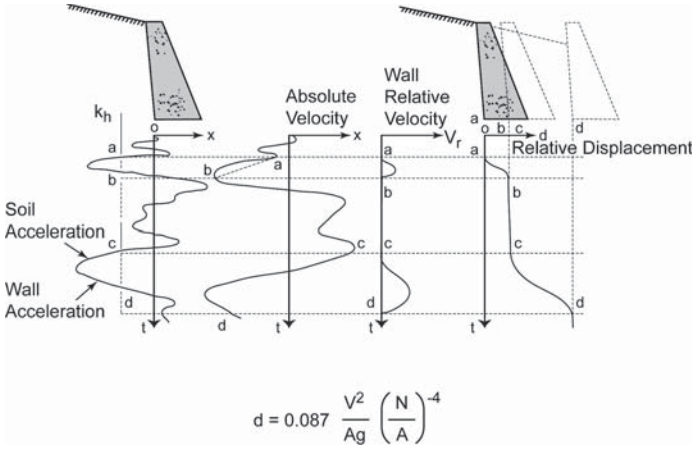

Figure 7-17. Concept of Newmark sliding block analysis (AASHTO, 2007).

using the Mononobe-Okabe method specified in Appendix A11, Article A11.1.1.1.1:

- The wall system and any structures supported by the wall can tolerate lateral movement resulting from sliding of the structure.
- The wall base is unrestrained against sliding, other than soil friction along its base and minimal soil passive resistance.
- If the wall functions as an abutment, the top of the wall must also be restrained, e.g., the superstructure is supported by sliding bearings.

The commentary for this Article notes that,

In general, typical practice among states located in seismically active areas is to design walls for reduced seismic pressures corresponding to 2 to 4 inches of displacement. However, the amount of deformation which is tolerable will depend on the nature of the wall and what it supports, as well as what is in front of the wall.

Observations of the performance of conventional cantilever gravity retaining walls in past earthquakes, and in particular during the Hyogoken-Nambu (Kobe) earthquake in 1995, have identified significant tilting or rotation of walls in addition to horizontal deformations, reflecting cyclic bearing capacity failures of wall foundations during earthquake loading. To accommodate permanent wall deformations involving mixed sliding and rotational modes of failure using Newmark block failure assumptions, it is necessary to formulate more complex coupled equations of motions.

Coupled equations of motion may be required for evaluating existing retaining walls. However, from the standpoint of performance criteria for the seismic design of new conventional retaining walls, the preferred design approach is to limit tilting or a rotational failure mode, to the extent possible, by ensuring adequate ratios of capacity to earthquake demand (that is, high C/D ratios) for foundation bearing capacity failures and to place the design focus on performance criteria that ensure acceptable sliding displacements (that is lower C/D ratios relative to bearing or overturning). For weaker foundation materials, this rotational failure requirement may result in the use pile or pier foundations, where lateral seismic loads would be larger than those for a sliding wall.

Much of the recent literature on conventional retaining wall seismic analysis, including the European codes of practice, focus on the use of Newmark sliding block analysis methods. For short walls (less than 20-feet high), the concept of a backfill active failure zone deforming as a rigid block is reasonable, as discussed in the previous paragraph. However, for higher walls, the dynamic response of the soil in the failure zone leads to non-uniform accelerations with height and negates the rigid-block assumption.

For wall heights greater than 20 feet, the use of height-dependent seismic coefficients is recommended to determine maximum average seismic coefficients for active failure zones, and may be used to determine k_{max} for use in Newmark sliding block analyses. In effect, this represents an uncoupled analysis of deformations as opposed to a fully coupled dynamic analysis of permanent wall deformations. However, this approach is commonly used for seismic slope stability analyses, as discussed in Chapter 8.

The existing AASHTO *LRFD Bridge Design Specifications* use an empirical equation based on peak ground acceleration to compute wall displacements for a given wall yield acceleration. This equation was derived from studies of a limited number of earthquake accelerations, and is of the form:

$$d = 0.087\left(V^2/k_{\max} g\right)\left(k_y/k_{\max}\right)^{-4} \qquad (7\text{-}3)$$

where

k_y = yield acceleration;
k_{max} = peak seismic coefficient at the ground surface;
V = maximum ground velocity (inches/sec), which is the same as PGV discussed in this report; and
d = wall displacement (inches).

Based on a study of the ground motion database described in Chapter 5, revised displacement functions are recommended for determining displacement.

For WUS sites and CEUS soil sites (Equation 5-8)

$$\log(d) = -1.51 - 0.74\log\left(k_y/k_{\max}\right) + 3.27\log\left(1 - k_y/k_{\max}\right) - 0.80\log\left(k_{\max}\right) + 1.59\log(\mathrm{PGV})$$

For CEUS rock sites (Equation 5-6)

$$\log(d) = -1.31 - 0.93\log\left(k_y/k_{\max}\right) + 4.52\log\left(1 - k_y/k_{\max}\right) - 0.46\log\left(k_{\max}\right) + 1.12\log(\mathrm{PGV})$$

where

k_{max} = peak seismic coefficient at the ground surface; and
PGV = peak ground velocity obtained from the design spectral acceleration at 1 second and adjusted for local site class (that is, F_v S_1) as described in Chapter 5.

The above displacement equations represent mean values and can be multiplied by 2 to obtain an 84 percent confidence level. A comparison with the present AASHTO equation is shown in Figure 7-18.

7.7 Conventional Gravity and Semi-Gravity Walls—Recommended Design Method for External Stability

Based on material presented in the previous paragraphs, the recommended design methodology for conventional gravity and semi-gravity walls is summarized by the following steps:

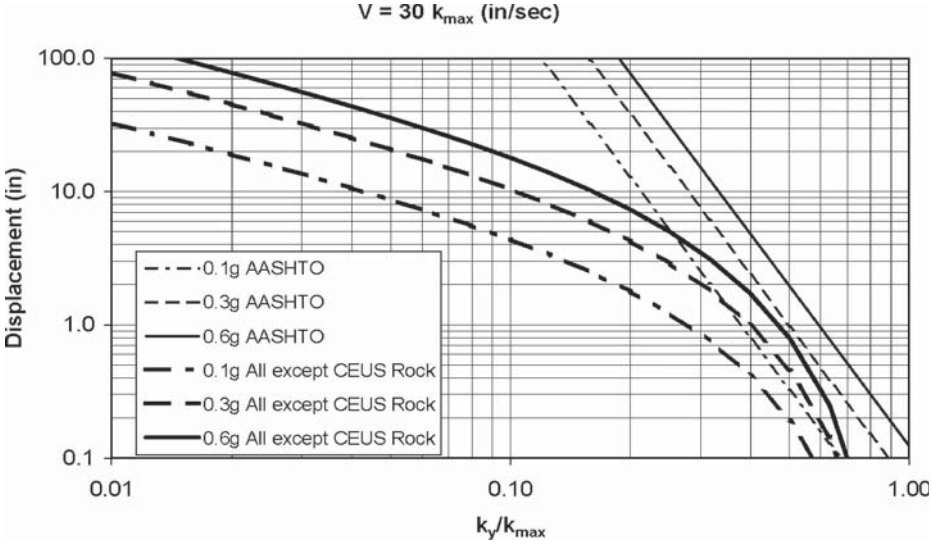

Figure 7-18. Comparison between all except CEUS-Rock and AASHTO correlations for PGV = 30 × k_{max}.

1. Establish an initial wall design using the AASHTO *LRFD Bridge Design Specifications* for static loading, using appropriate load and resistance factors. This establishes wall dimensions and weights.
2. Estimate the site peak ground acceleration coefficient (k_{max}) and spectral acceleration at 1 second (S_1) from the 1,000-year seismic hazards maps adopted by AASHTO (including appropriate site soil modification factors).
3. Determine the corresponding PGV from the correlation equation between S_1 and PGV (Equation 5-11, Chapter 5).
4. Modify k_{max} to account for wall height effects as described in Figure 7-16 of Section 7.5.
5. Evaluate the potential use of the M-O equation to determine P_{AE} (Figure 7-10) as discussed in Section 7.2, taking into account cut slope properties and geometry and the value of k_{max} from step 3.
6. If P_{AE} cannot be determined using the M-O equation, use a limit-equilibrium slope stability analysis (as described in Section 7.4) to establish P_{AE}.
7. Check that wall bearing pressures and overturning criteria for the maximum seismic load demand required to meet performance criteria. If criteria are met, check for sliding potential. If all criteria are met, the static design is satisfactory. If not, go to Step 8.
8. Determine the wall yield seismic coefficient (k_y) where wall sliding is initiated.
9. With reference to Figure 7-19, as both the driving forces [$P_{AE}(k)$, kW_s, kW_w] and resisting forces [$S_r(k)$ and $P_{PE}(k)$] are a function of the seismic coefficient, the determination of k_y for limiting equilibrium (capacity to demand = factor of safety = 1.0) requires an interactive procedure, using the following steps:
10. Determine values of P_{AE} as a function of the seismic coefficient k ($<k_{max}$) as shown in Figure 7-20a.
11. Determine horizontal driving and resisting forces as a function of k (using spreadsheet calculations) and plot as a function of k as shown in Figure 7-20b. The values of k_y correspond to the point where the two forces are equal, that is, the capacity to demand ratio against sliding equals 1.0.
12. Determine the wall sliding displacement (d) based on the relationship between d, k_y/k_{max}, k_{max}, and PGV described in Section 7.6.
13. Check bearing pressures and overturning criteria to confirm that the seismic loads meet performance criteria for seismic loading (possibly maximum vertical bearing pressure less than ultimate and overturning factor of safety greater than 1.0).
14. If step 13 criteria are not met, adjust footing dimensions and repeat steps 6-12 as needed.
15. If step 13 criteria are satisfied, assess acceptability of sliding displacement (d).

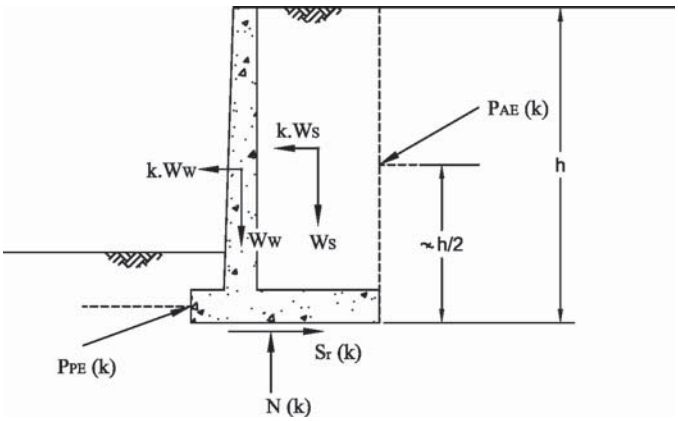

Figure 7-19. Seismic force diagram on retaining wall.

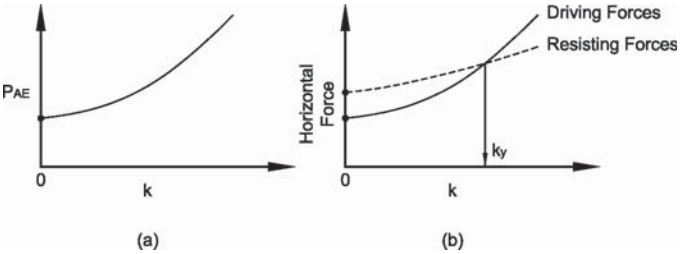

Figure 7-20. Design procedure steps.

From design examples and recognizing that static designs have inherently high factors of safety, a recommendation to eliminate step 7 and replace it by a simple clause to reduce the seismic coefficient from step 6 by a factor of 50 percent (as in the existing AASHTO Specifications) would seem realistic. This is particularly the case since the new displacement function gives values significantly less than the present AASHTO Specifications.

7.8 MSE Walls—Recommended Design Methods

The current AASHTO Specifications for MSE walls largely are based on pseudo-static stability methods utilizing the M-O seismic active earth pressure equation. In this approach dynamic earth pressure components are added to static components to evaluate external sliding stability or to determine reinforced length to prevent pull-out failure in the case of internal stability. Accelerations used for analyses and the concepts used for tensile stress distribution in reinforcing strips largely have been influenced by numerical analyses conducted by Segrestin and Bastick (1988), as described in Appendix H. (A copy of the Segrestin and Bastick paper was included in earlier drafts of the NCHRP 12-70 Project report. However, copyright restrictions precluded including a copy of the paper in this Final Report.)

7.8.1 Current Design Methodology

In the past 15 years since the adoption of the AASHTO design approach, numerous publications on seismic design methodologies for MSE walls have appeared in the literature. Publications have described pseudo-static, limit equilibrium methods, numerical methods using dynamic analyses, and model test results using centrifuge and shaking table tests. A comprehensive summary of much of this literature was published by Bathurst et al. (2002). It is clear from review of this literature that consensus on a new robust design approach suitable for a revised design specification has yet to surface due to the complexity of the problems and ongoing research needs.

Over the past several years, observations of geosynthetic slopes and walls during earthquakes have indicated that these types of structures perform well during seismic events. The structures have experienced small permanent deformations such as bulging of the face and cracking behind the structure, but no collapse has occurred. A summary of seismic field performance is shown in Table 7-1. The inherent ductility and flexibility of such structures combined with the conservatism of static design procedures is often cited as a reason for the satisfactory performance. Nevertheless, as Bathurst et al. (2002) note, seismic design tools are needed to optimize the design of these structures in seismic environments.

In the following sections, the current AASHTO design methods for external and internal stability are described, and recommendations for modifications, including a brief commentary of outstanding design issues, are made.

7.8.2 MSE Walls—Design Method for External Stability

The current AASHTO design method for seismic external stability is described in Article 11.10.7.1 in Section 11 of the Specifications, and is illustrated in Figure 7-21. The method evaluates sliding stability of the MSE wall under combined static and earthquake loads. For wall inertial load and M-O active earth pressure evaluations, the AASHTO method adopts the Segrestin and Bastick (1988) recommendations, where the maximum acceleration is given by:

$$A_m = (1.45 - A)A \tag{7-4}$$

where A is peak ground acceleration coefficient.

However, as discussed in Appendix H, the above equation is conservative for most site conditions, and the wall height-dependent average seismic coefficient discussed in Figure 7-16 in Section 7.5 is recommended for both gravity and MSE wall design.

A reduced base width of $0.5H$ is used to compute the mass of the MSE retaining wall used to determine the wall inertial load P_{IR} in the AASHTO method (Equation 11.10.7.1-3). The apparent rationale for this relates to a potential phase difference between the M-O active pressure acting behind the wall and the wall inertial load. Segrestin and Bastick (1988) recommend 60 percent of the wall mass compatible with AASHTO, whereas Japanese practice is to use 100 percent of the mass. A study of centrifuge test data shows no evidence of a phase difference. To be consistent with previous discussion on non-gravity cantilever walls, height effects, and limit equilibrium methods of analysis, the total wall mass should be used to compute the inertial load.

The AASHTO *LRFD Bridge Design Specifications* for MSE walls separate out the seismic dynamic component of the force behind the wall instead of using a total active force P_{AE} as discussed in Section 7.4. Assuming a load factor of 1.0, the

Table 7-1. Summary of seismic field performance of reinforced soil structures (Nova-Roessig, 1999).

Earthquake, Country, & Year	Mag (M_L)	Dist. to Epicenter (km)	Horiz Accel (g)	No. of Walls	Wall Type	Wall Height (m)	Seismic Design?	Reported Damage
Gemona, Italy 1976[1]	6.4	25-40		3	RE™	4-6	no	None
Leige, Belgium 1983[1]	5	0.8	0.15-0.2	2	RE™	4.5-6	no	None
Honshu, Japan 1983[1]	7.7	80-275	0.1-0.3 at 140 km	49	RE™			one wall-few cm of settlement
Edgecumbe, NZ 1987[1]	6.3	30		1	RE™	6		none
Chiba-Ken Toho-Oki Japan 1987[8, 9]	6.7	40	0.22-0.33	2	nonwoven geotextile	5.5		none
Loma Prieta, CA, USA 1989[1,2,3]	7.1	11-100	0.1-0.55	20	RE™	5-10	some	none
		11-130	0.1-0.4	> 1	geogrid	3-24	yes	one wall-0.2%H movement (top)
Kushiro-Oki Japan 1993[8]	7.8	40	0.30	1	geogrid	4.4		none
Northridge CA, USA 1994[1,4,5,8]	6.7	2.5-84	0.1-0.9	20	RE™	4-17		Panel spalling, cracking
		61	0.1	1	RE™	16		Bulged at center (3% H)
		8-113	0.2-0.5	> 1	geogrid	3-15		none
		19	0.35	1	MSE	12		cracking, 2.5 cm differential settlement
Hyogoken-Nanbu, Japan 1995[6,7]	6.9 (M_W)	16-40	up to 0.8	3	fiber grid	3-8	yes	none
		16	up to 0.8	1	fiber grid	6	yes	30 cm lateral movement, panel spalling, cracking
Chi-Chi, Taiwan 1999[10]	7.3	15-40	up to 1.0	6	geogrid	2-40		cracking, 2 m differential settlement-one wall, bulging
Nisqually, WA, USA 2001	6.8	23	up to 0.25	1	geogrid w/Allan block facing	4		collapse

[1] Reinforced Earth Co., 1990, 1991, 1994; [2] Collin et al., 1992; [3] Eliahu and Watt, 1991; [4] Stewart et al., 1994; [5] Sandri, 1994; [6] Sitar, 1995; [7] Tatsuoka et al., 1996; [8] Ling et al., 1997; [9] Ling et al., 1989; [10] Ling et al., 2001

following equation (Equation 11.10.7.1-2) is used to define the seismic dynamic component of the active force:

$$P_{AE} = 0.375\, A_m \gamma_s H^2 \qquad (7\text{-}5)$$

where

γ_s = soil unit weight; and
H = wall height.

The use of the symbol P_{AE} is confusing, as the seismic dynamic increment is usually defined as ΔP_{AE}. Whereas it is not immediately evident how this equation was derived, it is assumed that use was made of the approximation for K_{AE} suggested by Seed and Whitman (1970), namely:

$$K_{AE} = K_A + 0.75 k_h \qquad (7\text{-}6)$$

where

K_A = static active pressure coefficient; and
K_{AE} = total earthquake coefficient.

Hence using the AASHTO terminology,

$$\Delta P_{AE} = (0.75\, A_m) \times 0.5\, \gamma_s H^2$$
$$= 0.375 A_m\, \gamma_s\, H^2$$

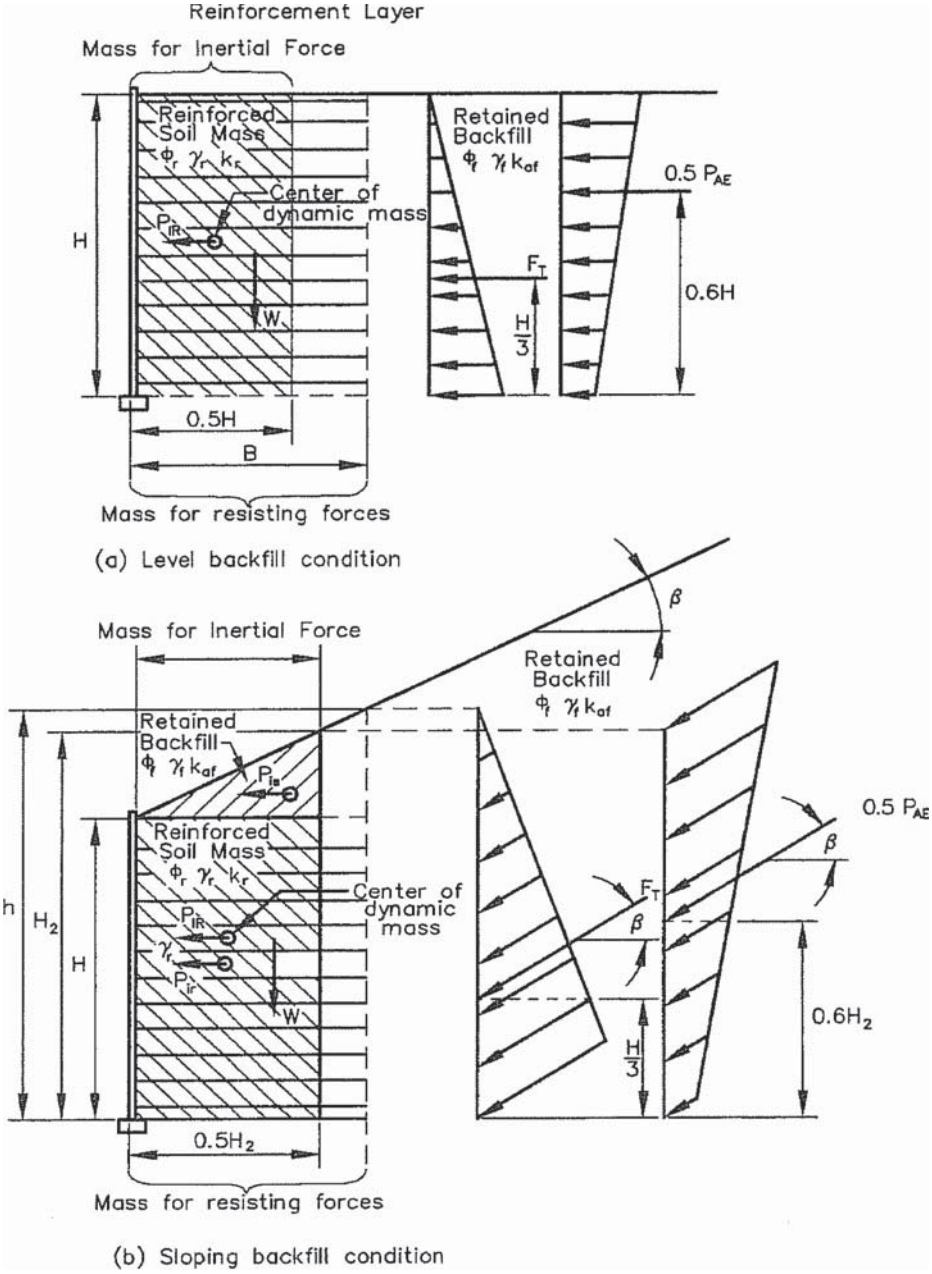

Figure 7-21. Seismic external stability of a MSE wall (AASHTO, 2007).

Note that the Seed and Whitman (1970) simplified approach was developed for use in level-ground conditions. If the Seed and Whitman simplification was, in fact, used to develop Equation (7-6), then it is fundamentally appropriate only for level ground conditions and may underestimate seismic earth pressures where a slope occurs above the retaining wall.

For external stability, only 50 percent of the latter force increment is added to the static active force, again reflecting either a phase difference with inertial wall loads or reflecting a 50 percent reduction by allowing deformation potential as suggested for cantilever walls. In lieu of the above, the recommended approach for MSE walls is a design procedure similar to that for gravity and semi-gravity walls (Section 7.6), where a total active earthquake force is used for sliding stability evaluations.

It also is noted that the AASHTO *LRFD Bridge Design Specifications* suggest conducting a detailed lateral deformation analysis using the Newmark method or numerical modeling if the ground acceleration exceeds 0.29g. However, as discussed for gravity and semi-gravity walls, due to the inherently high factors of safety used for static load design, in most cases yield seismic coefficients are likely to be high enough to minimize potential sliding block displacements.

7.8.3 MSE Walls—Design Method for Internal Stability

The current AASHTO design method for seismic internal stability is described in Article 11.10.7.2 of Section 11 of the AASHTO Specifications, and is illustrated in Figure 7-22. The method assumes that the internal inertial forces generating additional tensile loads in reinforcements act on an active pressure zone assumed to be the same for the static loading case. A bilinear zone is defined for inextensible reinforcements such as metallic strips and a linear zone for extensible strips. Whereas it could reasonably be anticipated that these active zones would extend outwards for seismic cases, as for M-O analyses, numerical and centrifuge models indicate that the reinforcement restricts such outward movements, and only relatively small changes in location are seen.

The internal inertial force in the AASHTO method is calculated using the acceleration A_m defined in Section 7.8.2 for the external stability case. As previously discussed, the acceleration equation used for external stability evaluations is too conservative for most site conditions, and the use of the wall-height dependent average seismic coefficient concept discussed in Section 7.5 is recommended.

In the AASHTO method, the total inertial force is distributed to the reinforcements in proportion to their effective resistant lengths L_{ei} as shown on Figure 7-22. This approach follows the finite element modeling conducted by Segrestin and Bastick (1988), and leads to higher tensile forces in lower reinforcement layers. This is the opposite trend to incremental seismic loading used by AASHTO for external stability evaluations based on the M-O equation. In the case of internal stability evaluation, Vrymoed (1989) used a tributary area approach that assumes the inertial load carried by each reinforcement layer increases linearly with height above the toe of the wall for equally spaced reinforcement layers. A similar approach was used by Ling et al. (1997) in limit equilibrium analyses. This concept would suggest that longer reinforcement lengths could be needed at the top of walls with increasing acceleration levels, and the AASHTO approach could be unconservative. In view of this uncertainty in distribution that has been widely discussed in the literature, a suggested compromise is to distribute the inertial force uniformly within the reinforcement. In essence, this represents an average of the tensile load

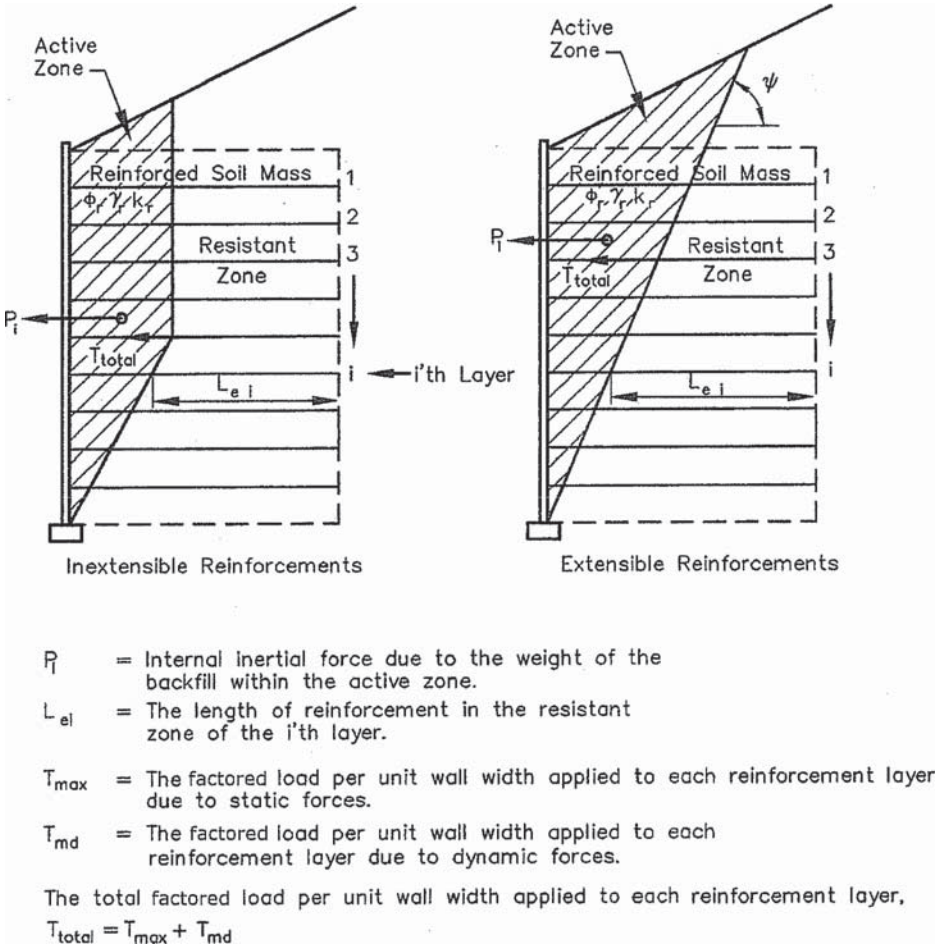

Figure 7-22. Seismic internal stability of a MSE wall (AASHTO, 2007).

distribution from the existing AASHTO approach with that determined using the tributary area of strips in the inertial active zone.

A computer program MSEW (ADAMA, 2005) has been developed and is commercially available to design MSE walls using the current AASHTO *LRFD Bridge Design Specifications.* An application of the program to design a representative wall is provided in Appendix I, where the older allowable stress design (ASD) specifications are compared to the LRFD specifications. A modest seismic coefficient of 0.1 is used for design. Slightly longer reinforcing strips are needed for the LRFD design, and seismic loading does not impact the design. The suggested recommendations to modify the seismic design procedure (acceleration coefficients and tensile load distribution) cannot be directly incorporated in the program, but changes to the source code could be made with little effort, and the design impact of the changes examined by studying several examples.

The work plan in Chapter 4 identified a methodology involving the application of limit equilibrium programs for assessing internal stability of MSE walls. In particular the computer programs, SLIDE and ReSSA (Version 2), were going to be used to conduct detailed studies. After performing a limited evaluation of both programs, the following concerns were noted relative to their application to AASHTO *LRFD Bridge Design Specifications:*

1. Since static and seismic design methodologies should desirably be somewhat consistent, the adoption of such programs for seismic design means that a similar approach should be used for static design. This would require a major revision to the AASHTO static LRFD design methodology.
2. Whereas the use of ReSSA (Version 2) for static analyses has been compared successfully to FLAC analyses by Leshchinsky and Han (2004), similar comparisons have not been identified for seismic loading problems. Such comparisons would provide more confidence in the use of a limit equilibrium program to simulate the mechanics of loading. In particular the main concern is the distribution of seismic lateral forces to reinforcing strips from the limit equilibrium analyses. It would be of value if in future centrifuge tests, for example, strips could be instrumented to measure loads during seismic loading.

In view of the these concerns, adoption of limit equilibrium analyses is not currently recommended for MSE internal stability analysis, although future research on their potential application is warranted.

Deformation design approaches are not identified for internal stability in the AASHTO Specifications. Such methods are complex as they involve sliding yield of reinforcing strips or possible stretch in the case of geosynthetic grids or geotextiles. Methods range from more complex FLAC computer analyses to simplified methods based on limit equilibrium and Newmark sliding block analyses. Bathurst et al. (2002) summarizes a number of these methods. Approaches based on limit equilibrium and Newmark sliding block methods are also described, for example, by Ling et al. (1997) and Paulsen and Kramer (2004). Comparisons are made in the latter two papers with centrifuge and shaking table test results, with some degree of success. However, the explicit application of these performance-based methods in the AASHTO *LRFD Bridge Design Specifications* at the present time is premature.

7.9 Other Wall Types

Three other wall types were considered during this Project: (1) nongravity cantilever walls, (2) anchored walls, and (3) soil nail walls. The treatment of these walls has been less detailed than described above for semi-gravity and MSE walls. Part of this reduced effort is related to the common characteristics of the nongravity cantilever, anchored, and soil nail walls to the walls that were evaluated. The following subsections provide a summary of the recommended approach for these wall types.

7.9.1 Nongravity Cantilever Walls

These walls include sheet pile walls, soldier pile and lagging walls (without anchors), and secant/tangent pile walls. Each of these walls is similar in the sense that they derive their resistance to load from the structural capacity of the wall located below the ground surface. The heights of these walls typically range from a few feet to as high as 20 to 30 feet. Beyond this height, it is usually necessary to use anchors to supplement the stiffness capacity of the wall system. The depth of the wall below the excavation depth is usually 1.5 to 2 times the height of the exposed wall face.

7.9.1.1 Seismic Design Considerations

The conventional approach for the seismic design of these walls is to use the M-O equations. Article C11.8.6 of the AASHTO *LRFD Bridge Design Specifications* indicates that a seismic coefficient of $k_h = 0.5A$ is to be used and that wall inertial forces can be ignored. In this context A is the peak ground acceleration for the site based on the AASHTO hazard map and the site classification. The use of the 0.5 factor implies that the wall is able to move, although this is not explicitly stated. As discussed in previous sections, the original development of the 0.5 factor assumed that the wall could move $10A$ (in inches), which could be several inches or more and which would often be an unacceptable condition for this class of walls.

Most nongravity cantilever walls are flexible and therefore the customary approach to static design is to assume that active earth pressure conditions develop. The amount of movement also will be sufficient to justify use of the M-O equation for estimating seismic active earth pressures. However, rather than the 0.5 factor currently given in the AASHTO Specifications, it is suggested that the wave scattering factors described in Section 7.5 of this chapter be used. For typical nongravity cantilever walls, which have a height of 25 feet or less, this means that the factor will range from 0.8 to 0.9 rather than 0.5.

The decision whether to use the 0.5 factor currently given in AASHTO will depend on the amount of permanent movement of the nongravity cantilever wall that is acceptable during the design seismic event. If the structural designer reviews the design and agrees that average permanent wall movements of 1 to 2 inches at the excavation level are acceptable, the seismic coefficient used for design (after reducing for scattering effects) can be further reduced by a factor of up to 0.5.

The acceptability of the 0.5 factor is based on several considerations:

- Allowable stresses within the wall are not exceeded during the earthquake and after the earthquake, since there is likely to be at least 1 to 2 inches of permanent wall movement at the excavation level.
- Weather conditions at the site will allow several inches of outward movement to develop. If pavements, sidewalks, or protective barriers prevent outward movement of 1 to 2 inches, then the reduction of 0.5 would not seem to be appropriate.
- Aesthetics of the wall after permanent movement are acceptable. Often there will be some rotation with the movement at the excavation line, resulting in a wall that is leaning outward. This wall may be structurally acceptable but it may result in questions whether the fill is falling over.
- Movement at the excavation level or at the top of the wall, which will likely be at least 1 to 2 several inches because of rotation, do not damage utilities or other infrastructure located above or below the wall.

Another important consideration is the characteristics of the soil being supported. Nongravity cantilever walls are normally constructed using a top-down method, where the structural support system is installed (that is, sheet pile or soldier pile) and then the earth is excavated from in front of the structural members. In many cases the natural soil behind the wall will have some cohesive content. As discussed in Section 7.3, the active earth pressure can be significantly reduced if the soil has a cohesive component. If site explorations can confirm that this cohesive component exists, then it makes sense that the design method accounts for this effect.

One important difference for this class of walls relative to gravity walls and MSE walls is that the capacity of the wall depends on the passive pressure at the face of the structural unit: either the sheet pile or the soldier pile. For static loading, the passive pressure is usually estimated from charts as shown in Article 3.11.5.4 of the AASHTO *LRFD Bridge Design Specifications.* For soldier piles the effective width of the structural element below the base of the wall is assumed to be from 1 to 3 pile diameters to account for the wedge-shape form of soil reaction. The upper several feet of soil are also typically neglected for static passive earth pressure computation. This is done to account for future temporary excavations that could occur. In view of the low likelihood of the excavation occurring at the time of the design earthquake, this approach can be neglected for seismic load cases.

Under seismic loading a reduction in the seismic passive pressure occurs. This reduction can be estimated using M-O equation for passive pressures (Equation A11.1.1.1-4). However, as noted earlier in this chapter, the M-O equation for passive earth pressures is based on a granular soil and Coulomb failure theory. Various studies have shown that Coulomb theory can be unconservative in certain situations. The M-O equation also does not include the contributions of any cohesive content to the soil. Similar to the previous discussion for active pressures, the effects of cohesion on the passive earth pressure have been found to be significant.

As an alternative to the M-O passive pressure equation, the seismic passive earth pressure can be estimated using the charts in Figures 7-23 through 25. These charts show the relationship between K_{PE} and k_h as a function of the normalized soil cohesion. The charts were developed using log spiral procedures, following the methodology published by Shamsabadi et al. (2007). The interface friction for these charts is 0.67 ϕ. Procedures described by Shamsabadi et al. can be used to estimate the seismic passive coefficient for other interface conditions.

Significant deformation is required to mobilize the passive pressure, and therefore, for static design, the resulting passive pressure coefficient is often reduced by some amount to control deformations. For static loading the reduction is usually 1.5 to 2. In the absence of specific studies showing otherwise, this same reduction may be appropriate for the seismic loading case in a limit equilibrium analysis, to limit the deformation of the nongravity cantilever. This approach would be taken if using the computer programs SPW 911 or SWALSHT.

Alternately, a numerical approach, such as followed within the computer program PY WALL (Ensoft, 2005) can explicitly account for the displacement through the use of p-y springs. Programs such as L-PILE and COM624 also can be used to make these analyses, although appropriate consideration needs to be given to the development of p-y curves. These programs are not specifically set up for evaluating seismic response

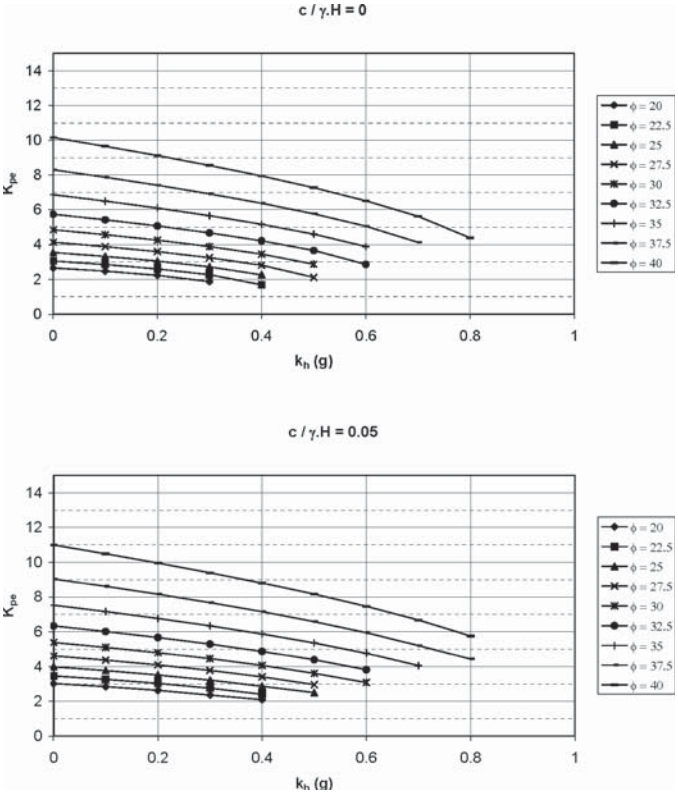

Figure 7-23. Seismic passive earth pressure coefficient based on log spiral procedure (c = soil cohesion, γ = soil total unit weight, and H is height).

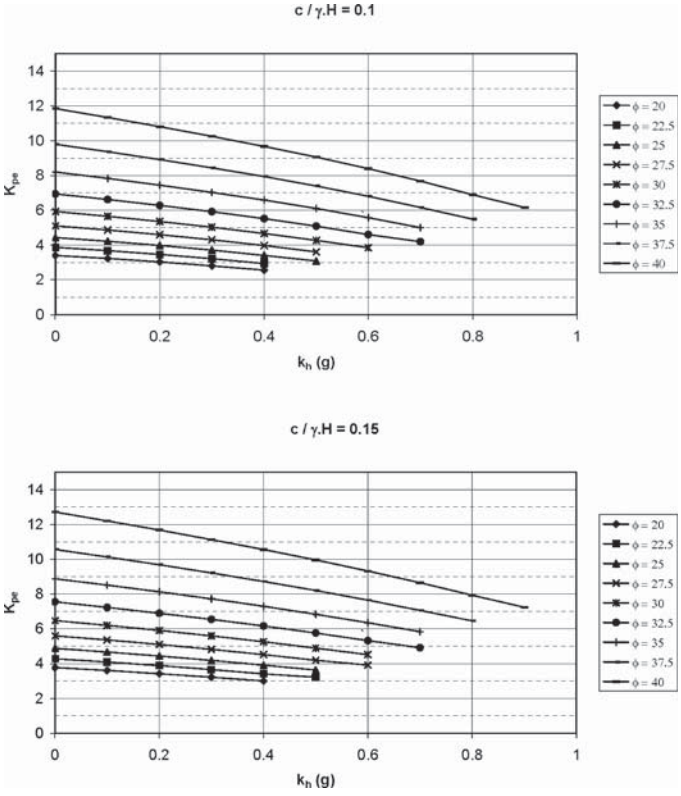

Figure 7-24. Seismic passive earth pressure coefficient based on log spiral procedure (cont.) (c = soil cohesion, γ = soil total unit weight, and H is height).

but can be used to evaluate seismic performance by introducing appropriate soil pressures and reactions consistent with those expected to occur during a seismic event. Appendix K describes a study that was part of the NCHRP 12-70 Project that demonstrates the use of the general beam-column approach to evaluate nongravity cantilever retaining walls under seismic loading. Included within the Appendix K discussion are recommendations on p- and y-multipliers to develop p-y curves for continuous (sheet pile) retaining walls.

7.9.1.2 Seismic Design Methodology

The following approach is suggested for design of nongravity cantilever walls:

1. Perform static design following the AASHTO *LRFD Bridge Design Specifications.*
2. Establish the site peak ground acceleration coefficient (k_{max}) and spectral acceleration S_1 at 1 second from the 1,000-year maps adopted by AASHTO (including appropriate site soil modification factors).
3. Determine the corresponding PGV from correlation equations between S_1 and PGV (provided in Chapter 5).
4. Modify k_{max} to account for wall-height effects as described in Section 7.6. Include cohesion component as

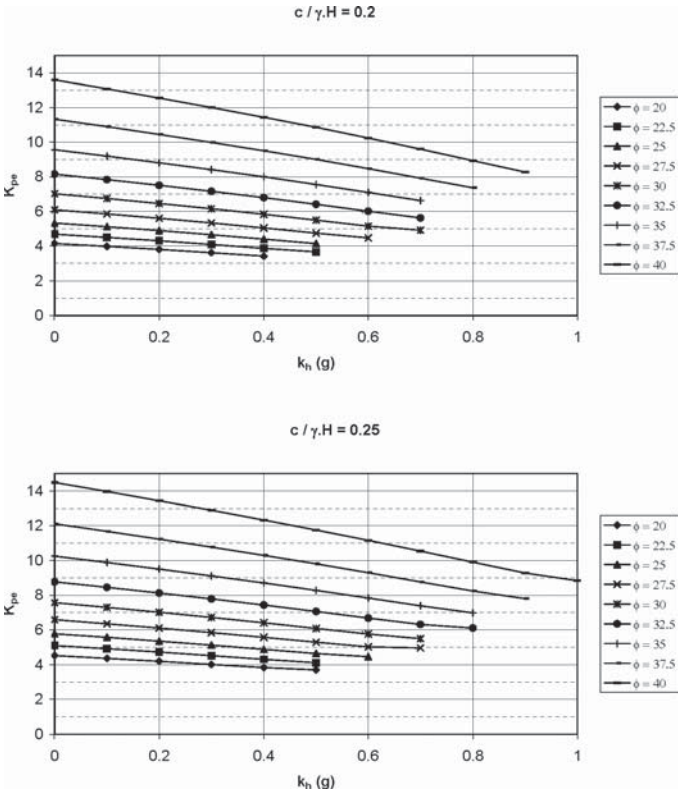

Figure 7-25. Seismic passive earth pressure coefficient based on log spiral procedure (cont.) (c = soil cohesion, γ = soil total unit weight, and H is height).

appropriate. *Apply a 0.5 factor to the resulting seismic coefficient if 1 to 2 inches of average permanent movement can be accepted and conditions are such that they will develop. Otherwise use the k_{max} without further reduction.*

5. Compute wall pressures using M-O equation for active pressure, the charts in Figures 7-11 and 7-12, or the generalized limit equilibrium method. Estimate earth pressure for passive loading using charts in Figure 7-25 or the methodology published by Shamsabadi et al. (2007). *Do not use the M-O equation for passive pressure.*
6. Evaluate structural requirements using a suitable software package or through use of hand methods (for example, free earth support). Confirm that displacements are sufficient to develop an active pressure state.
7. Check global stability under seismic loading using a limit equilibrium program such as SLIDE with the seismic coefficient modified for height effects. Assume that the critical surface passes beneath the structural element. If the capacity to demand ratio (that is, factor of safety) is less than 1.0, estimate displacements.

The generalized limit equilibrium approach can be used where soil conditions, seismic coefficient, or geometry warrant. In this analysis the contributions from the structural elements need to be included in the evaluation of stability. Programs such as SLIDE allow incorporation of the structural element through the use of an equivalent reaction, where the reaction of individual members is "smeared" to obtain an equivalent two-dimensional representation.

7.9.2 Anchored Walls

The next class of walls is essentially the same as nongravity cantilever walls; however, anchors are used to provide additional support to the walls. Typically the anchors are installed when the wall height exceeds 20 feet, or sometimes even at less height if a steep backslope occurs above the wall or the wall supports heavy loads from a structure. The height of anchored walls can exceed 100 feet.

The anchored wall can be used in either cut or fill conditions.

- For fill conditions the reaction is usually provided by a deadman anchor. This wall type is generally limited to use at port facilities, where a single deadman anchor is used to augment the capacity of the wall. While deadman can be used for highway construction, particularly for retrofits, other wall types, such as MSE or semi-gravity cantilever walls, are usually more cost-effective for new walls.
- For cut slope locations, the wall uses one or more grouted anchors to develop additional capacity. Anchors are usually installed at approximately 10-foot vertical spacing; horizontal spacing of the soldier piles is often 8 to 10 feet. AASHTO *LRFD Bridge Design Specifications* provide specific guidance on the minimum length of the anchors in Figure 11.9.1-1.

One of the key factors for the anchored wall is that each anchor is load tested during the construction process. The load test is used to confirm that the anchor will meet long-term load requirements. The testing typically includes applying from 1.5 to 2 times the design (working) load and monitoring creep of the anchor. Well-defined criteria exist for determining the acceptability of the anchor during proof or performance testing.

7.9.2.1 Seismic Design Considerations

The AASHTO *LRFD Bridge Design Specifications* provide limited guidance for the seismic design of anchored walls. Article 11.9.6 indicates that, "the provisions in Article 11.8.6 shall apply." The referenced article deals with nongravity cantilever walls, and basically states that the M-O equations should be used with the seismic coefficient $k_h = 0.5A$.

Various other methods also have been recommended for the seismic design of anchored walls:

- The FHWA report *Geotechnical Earthquake Engineering* (FHWA, 1998a) presents an approach for walls anchored with a single deadman. This method suggests using the M-O equations to estimate the seismic active and passive pressures. The design method recommends that the anchors be located behind the potential active failure surface. This failure surface is flatter than that used for the static stability analysis.
- A more recent FHWA document *Ground Anchors and Anchored Systems* (FHWA, 1999) provides discussions on the internal stability using pseudo-static theory and external stability. Again the approach is to use the M-O equations. The document notes that,

  > use of a seismic coefficient from between one-half and two-thirds of the peak horizontal ground acceleration divided by gravity would appear to provide a wall design that will limit deformations in the design earthquake to small values acceptable for highway facilities.

  The seismic active earth pressure is assumed to be uniformly distributed over the height of the wall.
  - For the grout tendon bond, considered a brittle element of the system, the report suggests using the site-adjusted PGA with no reductions in the M-O equations to obtain a peak force and that a factor of safety against brittle failure be 1.1 or greater.
  - For ductile elements (for example, tendons, sheet piles, and soldier piles) the seismic coefficient in the M-O method is 0.5 times the site-adjusted PGA. The Newmark method is used as the basis of this recommendation. For this condition the factor of safety should be 1.1 or greater.

A global check on stability also is recommended. Similar to the approach in *Geotechnical Earthquake Engineering,* the anchor zone should be outside the flattened failure surface.

- Another FHWA document *Design Manual for Permanent Ground Anchor Walls* (FHWA, 1998b) has a slight variation on the above methods. First, the method suggests using 1.5 times the site-adjusted PGA, but notes that Caltrans has been successful using a 25 percent increase over the normal apparent earth pressures. The justification for the lower loads is related to the test loads that are applied (133 percent times Load Group VII); these loads are higher than would be obtained using the AASHTO approach. Since the seismic loads are applied for a short period of time, the document suggests not increasing the soldier piles or wall facing for the seismic forces. For external stability the report identifies a deformation-based approach used at the time by Caltrans. This method is based on the Makdisi and Seed (1978) charts for computing deformations.
- Whitman (1990) in a paper titled, "Seismic Design and Behavior of Retaining Walls," presents a methodology that accounts for the increased support from the anchor as the wall deforms. In the Whitman approach, a limit equilibrium analysis is conducted with a program such as SLIDE. The anchor lock-off load is modeled as an external force oriented along the axis of the anchor (that is, typically 10 to 20 degrees). The yield acceleration is determined, and then the deformation is estimated using a Newmark chart. This deformation results in elongation of the anchor tendon or bar, which results in an increased reaction on the wall (that is, $\Delta = PL/AE$). Analyses are repeated until there is compatibility between the deformations and the anchor reaction. The final force is then checked against capacity of the tendon and grouted anchor.

With one exception, the documents summarized here do not suggest amplification within the zone between the retaining wall and the anchors. One reference was made to the use of an amplification factor identical to that used for the seismic design of MSE walls [that is, $A_m = (1.45 - A)A$]. No basis for this increase was provided. Most references do suggest that the location of the anchors be moved back from the wall to account for the flattening of the active zone during seismic loading. The potential that the pressure distribution behind the anchored walls changes during seismic loading is not currently addressed.

The most significant uncertainty appears to be whether to use the peak seismic coefficient, or a value that is higher or lower than the peak. Arguments can be made for higher values based on amplification effects. However, if several inches of movement occur as demonstrated by the example problem in Appendix J, a reduction in the peak seismic coefficient seems justified. If this reduction is, however, accepted, then careful consideration needs to be given to the stiffness of the wall-anchor system to confirm that the elongation of the anchor strand or bar and the stiffness of the wall are such that several inches of movement can occur.

While the methodologies for the seismic design of anchored walls seem to lack guidance on a number of topics, the FHWA documents note that anchored walls have performed well during past seismic events. It was noted that of 10 walls inspected after the 1987 Whittier earthquake and the 1994 Northridge earthquake, wall performance was good even though only one in 10 walls inspected was designed for earthquake loading.

7.9.2.2 Seismic Design Methodology

The following approach is suggested for design of anchored retaining walls:

1. Perform static design following the AASHTO *LRFD Bridge Design Specifications.*
2. Establish the site peak ground acceleration coefficient (k_{max}) and spectral acceleration S_1 at 1 second from the 1,000-year AASHTO maps, including appropriate site soil modification factors.
3. Determine the corresponding PGV from correlation equations between S_1 and PGV (provided in Chapter 5).
4. Modify k_{max} to account for wall-height effects as described in Section 7.6. *Do not use 1.5 factor given in the current AASHTO Specifications, unless the wall cannot be allowed to deflect.*
5. Compute wall pressures using the M-O equation for active pressure, the charts in Figures 7-11 and 7-12, or the generalized limit equilibrium method. Apply a factor of 0.5 if 1 to 2 inches of average permanent movement are acceptable and the stiffness of the wall and anchor system (that is, $\Delta = PL/AE$) will allow this movement. If 1 to 2 inches are not tolerable or cannot develop, then use the full seismic coefficient. Estimate earth pressure for passive loading using Figures 7-23 to 7-25 or the equations developed by Shamsabadi et al. (2007).
6. Use the same pressure distribution used for the static pressure distribution. For the resulting load diagram, check loads on tendons and grouted anchors to confirm that the seismic loads do not exceed the loads applied during performance or proof testing of each anchor. Confirm that the grouted anchors are located outside the seismic active pressure failure wedge.
7. Check global stability under seismic loading using a limit equilibrium program such as SLIDE with the seismic coefficient modified for height effects. Assume that the critical surface passes beneath the structural element. If the capacity to demand ratio is less than 1.0, estimate displacements.

For cases where M-O equations are not appropriate, such as for some combinations of a steep back slope and high site-adjusted PGA or if the soil behind the wall simply cannot be represented by a homogeneous material, then the generalized limit equilibrium methodology should be used to estimate the seismic active earth pressure. This pressure can be either distributed consistent with a static pressure distribution and the wall checked for acceptability, or the deformation approach recommended by Whitman (1990) can be used to evaluate the forces in the vertical structural members, anchor tendons, and grouted zone.

7.9.3 Soil Nail Walls

These walls are typically used where an existing slope must be cut to accommodate a roadway widening. The slope is reinforced to create a gravity wall. These walls are constructed from the top down. Each lift of excavation is typically 5 feet in thickness. Nails are installed within each lift. The spacing of the nails is usually about 4 to 5 feet center-to-center in both the vertical and horizontal direction. The nail used to reinforce the slope is high strength, threaded steel bar (60 to 75 ksi). Each bar is grouted in a hole drilled into the soil. The length of the bar will usually range from 0.7 to 1.0 times the final wall height. Most soil nail walls currently are designed using either of two computer programs, SNAIL, developed and made available by Caltrans, and GOLDNAIL, developed and distributed by Golder and Associates. These programs establish global and internal stability.

7.9.3.1 Seismic Design Considerations

The seismic design of soil nail walls normally involves determining the appropriate seismic coefficient and then using one of the two computer programs to check the seismic loading case. The AASHTO *LRFD Bridge Design Specifications* currently does not have any provisions for the design of soil nail walls. However, FHWA has a guidance document titled *Soil Nail Walls* (FHWA, 2003) used for soil nail wall design. This document has a section on the seismic design of these walls.

Key points from the seismic discussions are summarized below:

- Soil nail walls have performed very well during past earthquakes (for example, 1989 Loma Prieta, 1995 Kobe, and 2001 Nisqually earthquakes). Ground accelerations during these earthquakes were as high as 0.7g. The good performance is attributed to the intrinsic flexibility. These observations also have been made for centrifuge tests on model nail walls.
- Both horizontal and vertical seismic coefficient can be used in software such as SNAIL. A suggestion is made in the FHWA guidance document to use the same amplification factor used for MSE walls, that is, $A_m = (1.45 - A)A$. The basis of using this equation is not given, other than the FHWA report indicates that performance of the soil nail wall is believed to be similar to an MSE wall.
- The seismic coefficient for design ranges from 0.5 A_m to 0.67 A_m. This reduction is based on tolerable slip of 1 to 8 inches with most slip of 2 to 4 inches. The possibility of performing Newmark deformational analysis is noted for certain soil conditions and high ground accelerations.
- The M-O equation is used to estimate the seismic active pressure acting on the wall. Reference is made to the angle of the failure plane for seismic loading being different than static loading.
- Mention is made of the limitations of the M-O procedure for certain combinations of variables, in particular when the backslope is steeper than 22 degrees and does not capture many of the complexities of the system.
- A detailed design example based on the recommended approach is presented.

The earlier FHWA report *Geotechnical Earthquake Engineering* (FHWA, 1998a) also provides some discussion on the design of soil nail walls. It mentions use of (1) the amplification factor, $A_m = (1.45 - A)A$ and (2) for external stability using 0.5 times the site-adjusted PGA, as long as the wall can tolerate 10 A (inches displacement) where A is the peak ground acceleration. This document also references using a seismic design coefficient of 0.5A to check seismic bearing capacity stability. Limitations and assumptions for this approach are discussed in Appendix G.

Procedures used to evaluate the external or global stability of the soil nail wall during seismic loading will be the same as those described previously for evaluating the seismic performance of semi-gravity walls and MSE walls. The uncertainty with this wall type deals with the internal stability. The computer programs currently used in practice, SNAIL and GOLDNAIL, use pseudo-static, limit equilibrium methods to determine stresses in the nail. Checks can be performed to determine if pullout of the nail, tensile failure, or punching failure at the wall face occur. For the seismic loading case, the increased inertial forces are accounted for in the analysis. Similar to the internal stability of MSE walls, the mechanisms involved in transferring stresses from the soil to the nails and vice versa are complex and not easily represented in a pseudo-static, limit equilibrium model.

In principle it would seem that some significant differences might occur between the seismic response of the soil nail wall versus the MSE wall. The primary difference is that MSE walls are constructed from engineered fill whose properties are well defined, whereas nail walls are constructed in natural soils characterized by variable properties. Part of this difference

also relates to the angle of the nail. Most nails are angled at 10 to 20 degrees to the horizontal in contrast to the horizontal orientation of the reinforcement within the MSE wall. This would likely stiffen the soil nail wall relative to the MSE wall, all other conditions being equal. From a design standpoint, it also is not clear if seismic forces are adequately modeled by the pseudo-static approach currently taken. These issues need to be further evaluated during independent research efforts.

Many nail walls will be located in areas where there is a cohesive content to the soil into which the nails are installed. For these sites the effects of cohesion on the determination of seismic earth pressure coefficients, as discussed in Section 7.3, should be considered.

7.9.3.2 Seismic Design Methodology

Based on material presented in the previous paragraphs, the recommended design methodology is summarized by the following steps:

1. Establish an initial wall design using the computer program SNAIL or GOLDNAIL for static loading, using appropriate load and resistance factors. This establishes wall dimensions and weights.
2. Establish the site peak ground acceleration coefficient (k_{max}) and spectral acceleration S_1 at 1 second from the 1,000-year maps adopted by AASHTO (including appropriate site soil modification factors).
3. Determine the corresponding PGV from correlation equations between S_1 and PGV (provided in Chapter 5).
4. Modify k_{max} to account for wall height effects as described in Section 7.6. Use the modified k_{max} in the SNAIL or GOLDNAIL program. If the wall can tolerate displacements, use the SNAIL or GOLDNAIL program to estimate the yield acceleration, k_y. Use the yield acceleration to estimate displacements following the procedures in Chapter 5.

Note that both computer programs also provide an evaluation of global stability, and therefore, it is not necessary to perform an independent global stability analysis with a limit equilibrium program such as SLIDE.

7.10 Conclusions

This chapter summarizes the approach being recommended for the seismic design of retaining walls. Force-based methods using the M-O equations and a more generalized displacement-based approach were evaluated. The methodologies introduce new height-dependent seismic coefficients, as discussed in Chapters 5 and 6 and further refined in Section 7.5 for these analyses.

Results of the work completed for retaining walls includes charts showing the effects of cohesion within the soil on the seismic earth pressure coefficients that were developed. These effects can result in a 50 percent reduction in the seismic active earth pressure; however, it may be difficult in some cases to confidently rely on this benefit. In view of current uncertainties, the designer needs to consider the implications of overestimating the effects of cohesion on the seismic active and passive earth pressures.

Two wall types were considered in detail during this study: (1) semi-gravity walls and (2) MSE walls.

- The proposed approach for gravity walls uses either the M-O seismic active earth pressure equation, the charts in Figures 7-11 and 7-12, or the generalized limit equilibrium method to determine seismic active forces. These forces are used to conduct bearing, overturning, and sliding stability checks. A key question that still exists for this type of wall is whether inertial forces from the soil above the heel of a semi-rigid gravity wall (for example, Figure 7-10 in this report) is defined by the entire soil mass times the seismic coefficient or some lesser value.
- The MSE design methodology includes a critical review of the existing AASHTO guidance, including internal stability, and then identifies a step-by-step approach for evaluating stability. Reference is made to the need to change existing software to handle this approach. Questions also still exist on the distribution of stresses within the reinforcement strips during seismic loading.

Three other wall types were considered to lesser extents: nongravity cantilever walls, anchored walls, and soil nail walls. The design approach for each of these walls also used the results of work presented in previous sections and chapters.

- For nongravity cantilever walls, the M-O method is believed to be an appropriate method to determine seismic active pressures as long as there is flexibility in the wall and the soil behind the wall is primarily cohesionless. Otherwise, charts in Figures 7-11 and 7-12 or a generalized limit equilibrium method can be used to estimate the seismic active earth pressure. The seismic coefficient used for design can be reduced by a factor of 0.5 as long as 1 to 2 inches of average permanent deformation at the excavation level are acceptable. A structural engineer should make this evaluation. Checks on wall deflections also should be made to confirm that the basic assumptions associated with wall displacement are being met. Seismic passive pressures should be determined using a log spiral approach, such as suggested by Shamsabadi et al. (2007).
- In the case of the anchored wall, either a limit equilibrium procedure or a displacement based procedure suggested by

Whitman can be used. Seismic active earth pressures for the limit equilibrium approach can be estimated using the M-O equation, charts in Figures 7-11 and 7-12, or the generalized limit equilibrium approach. Soils must be homogeneous and cohesionless if using the M-O equation while the generalized limit equilibrium method can accept combinations of soil conditions. The seismic coefficient for these analyses can be reduced by 50 percent as long as 1 to 2 inches of average permanent movement are acceptable and as long as anchor tendons and grouted zones are not overstressed. The Whitman displacement-based approach accounts for changing anchor tendon forces during seismic loading and appears to represent the fundamental mechanisms that occur during seismic response of this wall type. However, the additional effort to make these evaluations may not be warranted in areas where seismicity is low, and the normal performance and proof testing of the anchors provides sufficient reserve capacity.

- Soil nail walls can be treated as semi-gravity walls from an external stability standpoint. In most cases seismic coefficients can be reduced by 0.5 since this type of wall can usually tolerate several inches of permanent movement. For internal stability there are still questions on the distribution of seismic forces to the nails within the reinforced zone and whether the current models adequately account for these distributions. Additional research is still required to evaluate these questions.

In a number of areas it was apparent that significant deficiencies exist with current design methodologies. These deficiencies reflect the complexity of the overall soil-structure interaction problem that occurs during seismic loading. The nature of these deficiencies is such that for several of the wall types (for example, MSE, anchored, and soil nail) independent research efforts involving specific model and prototype testing will be required to fully understand the mechanisms involved in seismic loading.

While there is considerable work to be done, past experience also suggests that many of these wall types have performed well during relatively high seismic loading, despite having either no provisions for seismic design or a very simple analysis. In most cases this good performance occurred when walls were flexible or exhibited considerable ductility. More problems were observed for rigid gravity walls and non-gravity cantilever walls, often because of the lack of seismic design for these walls. The methodologies suggested in this chapter should help improve the seismic performance of these walls in the future.

CHAPTER 8

Slopes and Embankments

This chapter summarizes the results of embankment and slope stability studies that were carried out for the Project. The primary objectives of these studies were to:

- Develop a methodology for evaluating the seismic response of embankments and slopes that can be easily used by designers;
- Account for the results of ground motion and wave scattering studies presented in Chapters 5 and 6 in the proposed approach; and
- Provide comments on the use of the proposed methodology in low seismicity areas, where a "no analysis" approach may be appropriate for the seismic analysis and design of embankments and slopes.

The proposed methodology is intended for use in constructed embankments or naturally occurring soil slopes. As noted in Section 4.3, rock slopes are not being considered in this development.

This chapter begins with a brief summary of the types of slopes and embankments commonly encountered during transportation projects. This discussion is followed by a brief summary of current practice, a summary of the methodology being proposed, and an example application of this methodology. The chapter is concluded with a discussion of other considerations relative to the seismic analysis and design of slopes and embankments. As with previous chapters, the approach identified in this chapter will form the basis of the proposed specifications, commentaries, and example problems given in Volume 2 of this Final Report.

8.1 Types and Performance of Slopes

Two general classes of slopes need to be considered for the methodology development: natural slopes and constructed or engineered slopes. These two categories of slopes will vary significantly in terms of geometry, material properties, and groundwater conditions. In most cases the constructed slopes will be relatively uniform in soil conditions, though the constructed material will vary from sands and gravels to fill that has high fines content (that is, cohesive soil content). On the other hand the natural slopes will usually be highly variable, with layers that range from gravels to clays and often the groundwater will be located within the slope.

8.1.1 Engineered Slopes and Embankments

These slopes generally will be constructed from an imported material. Depending on the geographic area, the imported materials can be predominantly sands or gravels or they can have a high percentage of cohesive soil. The slopes are compacted and will usually exhibit good strength characteristics. Slope angles often will range from 2H:1V (horizontal to vertical) to flatter than 3H:1V. Height of the slope can vary from a few feet to over 50 feet. A common example of these slopes would be the approach fill used at either end of a bridge. These approach fill slopes would be on the order of 30 feet in height.

These slopes are perhaps the easiest to evaluate from the standpoint that the fill is defined, and therefore determination of material properties is more straight-forward. If the fill is cohesionless, the friction angle (ϕ) will normally be 35 degrees or higher. If the fill has appreciable fines content, the compacted strength often will be in excess of 2,000 psf. The groundwater location for most of these slopes will be at some distance below the base of the fill. The designs of these slopes become problematic if the embankment fill is being placed on a soft or liquefiable foundation material. In these cases the determination of the strength of the foundation material under static and seismic loading becomes a key consideration during the analysis.

The geotechnical investigation of the engineered fill generally will be limited to investigating the characteristics of the

foundation material. Explorations often would be conducted to twice the slope height to define strength and compressibility properties of soil layers upon which the embankment will be constructed. The geometry and properties of the fill will be determined on the basis of right-of-way widths and costs of importing fill material.

From a seismic design perspective these types of slopes are routinely encountered as new roadways are constructed or existing roadways are modified. Both the field investigation and the analysis of slope stability for these slopes are routinely handled for gravity loading and, in more seismically active areas, for seismic loading. Performance of the constructed slope during seismic loading generally has been very good, except where liquefaction of the foundation material occurs. In this case, the loss of foundation strength from liquefaction has led to embankment slope failures.

8.1.2 Natural Slopes

Natural slopes present more difficulties because of the wide range of conditions that occur within these slopes. Relatively uniform soil conditions can exist within the slope; however, most often the slope involves layers of different geologic materials, and these materials often change from cohesionless to cohesive in characteristic. Groundwater often is found within the slope, and sometimes the water is intermittently perched on less permeable layers.

Further complicating the evaluation of the natural slope is the geometry. In areas where soils have been overconsolidated from glaciation, the slope angles can be steeper than 1H:1V, even where the fines content is minimal. Likewise in mountainous areas the natural slopes can be marginally stable in the existing state. Other natural slopes that are relatively flat can have thin bedding planes characterized by very low friction angles for long-term loading. Where located adversely to a planned slope cut, the removal of materials buttressing these slopes can initiate large slides under gravity loading and reactivate slides during seismic events.

Natural slopes are often the most difficult to characterize in terms of layering and material characteristics. Access to conduct site explorations can be difficult, particularly where steep slopes exist. The variability of natural deposits forming the slope often makes it difficult to locate or adequately model soil layers critical to the evaluation of slope stability, either under gravity or seismic loading.

From a seismic perspective, natural slopes are where most slope failures have been observed. Although there is no single cause of past failures, many of these failures have occurred where slopes are oversteepened, that is, barely stable under gravity loading. The size of the failure can range from small slides of a few yards of soil to movements involving thousands of yards of soil. In highly seismic areas of the WUS, the potential for seismic instability becomes a key consideration in some areas, particularly where critical lifeline transportation routes occur.

8.2 Current Practice

Earthquake-induced ground accelerations can result in significant inertial forces in slopes or embankments, and these forces may lead to instability or permanent deformations. Current practice for the analysis of the performance of slopes and embankments during earthquake loading is to use one of two related methods:

1. Limit equilibrium methods using a pseudo-static representation of the seismic forces. In this approach, induced seismic loads are used in a conventional limit equilibrium analysis to evaluate a factor of safety. The seismic loads are determined on the basis of the ground acceleration and the mass of soil being loaded.
2. Displacement-based analyses using either the Newmark sliding block concept shown schematically in Figure 8-1 or more rigorous numerical modeling methods. In Figure 8-1, when the acceleration exceeds the yield acceleration (that is C/D ratio = FS = 1.0), deformations accumulate leading to permanent ground deformation. This procedure is similar to that adopted for retaining wall analysis as discussed in Chapter 7.

Use of these methods for design has been widely adopted in the United States and in international design guidelines. For example, methods are described in detail in the FHWA report titled *Geotechnical Earthquake Engineering* (FHWA, 1998a) and a publication on *Guidelines for Analyzing and Mitigating Landslide Hazards in California* (SCEC, 2002).

8.2.1 Limit Equilibrium Approach

The limit equilibrium approach involves introducing a seismic coefficient to a conventional slope stability analysis and determining the resulting factor of safety. The seismic coefficient is typically assumed to be some percentage of the site-adjusted PGA occurring at a site. The value can range from less than 50 percent of the peak to the PGA, depending on the designer's views or agency requirements. Typically, a slope is judged to be safe if the resulting factor of safety is greater than 1.1 to 1.3.

As discussed in the FHWA publication, a wide variety of commercially available computer programs exist that can perform both static and pseudo-static limit equilibrium analyses. Most of these programs provide general solutions to slope stability problems with provisions for using the simplified Bishop, simplified Janbu, and Spencer's method of slices.

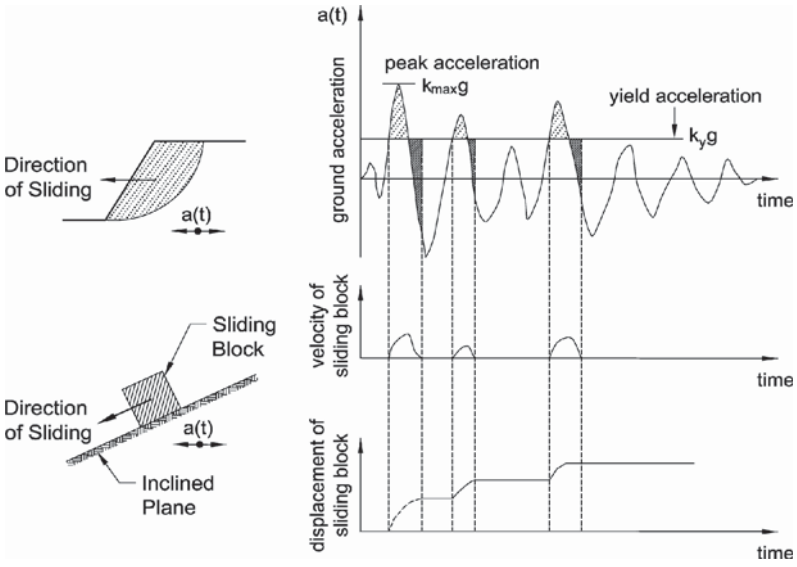

Figure 8-1. Newmark sliding block concept for slopes.

Potential sliding surfaces, both circular or polygonal, usually can be prespecified or randomly generated. Commonly used programs include PCSTABL (developed at Purdue University), UTEXAS4 (developed at the University of Texas at Austin), SLOPE/W (distributed by Geo-Slope International), and SLIDE (RocScience).

An important consideration in the limit equilibrium approach is that the rate of loading during the earthquake is relatively fast. For this reason, in most cases undrained total stress strength parameters should be used in the stability model, rather than drained or effective stress parameters. The undrained total stress parameters are obtained from static strength tests conducted in the laboratory, from in situ strength testing or from empirical relationships.

Although the rate effects associated with earthquake loading may result in a higher undrained strength during the first cycle of loading, various studies have shown that after 10 to 15 cycles of significant loading, as might occur during a seismic event, degradation of the undrained strength often occurs. In view of this potential for degradation, a conservative approach is to use the static undrained strength in the seismic stability analysis. Where this simplification is questionable, cyclic loading tests can be conducted in the laboratory to obtain a more precise definition of the strength parameters during cyclic loading.

In the limit equilibrium approach, a seismic coefficient is used to determine the inertial forces imposed by the earthquake upon the potential failure mass. The seismic coefficient used in the analysis is based on the site-adjusted PGA adjusted for wave scattering effects using the α factor defined in Chapters 6 or 7. The vertical acceleration is normally set equal to zero based on studies that have shown vertical accelerations have a minor effect on the seismic stability evaluation for most cases.

A factor of safety is determined by applying the seismic coefficient in the limit equilibrium stability program. An allowable factor of safety is selected such that behavior of the slope, in terms of permanent deformation, is within a range considered acceptable. A factor of safety (or C/D ratio) of more than 1.0 when using the peak seismic coefficient implies no slope movement, while a factor of safety less than 1.0 when using the peak seismic coefficient implies permanent movement. Typically, the seismic coefficient is assumed to be 50 percent of the peak, as noted above, reflecting the acceptance of 1 to 2 inches of permanent movement. In this case, as long as the factor of safety is greater than 1.1 to 1.3, the deformations are assumed to be minimal.

The drawback of the limit equilibrium approach lies in the difficulty of relating the value of the seismic coefficient to the characteristics of the design earthquake. Use of either the peak ground acceleration coefficient or the peak average horizontal acceleration over the failure mass, in conjunction with a pseudo-static factor of safety of 1.0, usually gives excessively conservative assessments of slope performance in earthquakes. However, often little guidance on selection of the seismic coefficient as a fraction of the peak ground acceleration is available to the designer.

Los Angeles County uses a nominal seismic coefficient of 0.15 and requires a factor of safety >1.1. The recently published guidelines by Southern California Earthquake Center (SCEC) (2002) for the State of California suggests reducing peak ground acceleration map values in California by about 0.3 to 0.6 (depending on earthquake magnitude and peak ground acceleration values) to ensure slope displacements are

less than about 6 inches, a screening value suggested as a potential criteria to determine if a Newmark displacement analysis is necessary.

8.2.2 Displacement-Based Approach

In contrast to the limit equilibrium approach, the displacement-based approach involves the explicit calculation of cumulative seismic deformation. The potential failure mass is treated as either a rigid body or deformable body, depending on whether a simplified Newmark sliding block approach or more advanced numerical modeling is used.

8.2.2.1 Newmark Sliding Block Approach

The Newmark sliding block approach treats the potential failure mass as a rigid body on a yielding base. The acceleration time history of the rigid body is assumed to correspond to the average acceleration time history of the failure mass. Deformation accumulates when the rigid body acceleration exceeds the yield acceleration of the failure mass (k_y) where k_y is defined as the horizontal acceleration that results in a factor of safety of 1.0 in a pseudo-static limit equilibrium analysis.

This approach may be used to calibrate an appropriate pseudo-static seismic coefficient reflecting acceptable displacement performance, as discussed in Chapter 7 for retaining wall analysis. Similar discussions for slopes are presented in the FHWA publication *Geotechnical Earthquake Engineering* (FHWA, 1998a). For example, Figure 8-2 shows results of Newmark seismic deformation analyses performed by Hynes and Franklin (1984) using 348 strong motion records (all soil/rock conditions; $4.5 < M_w < 7.4$) and six synthetic records.

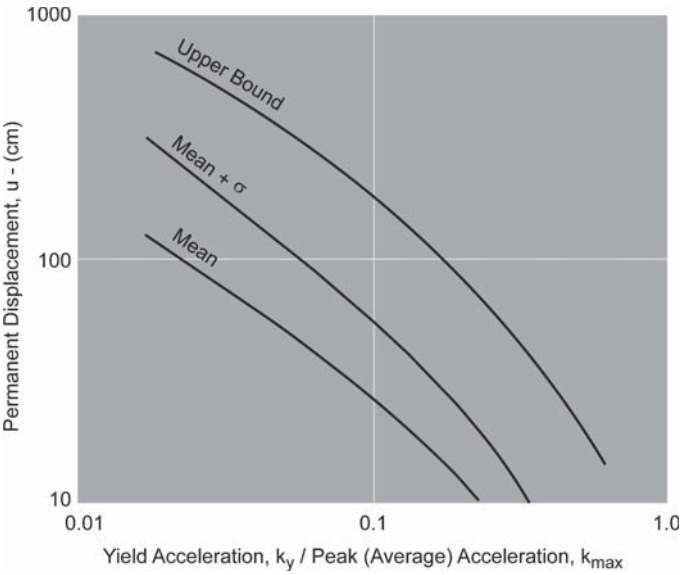

Figure 8-2. Permanent seismic deformation chart (Hynes and Franklin, 1984).

The Hynes and Franklin "upper bound" curve presented in Figure 8-2 suggests that deformations will be less than 12 inches (30 cm) for yield accelerations greater than or equal to one-half the peak acceleration.

In utilizing such curves, it must be recognized that slope-height effects should be taken into account to determine a height-dependent, average maximum acceleration for use as the k_{max} value (as was the case for retaining walls discussed in Chapter 7). This was recognized by the studies published by Makdisi and Seed (1978), who developed slope displacement design charts for the seismic design of earth dams.

Results from the Makdisi and Seed (1978) analyses are shown in Figure 8-3. Analyses were conducted for a limited number of dam heights (for example, 75 to 135 feet) and earthquake records. The lower left figure illustrates the normalized reduction in average maximum seismic coefficient with slide depth (equivalent to an α factor using the terminology from Chapters 6 and 7), and equals an average of 0.35 for a full height slide (average height studied equals approximately 100 feet) which is compatible with values noted in Chapters 6 and 7. A range of displacements as a function of k_y/k_{max} is noted on the lower right figure and shows earthquake magnitude variation.

The Newmark displacement equations discussed in Chapter 5 show insensitivity to earthquake magnitude, which is believed to be better reflected in PGV. Makdisi and Seed note that variability is reduced by normalizing data by k_{max} and the natural period of embankments. The height parameter used in the analyses conducted for this Project reflects changes in natural period, and k_{max} is included in the Newmark equation.

In 2000 an updated approach for estimating the displacement of slopes during a seismic event was developed through the SCEC. The displacement analysis procedures documented in the SCEC (2002) Guidelines are relatively complex and would require simplification for use in a nationwide specification document. Recommended procedures described in the SCEC Guidelines are illustrated by Figures 8-4 and 8-5.

Figure 8-4 shows the ratio of the maximum average seismic coefficient (averaged over the slide mass) to the maximum bedrock acceleration multiplied by a nonlinear response factor (NRF) (equals 1.00 for 0.4g) plotted against the natural period (T_s) of the slide mass ($4H/V_s$, where H is the average height of slide and V_s is the shear wave velocity) divided by the dominant period T_m of the earthquake. In effect, this plot is analogous to the plot of α versus the wall height (assuming the height of the slide equals the wall height) discussed in Chapter 6. For example, if $T_m = 0.3$ sec, $H = 20$ feet, NRF = 1, $V_s = 800$ ft/sec, then $T_s/T_m = 0.1/0.3 = 0.33$, and hence $\alpha = 1$ as would be expected. However, if $H = 100$ feet with the same parameters, $T_s/T_m = 0.5/0.3 = 1.66$ and hence $\alpha = 0.3$, which is reasonably compatible with the α curves presented in Chapter 6.

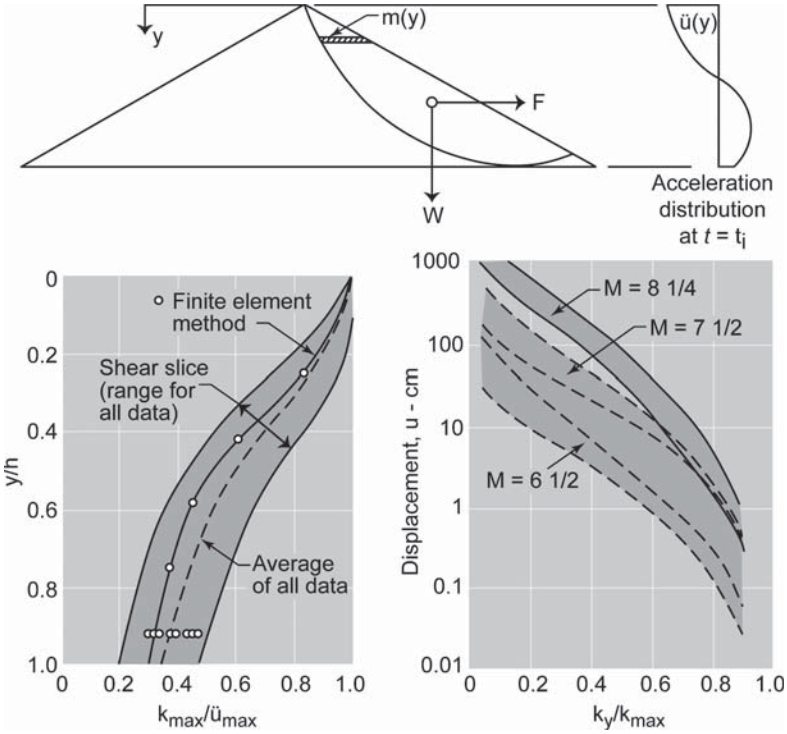

Figure 8-3. Permanent seismic deformation charts (Makdisi and Seed, 1978).

Figure 8-5 shows a median prediction sliding displacement chart, normalized by k_{max} and $D_{5–95}$, an earthquake duration parameter dependent on magnitude. For example, if $k_y/k_{max} = 0.2$, $k_{max} = 0.4$, $D_{5–95} = 10$ seconds, then u equals about 15 inches, compared to about 6 inches (or 12 inches to achieve an 84 percent confidence level) for the recommended Newmark chart shown on Figure 7-18 of this report. This difference is relatively small considering the general accuracy of the Newmark method.

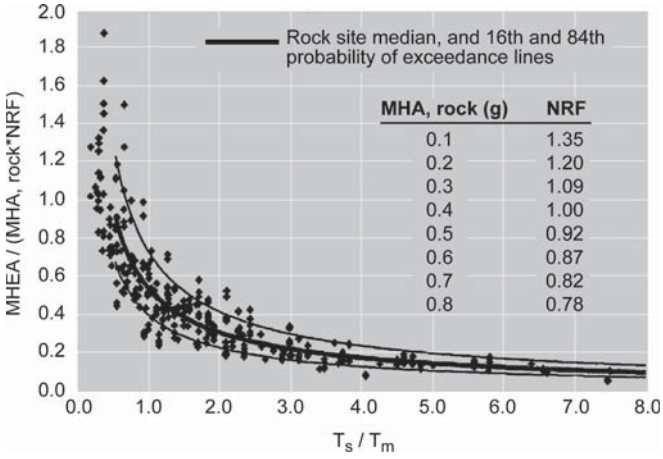

Figure 8-4. Normalized MHEA for deep-seated slide surface vs. normalized fundamental period of slide mass (Bray and Rathje, 1998).

8.3 Proposed Design Methodology

Two approaches for the seismic design of embankments and slopes are described in the previous section: (1) the limit equilibrium approach, and (2) displacement-based method. Both are relatively simple to use, and both involve essentially the same modeling effort. The advantage of the displacement-

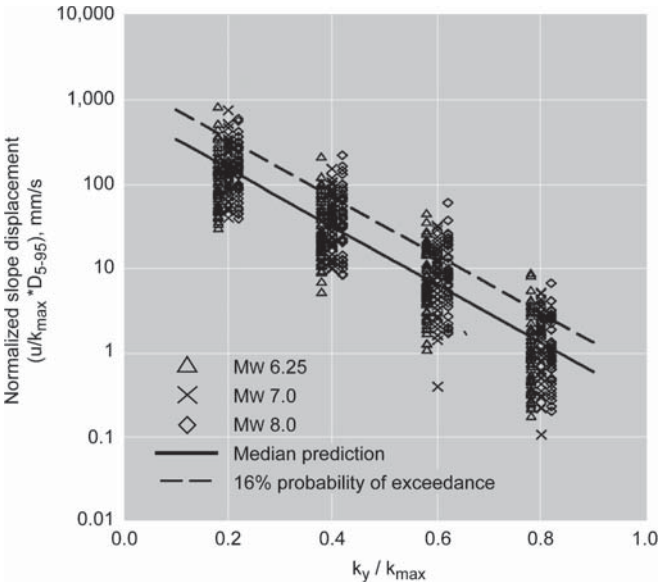

Figure 8-5. Normalized sliding displacement (SCEC, 2002; modified from Bray and Rathje, 1998).

based approach is that the amount of movement associated with the analysis is estimated, and sometimes this can be an important consideration. Note that both approaches assume that liquefaction or porewater pressure effects are not a consideration. Section 8.5.3 provides comments on the potential treatment of liquefaction.

8.3.1 Limit Equilibrium Approach

The limit equilibrium approach involves the following steps:

1. Conduct static slope stability analyses using appropriate resistance factors to confirm that performance meets static loading requirements. Typically these will be a C/D ratio of 1.3 to 1.5 for natural slopes and 1.5 for engineered slopes. A variety of factors should be considered when selecting the C/D ratio including the quality of the site characterization and the implications of failure. Both short-term, undrained stability, and long-term drained stability should normally be considered in this evaluation.
2. Establish the site peak ground acceleration coefficient k_{max} and spectral acceleration at one second, S_1 from the new AASHTO ground motions maps for a 1,000-year return period, including appropriate site soil modification factors.
3. Determine the corresponding PGV from correlation equations between S_1 and PGV (provided in Chapter 5).
4. Modify k_{max} to account for slope height effects for full slope or embankment height stability analyses (note that α factors described in Chapter 7 for retaining walls appear compatible with those for slopes based on comparison with analysis methods described above).
5. Reduce the resulting k_{max} by a factor of 0.5, as long as 1 to 2 inches of permanent displacement are permissible. If larger amounts of deformation are acceptable, further reductions in k_{max} are possible, but these would have to be determined by conducting separate calibration studies between displacement and the ratio of the yield acceleration (k_y) and k_{max}.
6. Conduct a conventional slope stability analysis using 0.5 k_{max}. If the factor of safety is at least 1.1, the slope meets seismic loading requirements.

8.3.2 Displacement-Based Approach

The following displacement-based methodology is recommended for slopes and embankments, where the static strength parameters can reasonably be assumed for seismic analyses:

1. Conduct static slope stability analyses using appropriate resistance factors to confirm that performance meets static loading requirements.
2. Establish the site peak ground acceleration coefficient k_{max} and spectral acceleration at one second, S_1 from the new AASHTO ground motion maps for a 1,000-year return period, including appropriate site soil modification factors.
3. Determine the corresponding PGV from correlation equations between S_1 and PGV (provided in Chapter 5).
4. Modify k_{max} to account for slope height effects for full slope or embankment height stability analyses (note that α factors described in Chapter 7 for retaining walls appear compatible with those for slopes based on comparison with analysis methods described above).
5. Determine the yield acceleration (k_y) using a pseudo-static stability analysis for the slope (that is, the seismic coefficient corresponding to a factor of safety equal to 1.0). Note that these stability analyses should normally be conducted using the undrained strength of the soil because of the short-term loading from the earthquake.
6. Establish the earthquake slope displacement potential corresponding to the value of k_y/k_{max} using the Newmark displacement chart recommendations given in Chapter 5.
7. Evaluate the acceptability of the displacement based on performance criteria established by the owner for the specific project site.

8.4 Example Application

The proposed displacement-based methodology is illustrated by considering an existing slope located in the State of Washington. This slope is next to a heavily traveled roadway. The roadway is being widened to accommodate projected increases in traffic. Stability analyses were required to determine the potential effects of seismic loading to the slopes located above and below the roadway.

8.4.1 Problem Description

Seismic stability of the natural slopes was evaluated for the following conditions:

- Slope angles ranging from 2H:1V up to 1H:1V.
- Soils comprised of glacial till and fill. Till is a dense silty sand with gravel. Standard penetration test (SPT) blowcounts range from 30 blows per foot to refusal. Soil strength values were interpreted from SPT blowcounts. (See Appendix J for sections and assigned properties).
- Groundwater located at the base of the slope.
- The firm-ground values of PGA, S_s, and S_1 for site are estimated to be 0.41g, 0.92g, and 0.30g, respectively, for the 1,000-year earthquake based on the USGS deaggregation website. (Note that at the time the example was developed, the new AASHTO ground motion hazard maps and implementation CD were not available to the NCHRP 12-70

Project Team.) The soil conditions are representative of Site Class C.

The objective of the seismic stability study was to evaluate the displacements that would be expected for the design earthquake. The owner also is interested in the risk to the roadway facility, and therefore, stability also was evaluated for a 10 percent probability of exceedance in 50 years (475-year event) and for a 2 percent probability of exceedance (2,475-year event). There is debate locally on the strength properties to assign till; therefore, each of the commonly used alternatives is evaluated.

8.4.2 Results

The ground motion criteria for the site were obtained from the USGS website for the three return periods, as summarized in Table 8-1; local site effects were considered using the procedures recommended in Chapter 5.

The computer program SLIDE was used to determine the static factor of safety and then the yield accelerations (k_y) for the various cases involved. With the yield acceleration, site-adjusted PGV, and the site-adjusted peak seismic coefficient (that is, PGA adjusted for site class and wave scattering), the equations in Chapter 5 were used to estimate permanent displacement. The estimated displacements from the analyses are summarized in Table 8-2.

The summary in Table 8-2 indicates that the displacements ranged from zero to a maximum of 73 inches, depending on assumptions made for soil properties and the design earthquake. Details for these analyses are included in Appendix J.

8.5 Other Considerations

There are three other considerations relative to the seismic design of slopes and embankments: (1) the use of the limit equilibrium method for determining acceptability of slope under seismic loading, (2) the acceleration level at which a "No Analysis" approach can be invoked, and (3) methods to consider when there is a liquefaction potential. These considerations are summarized below.

8.5.1 Limit Equilibrium Design Methods

Computer programs are routinely used for evaluating the static stability of slopes. As demonstrated in the example problem, the incremental effort to determine k_y is relatively minor. However, a particular state DOT may choose to develop a value of k_{max} to use either (1) in pseudo-static screening analyses (by calibrating against a displacement chart appropriate for seismic hazard levels in their state) in lieu of requiring a displacement analysis, or (2) if they feel a displacement level different than the several inches identified in Section 8.3.1 is permissible.

Table 8-1. Ground motions for example problem.

Parameter	Units	Site Class	Ground Motion Parameter		
			7% in 75 Years	10% in 50 Years	2% in 50 Years
PGA		B	0.41	0.31	0.58
S_s		B	0.92	0.68	1.30
S_1		B	0.30	0.22	0.44
$S_s/2.5$			0.37	0.27	0.52
Magnitude			6.8	6.8	6.8
F_{pga}		C	1.00	1.10	1.00
		D	1.10	1.20	1.00
F_v		C	1.50	1.58	1.36
		D	1.80	1.96	1.56
PGV	In/sec	C	25	19	33
	In/sec	D	30	24	38
$\beta = F_v S_1 / F_{pga}$ PGA*		C	1.10	1.02	1.03
		D	1.20	1.16	1.18
Failure Slope Height	ft		15	15	15
α Factor per Equation 7-2		C	0.93	0.93	0.93
		D	0.94	0.94	0.94
$K_{av} = PGA*F_{pga} * \alpha$		C	0.38	0.32	0.54
		D	0.42	0.35	0.54

Table 8-2. Results of ground displacement estimates for example stability evaluation.

Parameter	Slope Angle	Static C/D Ratio	k_{yield}	Ground Motion Displacement (inches)		
				7% in 75 Years	10% in 50 Years	2% in 50 Years
Upper Bound Till (ϕ = 42 degrees)						
Case 1	1H to 1V	0.9	NA	NA	NA	NA
Case 2	1.5H to 1V	1.3	0.13	6-9	3-5	14-18
Case 3	2H to 1V	1.7	0.25	<1	<1	3-4
Upper Bound Till (ϕ = 38 degrees, c = 200 psf)						
Case 1	1H to 1V	1.2	0.09	12-19	7-11	26-32
Case 2	1.5H to 1V	1.6	0.26	<1	0	3
Case 3	2H to 1V	2.0	0.32	0	0	<1
Lower Bound Till (ϕ = 36 degrees)						
Case 1	1H to 1V	0.8	NA	NA	NA	NA
Case 2	1.5H to 1V	1.2	0.07	18-27	11-17	36-44
Case 3	2H to 1V	1.5	0.17	3-5	1-2	8-11

Typically, if the site is nonliquefiable (that is, significant loss in strength does not occur during seismic loading), a seismic coefficient of 50 percent of the site-adjusted PGA (after adjustments for site soil effects and wave scattering) will result in ground displacements of less than 1 to 2 inches, as long as the resulting C/D ratio (that is, factor of safety) is greater than 1.0. In view of the simplifications associated with this method, common practice is to use a C/D ratio > 1.1 to define acceptable slope conditions. It is a fairly simple task to calibrate the reduction based on the typical site-adjusted PGA and PGV for the area, the shape of the normalized response spectrum, and the displacement that is acceptable. Newmark curves in Chapter 5 then can be used to "back out" the k_y value. If the k_y value is used in the slope stability computer program as the seismic coefficient, and the resulting factor of safety is greater than 1.0, acceptable slope displacements are predicted.

8.5.2 No Analysis Cut-off

The same concept as described in the preceding subsection can be used to define a "no analysis" area. In this case, if the C/D ratio for gravity loading is greater than a predetermined value, then the slope will be inherently safe during seismic loading, as long as liquefaction does not occur. For engineered slopes, most transportation agencies require that the minimum C/D ratio is 1.5 or more, and for natural slopes the acceptable C/D ratio ranges from 1.3 to 1.5, depending on the potential consequences of slope instability.

The following results were developed to define combinations of slope angles and the site-adjusted PGA values below which a seismic stability analysis did not appear warranted.

This guidance must be used with some care. It works best when the slope is relatively homogeneous in consistency and there is no water table within the slope. As the slope becomes more complicated, particularly if there are thin, low-strength bedding planes, then this screening criteria identified in Table 8-3 should not be used and a detailed slope stability analysis performed, in which the strength in each soil layer is modeled.

8.5.3 Liquefaction Potential

No effort has been made within this Project to introduce liquefaction effects into the seismic stability analysis. This topic has been specifically avoided due to the complexity of the issues involved and the on-going debate regarding the best approach for addressing liquefaction.

Several approaches are currently being used or proposed.

- The simplest are the empirical relationships suggested by Youd et al. (2002) for estimating displacement during lat-

Table 8-3. Proposed screening levels for no-analysis cut-off.

Slope Angle	F_{pga} PGA
3H:1V	0.3
2H:1V	0.2

eral spreading. These relationships are based on empirical correlations between observed lateral displacement, earthquake parameters, and soil conditions. This approach is typically applied near rivers or other locations where slopes are gentle and a free face might exist. Generally, results from these methods are considered most suitable for screening of potential displacement issues and involve too much uncertainty for design.

- An approach was suggested in the NCHRP 12-49 Project (NCHRP Report 472, 2002) for addressing liquefaction of bridge abutments. This approach includes the effects of foundation pile pinning. Combinations of earthquake magnitude, site-adjusted PGA, and SPT blowcounts are used to decide whether the liquefaction analysis is required. A residual strength is assigned to the liquefied layer using either of two empirical relationships (Seed and Harder, 1990; Olson and Stark, 2002). While this approach is relatively simple to apply, it is often criticized that it relies on triggering relationships for liquefaction and does not properly account for the dilation effects that occur under large ground displacement. Results of recent centrifuge research programs also indicate the methodology may not replicate important mechanisms that occur during seismic loading.
- Various computer models, such as FLAC, also are used commonly to investigate the seismic stability problem where liquefiable soils have been identified. These methods seem to be used extensively by designers, often without having a particularly good understanding or appreciation for the uncertainties of the model. One significant criticism of this method is that thin layers that lead to ground displacement during liquefaction are often ignored.
- The NCHRP 20-07 Project initially suggested that the entire issue of liquefaction could be ignored if the magnitude of the design earthquake is less than a value of approximately 6.5. The controlling magnitude was taken from a study conducted by Dickenson et al. (2002) for the Oregon Department of Transportation. It is likely that Dickenson and his co-authors did not intend for his work to be used in this manner, and preliminary feedback from the geotechnical community suggested that this approach was too unconservative for adoption by AASHTO.

There is little doubt that liquefaction-related slope instability is an important consideration in some locations. However, in the absence of a consensus approach within the profession for handling this issue, it is difficult to provide specific guidance. The current difficulty in developing an approach results from uncertainties in two areas: (1) the capacity of the soil in its liquefied state, particularly where there are static shearing stresses (that is, sloping ground effects) for the site and also where the soil could dilate under large deformations, and (2) the ground motions to use after the seismic wave travels through the liquefied soil. While numerical methods, such as DESRA (1978), are available to address the latter issue, these methods are limited in availability to designers.

The approach used to address liquefaction during seismic slope and embankment design has and likely will continue to require more research. Until a consensus is reached within the profession, the NCHRP 12-70 Project team recommends using the methodology summarized in the NCHRP 12-49 Project, but providing more cautionary words on the limitations of this method.

8.6 Conclusions

This chapter summarizes the approach recommended for the seismic analysis and design of slopes. The methodology uses conventional limit equilibrium slope stability analysis methods, in combination with the Newmark method for estimating displacements. Relative to existing methods, the approach:

- Incorporates the results of wave scattering and ground motion studies summarized in Chapters 5 and 6, including an equation that relates the PGV to the spectral acceleration at one second.
- Uses a new set of equations for estimating displacements that were calibrated against the USNRC strong motion database, making the equations applicable to the CEUS as well as the WUS.

The proposed method is thought to be relatively simple to use and easily adopted by designers. The primary outstanding issues are (1) the use of this method to develop a "no analysis" approach and (2) an appropriate methodology for introducing liquefaction potential into the analysis. Interim approaches for addressing each of these issues are given in the chapter; however, further research on each is required.

CHAPTER 9

Buried Structures

This chapter provides results of analyses and sensitivity studies conducted for buried structures. These studies dealt with the TGD and not PGD. The primary objectives of the TGD work were to:

- Identify methodologies for evaluating the ovaling response of circular conduits, as well as the racking response of rectangular conduits, and
- Conduct parametric studies and parametric evaluations for the methods being proposed.

Results of analyses conducted to address these objectives are summarized in the following sections. These analyses focused on deriving a rational procedure for seismic evaluation of buried culverts and pipelines that consider the following subjects: (1) general properties and characteristics of culverts and pipes, (2) potential failure modes for buried culverts and pipes subject to seismic loading, (3) procedures used in current design practice to evaluate seismic response of buried structures, (4) derivation of detailed rational procedures for seismic evaluation of both rigid and flexible culverts and pipes subject to TGD, taking into consideration soil-structure interaction, and (5) providing recommendations on a general methodology for seismic evaluation under the effects of PGD. These results consider both flexible and rigid culverts, burial depths that range from 0.5 to 5 diameters, various cross-sectional geometries (for example, circular and rectangular) and wall stiffnesses, and different properties of the surrounding soil.

9.1 Seismic Performance of Culverts and Pipelines

Damage to buried culverts and pipelines during earthquakes has been observed and documented by previous investigators (NCEER, 1996; Davis and Bardet, 1999 and 2000; O'Rourke, 1999; Youd and Beckman, 2003). In general, buried structures have performed better in past earthquakes than above-ground structures. Seismic performance records for culverts and pipelines have been very favorable, particularly when compared to reported damages to other highway/transportation structures such as bridges.

The main reason for the good performance of buried structures has been that buried structures are constrained by the surrounding ground. It is unlikely that they could move to any significant extent independent of the surrounding ground or be subjected to vibration amplification/resonance. Compared to surface structures, which are generally unsupported above their foundations, buried structures can be considered to display significantly greater degrees of redundancy, thanks to the support from the ground. The good performance also may be partly associated with the design procedures used to construct the embankment and backfill specifications for the culverts and pipes. Typical specifications require close control on backfill placement to assure acceptable performance of the culvert or pipe under gravity loads and to avoid settlement of fill located above the pipe or culvert, and these strict requirements for static design lead to good seismic performance.

It is important that the ground surrounding the buried structure remains stable. If the ground is not stable and large PGD occur (for example, resulting from liquefaction, settlement, uplift, lateral spread, or slope instability/landslide), then significant damage to the culvert or pipe structures can be expected. Although TGD due to shaking also can damage buried structures, compared to the effects of PGD, the damage is typically of a more limited extent.

9.2 Culvert/Pipe Characteristics

Culvert/pipe products are available over a large range in terms of material properties, geometric wall sections, sizes, and shapes. Pipe sizes as small as 1 foot and as large as culverts with spans of 40 feet and larger are used in highway applications. They can be composed of concrete, steel, aluminum, plastic, and other materials. Detailed information about their

shapes, range of sizes, and common uses for each type of culvert or pipe are summarized by Ballinger and Drake (1995).

9.2.1 Flexible Culverts and Pipes

In general, culverts and pipes are divided into two major classes from the static design standpoints: flexible and rigid. Flexible culverts and pipes typically are composed of either metal (for example, corrugated metal pipe (CMP) made of steel or aluminum) or thermoplastic materials (for example, HDPE or PVC). Flexible culverts and pipes respond to loads differently than rigid culverts and pipes. Because their ovaling stiffness is small, relative to the adjacent soil, flexible culverts and pipes rely on firm soil support and depend upon a large strain capacity to interact with the surrounding soil to hold their shape, while supporting the external pressures imposed upon them.

For static design, current AASHTO *LRFD Bridge Design Specifications* require as a minimum the following main design considerations (in addition to the seam failure) for flexible culverts and pipes: (1) buckling (general cross sectional collapse as well as local buckling of thin-walled section), and (2) flexibility limit for construction. Except for large box structures or other large spans with shapes other than circular [per McGrath, et al., (2002) NCHRP Report 473], the flexural strength consideration (that is, bending moment demand) is generally not required for flexible culverts and pipes.

Neither current AASHTO *LRFD Bridge Design Specifications* nor the McGrath, et al. (2002) study has addressed seismic design concerns for culvert structures. From the seismic design standpoint, there are two main factors that must be considered:

1. Bending moment and thrust evaluations: Seismic loading is in general nonsymmetric in nature and therefore may result in sizable bending in the culvert structures (even for circular shape culverts). Furthermore, the behavior of thin-walled conduits (such as for the flexible culverts and pipes) is vulnerable to buckling. This behavior differs somewhat from that of a rigid concrete culvert structure, for which bending moments are often the key factor in judging structural performance. For buckling, thrust (that is, hoop force) is the key factor and seismically induced thrust can be significant, particularly if the interface between the culvert or pipe structure and the surrounding soil is considered a nonslip condition (Wang, 1993). Therefore, it is important that both seismically induced bending and thrust be evaluated using published solutions for circular tube (Moore, 1989; Janson, 2003) as failure criteria for evaluating the seismic performance of CMP and polymeric conduits (for example, corrugated HDPE pipes).
2. Soil-support considerations: Implicit in the current AASHTO design assumptions for flexible culverts is the existence of adequate soil support. This may be the weakness of flexible culverts, in case of earthquakes, in that the soil support can be reduced or lost during liquefaction or other permanent ground failure mechanisms associated with seismic events. Significant distortion or collapse of the culvert cross section is likely if soil support is reduced or lost.

9.2.2 Rigid Culverts and Pipes

Rigid highway culverts and pipes consist primarily of reinforced concreted shapes that are either precast or cast-in-place. Unreinforced concrete culverts and pipe structures are not recommended for use in seismic regions. The sizes of reinforced concrete pipe (RCP) range (in diameter) from about 1 foot to 12 feet. Larger RCP can be precast on the site or constructed cast-in-place. Rectangular four-sided box culverts can be furnished precast in spans ranging from 3 feet to 12 feet. Larger spans can be constructed cast-in-place. Three-sided precast box culverts can be furnished in spans up to 40 feet.

Unlike the flexible culverts and pipes, the strain capacity of rigid culverts and pipes is much lower. Rigid culverts must develop significant ring stiffness and strength to support external pressures. Hence, they are not as dependent upon soil support as flexible culverts.

For static design, the primary design methods used for precast concrete pipe, either reinforced or unreinforced, include: (1) the Indirect Design Method, based on the laboratory three-edge bearing test, known as the test; (2) a more direct design procedure that accounts for bending moment, shear, thrust/tension, and crack width (bucking is generally not an issue with rigid converts and pipes) around the periphery of the culvert wall; and (3) methods employing computerized numerical models accounting for soil-structure interaction effects.

For box culverts the static design uses the same criteria as other reinforced concrete structures (for example, beams and columns). In general, the effect of surrounding soils is accounted for by applying the soil pressures (active or at-rest) directly against the wall in the model, instead of fully taking advantage of the soil-structure interaction effect. Most current commercially available computer software can perform the structural analysis required for this design. For other structural shapes, consideration of soil-structure interaction becomes important and therefore is generally accounted for by using computerized numerical models.

9.3 General Effects of Earthquakes and Potential Failure Modes

The general effects of earthquakes on culverts and pipe structures can be grouped into two broad categories: ground shaking and ground failure. The following sections discuss each category. As it will be demonstrated, soil-structure inter-

action plays a critical role in the evaluation of the effect of seismic loading for both flexible and rigid culverts and pipes. A unified evaluation procedure is developed in this chapter to provide a rational and reliable means for seismic evaluations as well as realistic design for buried culvert and pipe structures.

9.3.1 Ground Shaking

Ground shaking refers to the vibration of the ground produced by seismic waves propagating through the earth's crust. The area experiencing this shaking may cover hundreds of square miles in the vicinity of the fault rupture. The intensity of the shaking attenuates with distance from the fault rupture.

Ground shaking motions are composed of two different types of seismic waves, each with two subtypes:

- Body waves travel within the earth's material. They may be either longitudinal compressional (P-) waves or transverse shear (S-) waves, and they can travel in any direction in the ground.
- Surface waves travel along the earth's surface. They may be either Rayleigh waves or Love waves.

As stable ground is deformed by the traveling waves, any culverts or pipelines in the ground also will be deformed. The shaking or wave traveling induced ground deformations are called transient ground deformations.

When subject to transient ground deformations, the response of a buried linear culvert or pipe structure can be described in terms of three principal types of deformations: (1) axial deformations, (2) curvature deformations (refers to Figure 9-1), and (3) ovaling (for circular cross section) or racking (for rectangular cross section) deformations (refers to Figure 9-2).

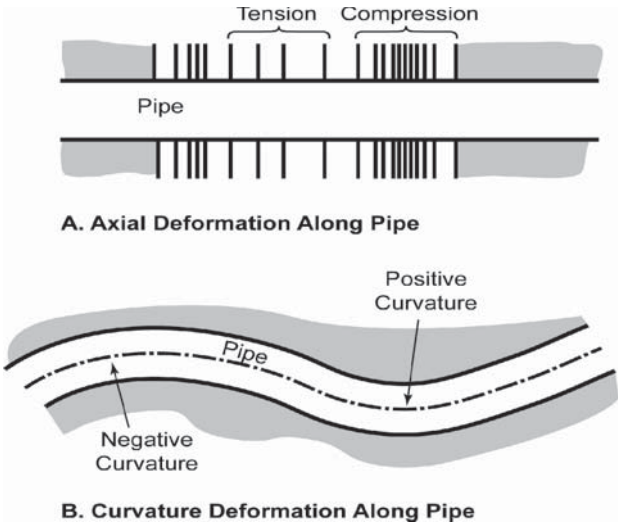

Figure 9-1. Axial and curvature deformations.

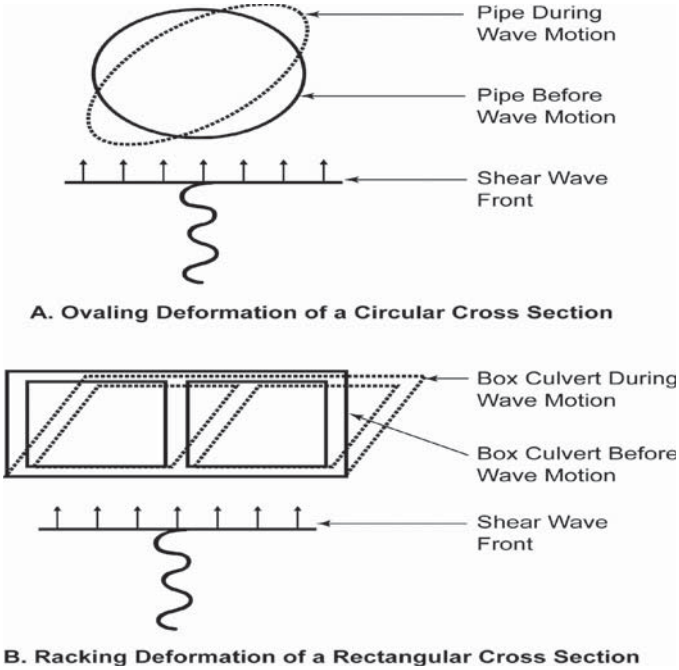

Figure 9-2. Ovaling and racking deformations.

The axial and curvature deformations are induced by components of seismic waves that propagate along the culvert or pipeline axis. Figure 9-1 shows the idealized representations of axial and curvature deformations. The general behavior of the linear structure is similar to that of an elastic beam subject to deformations or strains imposed by the surrounding ground.

Current design and analysis methodologies for pipeline systems were developed typically for long, linear structures. The principal failure modes for long, continuous pipeline structures consist of (1) rupture due to axial tension (or pull out for jointed segmented pipelines), and (2) local bucking (wrinkling) due to axial compression and flexural failure. If the pipelines are buried at shallow depth, continuous pipelines in compression also can exhibit beam-buckling behavior (that is, global bucking with upward buckling deflections). If the axial stiffness of the structures is large, such as that for a large sectional concrete pipe, then the buckling potential in the longitudinal direction is small for both local buckling and global buckling. The general failure criteria for the above-mentioned potential failure modes have been documented by previous studies (O'Rourke and Liu, 1996).

It should be noted, however, that typical culvert structures for transportation applications are generally of limited length. For this condition, it is in general unlikely to develop significant transient axial/curvature deformations along the culvert structures. The potential failure modes mentioned above are not likely to take place during the earthquake. The main focus of this chapter will not be on the effects of axial/curvature deformations. Instead, the scope of this chapter will concentrate on transverse deformations of culverts and pipes.

The ovaling or racking deformations of a buried culvert or pipe structure may develop when waves propagate in a direction perpendicular or nearly perpendicular to the longitudinal axis of the culvert or pipe, resulting in a distortion of the cross-sectional shape of the structure. Design considerations for this type of deformation are in the transverse direction. Figure 9-2 shows the ovaling distortion and racking deformation associated with a circular culvert or pipe and a rectangular culvert, respectively. The general behavior of the structure may be simulated as a buried structure subject to ground deformations under a two-dimensional, plane-strain condition.

Ovaling and racking deformations may be caused by vertically, horizontally, or obliquely propagating seismic waves of any type. Previous studies have suggested, however, that the vertically propagating shear wave is the predominant form of earthquake loading that governs the ovaling/racking behavior for the following reasons: (1) except possibly in the very near-source areas, ground motion in the vertical direction is generally considered less severe than its horizontal component, (2) vertical ground strains are generally much smaller than shearing strain because the value of constrained modulus is much higher than that of the shear modulus, and (3) the amplification of vertically propagating shear wave, particularly in the soft or weak soils, is much higher than vertically propagating compressional wave and any other type of waves traveling in the horizontal direction. Therefore the analysis and methodology presented in this chapter addresses mainly the effects of vertically propagating shear waves on ovaling/racking behavior of the buried culverts or pipes.

When subject to ovaling/racking deformations, a flexural type failure mode due to the combined effects of bending moment and thrust force must be checked. The flexural failure mode is typically the main concern for rigid culverts and pipes, such as those constructed with reinforced concrete. For flexible culverts and pipes (typically, thin-walled conduits constructed with steel, aluminum, or thermoplastic such as HDPE or PVC), they are likely to be controlled by buckling, which can occur in the elastic range of stresses. For buckling, thrust is the key factor and conservative assumption must be made regarding interface condition (slip or nonslip) between the exterior surface of the conduit and the surrounding ground. An elastic buckling criterion for circular conduits in uniform soil was proposed by Moore (1989) and may be used for buckling potential evaluation purpose.

9.3.2 Ground Failure

Ground failure broadly includes various types of ground instability such as faulting, landslides, liquefaction (including liquefaction-induced lateral spread, settlement, flotation, etc.), and tectonic uplift and subsidence. These types of ground deformations are called permanent ground deformations. Each permanent ground deformation may be potentially catastrophic to culvert or pipeline structures, although the damages are usually localized. To avoid such damage, some sort of ground improvement is generally required, unless the design approach to this situation is to accept the displacement, localize the damage, and provide means to facilitate repairs.

Characteristics of permanent ground deformation and its effects on culvert and pipes are extremely complex and must be dealt with on a case-by-case basis. It is unlikely that simple design procedures or solutions can be developed due to the complex nature of the problem. In this chapter, detailed study of problems associated with permanent ground deformation will not be conducted. Instead, only general guidelines and recommendations on methodology for seismic evaluation under the effects of permanent ground deformation will be provided.

9.4 Current Seismic Design Practice for Culverts or Other Buried Structures

Currently there is no standard seismic design methodology or guidelines for the design of culvert structures, including Section 12 within the current AASHTO *LRFD Bridge Design Specifications.* The NCHRP Report 473 *Recommended Specifications for Large-Span Culverts,* (NCHRP, 2002) does not address issues related to seismic evaluation of long-span culverts.

In the past, design and analysis procedures have been proposed by some researchers and design engineers for pipelines (for example, gas and water) or tunnel (that is, transportation or water) systems. While some of these procedures can be used for the design and analysis of culverts and pipes (for example, the transverse ovaling/racking deformation of the section, Figure 9-2), others cannot be directly applied because they are only applicable for buried structures with a long length, or with a deep burial depth. Furthermore, significant disparity exists among engineers regarding the appropriate design philosophy and methods of analysis applicable to various types of culvert structures.

The following two paragraphs provide a brief description of procedures and methodologies proposed in the past for seismic evaluation of buried structures in general:

- O'Rourke (1998) provides a general overview of lifeline earthquake engineering, including the treatment of seismic evaluation of pipelines. O'Rourke and Liu (1996) present a detailed methodology for evaluating response of buried pipelines subject to earthquake effects. Pipelines responses to both transient ground deformation and permanent ground deformation were addressed in these two studies. However, the focus of these studies was on pipeline behavior in the longitudinal direction which is more suitable for a long continuous buried pipeline structure. Although failure

criteria for axial tension and axial compression (local buckling/wrinkling and beam buckling) were developed, there were no discussions related to the procedure for evaluating the transverse ovaling deformation of the pipe's cross-sectional behavior.

- Based on the field performance of 61 corrugated metal pipes (CMP) that were shaken by the 1994 Northridge Earthquake, Davis and Bardet (2000) provided an updated approach to evaluating the seismic performance of CMP conduits. The focus of their study was on the ovaling and buckling (of the thin metal wall) of the transverse section behavior of the CMP. This approach involves the following general steps:
  1. Estimate the initial condition of compressive strain in the conduit, which is related to depth of burial.
  2. Estimate the compressive ground strain induced by a vertically propagating shear wave, which was calculated from the closed-form solution for transient shearing strain, as $\frac{1}{2}\,\gamma_{max} = v_p/2V_s$, where γ_{max} is the maximum transient shearing strain of the ground, v_p is the horizontal peak particle velocity transverse to the conduit, and V_s is the average shear wave velocity of the surrounding ground.
  3. Add the static and transient compressive strains.
  4. Compare the strain so determined with the critical compressive strain that would cause dynamic buckling (due to hoop force) of the CMP pipe. The critical buckling strain (or strength) was assumed to be dependent on the stiffness of the surrounding soil (Moore, 1989).

The methodology derived by Davis and Bardet, although more rational than most of the other procedures, has some drawbacks, including:

- The procedure is applicable for thin-walled pipes only. The failure mode considered by using this procedure is primarily for buckling and does not include flexural (that is, bending) demand and capacity evaluation. The latter is a very important failure mode that must be considered for rigid culverts and pipes (such as those constructed with reinforced concrete).
- The soil-structure interaction effect was considered in evaluating the buckling capacity, but not in the evaluation of the demand (that is, earthquake-induced ground strains).
- The method assumed that the strains in the pipe coincide with those in the surrounding ground (that is, pipe deforms in accordance with the ground deformation in the free-field), on the basis of the assumption that there is no slippage at the soil-pipe interface. This assumption was incorrect, as Wang (1993) pointed out in his study. Wang concluded that the strains and deformations of a buried conduit can be greater, equal, or smaller than those of the surrounding ground in the free-field, depending on the relative stiffness of the conduit to the surrounding ground.

To account for the effects of transient ground deformation on tunnel structures, Wang (1993) developed closed-form and analytical solutions for the determination of seismically induced ovaling/racking deformations and the corresponding internal forces (such as moments and thrusts) for bored as well as cut-and-cover tunnel structures. The procedure presented by Wang for the bored tunnels was developed from a theory that is familiar to most mining/underground engineers (Peck et al., 1972). Simple and easy-to-use seismic design charts were presented. The design charts are expressed primarily as a function of relative stiffness between the structure and the ground. Solutions for both full-slip and nonslip conditions at the interface between soil and the exterior surface of the tunnel lining were developed. These solutions fully account for the interaction of the tunnel lining with the surrounding ground. The results were validated through a series of finite element/difference soil-structure interaction analyses.

For the cut-and-cover tunnels (with a rectangular shape), the design solutions were derived from an extensive study using dynamic finite-element, soil-structure interaction analyses. A wide range of structural, geotechnical, and ground motion parameters were considered by Wang in his study. Specifically, five different types of cut-and-cover tunnel geometry were studied, including one-barrel, one-over-one two-barrel, and one-by-one twin-barrel configurations. To quantify the effect of relative stiffness on tunnel lining response, varying ground profiles and soil properties were used in the parametric analyses. Based on the results of the parametric analyses, a deformation-based design chart was developed for cut-and-cover tunnels.

Although these solutions were intended originally for tunnel structures (considered a fairly rigid type of structure), the methodology is rational and comprehensive and provides a consistent and unified approach to solving the problem of buried conduits subject to ground shaking regardless of whether they are rigid or flexible structures. With some adjustments this approach also is applicable to the culvert and pipe structures typically used for highway construction. Therefore, a more detailed discussion of Wang's approach is given in the following section.

9.5 General Methodology and Recommended Procedures

The general methodology and recommended procedures for the ovaling of circular conduits and the racking of rectangular conduits developed by Wang (1993) are presented in the following two sections, respectively.

9.5.1 Ovaling of Circular Conduits

The seismic ovaling effect on the lining of a circular conduit is best defined in terms of change of the conduit diameter

(ΔD_{EQ}) and incremental seismically induced internal forces [for example, bending moment (M) and thrust/hoop force (T)]. It should be noted that for flexible types of conduits (such as thin-walled metal, corrugated or noncorrugated, and thermoplastic pipes) buckling is the most critical failure mode and therefore the thrust force, (T) is the governing quantity in the evaluation. For rigid conduits (for example, constructed with reinforced concrete), the deformation of the lining, the bending, the thrust as well as the resulting material strains are all important quantities. These quantities can be considered as seismic ovaling demands for the lining of the conduit and can be determined using the following general steps:

Step 1: Estimate the expected free-field ground strains caused by the vertically propagating shear waves of the design earthquakes using the following formula:

$$\gamma_{max} = V_s / C_{se} \quad (9\text{-}1)$$

where

γ_{max} = maximum free-field shearing strain at the elevation of the conduit;
V_s = shear (S-) wave peak particle velocity at the conduit elevation; and
C_{se} = effective shear wave velocity of the medium surrounding the conduit.

It should be noted that the effective shear wave velocity of the vertically propagating shear wave (C_{se}) should be compatible with the level of shearing strain that may develop in the ground at the elevation of the conduit under the design earthquake shaking.

An important aspect for evaluating the transient ground deformation effects on culvert and pipe structures is to first determine the ground strain in the free-field (in this case free-field shear strain, γ_{max}) and then determine the response of the structures to the ground strain. For a culvert or pipe structure constructed at a significant depth below the ground surface, the most appropriate design ground motion parameter to characterize the ground motion effects is not PGA. Instead, PGV (in this case S-wave peak particle velocity, V_s) is a better indicator for ground deformations (strains) induced during ground shaking. This is particularly important because given the same site-adjusted PGA value, the anticipated peak ground velocity for CEUS could be much smaller than that for the WUS. The results based on the PGA versus PGV study presented in Chapter 5 in this report should be used in evaluating the maximum free-field shearing strain in Equation (9-1).

However, for most highway culverts and pipes, the burial depths are generally shallow (that is, within 50 feet from the ground surface). Under these conditions, it is more reasonable to estimate the maximum free-field shearing strain using the earthquake-induced shearing stress and the strain-compatible shear modulus of the surrounding ground. In this approach, the expected free-field ground strain caused by the vertically propagating shear waves for the design earthquake is estimated using the following equation.

$$\gamma_{max} = \tau_{max} / G_m \quad (9\text{-}2)$$

τ_{max} = maximum earthquake-induced shearing stress;
= (PGA/g) σ_v R_d;
σ_v = total vertical overburden pressure at the depth corresponding to the invert of the culvert or pipe;
= γ_t ($H + D$);
γ_t = total unit weight of soil;
H = soil cover thickness measured from the ground surface to the crown elevation;
d = diameter of the circular culvert or pipe;
R_d = depth-dependent stress reduction factor;
= 1.0 – 0.00233z for z <30 feet where z is the depth to the midpoint of the culvert or pipe;
= 1.174 – 0.00814z for 30 feet < z <75 feet; and
G_m = effective, strain-compatible shear modulus of the ground surrounding the culvert or pipe.

Alternatively, the maximum free-field shearing strain also can be estimated by a more refined free-field site response analysis (for example, conducting SHAKE analyses).

Step 2: Given γ_{max}, the free-field diameter change of the conduit would be:

$$\Delta D_{EQ\text{-}FF} = 0.5 \gamma_{max} D \quad (9\text{-}3)$$

However, if the fact that there is a hole/cavity in the ground (due to the excavation of the conduit) is considered, then the diameter change in the ground with the cavity in it would be:

$$\Delta D_{EQ} = \pm 2 \gamma_{max} (1 - \nu_m) D \quad (9\text{-}4)$$

where

ν_m = Poisson's ratio of the surrounding ground; and
D = diameter of the conduit structure.

It is to be noted that Equation (9-3) ignores the fact that there is a cavity and a conduit structure in the ground, while Equation (9-4) accounts for the presence of the cavity but ignores the stiffness of the conduit. Equation (9-4) is applicable for a flexible conduit in a competent ground. In this case, the lining of the conduit can be reasonably assumed to conform to the surrounding ground with the presence of a cavity in it.

In the study by Davis and Bardet (2000), it was assumed that the CMP conform to the free-field ground deformation (that is, Equation 9-3). For flexible conduits such as the CMP studied by Davis and Bardet, the actual pipe deformations/

strains should have been closer to the values predicted by Equation (9-4) rather than by Equation (9-3), suggesting that the strains in the pipes calculated in that study were probably well underestimated.

This very simplified design practice has been used frequently in the past (that is, estimate the free-field ground deformations and then assume that the conduit structure would conform to the free-field ground deformations). By doing this, the soil-structure interaction effect was ignored. This practice may lead to either overestimated or underestimated seismic response of the structural lining, depending on the relative stiffness between the surrounding ground and the culvert.

Further studies by Wang (1993) led to a more rational procedure in estimating the actual lining deformation by defining the relative stiffness between a circular lining and the surrounding ground using two ratios designated as the compressibility ratio (C) and the flexibility ratio (F), as follows (Peck et al., 1972):

$$C = \{E_m(1-\nu_l^2)R\}/\{E_l A_l(1+\nu_m)(1-2\nu_m)\} \quad (9\text{-}5)$$

$$F = \{E_m(1-\nu_l^2)R^3\}/\{6E_l I_l(1+\nu_m)\} \quad (9\text{-}6)$$

where

E_m = strain-compatible elastic modulus of the surrounding ground;
ν_m = Poisson's ratio of the surrounding ground;
R = nominal radius of the conduit;
E_l = Elastic modulus of conduit lining;
ν_l = Poisson's ratio of the conduit lining;
A_l = lining cross-sectional area per unit length along culvert axial alignment;
t = lining thickness; and
I_l = moment of inertia of lining per unit length of tunnel (in axial direction).

The flexibility ratio (F) tends to be the governing factor for the bending response of the lining (distortion) while the compressibility ratio (C) tends to dominate the thrust/hoop forces/strains of the lining. When $F < 1.0$, the lining is considered stiffer than the ground, and it tends to resist the ground and therefore deforms less than that occurring in the free-field. On the other hand, when $F > 1$, the lining is expected to deform more than the free-field. As the flexibility ratio continues to increase, the lining deflects more and more than the free-field and may reach an upper limit as the flexibility ratio becomes infinitely large. This upper limit deflection is equal to the deformations displayed by a perforated ground, calculated by the Equation (9-4) presented above.

The strain-compatible elastic modulus of the surrounding ground (E_m) should be derived using the strain-compatible shear modulus (G_m) corresponding to the effective shear wave propagating velocity (C_{se}).

Step 3: The diameter change (ΔD_{EQ}) accounting for the soil-structure interaction effects can then be estimated using the following equation:

$$\Delta D_{EQ} = \pm 1/3(k_1 F \gamma_{max} D)(\text{full-slip}) \quad (9\text{-}7)$$

where

k_1 = seismic ovaling coefficient

$$= 12(1-\nu_m)/(2F+5-6\nu_m) \quad (9\text{-}8)$$

The seismic ovaling coefficient curves plotted as a function of F and ν_m are presented in Figure 9-3.

The resulting maximum thrust (hoop) force (T_{max}) and the maximum bending moment (M_{max}) in the lining can be derived as follows:

$$T_{max} = \{(1/6)k_1[E_m/(1+\nu_m)]R\gamma_{max}\}(\text{full slip}) \quad (9\text{-}9)$$

$$M_{max} = \{(1/6)k_1[E_m/(1+\nu_m)]R^2\gamma_{max}\}$$

$$= RT_{max}(\text{full slip}) \quad (9\text{-}10)$$

It should be noted that the solutions provided here are based on the full-slip interface assumption (which allows normal stresses, that is, without normal separation, but no tangential shear force). According to previous investigations, during an earthquake, slip at interface is a possibility only for a conduit in soft soils, or when the seismic loading intensity is very high. In most cases, the condition at the interface is between full-slip and no-slip.

In computing the forces and deformations in the lining, it is prudent to investigate both cases, and the more critical one should be used in design. The full-slip condition gives more conservative results in terms of maximum bending moment (M_{max}) and lining deflections (ΔD_{EQ}). This conservatism is desirable to offset the potential underestimation (about 15 percent) of lining forces resulting from the use of a pseudo-static

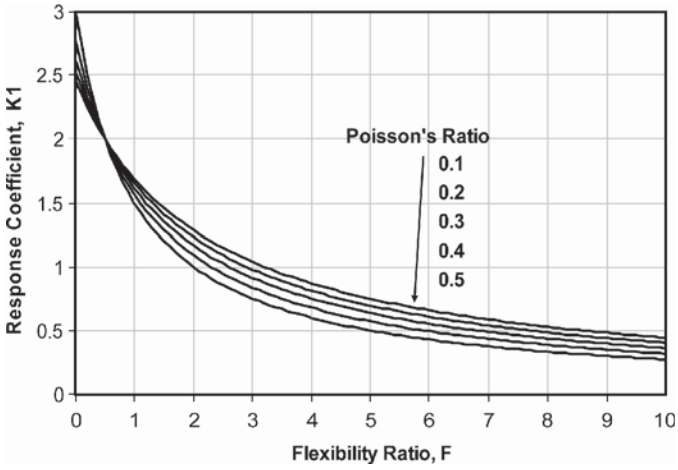

Figure 9-3. Seismic ovaling coefficient, K1.

model in deriving these close-form solutions in lieu of the dynamic loading condition (that is, some dynamic amplification effect). Therefore, the solutions derived based on the full-slip assumption should be used in evaluating the moment (Equation 9-10) and deflection (Equation 9-7) response of a circular conduit (that is, culvert/pipe in this study).

The maximum thrust/hoop force (T_{max}) calculated by Equation (9-9), however, may be significantly underestimated under the seismic simple shear condition and may lead to unsafe results, particularly for thin-wall conduit (flexible culverts and pipes) where buckling potential is the key potential failure mode. It is recommended that the no-slip interface assumption be used in assessing the lining thrust response. The resulting expression, after modifications based on Hoeg's work (Schwartz and Einstein, 1980), is:

$$T_{max} = \{k_2 [E_m / 2(1+\nu_m)] R\gamma_{max}\} \text{no-slip} \qquad (9\text{-}11)$$

Where the thrust/hoop force response coefficient k_2 is defined as:

$$k_2 = 1 + \{F[(1-2\nu_m) - (1-2\nu_m)C] - \tfrac{1}{2}(1-2\nu_m)^2 C + 2\} / \{F[(3-2\nu_m) + (1-2\nu_m)C] + C[5/2 - 8\nu_m + 6\nu_m^2] + 6 - 8\nu_m\} \qquad (9\text{-}12)$$

A review of Equation (9-11) and the expression of k_2 suggests that the maximum lining thrust/hoop force response is a function of compressibility ratio, flexibility ratio, and Poisson's Ratio. Figures 9-4 through 9-6 graphically describe their interrelationships. As the plots show:

- The seismically induced thrust/hoop force increases with decreasing compressibility ratio and decreasing flexibility

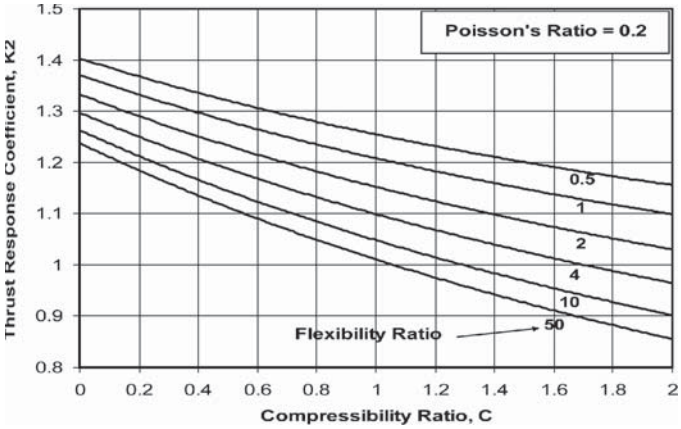

Figure 9-4. Seismic thrust/hoop force response coefficient, k_2 (no-slip interface; soil Poisson's ratio = 0.2).

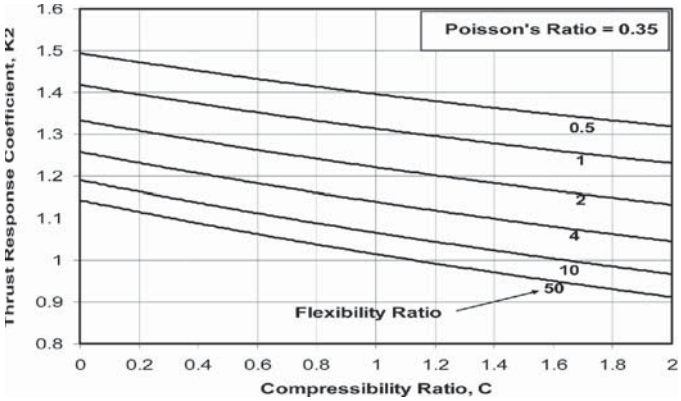

Figure 9-5. Seismic thrust/hoop force response coefficient, k_2 (no-slip interface; soil Poisson's ratio = 0.35).

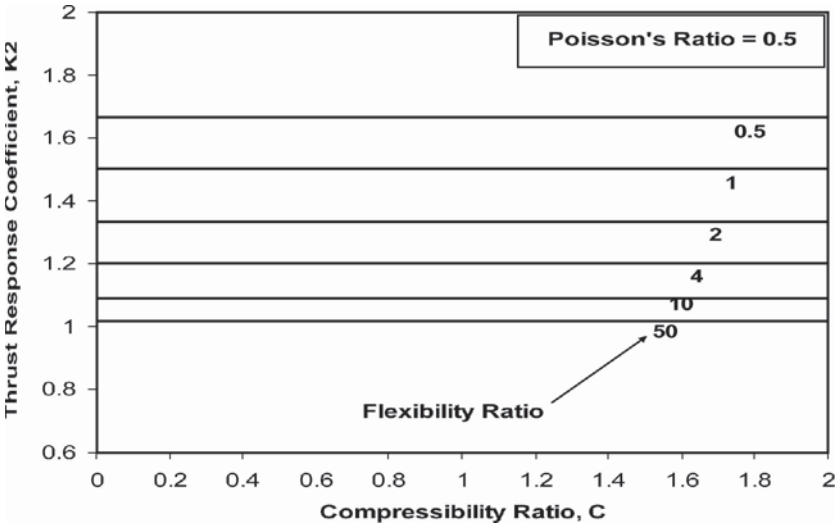

Figure 9-6 Seismic thrust/hoop force response coefficient, k_2 (no-slip interface; soil Poisson's ratio = 0.5).

ratio when the Poisson's ratio value of the surrounding ground is less than 0.5.
- When the Poisson's ratio approaches 0.5 (for example, for saturated undrained clay), the thrust response of the lining is essentially independent of the compressibility ratio.

The theoretical solutions and their applicability to typical culvert and pipeline structures is further verified for reasonableness by numerical analysis presented in the next section.

9.5.2 Racking of Rectangular Conduits

Racking deformations are defined as the differential sideways movements between the top and bottom elevations of rectangular structures, shown as "Δ_s" in Figure 9-7. The resulting structural internal forces or material strains in the lining associated with the seismic racking deformation (Δ_s) can be derived by imposing the differential deformation on the structure in a simple structural frame analysis.

The procedure for determining Δ_s and the corresponding structural internal forces [bending moment (M), thrust (T), and shear (V)], taking into account the soil-structure interaction effects, are presented below (Wang, 1993).

Step 1: Estimate the free-field ground strains γ_{max} (at the structure elevation) caused by the vertically propagating shear waves of the design earthquakes, refer to Equation (9-1) or Equation (9-2) and related discussions presented earlier in Section 9.4.1. Determine the differential free-field relative displacements ($\Delta_{free\text{-}field}$) corresponding to the top and the bottom elevations of the rectangular/box structure by:

$$\Delta_{free\text{-}field} = H * \gamma_{max} \tag{9-13}$$

where H is height of the structure.

Step 2: Determine the racking stiffness (K_s) of the structure from a simple structural frame analysis. For practical purposes, the racking stiffness can be obtained by applying a unit lateral force at the roof level, while the base of the structure is restrained against translation, but with the joints free to rotate. The structural racking stiffness is defined as the ratio of the applied force to the resulting lateral displacement.

Step 3: Derive the flexibility ratio (F_{rec}) of the rectangular structure using the following equation:

$$F_{rec} = (G_m / K_s) * (L/H) \tag{9-14}$$

where

L = width of the structure; and
G_m = average strain-compatible shear modulus of the surrounding ground.

The flexibility ratio is a measure of the relative racking stiffness of the surrounding ground to the racking stiffness of the structure. The derivation of F_{rec} is schematically depicted in Figure 9-8.

Step 4: Based on the flexibility ratio obtained form Step 3 above, determine the racking ratio (R_{rec}) for the structure using Figure 9-5 or the following expression:

$$R_{rec} = 2F_{rec} / (1 + F_{rec}) \tag{9-15}$$

The racking ratio is defined as the ratio of actual racking deformation of the structure to the free-field racking deformation in the ground. The solid triangular data points in Figure 9-9 were data generated by performing a series of dynamic finite element analyses on a number of cases with varying soil and structural properties, structural configurations, and ground motion characteristics. Note, however, these data were generated by using structural parameters representative of typical transportation tunnels during the original development of this design methodology. The validity of this design chart was later verified and adjusted as necessary by performing

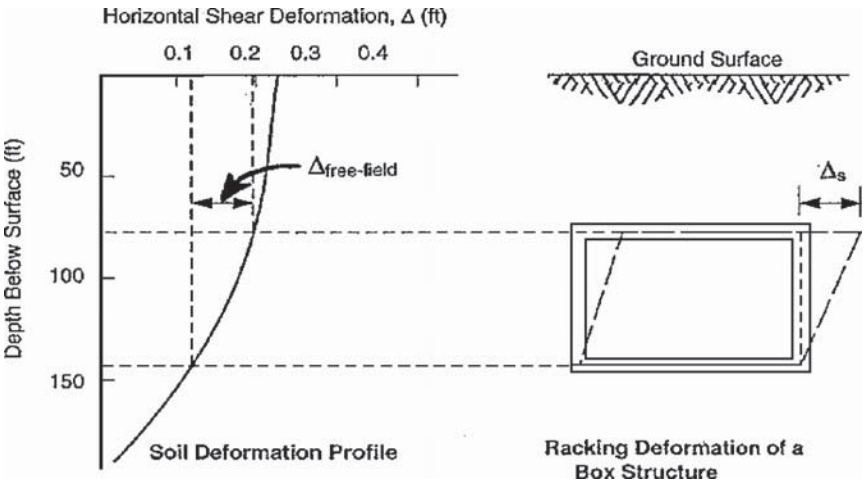

Figure 9-7. Racking deformations of a rectangular conduit.

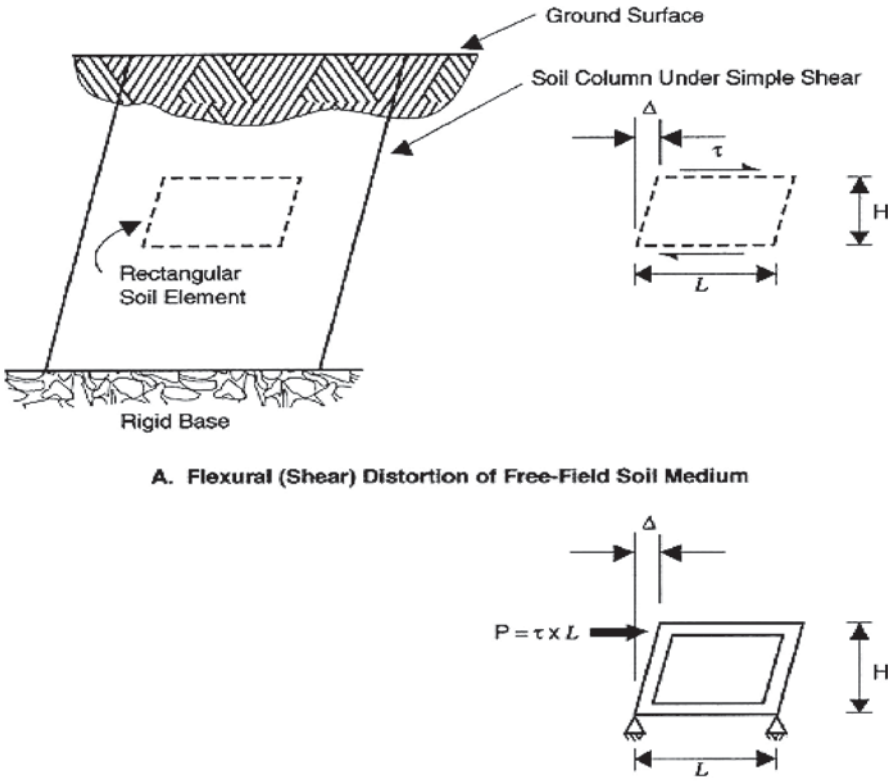

Figure 9-8. Relative stiffness of soil versus rectangular frame.

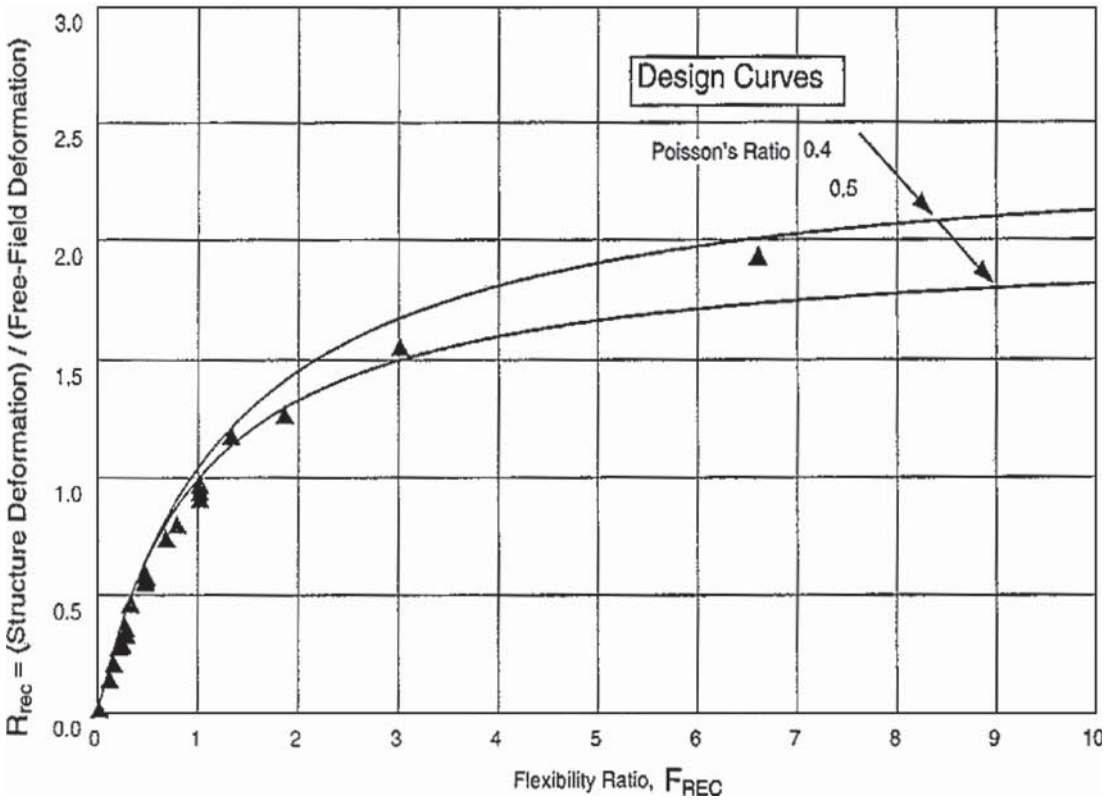

Figure 9-9. Racking ratio between structure and free-field.

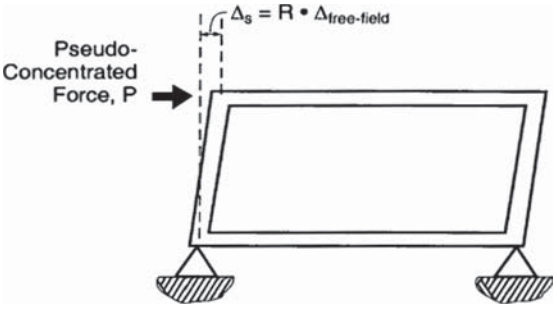

Figure 9-10. Simple frame analysis of racking deformations.

similar numerical analysis using parameters that are representative of highway culvert structures.

As indicated in Figure 9-9, if $F_{rec} = 1$, the structure is considered to have the same racking stiffness as the surrounding ground, and therefore the racking distortion of the structure is about the same as that of the ground in the free field. When F_{rec} is approaching zero, representing a perfectly rigid structure, the structure does not rack regardless of the distortion of the ground in the free field. For $F_{rec} > 1.0$ the structure becomes flexible relative to the ground, and the racking distortion will be magnified in comparison to the shear distortion of the ground in the free field. This magnification effect is not caused by the effect of dynamic amplification. Rather it is attributed to the fact that the ground has a cavity in it as opposed to the free field condition.

Step 5: Determine the racking deformation of the structure (Δ_s) using the following relationship:

$$\Delta_s = R_{rec} * \Delta_{free\text{-}field} \quad (9\text{-}16)$$

Step 6: The seismic demand in terms of internal forces (*M, T,* and *V*) as well as material strains can be calculated by imposing Δ_s upon the structure in a frame analysis as depicted in Figure 9-10.

It should be noted that the methodology developed above was intended to address the incremental effects due to earthquake-induced transient ground deformation only. The seismic effects of transient racking/ovaling deformations on culverts and pipes must be considered additional to the normal load effects from surcharge, pavement, and wheel loads, and then compared to the various failure criteria considered relevant for the type of culvert structure in question.

9.6 Parametric and Verification Analysis

Section 9.5 presents rational ovaling and racking analysis procedures robust enough to treat various types of buried conduit structures. Some simple design charts have also been developed to facilitate the design process. These design charts have been validated through a series of parametric numerical analyses. The applications of these simple design charts to vehicular/transit tunnels also have been successfully applied in real world projects in the past, particularly for deep tunnels surrounded by relatively homogeneous ground.

There are, however, differences between vehicular/transit tunnels and buried culverts and pipes. For example, tunnel structures are generally of large dimensions and typically have much greater structural stiffness than that of culverts and pipe structures. In addition, culverts and pipes are generally buried at shallow depths where the simplified procedure developed for deep tunnels may not necessarily be directly applicable.

To address the issues discussed above, numerical analysis using finite element/finite difference procedures was performed for a wide range of parameters representative of actual culvert properties and geometries (that is, for flexible as well as rigid culverts). In addition, the parametric analysis included the construction condition in terms of burial depth. The analysis, assumptions, and results are presented in the following sections.

9.6.1 Types of Structures and Other Parameters Used in Evaluation

The various parameters studied in this analysis are summarized in Table 9-1.

9.6.2 Model Assumptions and Results

Six sets of parametric analyses were conducted. Assumptions made and results from these analyses are summarized in the following sections.

9.6.2.1 Parametric Analysis—Set 1

Model Assumptions—Set 1. The parametric analysis—Set 1 (the Reference Set) started with a 10-foot diameter corrugated steel pipe (or an equivalent liner plate lining) and a 10-foot diameter precast concrete pipe to represent a flexible and a rigid culvert structure, respectively. Specific properties used for these two different types of culvert structures are presented in Table 9-2.

The soil profile used for Set 1 parametric analysis was assumed to be a homogeneous deep (100-foot thick) soil deposit overlying a rigid base (for example, base rock). The assumed Young's modulus and Poisson's ratio are $E_m = 3{,}000$ psi and $\nu_m = 0.3$, respectively. It is recognized that this is an ideal representation of actual conditions; however, these conditions provide a good basis for making comparison in parametric analysis.

To account for the effects of shallow soil cover, five cases of varying embedment depths were analyzed for each culvert

Table 9-1. Parameters used in the parametric analysis.

Parameters	Descriptions
Structure Types	***FLEXIBLE CULVERTS:*** • Corrugated Aluminum Pipe • Corrugated Steel Pipe • Corrugated HDPE Pipe ***RIGID CULVERTS:*** • Reinforced Concrete Pipe • Reinforced Concrete Box Type
Burial Depths	5d, 3d, 2d, 1d, 0.5d, ("d" represents the diameter of a circular pipe or the height of a box concrete culvert)
Cross Section Geometry Types	• Circular • Square Box • Rectangular Box • Square 3-sided • Rectangular 3-sided
Diameters of Circular Culverts	• 5 feet (Medium Diameter) • 10 feet (Large Diameter)
Wall Stiffness of Circular Culverts	***FLEXIBLE CULVERTS:*** • I=0.00007256 ft^4/ft, E= 2.9E+07 psi (Steel) • I=0.00001168 ft^4/ft, E= 1.0E+07 psi (Aluminum) • I=0.0005787 ft^4/ft, E= 1.1E+05 psi (HDPE)
Size Dimensions of Box Culverts	• 10 feet x 10 feet: Square Box and Square 3-sided • 10 feet x 20 feet: Rectangular Box and Rectangular 3-sided
Wall Stiffness of Box Culverts	***RIGID CULVERTS:*** • I=0.025 ft^4/ft, t=0.67 ft, E= 4.0E+06 psi (Concrete) • I=0.2 ft^4/ft, t=1.33 ft, E= 4.0E+06 psi (Concrete)
Properties of Surrounding Ground*	• E=3,000 psi (Firm Ground) • E=7,500 psi (Very Stiff Ground) • Total Unit Weight = 120 psf

* Note: The Young's Modulus values used in this study are for parametric analysis purposes only.

Table 9-2. Parametric Analysis Set 1—culvert lining properties (Reference Set).

Culvert Properties	Rigid Culvert (Concrete Pipe)	Flexible Culvert (Corrugated Steel Pipe)
Culvert Diameter, ft	10	10
Young's Modulus, $E/(1-\nu^2)$, used in 2-D Plane Strain Condition, psi	4.0E+06	2.9E+07
Moment of Inertia I, ft^4/ft	0.025 ft^4/ft	0.00007256 ft^4/ft (=1.505 in^4/ft)
Sectional Area A, ft^2 per ft	0.67	0.02
EI (lb-ft^2 per ft)	1.44E+07	3.03E+05
AE (lb per ft)	3.86E+08	8.35E+07
Poisson's Ratio	0.3	0.3

Note: Ground condition (firm ground with E_m = 3000 psi, ν_m = 0.3).

Table 9-3. Analyses performed for variable embedment depths.

Cases Analyzed	Soil Cover H (feet)	Culvert Diameter d (feet)	Embedment Depth Ratio, H/d
Case 1	50	10	5
Case 2	30	10	3
Case 3	20	10	2
Case 4	10	10	1
Case 5	5	10	0.5
Case 6	2	10	0.2

type (that is, the flexible type and the rigid type). The six cases of embedment depths are listed in Table 9-3.

Figures 9-11 through 9-15 show the finite difference meshes (using computer program FLAC) used for the parametric analysis accounting for the variable culvert embedment depths. Figure 9-16 graphically defines the "Embedment Depth Ratio" cited in Table 9-3. Figure 9-17 shows the culvert lining modeled as continuous beam elements in the finite difference, soil-structural interaction analysis.

The entire soil-structure system was subjected to an artificially applied pseudo-horizontal acceleration of 0.3g (acceleration of gravity), simulating earthquake-induced vertically propagating shear waves. As a result, lateral shear displacement in the soil overburden will occur. A simple, uniform pseudo acceleration and a simple, uniform soil profile (with a uniform soil stiffness modulus) were assumed for simplicity and are desirable in parametric analysis. Figure 9-18 presents the resulting lateral soil displacement profile under lateral acceleration of 0.3g.

Results of Analysis—Set 1. Figures 9-19 and 9-20 show examples of culvert lining response in terms of lining thrust/hoop forces and bending moments, respectively. Examples presented in Figures 9-19 and 9-20 are for the flexible culvert under the Case 1 conditions (that is, with a soil cover of 50 feet deep). As indicated, the maximum response (that is, the most vulnerable locations) occurs at the knee-and-shoulder locations around the lining, consistent with the generally observed damage/damage mechanism for buried pipes/culverts (as well as circular tunnels) during major earthquakes in the past (refer to the mechanism sketch depicted in Figure 9-2).

Using the lining information presented in Table 9-2 and the soil properties of the surrounding ground (that is, E_m = 3,000 psi, $\nu_m = 0.3$), the compressibility ratio (C) and flexibility ratio (F) for the two culverts were calculated using Equation (9-5) and Equation (9-6), respectively. Their values are presented in Table 9-4. The results of the analysis in terms of

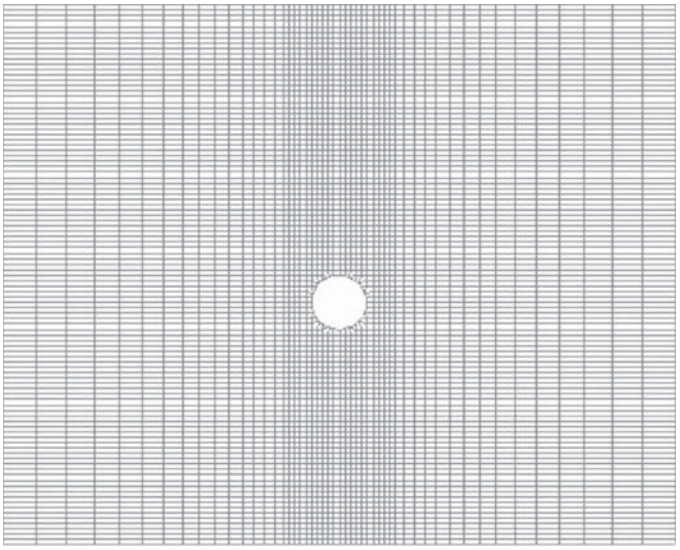

Figure 9-11. Case 1 finite difference mesh (soil cover = 50 feet).

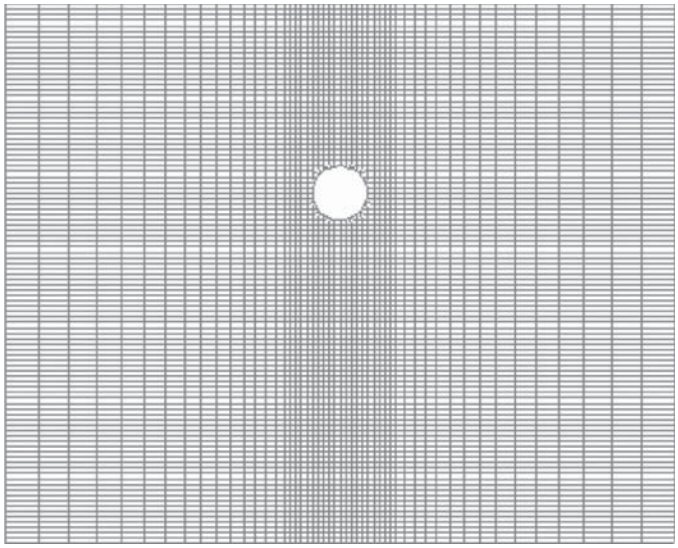

Figure 9-12. Case 2 finite difference mesh (soil cover = 30 feet).

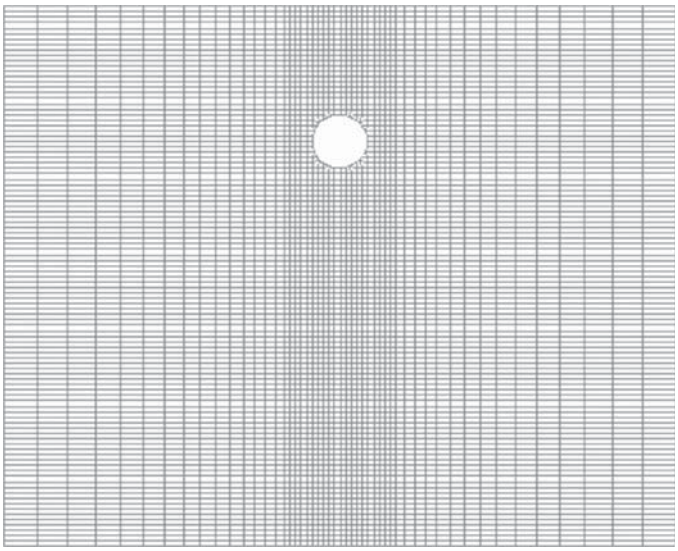

Figure 9-13. Case 3 finite difference mesh (soil cover = 20 feet).

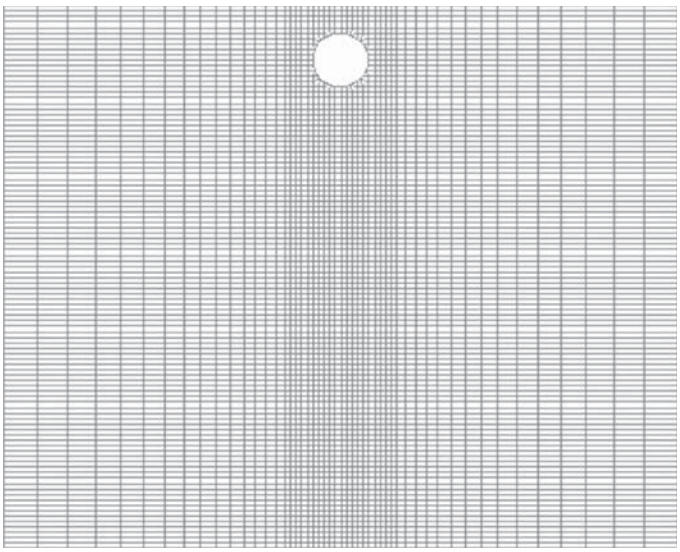

Figure 9-15. Case 5 finite difference mesh (soil cover = 5 feet).

lining deformations (diameter changes) are presented in Tables 9-5 and 9-6.

From these analyses the following observations were made:

- Flexible culverts experience greater deformation than the ground deformation in the free-field for both full-slip and no-slip cases.
- Rigid culverts experience less deformation than the ground deformation in the free-field for both full-slip and no-slip cases.
- The full-slip condition gives more conservative values of lining deflections (ΔD_{EQ}) than the nonslip condition by about 15 percent to 20 percent. This result is consistent with previous studies as discussed in Section 9.5.1.

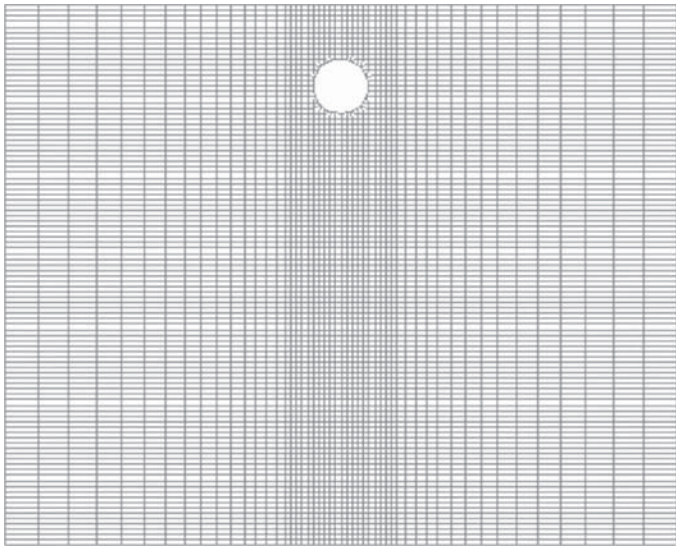

Figure 9-14. Case 4 finite difference mesh (soil cover = 10 feet).

The data contained in Table 9-6 is graphically presented in Figure 9-21. As seen, the flexible culvert deforms significantly more than the free field because its flexibility ratio ($F = 22.6$) is significantly greater than 1.0, suggesting the ground is much stiffer than the lining. For the rigid culvert with $F = 0.482 < 1.0$, the lining is stiffer than the ground and therefore deforms less than the free-field.

Figure 9-22 shows the effects of culvert embedment depth on the lining deformations, expressed by the ratios of the lining to free-field deformation. It can be seen that the ratios of the lining to free-field deformation remained almost unchanged for an embedment ratio of 1.0 or greater. When the embedment

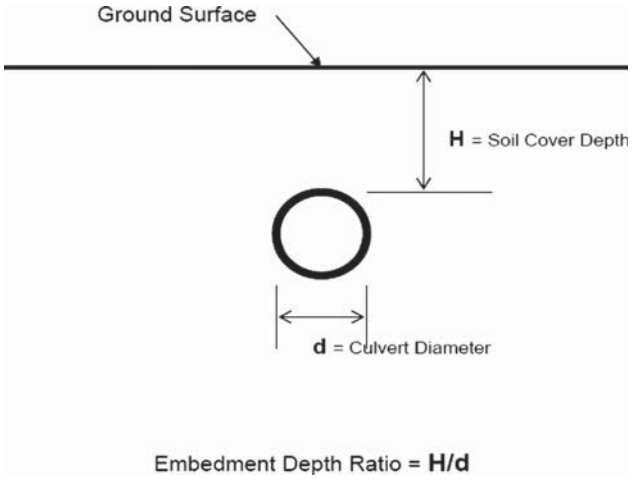

Figure 9-16. Definition of embedment depth ratio.

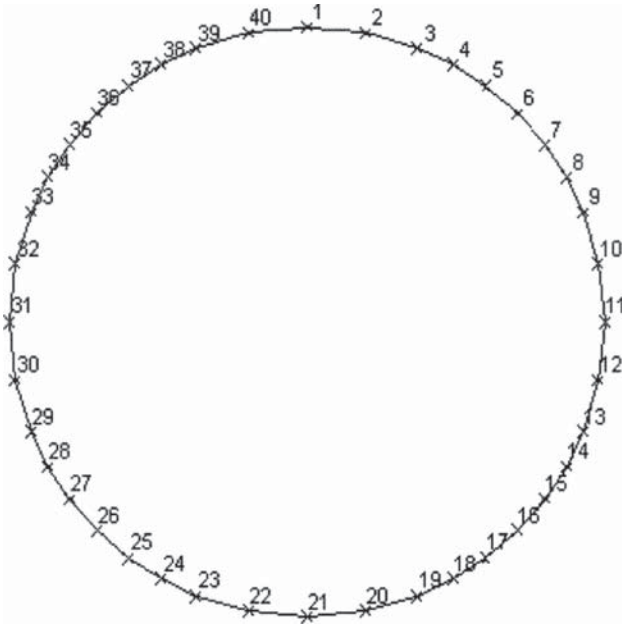

Figure 9-17. Culvert beam element number.

ratio is less than 1.0, the ratio of the actual culvert diameter change to the free-field deformation decreases gradually.

The culvert embedment depth, however, showed some effects on the thrust/hoop force and bending response of the lining, as indicated in Figures 9-23 and 9-24. The embedment effect on the thrust response is more obvious for the rigid culvert than for the flexible culvert. The thrust ratio presented in Figure 9-23 is defined as the maximum lining thrust obtained from the finite difference analysis normalized to that derived using the close-form solutions in Equations (9-11) and (9-12) (for the no-slip interface condition). As indicated, the theoretical close-form solution somewhat overestimates the lining thrust/hoop forces when the culvert is buried at shallow depth. For a rigid culvert, the overestimation is no more than 15 percent. For a flexible culvert the overestimation is negligible. The figure also shows that the effect of embedment is negligible when the embedment ratio is greater than about 3 or 4.

The embedment effects on bending response are illustrated in Figure 9-24. Based on the results from the analysis, it appears that the potential for overestimation of bending demand would occur for rigid types of culvert structures buried at shallow depths by as much as 30 to 35 percent. Figure 9-24 also suggests that the effects of embedment depth on bending response are insignificant when the embedment depth ratio is greater than about 3.

It should be noted that the main reason for the overestimation in thrust and bending forces is that the maximum free-field ground shearing strain used in calculating the close-form solutions (Equation 9-11 and Equation 9-12) is the maximum shearing strain that occurs at the culvert invert (instead of the average free-field shearing strain within the culvert depth). These results suggest that the maximum free-field ground strain is on the safe side.

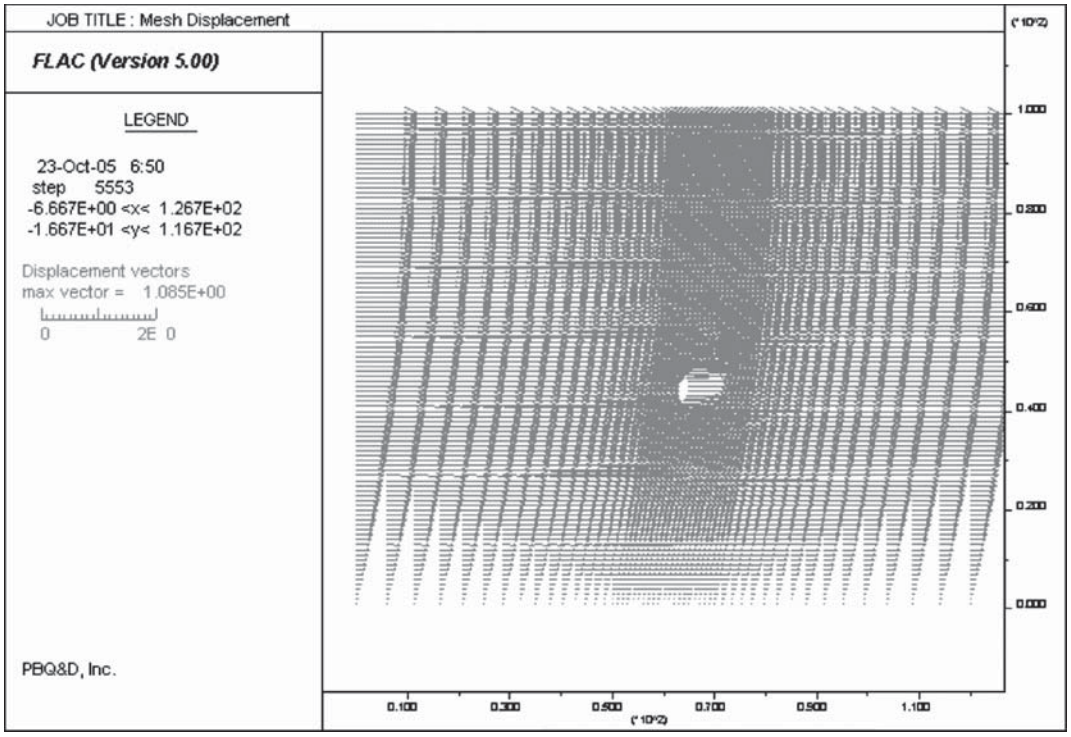

Figure 9-18. Soil deformations subjected to pseudo lateral acceleration of 0.3g.

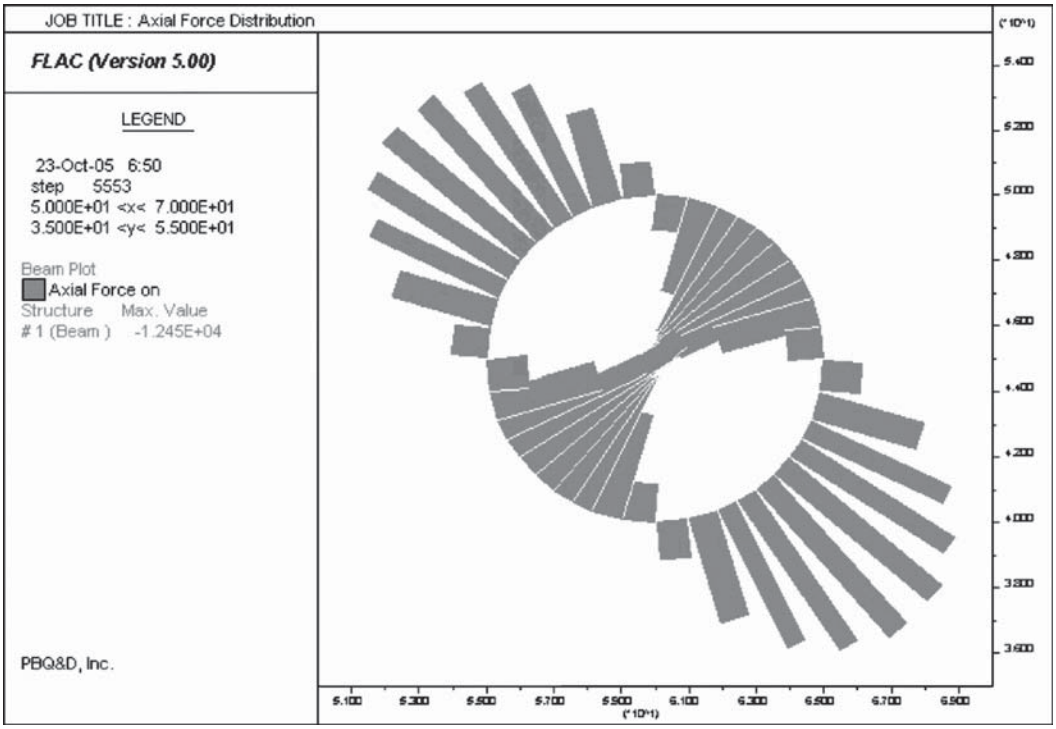

Figure 9-19. Culvert lining thrust/hoop force distribution (for flexible culvert in Set 1, Case 1 geometry).

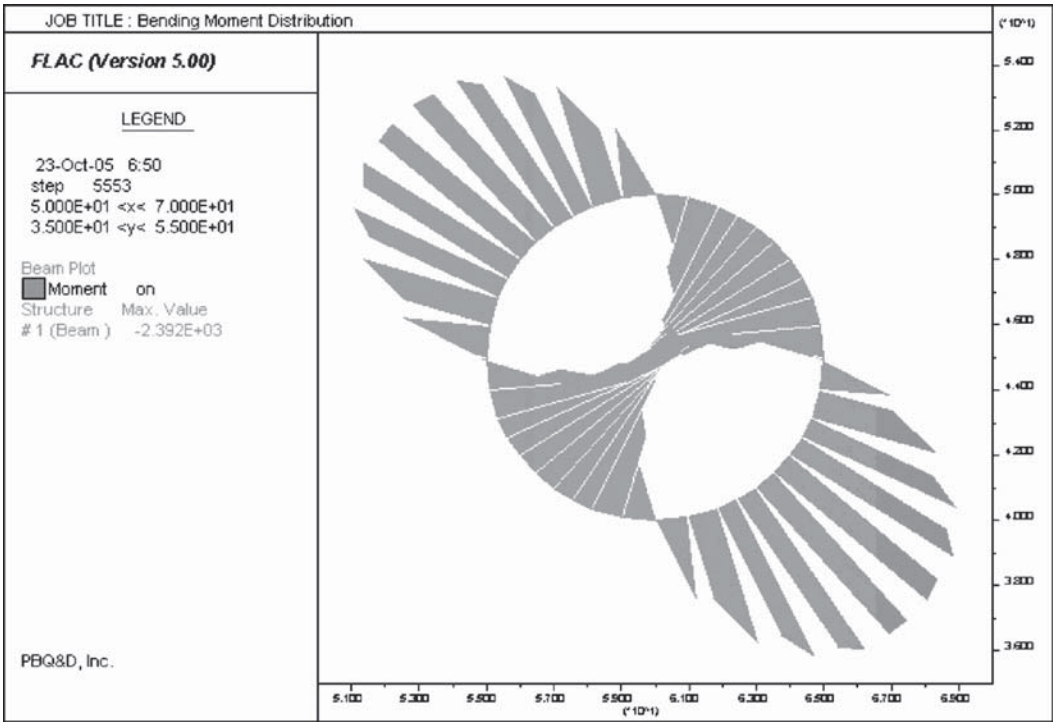

Figure 9-20. Culvert lining bending moment distribution (for flexible culvert in Set 1, Case 1 geometry).

Table 9-4. Culvert lining compressibility and flexibility used in analysis.

Properties	Rigid Culvert (Concrete Pipe)	Flexible Culvert (Corrugated Steel Pipe)
Compressibility Ratio, ***C***	0.011	0.05
Flexibility Ratio, ***F***	0.482	22.6

Table 9-5. Free-field ground strain and diameter change.

Case No. (Embedment Ratio)	Free-Field Maximum Ground Shear Strain (from FLAC Analysis) γ_{max}	Closed-Form Free-Field Ground Diameter Change Using Eq. 9-3 $\Delta D=0.5*D*\gamma max$ (feet)
Case 1 (H/d=5)	0.0129	0.065
Case 2 (H/d=3)	0.0085	0.043
Case 3 (H/d=2)	0.0064	0.032
Case 4 (H/d=1)	0.004	0.02
Case 5 (H/d=0.5)	0.003	0.015
Case 6 (H/d=0.2)	0.0022	0.011

Note: The maximum free-field ground shearing strain is the maximum shearing strain that could occur within the full depth of the culvert (that is, from the crown to the invert). In the pseudo-static FLAC analysis, the maximum ground shearing strains occur at the invert in all cases.

Table 9-6. Culvert diameter change—effect of interface slippage condition.

Case No. (Embedment Ratio)	Culvert Diameter Change (ft) for Full-Slip Interface Using Eq. 9-7	Culvert Diameter Change (ft) for No-Slip Interface Using FLAC Analysis	Diameter Change Ratio for No-Slip to Full-Slip
For Flexible Culvert			
Case 1 (H/d=5)	0.169	0.129	0.77
Case 2 (H/d=3)	0.111	0.082	0.74
Case 3 (H/d=2)	0.084	0.059	0.70
Case 4 (H/d=1)	0.052	0.036	0.68
Case 5 (H/d=0.5)	0.039	0.024	0.62
Case 6 (H/d=0.2)	0.029	0.018	0.62
For Rigid Culvert			
Case 1 (H/d=5)	0.042	0.034	0.80
Case 2 (H/d=3)	0.028	0.021	0.77
Case 3 (H/d=2)	0.021	0.015	0.72
Case 4 (H/d=1)	0.013	0.009	0.67
Case 5 (H/d=0.5)	0.010	0.006	0.57
Case 6 (H/d=0.2)	0.007	0.004	0.51

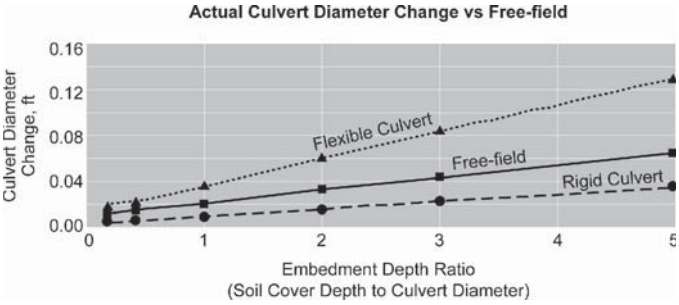

Figure 9-21. Culvert deformations versus free-field deformations.

Additional Parametric Analysis and Results. Additional parametric analyses included (1) different circular culvert/pipe sizes; (2) different culvert/pipe material, such as corrugated aluminum and HDPE pipes; (3) different soil stiffness; (4) square and rectangular shape culverts (constructed with reinforced concrete; (5) 3-sided flat roof rectangular concrete culverts; and (6) different culvert/pipe wall stiffness. These additional analyses were used to further verify that with some modifications, the close-form solutions developed for deep circular bored tunnels and rectangular cut-and-cover tunnels (refer to Section 9.5) also can be used for circular and rectangular culvert structures.

9.6.2.2 Parametric Analysis—Set 2

Model Assumptions—Set 2. Assumptions and parameters used in parametric analysis Set 2 are the same as those used in Set 1 (the Reference Case) except (1) the culvert diameter was reduced from 10 feet to 5 feet; (2) the total soil profile depth has been reduced from 100 feet to 50 feet; and (3) the culvert embedment depth was halved in each respective case to maintain the same embedment ratio (H/d). Because of this reduction in culvert size the resulting compressibility ratio (C) was reduced from 0.011 to 0.005 and the flexibility ratio (F) was reduced from 0.482 to 0.061 for the rigid culvert. Similarly for the flexible culvert, C and F were reduced from 0.05 to 0.025 and from 22.6 to 2.856, respectively (see Table 9-7).

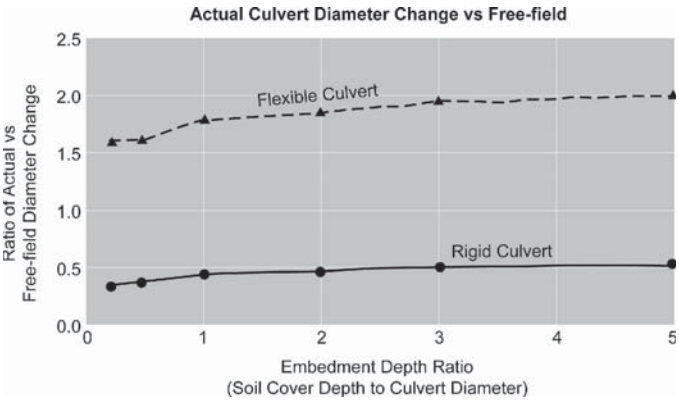

Figure 9-22. Ratios of culvert deformations versus free-field deformations.

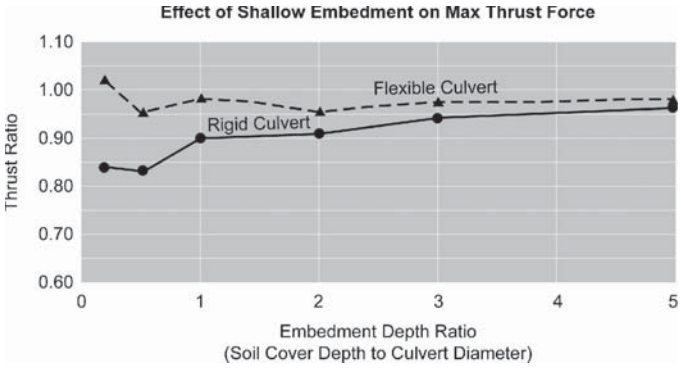

Figure 9-23. Embedment effects on culvert maximum thrust/hoop forces.

Results of Analyses—Set 2. Figures 9-25 through 9-27 present the results of FLAC analysis. Compared to results from Set 1 analysis (refer to Figures 9-22 through 9-24), the Set 2 results indicated that:

- The ratios of the actual culvert deformation to free-field ground deformation were significantly reduced, reflecting the effect of higher culvert lining stiffness because of the reduced culvert diameter.
- The bending and thrust force response of the smaller 5-foot diameter culvert, when normalized to the close-form solutions, show similar trends to that of the larger culvert (10-foot diameter). Based on results in Figure 9-26, when the burial depth is small, the close-form solutions (using the conservative maximum free-field ground strain value at the culvert invert elevation) tend to overestimate the thrust response by up to about 20 percent for the flexible culvert. For the rigid culvert the overestimation is greater than about 30 percent at very shallow burial depth.

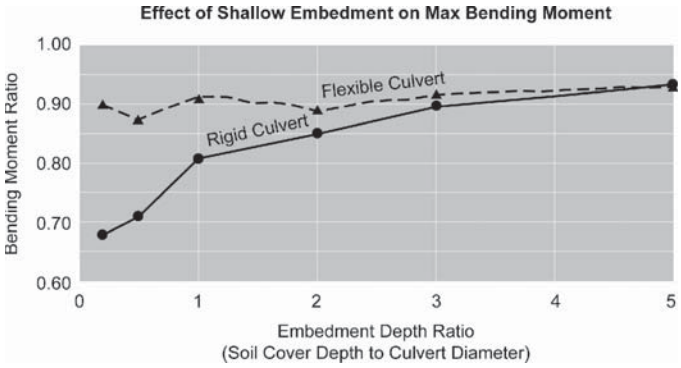

Figure 9-24. Embedment effects on culvert maximum bending moments.

Table 9-7. Parametric analysis set 2—culvert lining properties.

Culvert Properties	Rigid Culvert (Concrete Pipe)	Flexible Culvert (Corrugated Steel Pipe)
Culvert Diameter, ft	5	5
Young's Modulus, $E/(1-\nu^2)$, psi	4.0E+06	2.9E+07
Moment of Inertia, ft^4/ft	0.025	0.00007256
Sectional Area, ft^2 per ft	0.67	0.02
EI ($lb\text{-}ft^2$ per ft)	1.44E+07	3.03E+05
AE (lb, per ft)	3.86E+08	8.35E+07
Poisson's Ratio	0.3	0.3
Compressibility, **C**	0.005	0.025
Flexibility Ratio, **F**	0.061	2.856

Note: Ground condition (firm ground with E_m = 3000 psi, ν_m = 0.3).

The effect of shallow embedment depth on bending shows similar trends to the thrust response (refer to Figure 9-27).

9.6.2.3 Parametric Analysis—Set 3

Model Assumptions—Set 3. In this set of analyses the assumptions and parameters are the same as those used in Set 1 (the Reference Case) except (1) the flexible culvert was changed from corrugated steel pipe to corrugated aluminum pipe (with lower bending and compression stiffness compared to the steel pipe); and (2) the rigid concrete pipe was made even more rigid by increasing its wall thickness from 0.67 feet to 1.33 feet. The resulting compressibility ratio and flexibility ratio, along with other lining properties are presented in Table 9-8.

Results of Analyses—Set 3. Results from the analysis are shown in Figures 9-28 through 9-30. As indicated, the results are following the same trend as shown in results from Sets 1 and 2 analysis, even though a much more flexible culvert and a much more rigid culvert were used in this set of analysis. This suggests that the analytical methodology and procedure previously presented in Section 9.5 provide a robust approach to accounting for the soil-structure interaction effect in evaluating the seismic behavior of culverts with varying characteristics.

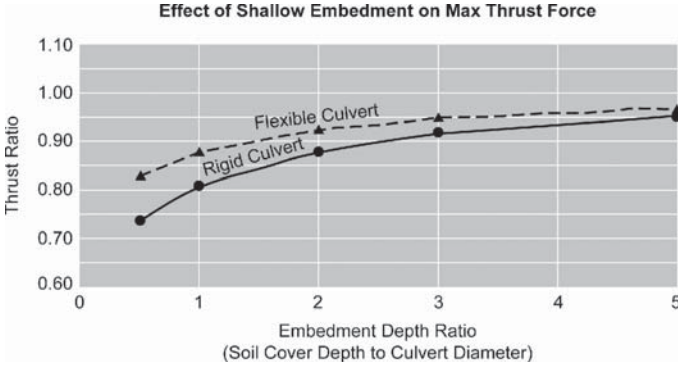

Figure 9-26. Embedment effects on culvert maximum thrust/hoop forces (parametric analysis—Set 2).

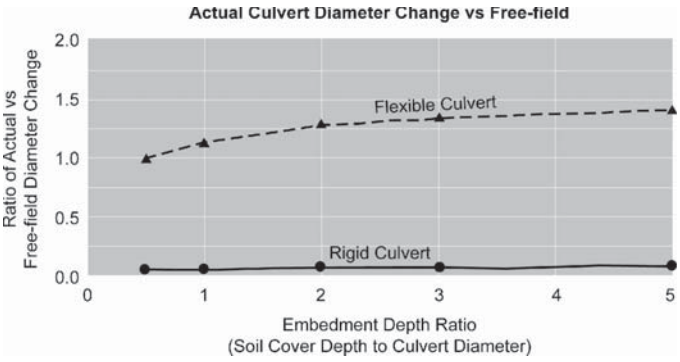

Figure 9-25. Ratios of culvert deformations versus free-field deformations (parametric analysis—Set 2).

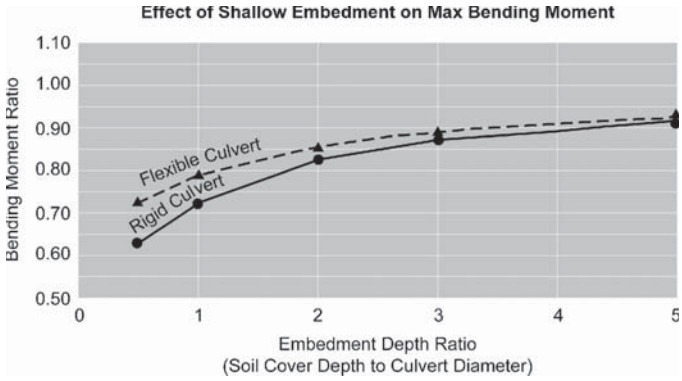

Figure 9-27. Embedment effects on culvert maximum bending moments (parametric analysis—Set 2).

Table 9-8. Parametric analysis set 3—culvert lining properties.

Culvert Properties	Rigid Culvert (Concrete Pipe)	Flexible Culvert Aluminum CMP
Culvert Diameter, ft	10	10
Young's Modulus, $E/(1-\nu^2)$, psi	4.0E+06	1.0E+07
Moment of Inertia, ft^4/ft	0.2	0.00001168
Sectional Area, ft^2 per ft	1.333	0.01125
EI ($lb\text{-}ft^2$ per ft)	1.152E+08	1.682E+04
AE (lb, per ft)	7.678E+08	1.62E+07
Poisson's Ratio	0.3	0.3
Compressibility, **C**	0.005	0.256
Flexibility Ratio, **F**	0.060	411.7

Note: Ground condition (firm ground with E_m = 3,000 psi, ν_m = 0.3).

9.6.2.4 Parametric Analysis—Set 4

Model Assumptions—Set 4. Only one type of lining was analyzed in this set of analysis. The lining modeled in this analysis is a 5-foot diameter corrugated HDPE pipe. The reason for selecting HDPE in this analysis is because polymeric conduits are being used with increasing frequency, and polymers, especially high density polyethylene, are likely to be the material of choice for many drainage applications in the future. The typical properties of the HDPE material are presented in Table 9-9. Young's modulus of 110,000 psi is appropriate for short term loading effects on HDPE pipe. Poisson's ratio of HDPE pipe is estimated to be about 0.45.

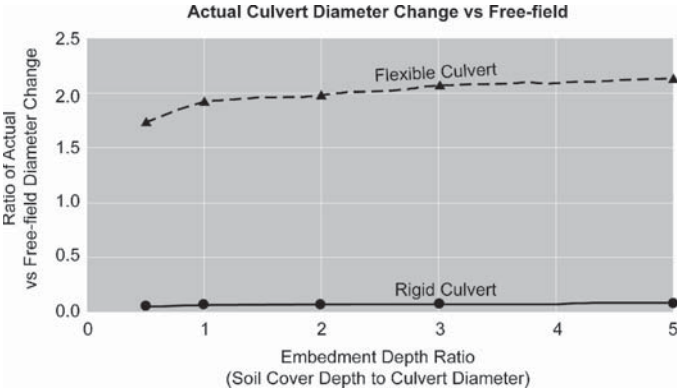

Figure 9-28. Ratios of culvert deformations versus free-field deformations (parametric analysis—Set 3).

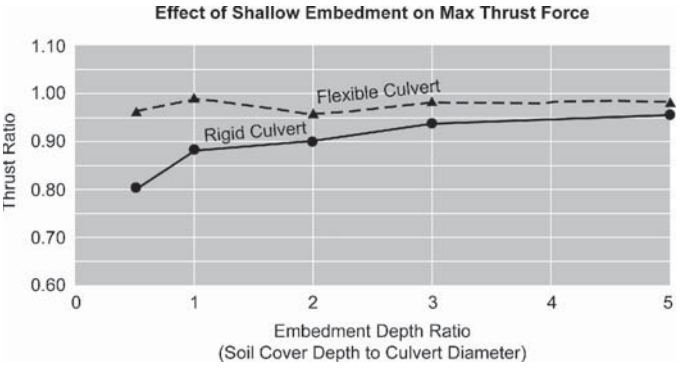

Figure 9-29. Embedment effects on culvert maximum thrust/hoop forces (parametric analysis—Set 3).

Results of Analyses—Set 4. Figures 9-31 through 9-33 present the results of the HDPE culvert analysis. As indicated, the seismic behavior of the HDPE pipe also can be predicted reasonably well using the analytical procedure presented in Section 9-5. Like in other cases, if necessary, some adjustments may be made to correct the overestimation of thrust forces and bending moments when the pipe is buried at a very shallow depth. For conservative design purposes, however, it is recommended that no force reduction be made.

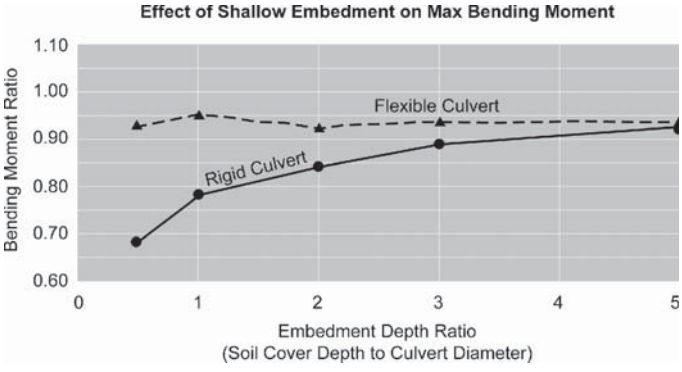

Figure 9-30. Embedment effects on culvert maximum bending moments (parametric analysis—Set 3).

Table 9-9. Parametric analysis set 4—culvert lining properties.

Culvert Properties	Flexible Culvert (Corrugated HDPE)
Culvert Diameter, ft	5
Young's Modulus, $E/(1-\nu^2)$, psi	1.1E+05
Moment of Inertia, ft^4 per ft	0.0005787
Sectional Area, ft^2 per ft	0.0448
EI ($lb\text{-}ft^2$ per ft)	9.17E+03
AE (lb, per ft)	7.10E+05
Poisson's Ratio	0.45
Compressibility, C	2.927
Flexibility Ratio, F	94.424

Note: Ground condition (firm ground with E_m = 3,000 psi, ν_m = 0.3).

9.6.2.5 Parametric Analysis—Set 5

Model Assumptions—Set 5. In this set of parametric analysis, the culvert lining properties used are identical to those assumed in Set 1 (the Reference Case, refer to Tables 9-2 and 9-10). However, the soil stiffness has been increased from E_m=3,000 psi (firm ground) to E_m=7,500 psi (very stiff ground). The entire soil profile was assumed to be homogeneous. The soil overburden thickness (100-foot thick) and other conditions are the same as those in Set 1.

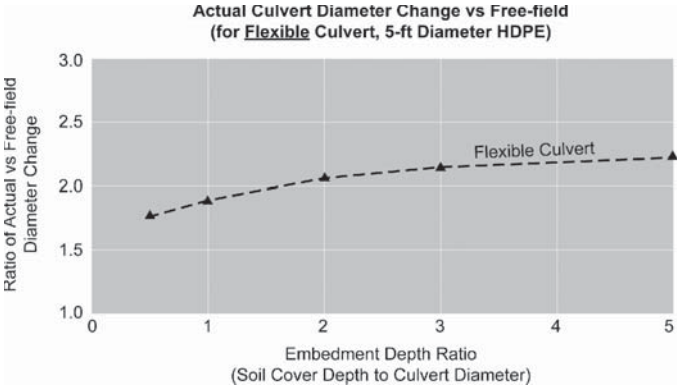

Figure 9-31. Ratios of culvert deformations versus free-field deformations (parametric analysis—Set 4).

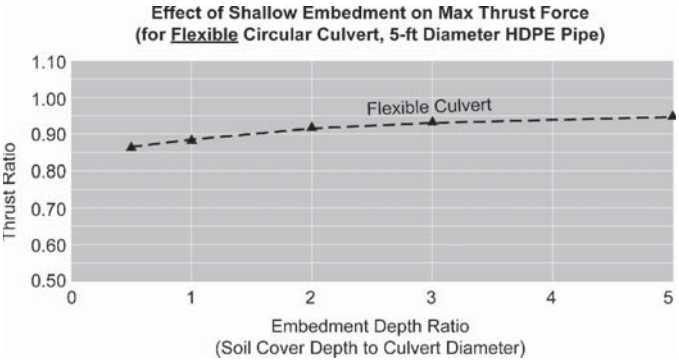

Figure 9-32. Embedment effects on culvert maximum thrust/hoop forces (parametric analysis—Set 4).

Results of Analyses—Set 5. The calculated compressibility and flexibility ratios also are included in Table 9-10. Because of the increased ground stiffness, the flexibility ratio for the rigid culvert was computed to be 1.217, slightly greater than 1.0. This suggests that the ovaling stiffness of the ground is only slightly greater than the ovaling stiffness of the rigid culvert. Based on the discussions presented in Section 9-4, when the flexibility ratio is close to 1.0, the ovaling deformation of the lining should be about the same as that of the surrounding ground.

Results from the FLAC analysis in Figure 9-34 show that for the rigid culvert the ratio of the culvert deformation to the ground deformation is very close to 1.0, verifying the validity

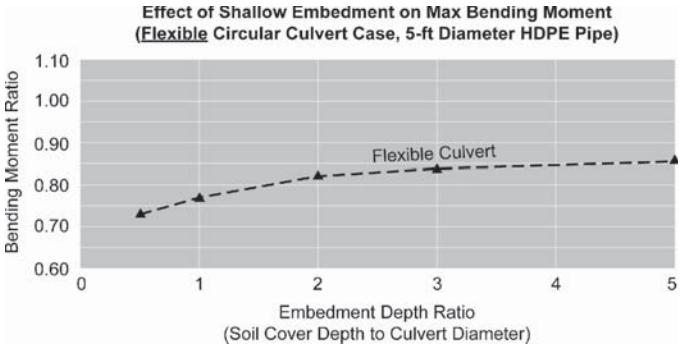

Figure 9-33. Embedment effects on culvert maximum bending moments (parametric analysis—Set 4).

Table 9-10. Parametric analysis set 5—very stiff ground condition.

Culvert Properties	Rigid Culvert (Concrete Pipe)	Flexible Culvert (Corrugated Steel Pipe)
Culvert Diameter, ft	10	10
Young's Modulus, E/(1-ν^2), psi	4.0E+06	2.9E+07
Moment of Inertia, ft^4/ft	0.025	0.00007256
Sectional Area, ft^2 per ft	0.67	0.02
EI (lb-ft^2 per ft)	1.44E+07	3.03E+05
AE (lb, per ft)	3.86E+08	8.35E+07
Poisson's Ratio	0.3	0.3
Compressibility, C	0.027	0.127
Flexibility Ratio, F	1.217	57.122

Note: ground condition (very stiff ground with E_m = 7,500 psi, ν_m = 0.3).

of the analytical solutions discussed in Section 9-4. Figures 9-35 and 9-36 display similar results (normalized thrust forces and bending moments) presented in other parametric analysis cases even though the ground stiffness was significantly changed (from E_m = 3,000 psi to E_m = 7,500 psi).

9.6.2.6 Parametric Analysis—Set 6

Model Assumptions—Set 6. The parametric analyses discussed thus far focused on the ovaling behavior of culverts. In this section, a series of parametric analysis is performed for the rectangular and square shaped culverts. These culverts are assumed to be constructed with reinforced concrete. The sizes and geometry of these concrete box culverts are graphically presented in Figure 9-37.

The concrete lining was modeled as continuous beam elements in the finite difference, soil-structural interaction analysis having the following properties:

- Young's Modulus, $E/(1-\nu^2)$ = 4.0E+06 psi
- Poisson's Ratio, ν = 0.3
- Thickness, t = 0.67 ft
- Moment of Inertia, I = 0.025 ft^4/ft

Five sets of parametric analyses have been performed considering the following combinations of variables: (1) culvert sizes; (2) culvert sectional configurations; (3) soil stiffness; and (4) culvert burial depths. Table 9-11 below summarize specific parameters used in each case of analysis.

The main purpose of this parametric analysis is to verify that the rectangular flexibility ratio (F_{rec}) developed in Equation (9-14), $F_{rec} = (G_m / K_s) * (w/h)$, is a proper representation of the relative stiffness between the culvert's racking stiffness and the ground's racking stiffness. By using F_{rec}, it is possible to accurately estimate the actual racking deformation of the culvert as long as the free-field ground deformation ($\Delta_{free\text{-}field}$) is known.

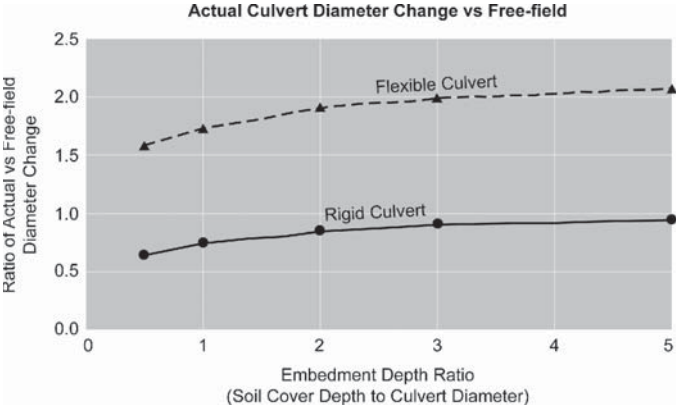

Figure 9-34. Ratios of culvert deformations versus free-field deformations (parametric analysis—Set 5).

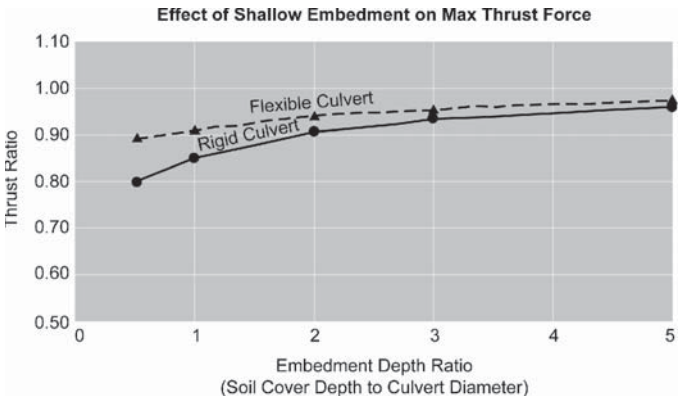

Figure 9-35. Embedment effects on culvert maximum thrust/hoop forces (parametric analysis—Set 5).

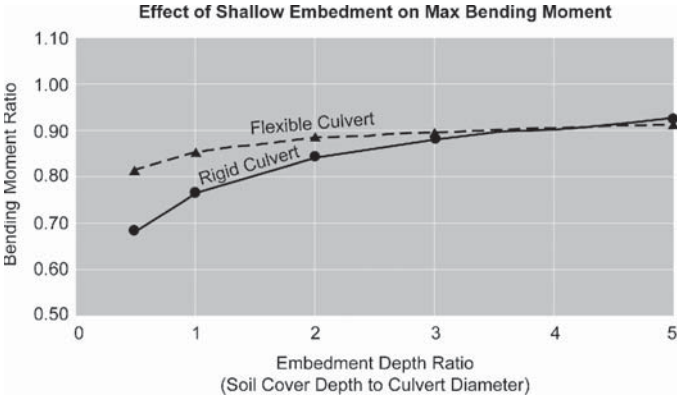

Figure 9-36. Embedment effects on culvert maximum bending moments (parametric analysis—Set 5).

The verification procedure is:

1. Determine the free-field racking deformation of the ground ($\Delta_{free\text{-}field}$). This was achieved in this analysis by applying a pseudo-horizontal acceleration in the entire free-field soil deposit in the FLAC analysis. Note that at this time the FLAC model is a free-field soil deposit model that does not contain the culvert structure in it. The resulting free-field racking deformations then can be directly read out from the output of the FLAC analysis.
2. Given $\Delta_{free\text{-}field}$, the racking deformation of the culvert can be manually estimated by using the simple relationship presented in Equation (9-16), $\Delta_s = R_{rec} * \Delta_{free\text{-}field}$.
3. The manually estimated racking deformation derived above then is compared to the actual racking deformation of the culvert from the soil-structure interaction FLAC analysis. In this FLAC analysis, the culvert structure is included in the soil deposit model and subject to the same pseudo-horizontal acceleration used in the free-field FLAC analysis mentioned in Step 1 above. Note that since Δ_s is related to $\Delta_{free\text{-}field}$ directly through R_{rec}, the racking ratio, the comparison therefore also can be made between the manually calculated $R_{rec} = [2F_{rec}/(1+F_{rec})]$, and R_{rec} computed from the FLAC analysis.
4. If the manually estimated racking deformations (or the R_{rec} values) are comparable to those computed by the soil-structure interaction FLAC analysis, then the simplified procedure developed in Section 9.5.2 can be considered to be validated.

Results of Analyses—Set 6. Based on the results from the FLAC analysis (from both the free-field analysis run and the soil-structure interaction analysis run), the free-field racking deformations and the actual culvert racking deformations were obtained. Ratios of the culvert to free-field racking deformations are plotted for all five cases (for five different burial depths in each case) in Figures 9-38 through 9-42. Based on the data presented in these figures, it appears that burial depth does not have significant influence on the racking deformation ratio for the rectangular type of rigid culverts.

In the meantime, the structural racking stiffness (K_s) of the culvert structure in each case was determined by a simple frame analysis based on the properties of the culvert structure; the results are presented in Table 9-12. Then the rectangular flexibility ratio (F_{rec}) was calculated using Equation (9-14), and results also presented in Table 9-12 for each case.

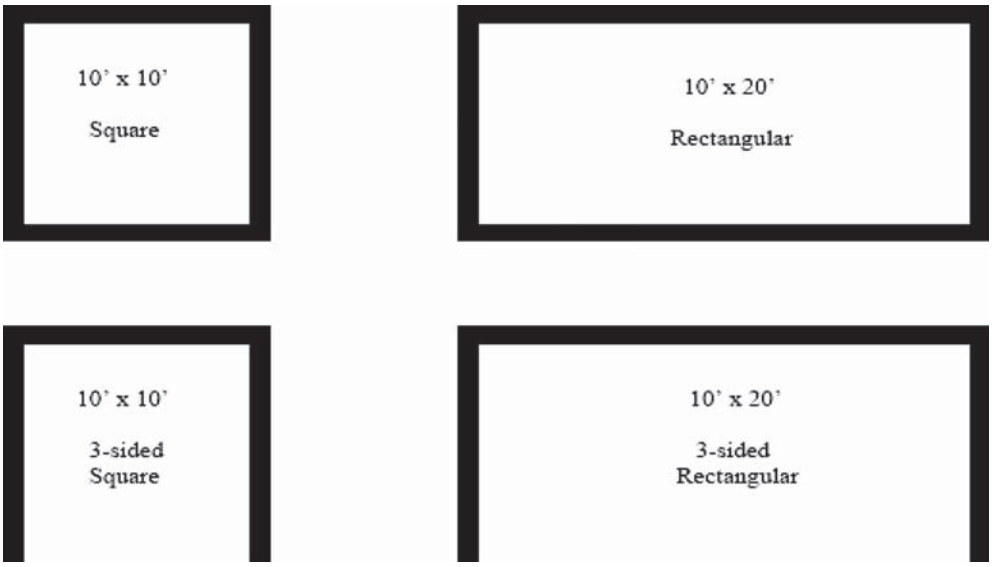

Figure 9-37. Various concrete box culvert sectional shapes and sizes used in the parametric analysis—Set 6.

Table 9-11. Soil and structure parameters used in the analysis.

	Structural Configurations and Soil Properties
Case 1	10' x 10' Square Box, in Firm Ground (E_m = 3,000 psi, ν_m = 0.3)
Case 2	10' x 10' Square Box, in Very Stiff Ground (E_m = 7,500 psi, ν_m = 0.3)
Case 3	10' x 20' Rectangular Box, in Firm Ground (E_m = 3,000 psi, ν_m = 0.3)
Case 4	10' x 10' Square 3-Sided, in Very Stiff Ground (E_m = 7,500 psi, ν_m = 0.3)
Case 5	10' x 20' Rectangular 3-Sided, in Very Stiff Ground (E_m = 7,500 psi, ν_m = 0.3)

Note: For each case, the effects of culvert embedment depth (of 50 feet, 30 feet, 20 feet, 10 feet, and 5 feet, measured from ground surface to top of the culvert roof) were studied.

The results show that for Case 1 the relative racking stiffness of the ground to the structure is about 1.0, suggesting that the structure would rack in conformance with the free-field racking deformation in the ground. The results presented in Figure 9-38 show clearly that the FLAC calculated racking deformations are about the same as the free-field deformations, validating the definition of flexibility ratio (F_{rec}) derived in Section 9-5. For Cases 2 through 5, the flexibility ratios are all greater than 1.0, suggesting that the structure would deform more than the ground in the free-field, and results shown in Figures 9-39 through 9-42 support this theory.

Figure 9-43 plots the racking ratio as a function of the flexibility ratio based on the results obtained from the FLAC analysis and then compares them with the recommended

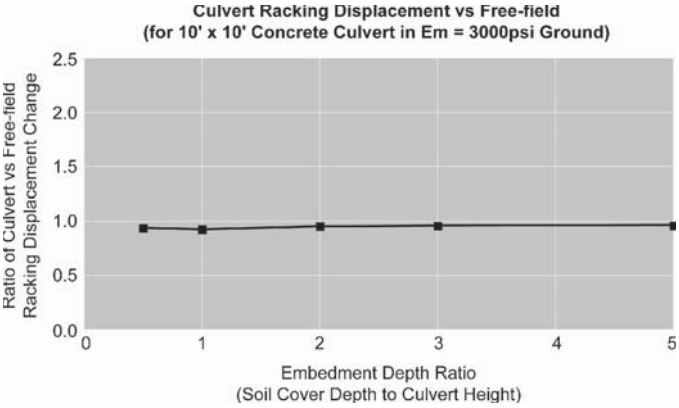

Figure 9-38. Racking ratios from FLAC analysis—Case 1.

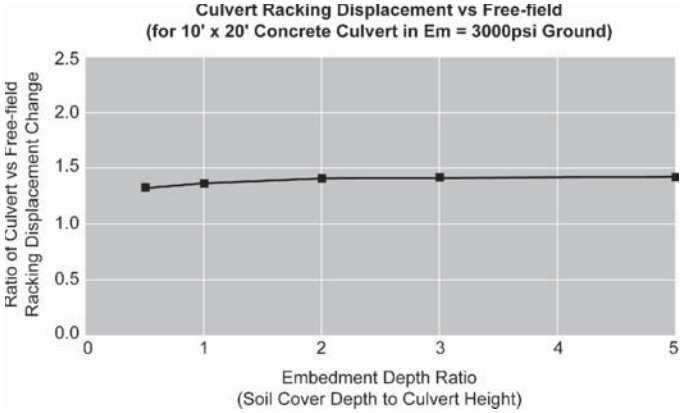

Figure 9-40. Racking ratios from FLAC analysis—Case 3.

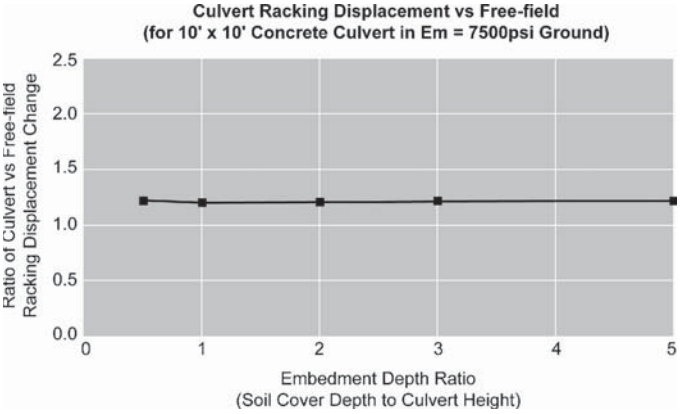

Figure 9-39. Racking ratios from FLAC analysis—Case 2.

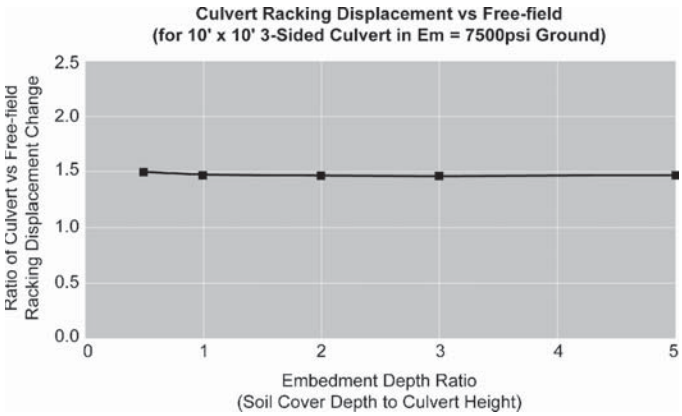

Figure 9-41. Racking ratios from FLAC analysis—Case 4.

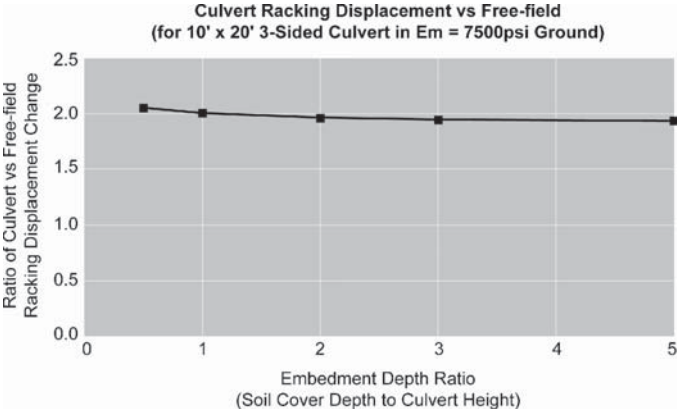

Figure 9-42. Racking ratios from FLAC analysis—Case 5.

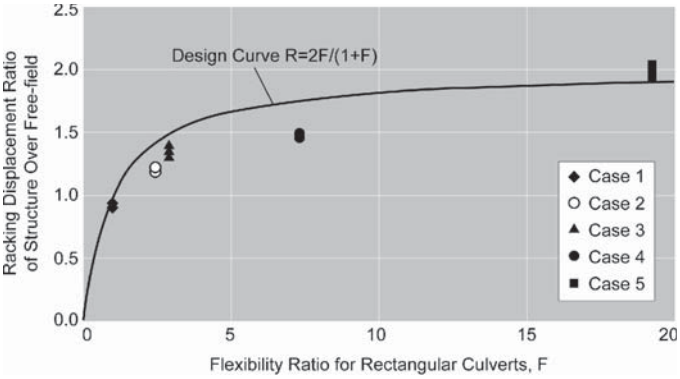

Figure 9-43. Recommended design racking curve.

design curve expressed by Equation (9-15), $R_{rec} = [2F_{rec}/(1+F_{rec})]$. The comparison shows reasonably good agreement between the recommended simple design solution charts and the results obtained from the numerical analyses.

9.7 Conclusions and Recommendations

Simplified seismic analysis procedures for evaluating culvert and pipe structures subjected to transient ground deformations induced by ground shaking proposed in this chapter. The analysis procedures use a deformation-based methodology that can provide a more reliable prediction of culvert/pipe performance. The approach focuses on the deformations in the transverse section of the structure (that is, ovaling/racking deformations) instead of the longitudinal axial/curvature deformations, due primarily to the general condition that typical culvert structures for transportation applications are of limited length, and as such it is in general unlikely to develop significant transient axial/curvature deformations along the longitudinal direction of the culvert structures.

Based on the results of a series of parametric soil-structure interaction analysis taking various factors into consideration, the following conclusions and recommendations are provided:

- For circular culverts and pipes subject to ovaling deformations, the simplified close-form solutions and procedure presented in Section 9.5.1 should provide reliable results under general conditions, with the following notes:
  - In selecting the design transient ground deformation parameter for a culvert or pipe constructed at a significant depth below the ground surface, PGV is a better parameter in the deformation-based procedure than the site-adjusted PGA, because PGV can be used directly for estimating the shearing strain in the ground (Equation 9-1). Discussions and recommendations on PGV values developed in Chapter 5 for retaining walls, slopes, and embankment should be used in evaluating the maximum free-field shearing strain in Equation (9-1). For culverts and pipes buried at relatively shallow depths (that is, within 50 feet of the ground surface), it is more reasonable to estimate the free-field shearing strain in the ground using the earthquake-induced shearing stress divided by the stiffness of the surrounding ground (Equation 9-2).
  - If a more accurate prediction of the maximum free-field shearing strain is required, a more refined free-field site response analysis (for example, using the SHAKE computer program) should be performed.
  - In using the simplified approach, the no-slip interface assumption should be used in calculating the maximum thrust/hoop forces (T_{max} based on Equation 9-11) in the culvert structure for conservative purposes. Results based

Table 9-12. Racking stiffness of culverts and flexibility ratios.

	Structural Racking Stiffness K_S (kips/ft)	Flexibility Ratio F_{REC}
Case 1	172	0.97
Case 2	172	2.4
Case 3	115	2.9
Case 4	57	7.3
Case 5	43	19.3

on the full-slip assumption tend to under-estimate the thrust/hoop forces.

– In using the simplified approach, the full-slip interface assumption should be used in calculating the maximum bending moments (M_{max}, based on Equation 9-10) and culvert deformation (ΔD_{EQ}, based on Equation 9-7) because it provides more conservative results than the no-slip interface assumption. A flexural type failure mode due to the combined effects of bending moment and thrust force must be checked for both rigid and flexible culverts. The flexural failure criteria may be established using the conventional capacity evaluation procedures for reinforced concrete or metals.

  Based on results from the soil-structure interaction analysis, the effect of shallow burial depth appears to be on the safe side, provided that the maximum free-field ground shearing strain is calculated at the most critical elevation (where the maximum ground shearing strain occurs, rather than the average ground shearing strain within the culvert depth profile).

- For rectangular shape culverts subject to racking deformations, the simplified procedure presented in Section 9.5.2 should provide reliable results under general conditions, with the following notes:
  – A series of parametric analysis was conducted verifying that the procedure can provide a reasonable estimate for the culvert racking deformations. To derive the internal forces in the structural elements, a simple frame analysis is all that is required (refer to Figure 9-10).
  – Based on the results of the parametric analysis, it appears that burial depth has insignificant effects on the culvert racking deformations and therefore no further modifications to the procedure presented in Section 9.5.2 is necessary.
- The seismic effects of transient racking/ovaling deformations on culverts and pipes must be considered additional to the normal load effects from surcharge, pavement, and wheel loads, and then compared to the various failure criteria considered relevant for the type of culvert structure in question.

CHAPTER 10

Recommendations for Future Work

During completion of the NCHRP 12-70 Project, it became apparent that additional work would be required to develop simplified recommendations for the seismic design of retaining walls, slopes and embankments, and buried structures. The required work generally occurs in two categories: (1) fundamental research into seismic performance related to specific issues, and (2) testing of recommended procedures described in this Final Report and as set forth in the specifications and commentaries contained in Volume 2. The following discussions summarize some of the topics that will require further research or evaluation.

10.1 Ground Motions and Displacements

Applicable ground motion criteria have been established by the AASHTO decision to adopt the 1,000-year ground motion maps and the NEHRP-type site factors as a basis for seismic design. This decision on the part of AASHTO resolves many of the uncertainties that existed during this Project and should provide a sufficient basis for the seismic design of retaining walls, slopes and embankments, and buried structures. The revised Newmark displacement charts given in this Final Report also provide an up-to-date method of estimating permanent ground displacements suitable for WUS and CEUS. Height-dependent coherency, or wave scattering, factors also were introduced in this Final Report, and these will be useful for seismic design of walls over 20 to 30 feet in height.

The following topics in the areas of ground motions and displacement determination appear to warrant either future consideration or development:

- Maps are needed from the USGS that provide PGV for the 1,000 year return period. These maps would eliminate the need to use empirical equations based on the 1-second spectral ordinates for making the PGV determination and could contribute to simpler estimates of permanent ground displacements.
- Simple but rational methods for estimating site factors at locations should be developed for locations where NEHRP site factors may not be appropriate. These locations include deep soil sites located in CEUS, where the frequency characteristics of ground motions in combination with the depth and shear wave velocity of the soil profile make the NEHRP factors inaccurate in some situations. Likewise, locations where thin soil layers (for example, less than 50 feet) occur over rock also may not be adequately modeled by the NEHRP site factors.
- An approach for introducing the effects of liquefaction into ground motion computations is needed. Although one-dimensional, nonlinear effective stress computer programs are available, use of these methods is relatively limited. Either simple ground motion adjustment procedures that account for liquefaction should be developed, or easier-to-use, commercially available, effective stress computer programs are needed. In the absence of these methods, it is difficult to properly account for changes in ground motion above sites where liquefaction is predicted.
- Revised equations are needed for estimating the site-adjusted PGA in Equations (5-7) and (5-9) at a predetermined permanent displacement. The current equations cannot be applied by a designer within a spreadsheet analysis procedure to estimate limiting PGA values if the displacement (d) is specified.
- Additional evaluations should be conducted to confirm that the wave scattering factors described in Chapters 6 and 7 are applicable for a variety of site, retaining wall, and slope conditions.

10.2 Retaining Walls

A relatively simple methodology was identified during this work for the seismic evaluation of retaining walls. This methodology was based on either M-O equations for cases where soil is homogenous behind the retaining structure, or a more

generalized limit equilibrium method using conventional slope stability software, for cases involving layered soils. Charts that included the effects of soil cohesion on seismic active and passive pressures were developed. A key consideration within the methodology was the amount of movement that would develop or could occur during seismic loading, and how this movement would affect the seismic demand on the retaining wall.

A number of retaining wall topics were identified as requiring further evaluation or investigation. These topics fall into two categories: (1) generic issues and (2) wall-specific issues:

1. Generic issues, relating to the demand and capacity evaluations
   - Simplified methods of estimating seismic passive earth pressures, particularly for cases involving cohesion, should be developed. Rigorous procedures involving the use of log spiral methods are recommended and charts showing typical results are provided. However, the log spiral approach to passive pressure determination is not easily performed, and in the absence of simple log spiral methods, the designer is likely to resort to less accurate Coulomb or even Rankine methods of estimating passive earth pressures.
   - The potential for shear banding in cohesionless soils limiting the development of seismic active earth pressures needs to be researched. This idea has been suggested by Japanese researchers and by some researchers in North America (for example, R. J. Bathurst and T. M Allen) as potentially limiting the development of seismic earth pressures. The concept is that failure during seismic loading will occur along the same failure surface as developed during static active earth pressure mobilization, rather than changing to some flatter slope angle. This mechanism would limit the development of seismic active earth pressures to much lower values than currently calculated. Unfortunately, the amount of information supporting this concept is currently limited, though it does appear to have some promise.
2. Wall-specific issues
   - The inertial force associated with the soil mass above the heel of a semi-gravity cantilever wall remains a design issue. The recommendations in this report assume that the only seismic force that must be considered is the incremental earth pressure from the active failure wedge, and that the soil mass above the heel of the wall does not provide any additional seismic load to the stem of the wall. Detailed finite element analyses could help resolve this issue.
   - Several issues were identified for MSE walls, including the amount of inertial mass that should be considered for sliding analyses and for the internal design of the reinforcing system. The approach taken during this Project was to assume that the entire mass within the reinforcing strips would respond as a rigid mass, and therefore should be included within the sliding analyses and internal stability evaluation. This approach can lead to very large inertial forces, which may not develop because of the flexibility of the MSE wall system. As noted in the section on MSE wall design, there are also significant issues regarding the approach used to estimate tensile forces in the reinforcement during internal stability evaluations, and there is a need to upgrade the two standard software packages, MSEW and ReSSA, once a consensus is reached on the approach used to design MSE walls. Part of the design issue associated with MSE walls is how to properly account for the flexibility of the wall system in the method of analysis being used. Additional research on the use of the generalized limit equilibrium approach and evaluation of deformations to define wall performance also is needed.
   - Nongravity cantilever walls and anchored walls both involved a similar question on whether movement of the soil wedge behind the retaining wall will be sufficient to allow use of a lower seismic coefficient. For both wall types the approach being recommended, assumes there is no amplification of ground motions behind the retaining wall and that the wall will displace enough to support using a seismic coefficient in design that has been reduced by 50 percent. The potential for amplification of forces to values higher than the free-field ground motions is a particular concern for the anchored walls. The process of pretensioning each anchor to a design load ties the soil mass together, and though the strands or bars used for prestressing can stretch, there is a fundamental question whether the wall-tendon-grouted anchor zone can be simplified by eliminating any interaction effects.
   - Whereas soil nail walls appear to be relatively simple in terms of overall seismic design, there are still fundamental questions about the development of internal forces within the soil mass during seismic loading. These questions include whether the internal forces are transferred to the nails in the same manner as during static loading. The AASHTO *LRFD Bridge Design Specifications* also needs to be supplemented with specific discussions on the static design of soil nail walls, and then these static provisions need to be reviewed relative to provisions appropriate for seismic loading.

10.3 Slopes and Embankments

The seismic design of slopes and embankments was identified as a more mature area of seismic design, where both simplified limit equilibrium and displacement-based approaches

are conventionally used to investigate the seismic stability of engineered slopes and natural cut slopes.

The primary topics that require further study area are as follows:

- The appropriate liquefaction strength to use when assessing the stability of slopes comprised of or resting on liquefiable materials needs to be established. A number of issues about the liquefaction strength remain difficult to quantify, and these difficulties lead to uncertainty in design. Issues include simple methods of estimating the liquefied strength at locations involving sloping ground (that is, where a static shearing stress is imposed) and appropriate liquefied strength values for cohesionless soil where limited deformations occur. Included within this topic is the potential for ratcheting movements and how to adequately represent this mechanism.
- Stability of rock slopes requires further evaluation. This topic was not addressed during this Project because of the complexity of the problem. Although a transparent approach does not seem possible, some additional guidance on factors to consider when conducting a site-specific seismic evaluation would assist designers when they have to deal with rock slope stability.

10.4 Buried Structures

The buried structures portion of the Project provided design equations for rigid and flexible culverts and pipelines subjected to TGD. Guidance also was provided on design considerations for PGD such as might occur during liquefaction-induced lateral spreading or seismic-induced embankment failures. Section 12 of the current AASHTO *LRFD Bridge Design Specifications* does not cover seismic response of culverts and pipelines, and therefore the developments summarized in this report address a current deficiency in the AASHTO Specifications.

The treatment of buried structures in this Project was relatively limited in terms of levels of effort, and additional studies will be required to advance design methods for buried structures:

- Methods suggested in Chapter 9 need to be tested on a range of pipe configurations, ground conditions, and earthquake shaking levels to confirm that the recommended approaches for TGD design are practical. Experimental studies involving TGD also are needed to confirm the validity of the numerical methods being suggested.
- Further guidance needs to be developed for modeling pipeline behavior in conditions where PGD occurs. These developments include appropriate spring constants to use in modeling soil-pipe interaction for moving ground conditions.
- The seismic effects of transient racking/ovaling deformations on culverts and pipe structures need to be incorporated into the updated CANDE analysis. It is anticipated that an option will be required in the CANDE program to allow ground displacement profile as a loading input to the CANDE analysis.

10.5 Need for Confirming Methods

One clear conclusion from this Project was that various methods are available to the designer to use for the seismic design of retaining walls, slopes and embankments, and buried structures. These methods range from simple equations to advanced numerical methods. The focus of this Project has been to develop simple methods of analysis suitable for use in AASHTO *LRFD Bridge Design Specifications.* By focusing on simple methods, a number of simplifying assumptions and approaches had to be taken. Whereas checks and then example problems were completed to test these proposed methods, additional test cases will be required to identify areas where the simplifications are not appropriate, are too conservative, or lack conservatism. For example, test cases involving advanced numerical methods or experimental centrifuge testing could be used to confirm the simplified methods.

References

1. Abrahamson, N. (2005). "Selection of Ground Motion Time Series and Limits on Scaling," Personal Communication.
2. ADAMA Engineering (2005a). "Mechanically Stabilized Earth Walls: Program MSEW 3.0." www.GeoPrograms.com.
3. ADAMA Engineering (2005b). "ReSSA (2.0) Reinforced Slope Stability Analysis." www.GeoPrograms.com.
4. American Association of State Highway and Transportation Officials (2007). "AASHTO LRFD Bridge Design Specifications, Customary U.S. Units." 4th Edition.
5. American Association of State Highway and Transportation Officials (2002). "Standard Specification for Highway Bridges." 17th Edition.
6. American Lifelines Alliance (2001). "Seismic Fragility Formulations for Water System," ASCE, Part 1—Guidelines, April.
7. ASCE (1994). "Guidelines for the Seismic Design of Oil and Gas Pipeline Systems." ASCE, Committee on Gas and Liquid Fuel Lifelines, ASCE Technical Council on Lifeline Earthquake Engineering, ASCE.
8. Ballinger, C. A. and P. G. Drake (1995). "Culvert Repair Practices Manual: Volumes I and II." Report No. FHWA-RD-94-096, Federal Highway Administration, Washington, D.C.
9. Bathurst, R. J. and Z. Cai (1995). "Pseudo-Static Seismic Analysis of Geosynthetic Reinforced Segmental Retaining Walls." Geosynthetics International, Vol. 2, No. 5, pp 782–830.
10. Bathurst, R. J., D. Walters, K. Hatami, D. Saunders, N. Vlachopoulos, P. Burgess, and T. M. Allen (2002). "Performance Testing and Numerical Modeling of Reinforced Soil Retaining Walls." Seventh International Geosynthetics Conference, Nice, France.
11. Bray, J. D., and E. M. Rathje (1998). "Earthquake-Induced Displacements of Solid-Waste Landfills." *Journal of Geotechnical and Geoenvironmental Engineering,* ASCE, Vol. 124, No. 3, March.
12. Cai, Z. and R. J. Bathurst (1996). "Seismic-Induced Permanent Displacement of Geosynthetic-Reinforced Segmental Retaining Walls." *Canadian Geotechnical Journal,* Vol. 33, pp 937–955.
13. Chen, W. F. and X. L. Liu (1990). *Limit Analysis in Soil Mechanics.* Elsevier.
14. Chida S., K. Minami, and K. Adachi (1982). *Test de Stabilité de Remblais en Tere Armée.* Traduit du Japonais.
15. Chugh, A. K. (1995). "A Unified Procedure for Earth Pressure Calculations." Proceedings: Third International Conference on Recent Advances in Geotechnical Earthquake Engineering and Soil Dynamics, Volume III, St. Louis, Mo.
16. Das, B. M. (2001). *Principles of Foundation Engineering.* 4th Edition, Brooks/Cole Engineering Division, Monterey, Calif.
17. Davies, T. G., R. Richards, and K-H Chen (1986). "Passive Pressure During Seismic Loading.," *Journal of Geotechnical Engineering,* ASCE, Vol. 112, No. 4, April.
18. Davis, C. A. and J. P. Bardet (2000). "Responses of Buried Corrugated Metal Pipes to Earthquakes." *ASCE Journal of Geotechnical and Environmental Engineering,* Vol. 126, No. 1, pp 28–39.
19. Davis, C. A. and J. P. Bardet (1999). "Seismic Analysis of Buried Flexible Pipes." ASCE Geotechnical Special Publication No. 75—Geotechnical Earthquake Engineering and Soil Dynamics III, Vol. 2.
20. DESRA (1978). "DESRA-2: Dynamic Effective Stress Response Analysis of Soil Deposits with Energy Transmitting Boundary Including Assessment of Liquefaction Potential." Developed by M. K. W. Lee and W. D. Finn, Department of Civil Engineering, University of British Columbia, Soil Mechanics Series No. 38, 1978-06-23, Vancouver, BC, Canada.
21. Dickenson, S. E., N. J. McCullough, M. G. Barkau, and B. J. Wavra (2002). "Assessment and Mitigation of Liquefaction Hazards to Bridge Approach Embankments in Oregon." Oregon Department of Transportation and Federal Highways Administration, Nov.
22. Elms D. A., and G. R. Martin (1979). "Factors Involved in the Seismic Design of Bridge Abutments." Proceedings, Workshop on Seismic Problems Related to Bridges, Applied Technology Council, San Diego, Calif.
23. Ensoft (2005). "PY WALL 2.0: A Program for Analysis of Flexible Retaining Walls." Ensoft, Inc., www.ensoftinc.com.
24. FHWA (2003). "Soil Nail Walls." Geotechnical Circular No. 7, FHWA0-IF-03-017, Federal Highways Administration, March.
25. FHWA (1999). "Ground Anchors and Anchored Systems." Geotechnical Engineering Circular No. 4, FHWA-IF-99-015, Federal Highways Administration, June.
26. FHWA (1998a). "Geotechnical Earthquake Engineering." Publication No. FHWA HI-99-012, Federal Highways Administration, December.
27. FHWA (1998b). "Design Manual for Permanent Ground Anchor Walls." FHWA-RD-97-130, Federal Highways Administration, September.
28. FHWA (1996). "Geotechnical Engineering Circular No. 2—Earth Retaining Systems." FHWA-SA-96-038, Federal Highways Administration.
29. Golder (2006). "GoldNail: The Golder Modeling Program for Soil Nail Design." Golder Associates, www.golder.com.
30. Hamada, M., R. Isoyama, and K. Wakamatsu (1996). "Liquefaction-Induced Ground Displacement and Its Related Damage to Lifeline Facilities." Soils and Foundations, Special Issue.
31. Holzer, T. L., M. J. Bennett, J. C. Tinsley, III, D. J. Ponti, and R. V. Sharp (1996). "Causes of Ground Failure in Alluvium during the Northridge, California, Earthquake of January 17, 1994." Technical Report NCEER-96-0012, National Center for Earthquake Engineering Research.

32. Hynes, M. E. and A. G. Franklin (1984). "Rationalizing the Seismic Coefficient Method." Miscellaneous Paper GL-84-13, U.S. Army Waterways Experiment Station, Vicksburg, Miss.
33. IBC (2006). "International Building Code." International Code Council.
34. Imbsen, Roy A. (2006). "Recommended LRFD Guidelines for the Seismic Design of Highway Bridges." NCHRP Project 20-07, Task 193. Transportation Research Board of the National Academies, Washington, D.C.
35. Itasca (2007). "FLAC—Fast Lagrangian Analysis of Continua." HCItasca, www.itascag.com.
36. Janson, L-E. (2003). *Plastic Pipes for Water Supply and Sewage Disposal.* 4th Ed. Borealis, Stockholm, Sweden.
37. Johnson, E. R., M. C. Metz, and D. A. Hackney (2003). "Assessment of the Below-Ground Trans-Alaska Pipeline Following the Magnitude 7.9 Denali Fault Earthquake." TCLEE, Monograph 25, Technical Committee on Lifeline Earthquake Engineering, American Society of Civil Engineers.
38. Kramer, S. L. (1996). *Geotechnical Earthquake Engineering.* Prentice Hall.
39. Leschinsky, D. and J. Han (2004). "Geosynthetic Reinforced Multitiered Walls." *Journal of Geotechnical and Geoenvironmental Engineering,* ASCE, Vol. 130, No. 12, pp 1225–1235.
40. Ling, H. I., D. Leschinsky, and E. B. Perry (1997). "Seismic Design and Performance of Geosynthetic-Reinforced Soil Structures." *Geotechnique,* Vol. 47, No. 5, pp 933–952.
41. Makdisi, F. I., and H. B. Seed (1978). "Simplified Procedure for Estimating Dam and Embankment Earthquake-Induced Deformations." *Journal of Geotechnical Engineering,* ASCE, Vol. 104, GT7, pp 849–867.
42. Martin, G. R. and P. Qiu (1994). "Effects of Liquefaction on Vulnerability Assessment." NCEER Highway Project on Seismic Vulnerability of New and Existing Highway Construction, Year One Research Tasks, Technical Research Papers.
43. MCEER (2006). "Seismic Retrofitting Manual for Highway Structures: Part 2—Retaining Walls, Slopes, Tunnels, Culverts, and Roadways." MCEER-0-SP11, Multi-Disciplinary Center for Earthquake Engineering Research.
44. MCEER (1999). "Response of Buried Pipelines Subject to Earthquake Effects." MCEER Monograph Series No. 3, Multi-Disciplinary Center for Earthquake Engineering Research.
45. McGrath, T. J., I. D. Moore, E. T. Selig, M. C. Webb, and B. Taleb (2002). *NCHRP Report 473: Recommended Specifications for Large-Span Culverts.* TRB, National Research Council, Washington, D.C.
46. McGuire, R. K., W. J. Silva, and C. J. Costantino (2001). "Technical Basis for Revision of Regulatory Guidance on Design Ground Motions: Hazard- and Risk-Consistent Ground Motion Spectra Guidelines." NUREG/CR-6728, U.S. Nuclear Regulatory Commission, Office of Nuclear Regulatory Research, Washington.
47. Moore, I. D. (1989). "Elastic Buckling of Buried Flexible Tubes—A Review of Theory and Experiment." *Journal of Geotechnical Engineering,* ASCE, Vol. 115, No. 3, March, pp 340–358.
48. NCEER (1996). "Highway Culvert Performance During Earthquake." NCEER Technical Report NCEER-96-0015, National Center for Earthquake Engineering Research, November.
49. NCEER (1992). "Case Studies of Liquefaction and Lifeline Performance during Past Earthquakes." Technical Report NCEER-92-0001, Volume 1, M. Hamada, and T. D. O'Rourke Eds., National Center for Earthquake Engineering Research.
50. *NCHRP Report 472: Comprehensive Specification for the Seismic Design of Bridges* (2002). TRB, National Research Council, Washington, D.C.
51. NUREG/CR-6728 (2001). "Technical Basis for Revision of Regulatory Guidance on Design Ground Motions: Hazard- and Risk-Consistent Ground Motion Spectra Guidelines." Nuclear Regulatory Commission.
52. Olson, S. M. and T. D. Stark (2002). "Liquefied Strength Ratio from Liquefaction Flow Failure Case Histories." Canadian Geotechnical Journal, Vol. 39, June, pp 629–647.
53. O'Rourke, T. D. (1998). "An Overview of Geotechnical and Lifeline Earthquake Engineering." ASCE Geotechnical Special Publication No. 75—Geotechnical Earthquake Engineering and Soil Dynamics III, Vol. 2.
54. O'Rourke, M. J. and X. Liu (1996). "Continuous Pipeline Subject to Transient PGD: A Comparison of Solutions." Technical Report NCEER-96-0012, National Center for Earthquake Engineering Research.
55. Paulsen, S. (2002). A Numerical Model for Estimating Seismic Displacements of Reinforced Steep Slopes. Master of Science Thesis, University of Washington, Seattle.
56. Paulsen, S. B. and Kramer, S. L. (2004). "A Predictive Model for Seismic Displacements of Reinforced Slopes." Geosynthetics International, Vol. 11, No. 6, pp 407–428.
57. Peck, R. B., A. J. Hendron, and B. Mohraz (1972). "State of the Art of Soft Ground Tunneling." Proceedings of the Rapid Excavation and Tunneling Conference, Chicago, IL, Vol. 1.
58. Peng, J. (1998). "Seismic Sliding and Tilting of Retaining Walls in Kobe Earthquake." Master of Science Thesis, State University of New York, Buffalo.
59. Pockoski, M. and J. M. Duncan (2000). "Comparison of Computer Programs for Analysis of Reinforced Slopes." Virginia Polytechnic Institute and State University, the Charles E. Via, Jr., Department of Civil and Environmental Engineering, Center for Geotechnical Practice and Research, Blacksburg, VA, December.
60. Prakash S., and S. Saran (1966). "Static and Dynamic Earth Pressure Behind Retaining Walls." Proceedings, 3rd Symposium on Earthquake Engineering, Roorkee, India, Vol. 1, pp 273–288.
61. QUAD-4M (1994). "A Computer Program to Evaluate the Seismic Response of Soil Structures Using Finite Element Procedures and Incorporating a Compliant Base." University of California, Davis.
62. Richards R. and X. Shi (1994). "Seismic Lateral Pressures in Soils with Cohesion." *Journal of Geotechnical Engineering,* ASCE, Vol. 120, No. 7, pp 1230–1251.
63. Richards, R. and D. G. Elms (1979). "Seismic Behavior of Gravity Retaining Walls." *Journal of Geotechnical Engineering,* ASCE, Vol. 105, GT4, pp 449–464.
64. Richardson G. N., D. Feger, A. Fong, and K. Lee (1977). "Seismic Testing of Reinforced Earth Walls." *Journal of Geotechnical Engineering Division,* ASCE, Vol. 103, No. GT 11 pp 1–17.
65. RocScience (2005). "Slide: Stability Analysis for Soil and Rock Slopes." www.rocscience.com.
66. SCEC (2002). "Recommended Procedures for Implementation of DMG Special Publication 117 Guidelines for Analyzing and Mitigating Landslide Hazards in California." Southern California Earthquake Center, February.
67. Schnabel, P. B., J. Lysmer, and H. B. Seed (1972). "SHAKE: A Computer Program for Earthquake Response Analysis of Horizontally Layered Sites." University of California—Berkeley, Earthquake Engineering Research Center, Report No. EERC 72-12, December.
68. Schwartz, C. W., and H. H. Einstein (1980). "Improved Design of Tunnel Supports: Volume 1—Simplified Analysis for Ground-Structure Interaction in Tunneling." Report No. UMTA-MA-06-0100-80-4, prepared for U.S. DOT, Urban Mass Transportation Administration.

69. Seed H. B. and J. K. Mitchell (1981). "Earthquake Resistant Design of Reinforced Earth Walls." Internal Study, progress report, Berkeley, Calif.
70. Seed, H. B. and R. V. Whitman (1970). "Design of Earth Retaining Structures for Dynamic Loads." 1970 Specialty Conference Lateral Stresses in the Ground and Design of Earth Retaining Structures, ASCE, June, pp 103–147.
71. Seed, R. B. and L. F. Harder (1990). "SPT-Based Analysis of Pore Pressure Generation and Undrained Residual Strength." In Proceedings of the H. B. Seed Memorial Symposium, Vol. 2, pp 351–376.
72. Segrestin, P. and M. L. Bastick (1988). "Seismic Design of Reinforced Earth Retaining Walls—The Contribution of Finite Element Analysis." International Geotechnical Symposium on Theory and Practice of Earth Reinforcement, Fukuoka, Japan, October.
73. SHAKE91 (1992). "A Computer Program for Conducting Equivalent Linear Seismic Response Analyses of Horizontally Layered Soil Deposits." University of California, Davis.
74. Shamsabadi, A. (2006). *CT-FLEX—Computer Manual.* Office of Earthquake Engineering, California Department of Transportation, Sacramento, Calif.
75. Shamsabadi, A. (2000). "Static and Dynamic Evaluation of Bridge Abutment Capacity." Engineer Degree (Civil) Thesis, Department of Civil and Environmental Engineering, California State University, Long Beach, Long Beach, Calif.
76. Shamsabadi, A., K. M. Rollins, and M. Kapuskar (2007). "Nonlinear Soil-Abutment-Bridge Structure Interaction for Seismic Performance-Based Design." *Journal of Geotechnical and Geoenvironmental Engineering,* ASCE, Vol. 133, No. 6, pp 707–720.
77. Shastid, T., J. Prospero, and J. Eidinger (2003). "Southern Loop Pipeline—Seismic Installation in Today's Urban Environment." TCLEE, Monograph 25, Technical Committee on Lifeline Earthquake Engineering, American Society of Civil Engineers.
78. Siddharthan, R., S. Ara, and G. Norris (1992). "Simple Rigid Plastic Model for Seismic Tilting of Rigid Walls." *Journal of Structural Engineering,* ASCE, Vol. 118, No. 2, pp 469–467.
79. SNAIL. "SNAILZ: Soil Reinforcement Program." California Department of Transportation.
80. Udaka T. (1982). "A Method for Soil-Structure Interaction Analysis." Proceedings of the Symposium on the Use of Computers in Buildings Engineering, Japan, March.
81. USGS (2005). "USGS National Seismic Hazard Mapping Project." United States Geological Survey, http://earthquake.usgs.gov/hazmaps/products_data/48_States/index.htm
82. Vrymoed, J. (1989). "Dynamic Stability of Soil-Reinforced Walls." In *Transportation Research Board Record 1242,* TRB, National Research Council, Washington, D.C., pp. 29–45.
83. Wang, J., (1993). "Seismic Design of Tunnels—A Simple State-of-the-Art Design Approach." William Barclay Parsons Fellowship, Parsons Brinckerhoff, Monograph 7.
84. Whitman, R. V. (1990). "Seismic Analysis and Behavior of Retaining Walls." Geotechnical Special Publication No. 25, ASCE, Design and Performance of Earth Retaining Structures, ed. P. Lambe and L. Hansen, June, pp. 817–839.
85. Youd, T. L. and C. J. Beckman, (2003). "Performance of Corrugated Metal Pipe (CMP) Culverts during Past Earthquakes." TCLEE, Monograph 25.
86. Youd, T. L., C. M. Hansen, and S. F. Bartlett (2002). "Revised Multilinear Regression Equations for Prediction of Lateral Spread Displacements." *Journal of Geotechnical and Environmental Engineering,* ASCE, Vol. 128, No. 12, pp 1007–1017.

APPENDICES

Appendices to the contractor's final report for NCHRP Project 12-70, "Seismic Analysis and Design of Retaining Walls, Buried Structures, Slopes, and Embankments," are available on the TRB website at http://trb.org/news/blurb_detail.asp?id=9631. The appendices are the following:

A. Working Plan
B. Design Margin—Seismic Loading of Retaining Walls
C. Response Spectra Developed from the USGS Website
D. PGV Equation—Background Paper
E. Earthquake Records Used in Scattering Analyses
F. Generalized Limit Equilibrium Design Method
G. Nonlinear Wall Backfill Response Analyses
H. Segrestin and Bastick Paper
I. MSE Wall Example for AASHTO ASD and LRFD Specifications
J. Slope Stability Example Problem
K. Nongravity Cantilever Walls

Abbreviations and acronyms used without definitions in TRB publications:

AAAE	American Association of Airport Executives
AASHO	American Association of State Highway Officials
AASHTO	American Association of State Highway and Transportation Officials
ACI–NA	Airports Council International–North America
ACRP	Airport Cooperative Research Program
ADA	Americans with Disabilities Act
APTA	American Public Transportation Association
ASCE	American Society of Civil Engineers
ASME	American Society of Mechanical Engineers
ASTM	American Society for Testing and Materials
ATA	Air Transport Association
ATA	American Trucking Associations
CTAA	Community Transportation Association of America
CTBSSP	Commercial Truck and Bus Safety Synthesis Program
DHS	Department of Homeland Security
DOE	Department of Energy
EPA	Environmental Protection Agency
FAA	Federal Aviation Administration
FHWA	Federal Highway Administration
FMCSA	Federal Motor Carrier Safety Administration
FRA	Federal Railroad Administration
FTA	Federal Transit Administration
IEEE	Institute of Electrical and Electronics Engineers
ISTEA	Intermodal Surface Transportation Efficiency Act of 1991
ITE	Institute of Transportation Engineers
NASA	National Aeronautics and Space Administration
NASAO	National Association of State Aviation Officials
NCFRP	National Cooperative Freight Research Program
NCHRP	National Cooperative Highway Research Program
NHTSA	National Highway Traffic Safety Administration
NTSB	National Transportation Safety Board
SAE	Society of Automotive Engineers
SAFETEA-LU	Safe, Accountable, Flexible, Efficient Transportation Equity Act: A Legacy for Users (2005)
TCRP	Transit Cooperative Research Program
TEA-21	Transportation Equity Act for the 21st Century (1998)
TRB	Transportation Research Board
TSA	Transportation Security Administration
U.S.DOT	United States Department of Transportation